THE ROLE OF ENDOCRINE AND OTHER FACTORS IN THE REMODELLING UNDERPINNING GRAVES' ORBITOPATHY

Mohd Shazli Draman

This thesis is submitted in fulfilment of the requirements for the degree of Doctor of Philosophy (PhD)

Institute of Molecular and Experimental Medicine

School of Medicine

Cardiff University

Heath Park

Submitted September 2016

DECLARATION

This work has not been submitted in substance for any other degree or award at this or any other university or place of learning, nor is being submitted concurrently in candidature for any degree or other award.

Signed …… Date ……..……

STATEMENT 1

This thesis is being submitted in partial fulfilment of the requirements for the degree of PhD.

Signed …… Date ……..……

STATEMENT 2

This thesis is the result of my own independent work/investigation, except where otherwise stated. Other sources are acknowledged by explicit references. The views expressed are my own.

Signed …… Date ……..……

STATEMENT 3

I hereby give consent for my thesis, if accepted, to be available online in the University's Open Access repository and for inter-library loan, and for the title and summary to be made available to outside organisations.

Signed …… Date ……..……

STATEMENT 4: PREVIOUSLY APPROVED BAR ON ACCESS

I hereby give consent for my thesis, if accepted, to be available online in the University's Open Access repository and for inter-library loans **after expiry of a bar on access previously approved by the Academic Standards & Quality Committee.**

Signed …… Date ……..……

SUMMARY

In Graves' orbitopathy (GO) tissue remodelling by increased proliferation, excess adipogenesis and hyaluronan overproduction, cause exophthalmos. My initial work followed reports by others of enophthalmos in some glaucoma patients treated with Bimatoprost (prostaglandin $F_{2\alpha}$, $PGF_{2\alpha}$) eye drops. I hypothesized that this could be due to reduced proliferation or adipogenesis and/or increased lipolysis; any of which could improve GO. In vitro models used to investigate possible mechanisms demonstrated that $PGF_{2\alpha}$ reduced proliferation by prolongation of G2/M (flow cytometry) and adipogenesis (evaluated morphologically, by oil red O staining and Q-PCR measurement of adipogenesis markers) of 3T3-L1 and human orbital fibroblasts (OF). These effects were reversible upon drug withdrawal. GO OFs proliferated significantly more rapidly and also displayed higher adipogenic potential than non-GO. There was no effect of $PGF_{2\alpha}$, on basal or norepinephrine-induced lipolysis in 3T3-L1 or human OFs, either GO or non-GO.

The data helped us secure NISCHR funding for a clinical trial 'Prostaglandin F2-alpha eye drops (Bimatoprost) in thyroid eye disease: a randomised controlled double blind crossover trial'. Following informed consent, 31 clinically inactive (late phase) GO patients were randomised to receive Bimatoprost or placebo eye drops daily for three months followed by a two-month drug washout period before switching to the opposite treatment for three months. I concluded that 3 months Bimatoprost treatment is not effective in reducing proptosis in late phase GO patients.

My subsequent work investigated truncated *TSHR* variants (*TSHR*_v2) and thyrostimulin. The former could act as TSH/TRAB binding proteins whilst the latter could bind to and activate the TSHR and contribute to GO pathogenesis. I found no evidence of a role for thyrostimulin in GO. *TSHR*_v2 transcripts and protein are more abundant than full length *TSHR* in OF and during adipogenesis are significantly higher in GO than non-GO. TSHR_v2 may be secreted and provide a binding protein for TSHR ligands and thus alter intracellular TSHR signalling.

GD patients lose weight during active disease but gain more following treatment. Our group reported that TSHR activation leads to a 'browning' of fat from various depots. I performed ex vivo analysis on neck fat for brown, beige and white adipose tissue markers. The samples were GD patients (previously hyperthyroid/positive TSAB), toxic goitre (previously hyperthyroid/no TSAB) and euthyroid. I found no difference in expression of *UCP1 and* $PGC1_{\alpha}$. There were general reductions in *ZIC1*, *CITED1*, *HOXC9 and LEPTIN* markers in GD which may explain the altered body composition in these patients.

For

ABAH & MA

MY BEAUTIFUL WIFE & CHILDREN

ACKNOWLEDGEMENTS

In doing this work, I have been fortunate enough to have had a great amount of support and assistance from a large number of generous, helpful and talented people, more than I have space to name individually. There are a few people I must acknowledge, however, without whom I would have been unable to have put this work together.

I would like express my sincere gratitude to my supervisor Professor Marian Ludgate for her help and support to me during these years. There is no word to describe her outstanding mentorship, constructive attitude, encouragement and kindness to me and throughout my PhD study. I also would like to thank my mentor Professor Colin Dayan for believing in me and for his help and support to me during these years. I would like to extend this further to my co-supervisors Dr. Fiona Grennan-Jones and Dr. Lei Zhang for their continuous supports and assistance.

Finally, a massive thank you to my in-laws, brothers and sisters for their continued support and help throughout the whole of my studies.

PUBLICATIONS AND PRESENTATIONS

Publications:

1. Thyroid eye disease - An update. MS Draman, M Ludgate. Expert Review of Ophthalmology 2016. DOI:10.1080/17469899.2016.1202113.
2. Prostaglandin F2α (PGF2α) Effects on Adipocyte Biology Relevant to Graves' Orbitopathy. MS Draman, F Grennan-Jones, L Zhang, P Taylor, T Kyaw Tun, J McDermott, P Moriarty, D Morris, C Lane, S Sreenan, C Dayan, M Ludgate. Thyroid. 2013 Sep 3. [Epub ahead of print] doi:10.1089/thy.2013.0194.

Oral presentation:

1. Possible role for thyrotropin receptor variant (TSHRV) as a binding protein for TSHR ligands in Graves' orbitopathy (GO)? MS Draman, L Zhang, F Grennan-Jones, PN Taylor, I Muller, I Ladas, S Evans, B Skippen, D Morris, C Dayan, M Ludgate. International Thyroid Congress 2015, Florida; Thyroid. October 2015, 25(S1): P-1-A-337. doi:10.1089/thy.2015.29004. SOC 465 & British Thyroid Association, New Castle, supplement in Thyroid Research Journal 2016.
2. Differential proptosis in stable thyroid eye disease. S Evans, MS Draman, D Morris, C Dayan. Kestrel Cup Ophthalmology 2015 Cardiff.
3. Role of alternate TSHR ligands and binding proteins (TSHR-BP) In Graves' orbitopathy (GO). MS Draman, F Grennan-Jones, L Zhang, PN Taylor, D Morris, C Lane, C Dayan, M Ludgate. European Thyroid Association 2014, Santiago de Compostela, Spain. Eur Thyroid J Vol. 3, Suppl. 1, 2014: 25.

4. Potential role of prostaglandin eye drops for treatment of Graves' orbitopathy. MS Draman, WA Mahmood, T Kyaw Tun, JH McDermott, M. Ludgate, S. Sreenan. Annual Irish Endocrine Society meeting 2010, Belfast, Northern Ireland. Ir J Med Sci 2011; 180(13): 473-510.

Abstract presentations:

1. Possible role of physiological and pathological thyrotropin receptor (TSHR) activation in skin and its diseases. F Grennan-Jones, I Elmansori, MS Draman, L Zhang, F Ruge, T Easter, A Rees, A Elgadi, C Marcus, M Ludgate, R Porter. European Thyroid Association 2014, Santiago de Compostela. Eur Thyroid J Vol. 3, Suppl. 1, 2014: 46
2. Possible role of TSH/TSHR ligands in Graves' orbitopathy. MS Draman, F Grennan-Jones, L Zhang, PN Taylor, C Dayan, M Ludgate. High scoring abstract at 62nd Meeting of the British Thyroid Association Meeting, London Dec 2013 & Cardiff University Post Graduate day 2013.
3. Bimatoprost (PGF2α) effects on adipocyte biology? Relevant to Graves' orbitopathy. MS Draman, F Grennan-Jones, L Zhang, T Kyaw Tun, JH McDermott, S Sreenan, C Dayan, M Ludgate. European Thyroid Association meeting, Pisa. European Thyroid Journal 2012; 1(suppl 1); 195: P315.

TABLE OF CONTENTS

LIST OF TABLES

LIST OF FIGURES

ABBREVIATIONS

2D	Two dimension
3D	Three dimension
AC	Adenylate cyclase
ADP	Adenosine diphosphate
AITD	Autoimmune thyroid disease
ANOVA	Analysis of variance
APRT	Adenine Phosphoribosyltransferase
APS	Ammonium persulfate
ATF2	Activating transcription factor 2
ATP	Adenosine triphosphate
ATPase	Adenosine triphosphatase
Arp	Acidic ribophosphoprotein
AZT	Azathioprine
BAT	Brown adipose tissue
BC	Benign cyst
BMD	Bone mineral density
BMI	Body mass index
BSA	Bovine serum albumin
Ca^{2+}	Calcium
$CaCl_2$	Calcium chloride
CaMK	Calmodulin-dependent protein kinase
cAMP	Cyclic adenosine monophosphate
CAS	Clinical activity score
C/EBP	CCAAT/enhancer-binding protein
CD28	Cluster of Differentiation 28

CD52	Cluster of Differentiation 52
CD80	Cluster of Differentiation 80
CD86	Cluster of Differentiation 86
CDKs	Cyclin-dependent kinases
cDNA	Complementary DNA
CFA	Complete Freund's Adjuvant
CI	Confidence interval
CIRTED	Combined immunosuppression & radiotherapy in thyroid eye disease
CITED1	Cbp/p300-interacting transactivator, with Glu/Asp-rich carboxy-terminal domain 1
ClO_4^-	Perchlorate
CM	Complete medium
CN	Colloid nodules
CO_2	Carbon dioxide
COIP	Coimmunoprecipitation
CPRD	Clinical Practice Research Datalink
CRF	Case record form
CRE	cAMP response element
CREB	cAMP-response element binding protein
CSK	C-terminal Src kinase
CSRI	Client service receipt inventory
CT	Cycle threshold
CTLA4	Cytotoxic T lymphocyte-associated 4
CXCR4	C-X-C chemokine receptor type 4
D1	Deiodinase type 1
D2	Deiodinase type 2

D3	Deiodinase type 3
DIO1/2/3	Deiodinase type 1 or 2 or 3 gene
DAG	Diacylglycerol
DIT	Diiodotyrosine
DEHAL1	Iodotyrosine dehalogenase 1
DMSO	Dimethyl sulfoxide
DM	Differentiation medium
DNA	Deoxyribonucleic acid
DON	Dysthyroid optic neuropathy
DUOX 1/2	Dual oxidases 1 or 2
ECD	Extracellular domain
ECD-MBP	Extra cellular domain - maltose-binding protein fusion
ECM	Extracellular matrix
EGTA	Ethylene glycol-bis (β-aminoethyl ether)-N,N,N',N'-tetraacetic acid
ELISA	enzyme-linked immunosorbent assay)
EMNG	Euthyroid multinodular gland
EUGOGO	European Group on Graves Orbitopathy
FCS	Foetal calf serum
FOXP3	Forkhead box P3
FRET	Fluorescence resonance energy transfer
FP	Prostaglandin F receptor
FPS	Splice variant of Prostaglandin F receptor
FSH	Follicular secreting hormone
FT3	Free T3 (thyroid function test)
FT4	Free T4 (thyroid function test)
GABP	Guanine and adenine binding protein

GPCR	G protein coupled receptor
GPHA2	Glycoprotein hormone alpha-2
GPHB5	Glycoprotein hormone beta-5
GD	Graves’ disease
GFP	Green fluorescent protein
GO	Graves’ orbitopathy
GO-QOL	Graves’ orbitopathy – Quality of life questionnaire
Gpdh	Glycerol-3-phosphate-dehydrogenase
GPRD	General Practice Research Database
H_2O	Water
H_2O_2	Hydrogen peroxide
HA	Hyaluronan
HAS	HA synthetase
HAT	Histone transacetylase
HBSS	Hanks' Balanced Salt Solution
HCG	Human chorionic gonadotropin
HCl	Hydrochloric acid
HDA	Histone deacetylase activity
HLA	Human leucocyte antigen
HN	Hyperplastic nodules
HOXC9	Homeobox C9
HPETE	Hydroperoxyeicosatetraenoic acid;
I^-	Iodide
IBMX	3-isobutyl-1-methylxanthine
ICER	Inducible cAMP early repressor
IFA	Incomplete Freund's Adjuvant
IFN-γ	Interferon gamma

IGF1R	Insulin-like growth factor 1 receptor
IL-2	Interleukin-2
IL-4	Interleukin-4
IL-10	Interleukin-10
IL-23R	Interleukin 23 receptor
IMP	Investigational Medicinal Product
IP3	Inositol 1, 4, 5-trisphosphate
IQR	interquartile range
IOP	intraocular pressure
ISRCTN	International standard randomized controlled trial network
iTreg	Induced regulatory T cell
IV	Intravenous
IRISAB 2*	Mouse monoclonal TSAB
KCl	Potassium chloride
KH_2PO_4	Monopotassium phosphate
KO	Knockout
KOH	Potassium hydroxide
LB	Luria-Bertani
LBD	Ligand binding domain
LH	Luteinizing hormone
LH-CGR	Leutropin-choriogonadotropin receptor
LPL	Lipoprotein lipase
LRR	Leucine-rich repeats
LTA4-E4	Leukotriene A4-E4
M22	Human monoclonal TSHR antibodies
MA	Mature adipocyte
MAP	Mitogen-activated protein kinase

MCID	Minimal clinically important difference
MCT	Monocarboxylate transporter
$MgSO_4$	Magnesium sulfate
MHRA	Medicines and Healthcare Products Regulatory Agency
MIT	Monoiodotyrosine
MNG	Multinodular goitre
MMI	Methimazole
M-MLV	Moloney Murine Leukaemia Virus
mRNA	Messenger RNA
MS	Multiple sclerosis
MSC	Mesenchymal stem cells
Na+	Sodium
NaCl	Sodium chloride
NADP+/H	Nicotinamide adenine dinucleotide phosphate
$NaHCO_3$	Sodium bicarbonate
Na_2HPO_4	Disodium phosphate, or sodium hydrogen phosphate
NFAT	Nuclear factor of activated T-cells
NHANES III	National Health and Nutrition Examination Survey III
NIS	Sodium iodide symporter
NO	Normal individual
NSAID	Nonsteroidal anti-inflammatory agents
nTreg	Natural regulatory T cell
OF	Orbital fibroblast
OD	Optical density
PAGE	Polyacrylamide gel electrophoresis
PBS	Phosphate-buffered saline
PCR	Polymerase chain reaction

PDS	Pendrin or sodium-independent chloride/iodide transporter
PDT	Population doubling time
PEG	Polyethylene glycol
PET	Positron emission tomography
PKC	Protein kinase C
PLC	Phospholipase C
PG	Prostaglandin
PGC1α	Peroxisome proliferator-activated receptor gamma coactivator -1 alpha
PGD2	Prostaglandin D2
PGE2	Prostaglandin E2
$PGF_{2\alpha}$	Prostaglandin F2 alpha
PGI2	Prostaglandin I2 or prostacyclin
PMSF	Phenylmethylsulfonyl fluoride
PPARγ	Peroxisome proliferator-activated receptor gamma
PTPN22	Protein tyrosine phosphatase non-receptor 22
PTU	Propylthiouracil
PVDF	Polyvinylidene difluoride
QPCR	Quantitative polymerase chain reaction
RAPD	Relative afferent pupil defect
REC	Research Ethics Committee
RNA	Ribonucleic acid
rT3	Reverse triiodothyronine
rhTSH	recombinant TSH
RXRγ	Retinoid-X-receptor-γ
SAIL	Secure Anonymised Information linkage
SCN^-	Thiocyanate

SDS	Sodium dodecyl sulfate
SFM	Serum free medium
SEM	Standard error of mean
SI	Stimulation index
SOC	Super Optimal broth with Catabolite repression
SS	Disulphide
SSBP	Single strand binding protein
SST2	Somatostatin receptor-2
SST5	Somatostatin receptor-5
T3	Triiodothyronine
T4	Thyroxine
TA	Toxic adenoma
TBAB	Thyrotropin receptor blocking antibodies
TBG	Thyroid binding globulin
TBII	Thyrotropin binding inhibitory immunoglobulin
TCF21	Transcription factor 21
TCN	Transcript copy numbers
TCR	T cell receptor
TED	Thyroid eye disease
TEMED	Tetramethylethylenediamine
TES	Total eye score
TG	Thyroglobulin
TGAB	Thyroglobulin antibodies
TGF-β	Transforming growth factor beta
Th1	T helper cell type 1
Th2	T helper cell type 2
TXA2	Thromboxane

Tim-3	T-cell immunoglobulin mucin-3
TMD	Transmembrane domain
TMNG	Toxic multinodular gland
TNF	Tumour necrosis factor
TNG	Toxic nodular goitre
TPO	Thyroperoxidase
TPOAB	Thyroperoxidase antibodies
TR	Thyroid receptor
TRE	Thyroid response elements
Treg	Regulatory T cell
TRH	Thyrotropin-releasing hormone
TRH-R1	Thyrotropin-releasing hormone receptor type 1
TRH-R2	Thyrotropin-releasing hormone receptor type 2
TSAB	Thyroid stimulating hormone
TSH	Thyrotropin or thyroid stimulating hormone
TSHR	TSH receptor
TSHR_v	TSHR variants
TTF1	Thyroid transcription factor-1
UC	Universal container
UCP	Uncoupling protein
WAT	White adipose tissues
ZIC1	Zinc finger of cerebellum 1

Chapter One

1 INTRODUCTION

1.1 Origin of thyroid gland

The thyroid gland is named from its association with the laryngeal thyroid cartilage which resembles a Greek shield or ‘thyreos’. Thyroid gland is an important organ in human health. The hypothalamus and posterior portion pituitary gland are derived from down growth of the prosenchephalon (forebrain) and the anterior pituitary gland is from the up growth of the Rathke’s pouch of the oral ectoderm- The thyroid gland emerges from the primitive pharynx and visible as a bud around day 20-22. The bud proliferates ventrally and expands laterally to form the typical bilobed appearance of the thyroid gland. This is followed by caudal migration which completes by day 45-50 reaching its final destination. During the downward migration, it is joined laterally by the ultimobrachial body (from 4^{th} pouch) which contains C cells. Finally the onset of folliculogenesis begins at day 70 [1, 2]. At this stage thyroid hormone associated genes are expressed according to a strict temporal pattern- Thyroglobulin (TG), Thyroperoxidase (TPO) and TSH receptor (TSHR) followed by sodium iodide symporter (NIS) and dual oxidases Duox1/2. Therefore prior to this foetal development is fully dependent on maternal thyroid hormone.

1.2 Thyroid hormones biosynthesis and secretion

Inorganic form of iodine (iodide) enters the thyroid follicular cells and undergoes several metabolic steps to form thyroxine (T4) and triiodothyronine (T3). These steps and its inhibitors (see Table 1 and Figure 1) are as follows:

1. Active transport of iodide (iodide trapping)
2. Iodination of tyrosyl residues of TG
3. Coupling of iodothyrosine molecules
4. Storage
5. Colloid resorption
6. Proteolysis of TG with the release of T4, T3, rT3
7. Deiodination of iodothyrosine and recycling of the iodide

Table 1: Steps involved in thyroid hormone biosynthesis and respective inhibitors. $ClO4^-$, perchlorate; SCN-, thiocyanate; MMI, methimazole; PTU, propylthiouracil; I-, iodide; MIT, monoiodotyrosine; DIT, diiodotyrosine; T4, thyroxine.

Steps	Inhibitors
Iodide transport	$ClO4^-$, SCN^-
Iodination	MMI, PTU
Coupling	MMI, PTU
Colloid resorption	Colchicine, Lithium, I^-
Proteolysis	I^-
Deiodination of DIT & MIT	Dinitrotyrosine
Deiodination of T4	PTU

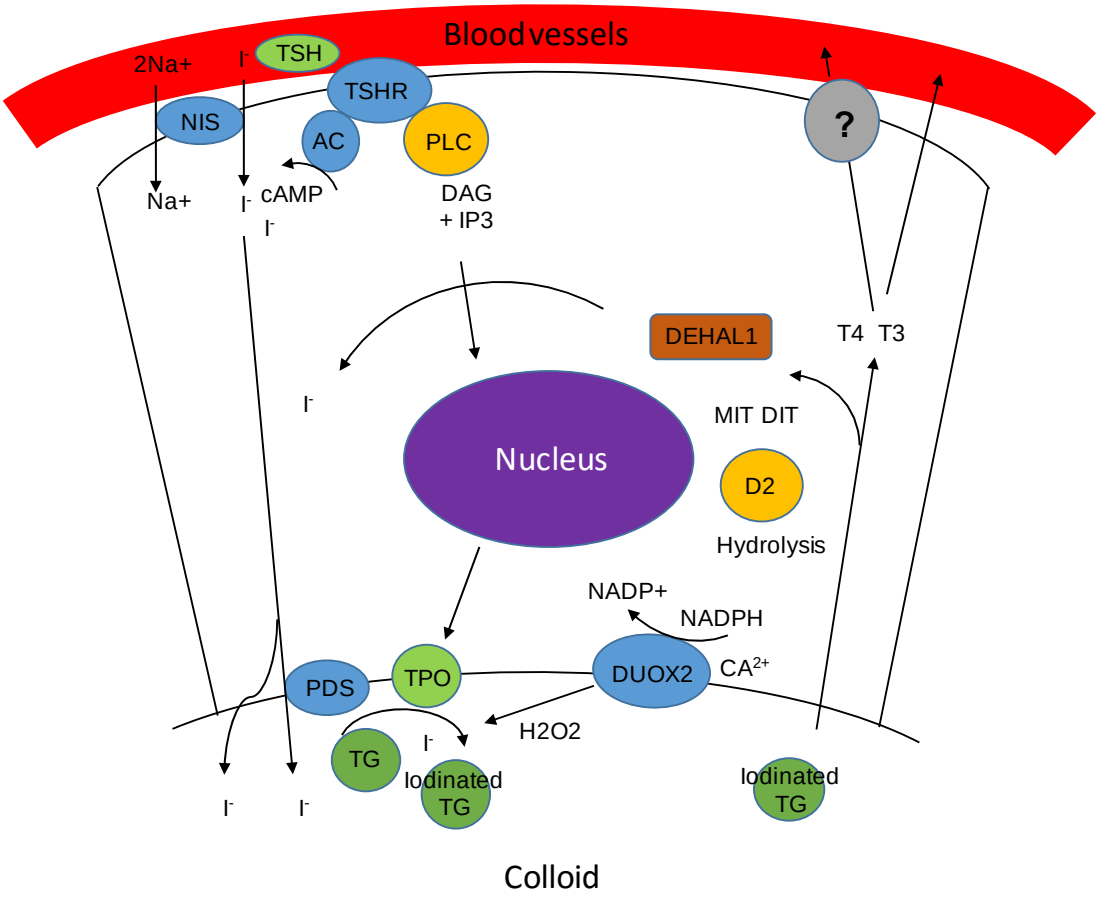

Figure 1: Schematic representation of a thyroid follicular cell illustrating the main steps in thyroid hormone biosynthesis. AC, Adenylate cyclase; Ca^{2+}, calcium; cAMP, cyclic adenosine monophosphate; D2, deiodinase 2, DAG, diacylglycerol; DIT, diiodotyrosine; H_2O_2, hydrogen peroxide; IP3, inositol 1,4,5-trisphosphate; DEHAL1, iodotyrosine dehalogenase 1; Na+, sodium; NADP+, nicotinamide adenine dinucleotide phosphate; NIS, sodium iodide symporter; PDS, Pendrin or sodium-independent chloride/iodide transporter; PLC, phospholipase C; MIT, monoiodotyrosine; T3, triiodothyronine; T4, thyroxine; TG, thyroglobulin; TPO, thyroperoxidase; TSH, thyrotropin; TSHR, thyrotropin receptor. Adapted from Hormone synthesis: Thyroid iodine metabolism, Alvin Taurog. Werner and Inghar's. The Thyroid, 7th edition 1996.

The pituitary thyrotropin (TSH) level controls all the steps of thyroid hormone metabolism including the iodide uptake and the release of thyroid hormones. This is achieved mainly via TSH binding to TSHR and activation of cAMP downstream signalling cascades [3]. The ability of thyroid gland to concentrate iodide is not unique to itself but also found in other tissues such as salivary gland, gastric mucosa,

mammary glands, choroid plexus, placenta and skin [4].

At the basolateral membrane, iodide is actively transported against an electrochemical gradient into the thyroid follicular cytoplasm by the sodium iodide symporter (NIS). NIS is dependent on the sodium gradient created by the Na+/K+ adenosine triphosphatase (ATPase). At the apical membrane, iodide efflux into the colloid is mediated partly by another transporter called Pendrin, also known as sodium-independent chloride/iodide transporter. Iodide molecules are also passively transported through other putative I^- channels across the apical membrane into the colloid.

At the apical-colloid interface, iodide is oxidized by TPO to generate active iodinating species in the presence of hydrogen peroxide (H_2O_2). The generation of hydrogen peroxide is mediated by the calcium-dependent reduced nicotinamide adenine dinucleotide phosphate (NADPH) dual oxidase type 2 (DUOX2) [5]. TG which is secreted into the colloid serves as a matrix for synthesis of T4 and T3. The thyroid hormones are formed firstly by iodination of selected tyrosyl residues (organification) catalysed by TPO enzyme which results in the formation of monoiodotyrosine (MIT) or diiodotyrosine (DIT). Subsequently, two iodotyrosines are coupled to form either T3 or T4 in a reaction that is also catalysed by TPO enzymes. The coupled thyroid hormones-thyroglobulin are stored as colloid in the follicular lumen. When needed, thyroglobulin is internalized into the follicular cell by pinocytosis and digested in lysosomes to generate T4 and T3. These are then released into the bloodstream through unknown mechanisms. Recent studies indicate that monocarboxylate transporter (MCT) 8 and 10 play major roles in the efflux of the thyroid hormones from the thyroid cells [6]. The remaining MIT and DIT in the follicular cell are then deiodinated by the iodotyrosine dehalogenase 1 (DEHAL1) to release iodide which is then recycled for thyroid hormone synthesis.

In the circulation, 99% of thyroid hormones are bound to plasma protein. Thyroid binding globulin (TBG) carries about 70% of the total T4 and T3. Albumin carries around 15-20% and Transthyretin/thyroxine-binding prealbumin around 10-15% of the total thyroid hormones. The latter 2 binding proteins have a lower binding affinity and hence readily available to be released rapidly. Lipoproteins transport a minor proportion of the circulating T4 and T3. Only 0.03% of T4 and 0.3% of T3 exist in free form.

1.3 Regulation of thyroid function

As mentioned above, TSH is the major stimulus of thyroid hormone production and secretion. It is produced in the anterior pituitary gland by thyrotroph cells. The TSH secretion is pulsatile with 6-18 pulses per 24 hours in adults and increase in both frequency and amplitude in the late evening and early morning. The exact mechanism controlling the pulsatility is unknown but more likely influenced by TRH secretion and the suprachiasmatic nucleus of the hypothalamus [7]. TRH is produced in the paraventricular nucleus of the hypothalamus and secreted into the portal circulation. This is then carried to the anterior pituitary gland where it activates TRH-R1 receptors to synthesize and secretes TSH α and β subunits, also posttranslational glycosylation-important for its biological activity. TRH-R2 has been identified in rodents but no role identified in human yet [8]. TRH also stimulates prolactin, and in some patients, growth hormones and gonadotropins.

TSH secretion is tightly regulated by T4 and T3 levels. TSH secretion is also controlled by other cell surface and nuclear receptors. These receptors include somatostatin receptor -2 and -5 (SST2 and SST5), catecholamine receptors, β2 isoforms of thyroid receptor, RXRγ (retinoid-X-receptor-γ) and glucocorticoid receptor. As the name implies, somatostatin is an inhibitor of growth hormone. It also inhibits

TSH secretion partly via a Gi coupled receptor which inhibits adenylyl cyclase [9]. Activation of α2 and β adrenergic receptors also stimulates the release of TSH. On the other hand, dopamine agonist probably via D2 receptor blocks TSH release via inhibition of cAMP accumulation [10]. The role of vitamin A analogues and inhibition of TSH release came about when bexarotene, an RXR ligand used to treat cutaneous T-cell lymphoma, was shown to cause reversible central hypothyroidism [11]. High dose steroid inhibits TSH secretion directly and indirectly via TRH release. With the exception of RXR ligand, none of the blocking substances cause hypothyroidism as the impact of T4 and T3 reduction on TSH release if far too potent and overcomes the inhibition process.

1.4 Thyroid hormone metabolism

Thyroxine is a prohormone and must be activated to T3 in order to exert its effect. The prolonged half-life of T4 (1 week) renders it very stable as opposed to T3 half-life of 1 day. Only approximately 20% of T3 is produced by the thyroid gland whilst the majority (80%) of T3 is produced by extra thyroidal deiodination. This is achieved by deiodinase enzymes with 3 subtypes namely Deiodinase-1, -2 and -3. D2 contributes more to plasma T3 by deiodination of outer tyrosyl ring of the T4. In contrast, both T4 and T3 can be inactivated by deiodination of the inner tyrosyl residue (Figure 2).

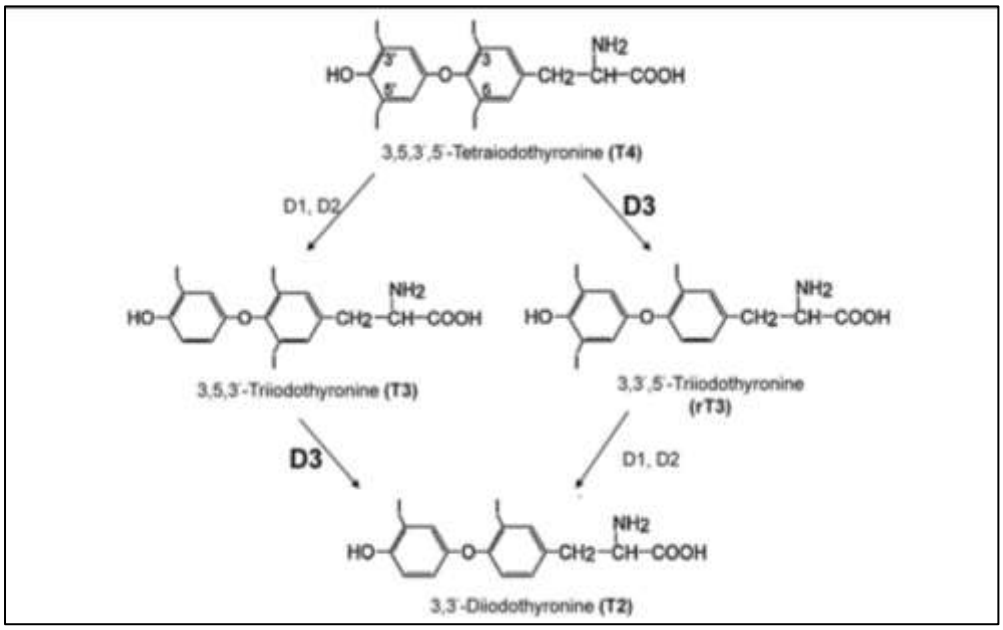

Figure 2: Thyroid hormone metabolism steps by 3 deiodinases. D1, deiodinase type 1; D2, deiodinase type 2; D3, deiodinase type 3; T4, tetraiodothyronine; T3, triiodothyronine; rT3, reverse triiodothyronine; T2, diiodothyronine.

The 3 deiodinase proteins share approximately 50% sequence homology and are membrane bound by a single transmembrane segment (Table 2). D1 and D3 are located in the cellular membrane with the catalytic region in the cytosol whilst D2 is located in the endoplasmic reticulum membrane again with catalytic region in the cytosol [12]. Deiodinase 1 is coded by *DIO1* gene located on chromosome 1 p32-p33. The D1 activities can be potentiated by T3 and selenium, and inhibited by cytokines TNF-α, IL-1β, interferon-γ and fasting state. Deiodinase 2 is coded by *DIO2* gene located on chromosome 14q24.3. Its action is enhanced by cold exposure, norepinephrine, isoproterenol, insulin and glucagon; and inhibited by growth hormone. The deiodinase 3 gene is located on chromosome 14q32. It is found predominantly in brain and skin. Elevated thyroid hormone, sex steroid level and critical illness have been associated with high D3 activity. Other nondeiodination metabolism pathways of thyroid hormones have been described, and include ether bond

cleavage [13], deamination/decarboxylation of the alanine side chain, glucuronidation and O-methylation [14, 15].

Table 2: Type of deiodinases with its locations and functions

Type	Location	Function
Deiodinase 1	Liver, kidney, thyroid, pituitary	Deiodinate either outer (5') and inner (5) tyrosyl residues
Deiodinase 2	Many tissues including bone, skin, skeletal muscle, CNS, fat, thyroid, pituitary, placenta, vascular smooth muscle	Major activating enzyme Deiodinate the outer (5') tyrosyl residues Also degrade rT3
Deiodinase 3	CNS, skin and placenta	Major inactivating enzyme Deiodinate the inner (5) tyrosyl residues

1.5 Thyroid hormone action

Thyroid hormones regulate a wide range of human biological and pathological activities. They play a crucial role in the foetal growth and development of the nervous system and also in the later part of childhood. In adulthood, thyroid hormones are primarily responsible for regulating metabolism (temperature, carbohydrates, lipids, protein) and also have an effect on mental status and bone turnover.

Thyroid hormone exerts its effects via its nuclear receptors. They are members of a

large family of nuclear receptors that include those of the steroid hormones. They function as hormone-activated transcription factors and modulate gene expression. In the absence of thyroid hormone, thyroid hormone receptors usually bind DNA leading to transcriptional repression. Hormone binding is associated with a conformational change in the receptor that causes it to function as a transcriptional activator. Human thyroid hormone receptors are encoded by two genes, designated α and β and located on chromosome 17 and 3 respectively [16, 17].

Like other nuclear receptors, thyroid hormone receptors consist of three functional domains:

1. A transactivation domain at the N-terminus that interacts with other transcription factors and forming complexes which can activate or suppress transcription.
2. A DNA-binding domain (DBD) that binds to sequences of promoter DNA known as thyroid response elements (TRE).
3. A ligand-binding domain (LBD) and dimerization domain at the C-terminus.

As shown in Figure 3 there is considerable variation among transactivation and ligand-binding domains. The α-2 isoform has a unique C-terminus consisting of 122 amino acids that replace part of LBD and does not bind triiodothyronine (T3). Therefore, α-2 may act as inhibitor of TH action by competing for binding to TREs.

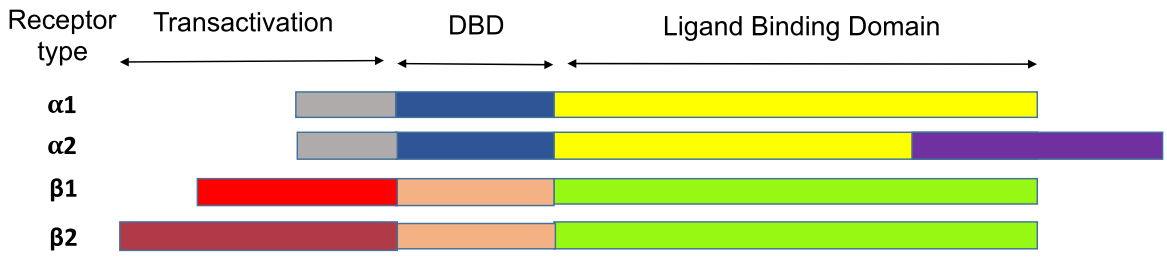

Figure 3: The different isoforms of thyroid receptors depicting highly conserved DNA binding (DBD) and Ligand binding domain (LBD) but marked divergence in terms of transactivating domain.

Currently, four different thyroid hormone receptors are recognized suggesting an extraordinary level of complexity of thyroid hormone effects. These are: TRα-1, α-2, β-1 and β-2. TRα-1 and β-1 proteins are expressed in almost all tissues with TRα-1 having highest expression in the brain, heart, brown fat and muscle. TR β-1 is highest in the liver and kidney. TRα-2 is highest in the brain and testis with TR β-2 is predominantly located in the anterior pituitary and hypothalamus.

Thyroid hormone receptors bind to thyroid or T3 response elements (TRE). A TRE is composed of two or more AGGTCA "half sites". The half sites of a TRE can be arranged as direct repeats, palindromes or inverted repeats [18]. Thyroid hormone receptors can bind to a TRE as monomers, as homodimers or as heterodimers with the retinoid X receptor (α, β, γ) with heterodimer being the major forms of the receptors. The TR can exist in a ligand-free state: where T3-free receptor/RXR heterodimer complex interacts with a group of corepressor molecules which has histone deacetylase activity (HDA). This forms a compact, "turned-off" conformation of chromatin leading to repression of gene transcription. In the ligand-bound state, the TR/RXR heterodimer complex binds to a group of coactivator proteins. This turns on histone transacetylase (HAT) activity, which imposes an open configuration on adjacent chromatin leading to gene transcription. Thyroid hormone resistance

syndrome has been identified in humans whereby they are clinically euthyroid but have elevated thyroid hormone with inappropriately normal TSH. It is an autosomal dominant disorder due to mutation in the carboxyl terminus of the TRβ. The mutation is mostly contained within 3 hotspots in the LBD and adjacent hinge region. The mutation renders TR less able to bind to thyroid hormone or leads to abnormal interaction with one of the cofactors involved in TH action [19, 20]. Recently, a mutation in TRA gene has been identified leading to mutant TRα-1 and α-2 proteins [21]. These patients have a distinct phenotype (macrocephaly, thickened calvarium, broad faces, skin tags, motor dyspraxia, slow speech), normal thyroid function test but low T4:T3 ratio.

1.6 Disorders of thyroid gland

Thyroid disorders are very common and tend mainly to occur in women. About 1 in 20 people suffer from some kind of thyroid disorder. Clinical presentations of thyroid disorders are commonly a result of lack of thyroid hormone secretion (Hypothyroidism) or excessive thyroid hormone secretion (Hyperthyroidism).

1.7 Hypothyroidism

Due to heterogeneous symptoms and signs of hypothyroidism the diagnosis of hypothyroidism relies heavily upon laboratory tests. Primary hypothyroidism is defined by a low serum free thyroxine (T4) concentration with elevated serum thyroid-stimulating hormone (TSH) concentration. As the name suggests the ‘primary’ indicates that the disorder is due to failure of the thyroid gland. Secondary hypothyroidism is characterized by a low serum T4 concentration and a normal or low serum TSH concentration. Subclinical hypothyroidism is defined by a normal free T4 concentration in the presence of an elevated TSH concentration above the normal

reference range and up to 10 mu/L. The prevalence of hypothyroidism using National Health and Nutrition Examination Survey data (NHANES III) is around 4.6 percent with the majority of this contributed by subclinical disease (4.3%) and smaller contribution by overt hypothyroidism (0.3%). Serum TPO autoantibody (please see below) concentrations are elevated in 11 % of this population. Whilst the Whickham survey revealed the UK prevalence of overt hypothyroidism of 0.1-2% [22].

1.7.1 Causes of hypothyroidism

Primary hypothyroidism may be caused by disease or treatment that destroys the gland itself. Worldwide iodine deficiency is still a major cause of hypothyroidism. In iodine sufficient areas, autoimmune thyroiditis is the commonest cause. Other causes of hypothyroidism are depicted in Table 3.

Table 3: Causes of hypothyroidism

Primary hypothyroidism
Chronic autoimmune thyroiditis
Iatrogenic e.g. Thyroidectomy
Radioiodine therapy or external irradiation
Iodine deficiency or excess
Drugs – iodine, thionamides, lithium, amiodarone, interferon-alfa, interleukin-2, perchlorate, tyrosine kinase inhibitors
Infiltrative diseases – amyloidosis, scleroderma, fibrous thyroiditis, hemochromatosis, sarcoidosis
Congenital thyroid dysgenesis, or defects in thyroid hormone synthesis
Transient hypothyroidism
Painless (silent, lymphocytic) thyroiditis or post-partum thyroiditis
Subacute granulomatous thyroiditis
Subtotal thyroidectomy
Following radioiodine therapy for Graves' hyperthyroidism
Following withdrawal of suppressive doses of thyroid hormone in euthyroid patients
Central hypothyroidism
Pituitary disease
Hypothalamic disease

1.7.2 Clinical manifestations of hypothyroidism

Clinical symptoms of hypothyroidism are heterogeneous but most patients with overt hypothyroidism will have symptoms and signs of hypothyroidism. On the other hand, patients may have minimal symptoms and signs, or at the other extreme, may present as myxoedema coma. Table 4 illustrated clinical manifestation of hypothyroidism.

Table 4: Common symptoms associated with hypothyroidism.

Symptoms of hypothyroidism
Fatigue
Lethargy
Cold intolerance
Weight gain
Mental sluggishness
Depression
Constipation
Hoarseness
Dry skin
Reduced appetite
Menorrhagia
Arthralgia
Myalgia
Paraesthesia

1.8 Hyperthyroidism

The term hyperthyroidism refers to overproduction of thyroid hormones while thyrotoxicosis refers to a clinical state that results from elevation of thyroid hormones in the blood stream from any cause [23]. From the NHANES III survey, hyperthyroidism was found in 1.3 % with 0.5 percent overt and 0.7 % subclinical [24]. The prevalence of overt hyperthyroidism from the Whickham survey is approximately the same around 1.3-1.9% [22].

The diagnosis of hyperthyroidism is based upon thyroid function tests with most patient having high free T4/T3 and suppressed TSH. Some patients may have only elevation in T3 (and suppressed TSH) due to an increase in thyroidal secretion of T3 and peripheral conversion of T4 to T3. This is called T3 thyrotoxicosis. Some hyperthyroid patients may have elevated T4 only with normal T3. This may be seen in patients with intercurrent illness whereby there is a reduction in extra thyroidal conversion of T4 to T3 due to reduced deiodinase activity. Upon recovery, these patients will subsequently have T3 elevation. With currently used sensitive assays, patients with minimal or no symptoms may present with suppressed TSH and normal T4 and T3. This is called subclinical hyperthyroidism. Very rarely patients will have elevated T4/T3 with non-suppressed TSH either due to TSH secreting pituitary adenoma or thyroid hormone resistance.

1.8.1 Causes of hyperthyroidism

The commonest cause of hyperthyroidism in any age group is Graves' disease followed by toxic multinodular goitre which is also the commonest cause in the older age group. Graves' disease will be discussed in detail below. A toxic nodular goitre (TNG) or Plummer's disease is a thyroid gland that contains autonomously functioning thyroid nodules, with resulting hyperthyroidism. The thyroid production is

independent of TSH and thyroid stimulating antibodies. It represents a spectrum of pathology ranging from a single hyperfunctioning nodule (toxic adenoma) to multiple hyperfunctioning nodules (toxic multinodular gland). The word ‘Toxic’ in thyroid terms means hyperthyroid state. It was first described by Dr. Henry Plummer in 1913. The hyperfunctioning nodule/s are readily seen on radioiodine or technetium scan with classical circumscribed increased uptake “hot nodules” on the imaging. In toxic multinodular goitre there may also be areas of reduced uptake or “cold nodules”.

The majority of these nodules are caused by somatic mutations leading to constitutive activation of TSHR G protein coupled receptor in 20-80% and less frequently in the adenylate cyclase-stimulating G alpha protein [25]. Signs and symptoms of TNG are similar to those of other types of hyperthyroidism.

Other causes of hyperthyroidism can be divided into normal or high radioiodine uptake against lower uptake. Table 5 illustrates causes of hyperthyroidism.

Table 5: Causes of hyperthyroidism

Hyperthyroidism with a normal or high radioiodine uptake
Autoimmune
Graves' disease
Hashitoxicosis
Autonomous thyroid tissue
Toxic adenoma (some may be due constitutively active mutant TSHR)
Toxic multinodular goitre
TSH-mediated hyperthyroidism
TSH secreting pituitary adenoma
Non-neoplastic TSH-mediated hyperthyroidism
Human chorionic gonadotropin-mediated hyperthyroidism
Hyperemesis gravidarum
Trophoblastic tumour
Choriocarcinoma
Familial gestational hyperthyroidism (Mutant TSHR sensitive to HCG)
Hyperthyroidism with low radioiodine uptake
Thyroiditis
Postpartum thyroiditis
Painless thyroiditis (silent thyroiditis, lymphocytic thyroiditis)
Subacute granulomatous (de Quervain's) thyroiditis
Amiodarone (Type II)

Radiation thyroiditis
Exogenous thyroid hormone intake
Excessive replacement therapy
Intentional suppressive therapy
Factitious thyrotoxicosis
Ectopic hyperthyroidism
Struma ovarii
Metastatic follicular thyroid cancer
Thyroid adenoma infarction

1.8.2 Clinical manifestations of hyperthyroidism

The diagnosis of hyperthyroidism is usually evident in patients with typical clinical and biochemical manifestation of the disease. Some other patients, especially the elderly, may have minor clinical signs, but definite biochemical hyperthyroidism. Majority of the patients will have symptoms as depicted in Table 6. Weight loss is a very common complaint due to the hypermetabolic states but some patients may present with weight gain due to excessive appetite stimulation.

Table 6: Symptoms of hyperthyroidism

Symptoms of hyperthyroidism
Anxiety
Tremor
Hyperactivity
Palpitation
Increased appetite
Weight loss
Increase sweat
Heat intolerance
Myopathy
Amenorrhea/Oligomenorrhea
Increase in bowel frequency

1.9 Graves' disease

Graves' disease (GD) which is the commonest cause of hyperthyroidism is caused by thyroid-stimulating autoantibodies (TSAB) that bind to the thyroid stimulating hormone (TSH) receptor (TSHR) on thyroid follicular cells causing excess production of thyroid hormone as well as thyroid growth causing goitre. Although the exact mechanism leading to its development is unknown, genetic and environmental factors are thought to be involved. GD prevalence is about 0.5 % with females being affected 7.5 times more often than men and peak incidence between 30-50 years old [26]. It is named after an Irish physician named Robert Graves who in his lecture in 1835

described a patient of his as “newly observed affectation of the thyroid gland in female” [27]. A decade prior to this, a Welsh physician Caleb Hillier Parry (1755-1822) gave a clinical picture of GD in 1786. This was not published but subsequently reported in his posthumous collection of unpublished writings in 1825 [28]. However going back 800 years ago in 12th century, a Persian physician Sayyid Ismail al-Jurjani has noted association of exophthalmos with goitre in his "Thesaurus of the Shah of Khwarazm", the major medical dictionary of its time [29]. In Europe, it is known as Basedow’s disease/syndrome after description by a German physician Karl Adolph von Basedow [30]. Other less common names include Parry’s disease, Begbie’s disease (named after Dr. James Begbie [31]) and Flajani’s disease after a description by 2 Italian physicians Giuseppe Flajani (1741-1808) in 1802 and Antonio Giuseppe Testa (1756-1814) in 1810 [32]. Clinically, patients present with hyperthyroidism alone but may be one of 3 pathognomonic features of GD namely exophthalmos, nail clubbing or pretibial myxoedema. The latter 2 are very rare phenomena. The thyroid is usually diffusely enlarged. The histology of the thyroid gland in patients with GD is characterized by diffuse hyperplasia and hypertrophy of follicular cells with retention of lobular architecture and prominent vascular congestion. Colloid is pale with scalloped margins. There may be lymphocytic infiltration in which the majority of the lymphocytes are T cells but B cells may be present.

1.9.1 Thyroid autoantibodies

Alterations in thyroid gland function result from the action of either stimulating or blocking autoantibodies on cell membrane receptors; or destructive nature of the autoantibodies on thyroid follicular cells. Three principal thyroid autoantigens are involved in autoimmune thyroid disease. These are TPO, TG and TSHR. These antigens will be further discussed in GO section below. Both TPO (TPOAB) and TG (TGAB) antibodies are found in 30% to 75% of GD patients [33, 34]. TPOAB is

normally found to be associated with Hashimotos's, atrophic and post-partum thyroiditis. It appears to be involved in the tissue destructive processes associated with the hypothyroidism. The appearance of TPOAB usually precedes the development of hypothyroidism. Some studies suggest that TPOAB may be cytotoxic to the thyroid via complement mediated pathway [35]. The role of TGAB is less clear. Rather than being pathogenic, TGAB presence probably reflects the destructive process in thyroid gland exposing TG leading to the formation of TGAB.

In 1956, GD sera was found to contain an immunoglobulin described as a long-acting thyroid stimulator (LATS) that inhibited the binding of radiolabelled TSH to thyroid membranes, suggesting that such activity was due to the presence of TRAB [36, 37]. More detail about TRAB will be provided below. Two most commonly used methods of assessing TRAB are competition assays and bioassays. The competition assays employ competition by TSHR autoantibodies for ligand (TSH or monoclonal antibody) binding to the TSHR. The ligand may be radiolabelled or tagged with an enzyme or fluorescent dye. This is also known as TBII (TSH-binding inhibitor immunoglobulin) assay. The assay quantifies patient's immunoglobulins that inhibit the binding of TSH to TSHR therefore it measures both TSAB and TSHR blocking antibodies (TBAB). Bioassays involve culturing thyroid cells or nonthyroidal cells expressing the recombinant human TSHR. They measure TSHR stimulating antibodies through their effect on cyclic adenosine monophosphate (cAMP) production in a cell line transfected with TSHR. TBAB is also measured using the bioassay by measuring the ability of patient's IgG or serum to inhibit TSH activity by 30%-40% depending the local laboratory reference range. Of note neither of the assays measure neutral TSHR antibodies, i.e. antibodies which bind the TSHR but have no biological activity and do not inhibit TSH binding. These currently used assays are also unable to measure antibodies that stimulate different pathways as described by Morshed et al [38].

TRAB can stimulate different subtypes of G proteins including Gs with cAMP pathways leading to an increase in NIS synthesis/activity and also thyroid hormones synthesis/secretion. TRAB also stimulate Gq and the PKC pathways leading to cell proliferation [39]. Weetman et al suggested TSAB are predominantly immunoglobulin G1 (IgG1) subclass suggesting that they are oligoclonal or possibly monoclonal in origin in contrast to TPOAB and TGAB which are polyclonal [40]. In terms of clinical utility, TRAB levels are frequently used to diagnose GD in the absence of extra thyroidal manifestations. Its predictive value for GD relapse remains questionable [41] possibly due to the presence of TRAB having varying biological activity and which may not be detected in all assays.

1.9.2 Risk factors for GD

Several factors that predispose to GD have been proposed. As mentioned above, the fact that GD is more common in females and age group of 30-50 years of age suggests there are hormones or age related factors that contribute to the susceptibility. Females are known to handle infections differently than males and respond better to infection and vaccine than males [42]. These protections are partly mediated by IL-4-mediated T helper type 2 (Th2) response by inhibition of IFN-γ production and by increasing anti-inflammatory T-cell immunoglobulin mucin-3 (Tim-3) and T regulatory (Treg) cell populations [43]. Oestrogen has been shown to increase production of antibody, IL4, IL10 and TGF-β. At high levels, such as in pregnancy, oestrogen inhibits T cells with the opposite effect at low level [44]. This explains why most autoimmune diseases go into remission during pregnancy and a similar phenomenon is observed in GD patients. Some patients even come off their anti-thyroid drug during pregnancy. Another explanation is likely due to suppression of the immune system in order to avoid rejecting the foetus through generation of specific regulatory T cells [45]. On the other hand, the postpartum period is well

known to be associated with GD onset or relapse [46]. Autoimmune diseases in males are characterized by acute inflammation, the appearance of autoantibodies, and a proinflammatory Th1 immune response whilst in female, these are associated with more with chronic, fibrotic Th2-mediated pathology and Th17 responses [47].

There is evidence of GD clustering in families suggesting there must be genetic susceptibility in these individuals. Although this is not an absolute risk factor but may collectively contribute towards the development of GD. Twin studies show that there is higher concordance of autoimmune thyroid disease (AITD) in monozygotic twins than dizygotic in which genetics have been suggested to explain up to 75% of the total phenotypic variance in GD [48-50]. Known genes that predispose patients to GD include human leucocyte antigen (*HLA*), cytotoxic T lymphocyte-associated 4 (*CTLA4*), forkhead box P3 (*FOXP3*), protein tyrosine phosphatase nonreceptor 22 (*PTPN22*) and the *TSHR* itself. Patients with GD express HLA-B8 more often than controls [51]. A North America study found that HLA-DRB1*08 and DRB3*0202 were associated with GD whilst DRB1*07 was protective [52]. This reflects the way the antigen being presented influences the autoimmune process. CTLA4 is expressed by activated T cells and transmits an inhibitory signal to T cells. CTLA4 is homologous to CD28 on T cells, and both molecules bind to CD80 and CD86 on antigen-presenting cells. CTLA-4 binds CD80 and CD86 with greater affinity than CD28. CTLA4 transmits an inhibitory signal to T cells whilst CD28 transmits a stimulatory signal [53]. An increase in frequency of the G (alanine) allele of CTLA-4 was seen in GD compared with control subjects (odds ratio = 1.58 corrected $P<0.0002$) [54]. FOXP3 is a regulatory factor for the development and function of Treg cells. Certain polymorphisms in *FOXP3* gene have been associated with GD [55, 56]. PTPN22 is involved in limiting the adaptive response to antigen by dephosphorylating and inactivating the T cell receptor (TCR). In lymphocytes, PTPN22 physically associates with CSK (c-Src kinase which is an important suppressor of the Src family kinases

that mediate TCR signalling). *TSHR* polymorphisms in the intron 1 gene region also have been shown to be associated with GD [57]. It is yet unknown how this region contributes to the susceptibility for GD but speculatively might be involved in generating TSHR splicing variant or microRNAs.

Multiple clinical studies support associations between cigarette smoking and both GD and GO. For example, Smoking carries a risk for GD with an odds ratio of 1.9 which can increase to 2.6 if the patient smokes more than 25 cigarettes per day [58, 59]. A meta-analysis from 8 studies showed an odds ratio for GD of 3.30 (95% CI, 2.09 to 5.22) among current smokers as compared with persons who had never smoked. In ex-smokers there was no significant excess risk of Graves' disease (OR=1.41, 95% CI: 0.77-2.58) [60] suggesting smoking cessation can reduce the risk of GD. A stronger correlation was noted with regard to the association of smoking with GO and will be discussed below. The proposed mechanism on how smoking contributes to the pathogenesis of GD include structural alterations in TRAB, making it more immunogenic, enhancement of immunologic responsiveness to factors responsible for the initiation of GD or impairment of tolerance to thyroid autoantigens [61].

Micro-organisms have long been thought to be implicated in GD, e.g. *Yersinia enterocolitica* has TSHR-like structures on its surface which have been suggested to trigger GD. This was elegantly demonstrated by Banga's work on murine monoclonal TSAB [62]. His group raised a germline precursor of TSAB which did not react with the TSHR, but instead binds the porins of *Yersinia enterocolitica*. The group also raised recombinant TSAB chimeras with heavy and light chain variable regions of mature TSAB. Only TSAB chimeras with a heavy chain recognizing the TSHR had TSHR stimulating properties. The data suggested early precursor B cells are expanded by *Yersinia enterocolitica* porins. These subsequently underwent somatic hypermutation to acquire a cross-reactive pathogenic response to TSHR. It also

showed the role of variable region of heavy chain in TSHR recognition.

Patients often reported stressful events prior to onset of GD. Using toxic nodular goitre as a control, Matos-Santos et al. has reported that there were higher stressful life events within 1 year prior to the GD onset [63]. Similar findings were reported by an Italian study [64]. Various drug treatments can induce GD. For example Interferon alpha treatment has been associated with autoimmune thyroid disease for both Hashimoto's thyroiditis and GD [65]. Between 10-30% multiple sclerosis (MS) patient on Alemtuzumab a monoclonal antibody against the T cell antigen CD52 developed GD. This will be discussed further below [66, 67].

1.9.3 Immune mechanism

There are several mechanisms known to be operated by our immune system in order for it to distinguish between self and foreign antigens and to make the decision between tolerance and immunity. One of the mechanisms is central tolerance by clonal deletion (reviewed in [68]). During lymphocyte development in the thymus or bone marrow for T and B lymphocytes respectively, cells that bind to self-MHC receptors are positively selected for maturation, those that do not die by apoptosis. Subsequently, these maturing lymphocytes are exposed to self-antigens presented by antigen presenting cells in these organs. Any cells that recognise self-antigens will be elimination or inactivated (anergy) before they develop into fully immunocompetent lymphocytes a process known as negative selection. Some of weakly self-recognizing T cells are not eliminated but differentiated into natural regulatory T cells (nTreg cells) which exert peripheral tolerance to any autoreactive T cells. Peripheral tolerance develops after T and B cells mature and enter the systemic circulation, peripheral tissues and lymph node [69]. Not all self-antigens are expressed in the thymus and bone marrow so additional mechanisms for tolerising autoreactive mature T and B

cells are necessary. In these cases, naive CD4+ helper T cells can be differentiated under influence of appropriate cytokines into induced Treg cells (iTreg cells). Peripheral deletion of CD4+ T cells seems to be dependent on signalling through Fas ligand and one of the molecular mechanisms responsible for inducing peripheral clonal anergy is signalling via CTLA4 molecule. There are different theories for breaking tolerance which include molecular mimicry resulting in cross-activation; epitope spreading- autoimmune responses to endogenous epitopes secondary to the release of self-antigens during an autoimmune/ inflammatory response; and bystander activation (adjuvant effect) [70].

There are various mechanisms that have been suggested as the means by which infections can initiate and/or exacerbate autoimmune diseases. One mechanism is molecular mimicry. This is where a foreign antigen shares sequence or structural similarities with self-antigens. This is then sufficient enough to result in the cross-activation of autoreactive T or B cells by that foreign-derived peptides. However current evidence for molecular mimicry in GD is very weak. Some GD sera have been found to interact with plasmid-encoded proteins of enteropathogenic *Yersinia enterocolitica* [71]. In Denmark discordant GD twin studies, GD twin has higher odds of prior *Yersinia enterocolitica* infection in this case measured by IgA or IgG towards *Yersinia enterocolitica* outer membrane protein [72]. Against this is the fact that the majority of patients who have had the infection do not develop GD.

Bystander activation as a mechanism leading to autoimmune disease has gained support through the use of experimental animal models such as for type 1 DM [73]. In this case local insult must have happened to thyroid follicular cells by any means (infections or immune attacks). This local reaction leads to inflammation, tissue damage, and the release of antigen/s (TSHR, IGF1R etc.) resulting in the re stimulation of resting autoreactive T cells. This is further supported by observation

that the normal thyroid gland does not express HLA class II molecules but in GD patients it does. This can be induced by viral infections of thyroid follicular cells, or it may be induced by cytokines such as IFN-γ produced by T cells [73]. Molecular mechanisms underlying breakdown of the immune-tolerance to TSHR are not fully understood.

1.9.4 In vivo models of GD

Most efforts have used TSHR-induced models in BALB/c mice and a wide range of GD and GO-like models have been described. Fibroblast transfected with full length TSHR with MHC class II molecule has been used successfully to induce GD in AKR/N mice [74]. Using chimeras of TSHR/ leutropin-choriogonadotropin receptor (LH-CGR), TBII but not TSAB was induced with TSHR lacking C-terminal part of ECD but not with the construct lacking N-terminal part [75]. Prabhakar's group later showed that immunization with TSHR ECD is sufficient to induce GD [76].

Whilst there were some successes in inducing GD, inducing GO has proven to be challenging. The first animal model with ocular changes suggestive of GO involved primed T cells transfer from BALB/c and NOD mice previously immunized with either TSHR extra cellular domain as a maltose-binding protein fusion (ECD-MBP) or by genetic immunization using cDNA for the full length human TSHR cloned into a eukaryotic expression vector [77, 78]. The latter was injected into muscle and assumed to be taken up by the muscle and expressed/presented on the cell surface. The T cells were further primed in vitro using ECD-MBP before being injected into the recipient mice. In approximately 20% of BALBc mice receiving TSHR primed cells the orbits appeared to have GO phenotypes. Different mouse strains exhibit different phenotypes when immunized with TSHR. In the BALBc mice, thyroid lymphocytic infiltration comprised B cells and immunoreactivity for IL-4 and IL-10 indicating

predominantly Th2 cell response. In contrast, in the NOD mice thyroids there were CD8+ T cells, and immunoreactivity for interferon gamma indicating Th1 response. None of the NOD recipients of primed and non-primed cells displayed GO. Unfortunately, the model could not be reproduced here in Cardiff despite using similar protocol, chow, housing and mice supplier [79] indicating that other factors, most likely the microbial environment, modulate the induced immune response. Recent progress has been made by Banga's group using in vivo electroporation of TSHR A-subunit plasmid into female BALB/c mice at 2 different locations. The group was able to reproduce functional antibodies to TSHR and antibodies to IGF-1 receptor α-subunit with GO histopathological evidence of adipogenesis, fibrosis, and muscle damage in both locations. In vivo MRI scans of mouse orbital region demonstrated evidence of orbital muscle hypertrophy and proptosis of the eye. Additionally, eyelid manifestations of chemosis, including congested and dilated orbital blood vessels, were apparent. Interestingly, there was no inflammatory infiltrate in orbital tissue suggesting "hit-and-run" immune-mediated inflammatory event [80, 81].

We can conclude from the animal models that TSAB can be generated with difficulty hence hyperthyroidism is rarely apparent. Since most researchers employ the human TSHR to induce disease, the sequence difference between the 2 species might explain this difficulty. One group has employed the adenovirus expressing mouse TSHR A subunit in wild-type BALB/c and B6 mice but failed to generate any TSHR antibodies even with Treg depletion [82] suggesting the difficulties in breaking mouse TSHR tolerance. However, the group managed to generate TSAB in TSHR KO BALB/c mice which further supports the concept that these mice were unable to develop central tolerance to the TSHR due to lack of thymic expression of the TSHR. As Graves-like hyperthyroidism cannot be expected to occur in TSHR KO mice, the same authors later performed adoptive transfer of splenocytes from the immunized TSHR KO mice to immunodeficient athymic nude BALB/c mice. This successfully

induced transient TSAB and hyperthyroidism (less than 4 weeks) in a small proportion of the mice (20%) and later was followed by development of TBAB and hypothyroidism. Interestingly macrophage infiltration was observed in the retrobulbar muscles and adipose tissues in 2 out of 9 mice which were TRAB positive but euthyroid throughout the experiments [83].

There is an induced human model of GD/GO which develops in multiple sclerosis patients treated with Alemtuzumab, a monoclonal antibody to CD52, resulting in elimination of >95% of circulating lymphocytes [66]. During immune reconstitution, B cells almost double but T cells at about 30-40% of pretreatment values. Approximately one third develop GD and a fifth of these have GO. GD patients displayed significantly higher CD8 lymphocyte counts 15-18 months later and lower memory: naive T cell ratio. Similar immune reconstitution phenomenon was noted from the report of three cases of GD after highly active antiretroviral therapy in patients with HIV infection [84]. These cases have given us a unique way of looking at mechanism of breakdown in self-tolerance in GD/GO.

1.9.5 Thyrotropin receptor (TSHR)

As mentioned above, the autoantigen in GD is the TSHR a member of the G protein coupled receptor family which in the thyroid signals mainly through Gs, although other cascades may also be involved. Virtually all patients with GD have TRAB indicating that TSHR probably is the most logical candidate autoantigen. TSHR belongs to a large family of G protein–coupled receptors and is encoded by 10 exons spread over 58 kilobases located on long (q) arm of chromosome 14 at position 31 (from base pair 80,954,989 to base pair 81,146,302) (Figure 4) [85, 86].

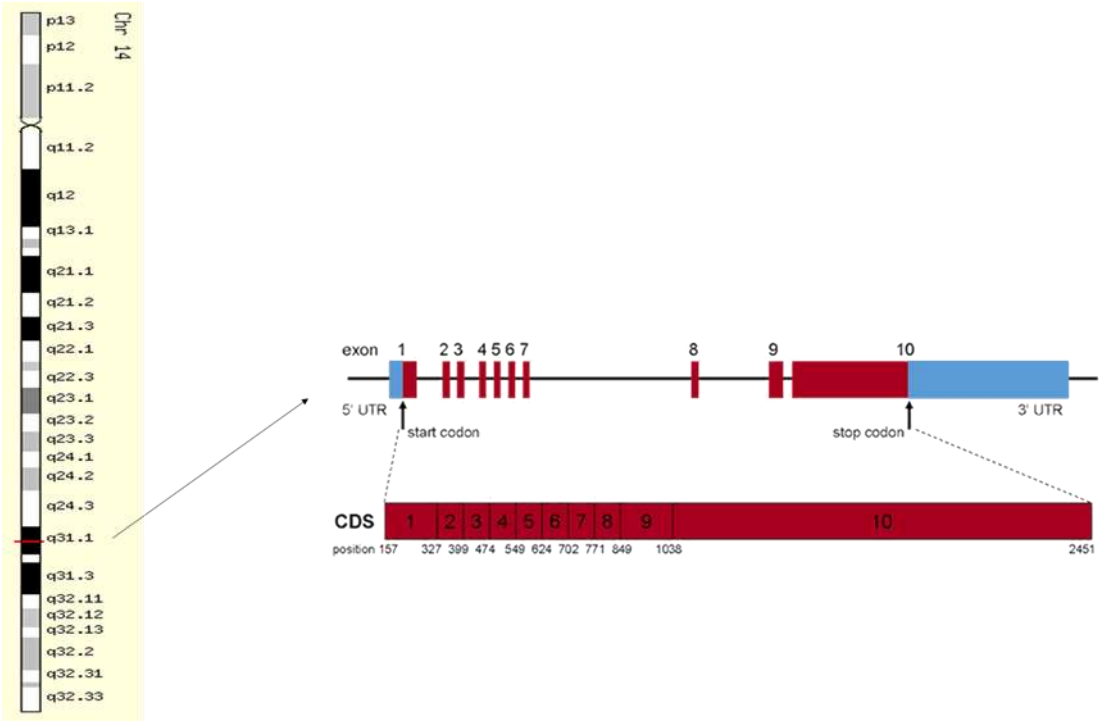

Figure 4: TSHR gene location on chromosome 14 at position q31.1 (left picture) and corresponding 10 exons and amino acid positions. Adapted from http://atlasgeneticsoncology.org/Genes/TSHRID290ch14q31.html

The TSHR expression is regulated by a TATA-less promoter containing binding sites for GABP (GA Binding protein- named due to the fact that it binds to DNA sequences rich in guanine and adenine) [87], TTF1 (Thyroid transcription factor-1) [88], CREB (cAMP-response element binding protein) [89], ATF2 (Activating Transcription Factor 2) [90], TR/RXR (Thyroid hormone receptor/retinoid X receptor) [91], SSBP (single strand binding protein) and ICER (inducible cAMP early repressor) [89] (Figure 5).

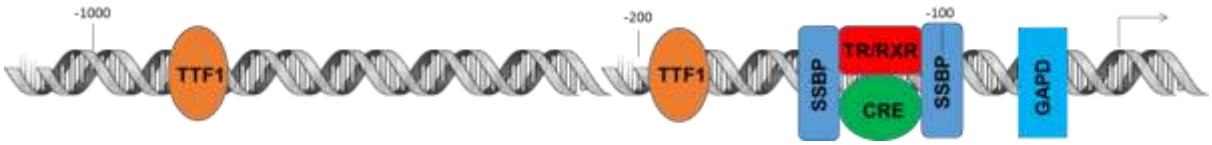

Figure 5: TSHR promoter with known regulatory elements with approximate locations. cAMP-response elements (CRE) is a constitutive enhancer and can be activated by CREB (CRE binding protein) or ATF2 (Activation Transcriptor 2) and repressed by ICER (inducible cAMP early repressor). This binding can be modulated by SSBP (single strand binding protein). TR (Thyroid hormone receptor) and RXR (retinoid X receptor) overlaps with CRE binding sites and can repress the TSHR transcription. There are 2 binding sites for TTF1 (Thyroid transcription factor-1). TTF1, TR, RXR are modulated by phosphorylation; GAPD is modulated by methylation and CRE is modulated by both. Modified from Garcia-Jimenez et al [92].

The TSHR gene codes for 764 amino acid protein consisting of seven transmembrane segments connected by three extra- and three intracellular loops. It contains two subunits; α/A subunit, corresponding to the extracellular domain (ECD) (residues 21-415) coded by first 9 exons plus the first 300 base pairs of exon 10 and, the β/B subunit, is mainly the transmembrane domain (TMD) (residues 416-764) encoded by the rest of exon 10 [90]. These A and B subunits are formed by sequential intermolecular cleavage by uncharacterized metalloprotease enzyme. This generates a C peptide of approximately 50 amino acids [93-95]. The intermolecular cleavage is almost complete in human thyroid tissue but full length uncleaved TSHR can be found on cell surface in L cells stably transfected with the TSHR receptor and also unprocessed mannose-rich monomeric precursor intracellularly [96]. The finding of high ratio of TSH B to A subunits (3:1) in thyroid membrane preparation suggests shedding phenomena of the TSHR A subunits [97] which can be found in the circulation [98]. The process is believed to be achieved by disulphide bridge break down by enzyme protein disulphide isomerase [99].

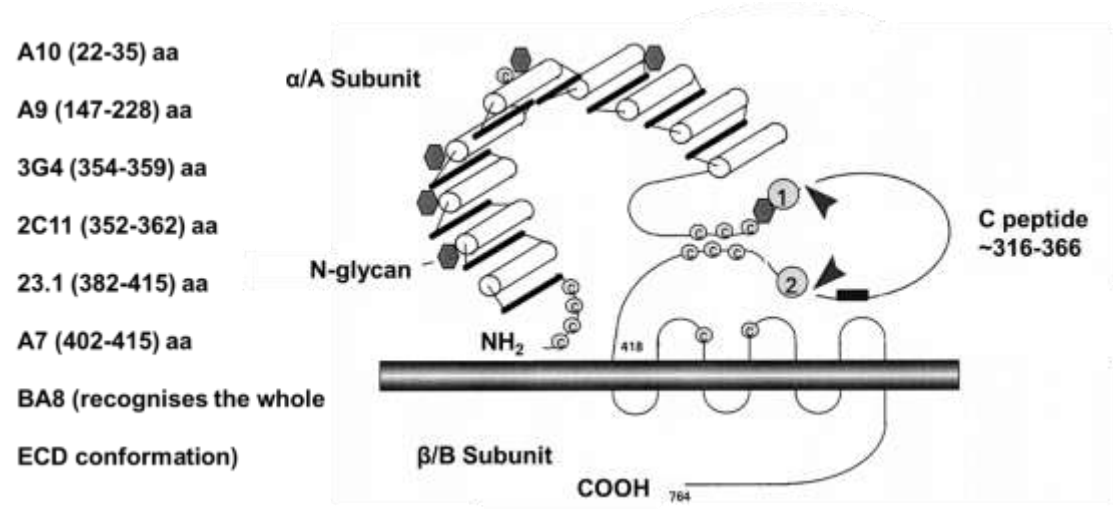

Figure 6: Schematic drawing of TSHR peptide anchored to the cell membrane by B subunit. The full length TSHR is derived from 21-764, extra cellular domain 21-415 amino acids with the first 20 amino acids as signal peptide. List of anti-TSHR antibodies with corresponding amino acid position (in brackets) in which the antibodies were raised. ECD = extracellular domain. Modified from Rapoport et al [100].

The Beta subunit of TSHR is constitutively active and the presence of TSH ECD [101] and interaction with trans membrane domain 6 [102] are critical for the maintenance of inactive state. TSHR binding sites have been studied through deletion-mutation analysis and antibodies panel (Figure 6) [103, 104]. These studies indicate that there are multiple discontinuous TSH binding regions mainly located in the A subunit and one segment (aa 381-385) for B subunits.

One of special features of TSHR is that it composed of two cysteine clusters flanking nine leucine-rich repeats (LRRs). The LRRs form a succession of β-strands and α-helices organized into a horseshoe-shaped structure. Each of LRR is made up of 20 ± 24 amino acids forming a β-strands followed by an α-helix [105]. These are arranged in such a way that β-strands form a concave surface of the horseshoe and α-helices form a convex surface of the receptor. It has been proposed that TSH interact with residues of the β-strands on the concave surface [105].

	LRR_1	LRR_2	LRR_3	LRR_4	LRR_5	LRR_6	LRR_7	LRR_8	LRR_9
X_1	**Q**55	**S**79	**T**104	**K**129	**F**154	**L**180	**D**203	**S**229	**K**250
X_2	**T**56	**R**80	**H**105	**F**130	**I**155	**T**181	**A**204	**L**230	**E**251
L									
X_3	**K**58	**Y**82	**E**107	**G**132	**E**157	**K**183	**Y**206	**D**232	**I**253
L									
X_4	**I**60	**S**84	**R**109	**F**134	**T**159	**Y**185	**N**208	**S**234	**R**255
X_5	**E**61	**I**85	**N**110	**N**135	**D**160	**N**186	**K**209	**Q**235	**N**256

Figure 7: Alignment of the β-strands of the nine LRRs of the TSHR ectodomain with the X residues are represented to better visualize the inner cusp of the ectodomain that putatively faces hormones and the possible interactions between side chains of these amino acids. Numbering starts from the first amino acid of the signal peptide of each receptor. Adapted from Smits et al [105].

The evidence that TSHR may exist in an oligomeric state is slowly gathering momentum and was initially provided by studies using antibodies [106] and more recently by fluorescence resonance energy transfer (FRET) technology [107]. The presence of dimerization influences TSHR behaviour. Unstimulated TSHRs has been shown to form oligomers [106] that return to the monomer state with TSH [108]. TSAB is proposed to favour formation of TSHR dimers whilst TSHR blocking antibodies, are unable to bring about this conformational change. After TSH binding, a constitutively oligomeric TSHR dissociates into active monomers (or dimers in TSAB binding case), which will be subsequently recruited to the lipid rafts to interact with G proteins thereby initiating the signalling cascade.

In the case of TSH, the signal is rapid and brief because of faster movement of monomers into the lipid rafts, in contrast to the retarded movement of the dimers. Multivalent blocking TSHR antibodies may cross-link the oligomers, thereby preventing them from dissociating and impeding their entry into lipid rafts [109].

The dominant monomer has been suggested to exert a negative effect on the

neighbouring monomer [110, 111]. On the other hand, if TSHR is present at low levels, it is less likely to form any kind of homo/heterodimer and so may activate different signalling cascades compared with cells undergoing adipogenesis where TSHRs are more abundant (will be described in more detail below). To add to the complexity, several TSHR variants (TSHR_v) have been described [112, 113] which lack the transmembrane domain and if expressed as protein would lead to soluble receptor products which could serve as TSH/TRAB binding proteins or even as autoantigens. NCBI describes two alternatively spliced variants, TSHR isoform 2 precursor (NM_001018036.1) and TSHR isoform 3 precursor (NM_001142626.1). According to NCBI (http://www.ncbi.nlm.nih.gov/ieb/research/acembly/) there are potentially 10 alternatively spliced variants, based upon cDNAs deposited in GenBank. These are derived from normal and neoplastic human tissues and cell lines. Currently, there is no evidence for protein expression of these splice variants. These will be discussed in more detail in chapter 4.

1.9.5.1 TSHR distribution

Initially thought to be thyroid specific, it is now clear that the TSHR is expressed in many other locations, predominantly adipose tissue. Several methodologies have been applied to investigate TSHR in fat including PCR, northern blot and functional studies. Using northern blot analysis and polymerase chain reaction, Cone et al have shown that TSHR mRNA was present in virtually all adipose tissue of the guinea pig but not in the retro orbital tissues [114]. This was later supported by in vitro study of human infant inguinal adipocytes obtained by collagenase digest. This showed the presence of TSHR in infant adipocytes [115] and that it is highly responsive to TSH and TSAB inducing lipolysis which can be blocked with blocking antibodies. Subsequently Feliciello et al were able to infer that TSHR transcripts are expressed in the human retro-orbital tissue [116] and was later confirmed by Crisp et al study by

northern blot analysis as 4.6 and 1.7kb transcripts [117]. The latter author also showed TSHR protein expression using immunohistochemistry [118]. TSHR expression was found to be increased during adipogenesis in rodents [119] and when human preadipocytes differentiate into mature adipocytes; indeed elevated TSHR expression in GO orbital fat is an indicator of ongoing adipogenesis [120]. The consensus is that in both rodents and humans, TSHR is expressed in any fat depot undergoing adipogenesis i.e. the lineage specific differentiation process in which new adipose cells are generated from mesenchymal stem cell precursors. Orbital fat derives from neural crest, unlike other adipose depots which originate in the mesoderm, consequently its regulation may differ from other depots as will be described later.

1.9.5.2 TSHR intracellular pathways

TSHR is known to activate mainly the Gs cAMP pathway but also activates several other G protein subtypes (Gi/o, Gαq/α11, and G12/13) [121, 122], non G protein pathways such as β-arrestin-1 [123] and other signalling pathways [124, 125]. Classically, upon TSH binding to TSHR there is an exchange of GDP for GTP bound to G-protein alpha-s subunits, followed by dissociation of the beta/gamma heterodimers. G-protein alpha-s in turn activates all isoforms of adenylate cyclase. After stimuli, adenylate cyclase increases levels of cAMP in the cell and activates Protein kinase, cAMP-dependent (PKA) inactive complex which results in PKA activation. The activated PKA phosphorylates multiple downstream target proteins one of which is cAMP responsive element binding protein (CREB) which will bind to its receptors on the promoter region of the DNA exerting various gene transcription processes including expression of thyroglobulin (TG), thyroid peroxidase (TPO), sodium iodide symporter (NIS), and the thyroid transcription factors TTF1/NKx2.1, TTF2/FoxE1, and PAX [126, 127]. Every intermediary in the pathway described above

may additionally interact with different molecules belonging to other pathways.

In human thyrocytes and rat FRTL-5, Gαq/α11 coupling stimulates Protein kinase C (PKC) pathways by generating phospholipase C (PLCβ). The PKC pathways has been associated with hyaluronan generation in GO [128]. The PKC pathways activation requires supraphysiological TSH concentrations [124, 129] although not all research agrees with this finding [130]. The PLC catalyses hydrolysis of phosphatidylinositols in the membrane yielding di-acyl-glycerol (DAG) and inositol tri phosphate (IP3) as second messengers. DAG directly stimulates PKC. IP3 increases cytosolic Ca+2 levels which act through a number of effectors including PKC itself [121, 131] and Nuclear factor of activated T-cells (NFAT) transcription factor protein. NFAT plays an important role on cytokine gene transcription regulation [132]. Calcium via calmodulin –a calcium sensor protein activates the serine/threonine phosphatase calcineurin (inhibited by ciclosporin and FK506). This in turn rapidly dephosphorylates NFAT proteins, resulting in a conformational change that exposes a nuclear localization signal leading to NFAT nuclear import [133]. In thyroid, the PLC-IP3-DAG pathway controls thyroid hormone production by activating production of H_2O_2 and subsequent iodination of thyroglobulin for thyroid hormone synthesis [134].

TSHR may also couple to Gαi1, which inhibits adenylyl cyclase and decrease cAMP levels whilst Gβγ dimers may induce multitudes of other pathways which include adenylyl cyclases [135], PI3K/AKT (PKB)-FOXO [136] and PLC [137] pathways.

1.9.6 Extra thyroidal manifestations of GD

GD also can be uniquely identified in clinical settings by its extra thyroidal manifestations. They are thyroid acropachy or clubbing, pretibial myxoedema and orbitopathy also known as Graves' orbitopathy (GO).

1.9.6.1 Thyroid acropachy

Thyroid acropachy is the least common manifestation of GD and characterized by digital clubbing, soft-tissue swelling of the hands and feet, and periosteal reaction with new bone formation. Rarely this can affect the midportion of the diaphysis of the phalanx and femur [138]. Its presence is normally associated with pretibial myxoedema and orbitopathy. It develops chronologically after the GD and GO onset. The skin can be pigmented and hyperkeratotic. It is often painless but some patients may have pain due to severe swelling [138]. It has similar pathological characteristic those of pretibial myxoedema [139].

1.9.6.2 Pretibial myxoedema

Pretibial myxoedema is also a rare manifestation of GD. It occurs in approximately 1.5% of GD and 6% of GO patients [140, 141]. It is also called localized myxoedema or thyroid dermopathy. Although commonly located in the pretibial area, it has been described in other locations including feet, nasal bridge [142] and traumatic areas such as shoulders [143] and surgical scars [144]. Histologically, skin biopsy shows a large amount of glycosaminoglycans especially hyaluronan in the dermis but not epidermis with some mononuclear cell infiltration and hyperkeratosis [145].

Clinically it is characterized by bilateral, asymmetric, non-pitting scaly thickening of the skin as one or a few well-demarcated papules or nodules. The pretibial myxoedema is usually asymptomatic but some patients might complain of itchiness or even pain. It takes several months for the lesion to develop before stabilizing. In some cases, it can regress spontaneously. In the worst case scenario it can develop into elephantiasis type of limbs [140]. The diagnosis of pretibial myxoedema is based upon the history and the characteristic appearance of the skin lesion; biopsy is rarely needed unless the diagnosis is uncertain.

The indications for treatment include pruritus, local discomfort, or for cosmetic reasons. As per management of GO, normalization of thyroid function is needed by means of anti-thyroid drug or surgery. RAI is feared to worsen the myxoedema due to higher TRAB titre following the treatment. Smoking cessation and losing weight are also highly recommended. Nightly topical application of corticosteroids is the preferred initial treatment. For those who are not responding intralesional injections of triamcinolone acetonide has been tried with success in a small case series [146]. In elephantiasic form the use of compressive stocking has been found beneficial [147]. Some have recommended complete decompressive physiotherapy [148].

1.10 Graves' orbitopathy

Graves' orbitopathy (GO), also known as thyroid eye disease (TED) usually occurs in people with Graves' disease. GO is a rare condition having an incidence of approximately 10-16 per million per year with the estimated prevalence of 2-4/10,000 [149]. Approximately 25-50% of GD patients will have GO with the majority of patients presenting with concurrent thyrotoxicosis.

1.10.1 Clinical manifestations of GO

Most of the signs and symptoms of GO are a direct consequence of expansion of intraorbital volume and the majority of patients present concomitantly with thyrotoxicosis. In about 20 percent of patients, GO precedes the onset of thyrotoxicosis by a number of months. Rarely the onset of GO and thyrotoxicosis can be separated by several years [150, 151]. In its mildest form GO causes irritation of the eye with excessive tearing, discomfort, and redness of the conjunctiva. Some symptoms are related to corneal exposure secondary to lid retraction or proptosis such as dry eyes, grittiness and photophobia. Most of these will be mistakenly treated for other conditions such as viral conjunctivitis or allergic reaction leading to a delay in treatment. All GD patients should be reminded about the possibility of eye disease and to be aware of these salient symptoms and also to remind their health professionals about this possibility. Even in its mildest form, GO can greatly interfere with the activity of daily life. Rarely, patient can present with severe eye disease with double vision and protrusion of the eyes and in 3-5% of cases this may lead to sight loss [26, 152]. Patients may complain of retro orbital pain on eye movements from swollen and inflamed retro orbital contents. In terms of double vision or diplopia, the symptoms could range from a mild form i.e. occurs only when the patient is tired to disabling constant double vision. In addition most patients with GO have reduced

quality of life [153] and suffer long-term psychological distress due to the disfiguring appearance resulting from the eye ball protrusion [154], an effect that is often underestimated by health care professionals.

GO signs are mainly related to orbital tissues inflammatory processes and oedema. At early stages, there could be evidence of periorbital soft tissue involvement such as conjunctival and periorbital erythema and/or oedema. This could extend to caruncle and plica inflammation. The periorbital oedema was thought to reflect decreased venous drainage due to vascular compression within the orbital space [155]. Eyelid retraction is the commonest sign of GO [156] and may be present on the primary gaze (Dalrymple's sign) or subtly during down ward gaze also known as lid lag (Von Graefe's sign). The phenomenon is primarily due to sympathetic hyperactivity of the levator and/or Muller's muscle [157] in the thyrotoxic state and levator hypertrophy and fibrosis at later stages [158] . Proptosis although unsightly is a natural process in an attempt to decompress the retroorbital content of an orbit. This is to protect the optic nerve but at the expense of exposure keratitis. Although this is a characteristic finding of GO, it is not always present and does not correlate with disease severity especially in elderly patients with enlarged muscles at the orbital apex. In the absence of proptosis, inflamed swollen retroorbital content can compress the optic nerve leading to dysthyroid optic neuropathy (DON). Any reduction of visual acuity, reduced colour perception, relative afferent pupil defect (RAPD) and/or visual field defect signs in GD patient should be treated as potential DON until proven otherwise. There will be evidence of restrictive diplopia which develops due to extraocular muscle oedema and/or fibrosis. This tends to affect inferior and medial rectus muscles. Of note, younger patients tend to have orbital fat expansion whereas older patients tend to have extraocular muscles swelling causing diplopia/DON in the absence of proptosis [159].

GO has a natural history first described by Rundle [160] where he did sequential measurements in untreated GO patients. After an initial rapid dynamic phase which usually lasts for 6 months but rarely can last more than 1 year [161], the disease continues to get worse until it reaches a point of maximum severity, and this is followed by a slow decrease in severity until it reaches a static/inactive plateau phase that is improved but not resolved to the baseline condition. Unfortunately approximately 50% of the patient will be left with the obvious signs of GO in the inactive phase [162]. The duration of the natural history is highly variable (from months to years) and unpredictable with some patients progressing whilst others regress or remain unchanged [163].

1.10.2 Clinical diagnosis and investigations

Clinical diagnosis of GO is largely based on history and typical findings of ocular examination. However, all patients should have baseline thyroid function test with TSH receptor antibody. Clinical evaluation should be thorough and to include visual acuity examination (LogMAR chart), relative afferent pupil defect (RAPD), colour vision (HRR or Ishihara plates), eyelid retraction, palpebral aperture (including lagophthalmos and Bell's phenomenon), motility assessment, corneal/optic disc assessment and measurement of intraocular pressure. Photographs can help documenting the change of appearances. Proptosis should be measured in standardized way ideally with the same Hertel exophthalmometer and fixed intercanthal distance. The GO should then be graded for activity using clinical activity score (CAS) and severity into mild, moderate to severe or sight-threatening to facilitate management decisions [164].

Computed tomography or magnetic resonance imaging of the orbits is indicated if there is any uncertainty about the cause of orbitopathy particularly in a patient with

unilateral proptosis. The differential diagnosis includes orbital cellulitis, orbital myositis and orbital inflammatory syndrome (also known as orbital pseudotumor). Patient with cellulitis will have evidence of infection such as fever and an increase in inflammatory markers. Extra ocular muscle tendons are involved in orbital myositis. Isolated enlargement of rectus muscle together with very rapid disease progression are suggestive of orbital pseudotumor rather than GO. Other rare differentials to include are orbital tumour, carotid artery cavernous sinus fistulas, acromegaly and other causes of infiltrative disease such as metastases, sarcoidosis, lymphoma and amyloidosis.

1.10.3 Risk factors

Current smoking, rather than lifetime exposure, is the strongest risk factor for developing GO [165-167]. Odds ratios as high as 20.2 for current smokers and 8.9 for combined current smokers and ex-smokers have been reported [168]. In general, GD patients who smoke are approximately 5 times more likely to develop GO than non-smokers [166, 169, 170]. Smokers tend to have more severe disease than non-smokers [166]. There is evidence for a dose-response relationship between smoking and the severity of GO [166, 169]. These patients responded poorly/delayed to treatment [171] especially after radioiodine therapy [172]. Passive smoking has also been indirectly linked to a higher GO prevalence in childhood GO (under 10 years old) [173]. In vitro studies have demonstrated that cigarette extract can increase the biological processes which underpin GO, i.e. adipogenesis and overproduction of hyaluronan (HA) [174]. Smoking also exerts other effects including changing the composition of tears [175], increasing IL-6 receptors [176], and HLA-DR expression on orbital fibroblasts [177]. GO is 3-6 times more common in women than men [156, 178] although men tend to have more severe disease this more likely confounded by the higher smoking rate in men [178]. Radioiodine treatment also has been

associated with risk of developing GO in the order of 15-30% [172, 179, 180]. This is probably due to thyroid follicular cell destruction and the release of the auto antigens, T cell activation, higher and prolonged TRAB antibodies [181] and an increase in serum inflammatory cytokines [182]. Thyroid dysfunction, and more so hypothyroidism [183] than hyperthyroidism, has been associated with an increased risk for severe GO with an odds ratio of 2.8 [184].

1.10.4 Genetics of GO

Genetic factors are important for some diseases, but in GO they are not absolute predisposition factors. The current dogma of the development of GO depends on complex interactions between genetic, environmental, and endogenous factors. The search for genetic susceptibility loci in GO has so far been disappointing and not to justify genetic testing to guide preventative strategies or therapy.

In GO, significant associations between exophthalmos and/or soft tissue changes were found with HLA DR3 with relative risk of approximately 3.7. These patients were found to be more resistant to radioiodine therapy than patients negative for these antigens [185]. Weetman et al. tested the possible association of HLA-DQB and HLA-DPB alleles with GD, with or without severe orbitopathy, by PCR of genomic DNA and allele-specific oligonucleotide probing. HLA-DPB 2.1/8 was found to be less prevalent in GO patients (2.5%) than in non-GO patients (20.8%) or controls (30%), albeit the GO protective effect of this HLA-DPB allele is weak [186].

Cytotoxic T lymphocyte antigen-4 (CTLA-4) is expressed on activated T cells. It binds to B7 present on APCs and functions as a negative regulator of T cell activation. CTLA4 gene is located on chromosome 2q33 [187]. The polymorphism in the CTLA-4 gene (A/G at codon 17) in GO confers a risk to GO as the strength of the association of the G allele with GO increases with the severity of GO with odds ratio up to 3.06

(p=0.01) for most severe GO. This was independent of male sex, smoking status, or previous radioiodine treatment. This is not specific for GO as it is found in other autoimmune conditions but rather confers a risk for autoimmune disease in general.

Lastly, polymorphisms in the IL23 receptor (IL-23R) gene are found to be associated with GO [188]. IL-23 is known to promote sustained cellular immunity by promoting survival and cytokine production (e.g. IFN-γ) of Th1 memory cells [188]. It is also a survival factor for the Th17 subset, recently identified as major effectors of autoimmune tissue damage [189]. Yet again, it is also found in other autoimmune conditions such as rheumatoid arthritis [190] and Crohn's disease [191]; it also hints at an important role for the innate immune system in autoimmune conditions including GO. However, none of these studies yield any confirmed susceptibility loci for GO because the various polymorphism data were found either to be weak or non-specific.

1.10.5 Treatments

For the majority of patients with mild disease the treatment is mainly supportive with ocular lubrication and oral selenium treatment [192]. Oral nonsteroidal anti-inflammatory agents (NSAIDs) may be considered. Patients should be advised to stop smoking and the disease symptoms and signs tend to resolve as thyroid function normalises. Rehabilitative surgery (Müllerectomy or blepharoplasty) can be offered once the disease becomes inactive and stable.

Current treatments for moderate to severe GO rely heavily on major immunosuppressive therapies. Glucocorticoids are the mainstay of treatment and used initially to suppress acute inflammatory changes. These are effective when given at an early active phase of the disease. They also have beneficial effect on soft tissue swelling, ocular motility and visual acuity but a limited effect on proptosis [193]. Although numerous different oral and parenteral regimes have been reported, high-

dose intravenous (IV) glucocorticoid pulses are superior to oral with response rates of about 80% compared to 60% for the oral route and significantly fewer adverse events than with oral glucocorticoid [194]. The morbidity and mortality of IV glucocorticoid therapy are around 6.5 and 0.6% respectively [193, 195]. These can be avoided by keeping the cumulative dose less than 8 grams in one course of therapy [196]. Other second-line immunosuppressive agents have been used with or without glucocorticoids with varying effects. However, the routine use of such drugs in the management of severe TED has been limited by fears about their potential toxicity.

The immune modulator rituximab, which is a chimeric mouse-human monoclonal antibody directed against the CD20 antigen on B lymphocytes, has been trialed in GO. The CD20 antigen presents on pre and mature B cells but not stem cells, B-cell precursors and antibody-producing plasma cells. Results were conflicting with Marius Stan and colleagues reporting that that there were no differences against the placebo with patients' clinical activity score and their secondary outcomes which included quality of life scores [197]. Mario Salvi's group described considerable improvement in their primary outcome measured which was clinical activity score and also secondary outcomes including eye motility, GO-QOL assessment, and the reduced number of surgical procedures in patients after rituximab treatment even at lower dose [198]. The reasons for this disagreement are unclear but may be related to the differences in the study designs and patient selection (The duration of GO was less than 6 months in Salvi's group compared to 1 year in the Stan's group).

Orbital radiotherapy given at cumulative dose of 20Gy per orbit is particularly useful in improving diplopia [199, 200]. Combinations of cyclosporine and glucocorticoids have been shown to achieve a better initial treatment response than either agent alone [201, 202]. Azathioprine (AZT) has not been shown to be of benefit as a single

[203] agent but the outcome of the multicentre CIRTED study, which has combined radiotherapy and/or AZT with the steroid is currently awaited [204]. Other unproven or being developed treatments includes IV immunoglobulins [205, 206], etanercept (anti-TNF) [207], somatostatin analogues [208, 209], Teprotumumab (IGF-1 receptor antagonist antibodies, NCT01868997), TSH-R-blocking antibodies and small-molecule-ligand antagonists [210].

Most patients with GO have mild disease which improves spontaneously and do not require corrective surgery. Surgical decompression is usually reserved for inactive GO but rarely has to be performed due to sight threatening GO unresponsive to medical treatment. This is normally followed by a rehabilitative surgery at a later stage.

1.10.6 Target Autoantigens in GO

1.10.6.1 TSHR as an autoantigen

TSHR was discussed in detail in previous sections and will be further described in Chapter 4. TSAB levels are associated with GO prevalence and severity [211-214] but TBII correlate only with GD and the hyperthyroid state but not GO [212, 213]. However, there are recent data showing close correlation between TSAB and to a lesser extent TBII with both activity and severity of GO [215, 216]. In terms of response to treatment, persistent elevation of both TBII and TSAB has been associated with non-response to treatment for GD [39] suggesting a role for TSHR autoantibodies in disease activity and its maintenance. This last study indicated that GD patients who relapses are most likely to develop GO. The lack of consistency with regard to TBII assays more likely reflects the mixture of stimulating and blocking

antibodies, thus studies showing an association with GO might have studied samples in which TSAB predominate and vice versa.

However, the fact that not all GO patients have TSAB and may even be euthyroid or hypothyroid has prompted people to seek other explanations. Work from our group [217] demonstrated 'neutral' TSHR antibodies able to bind but having no effect on known TSHR signalling. Indeed TSHR signalling may be far more complex than initially thought (reviewed by Latif et al [218]). Little is known about the effects of TSHR activation at various stages during differentiation from pre to mature adipocyte (see below) and the cascades stimulated will depend on the types and abundance of G proteins available in the cell [219]. As described above, G protein coupled receptors (GPCR) also can exist as monomers or oligomers. Oligomerization is the term used to describe dimeric, tetrameric, or higher-order complexes between GPCR monomers [220]. The activation of different GPCR complexes will have major influence on subsequent G protein signalling pathways. TSHR is generally found at low abundance in extra thyroidal tissue but during adipogenesis TSHR levels were found to increase [118].

1.10.6.2 Insulin like growth factor-1 receptor (IGF1R)

Others have searched for additional autoantigenic targets; the IGF1R was first proposed by Weightman and colleagues who demonstrated high affinity IGF1 binding sites on orbital fibroblasts [221]. More recently extensive work from Terry Smith and his colleagues has confirmed this finding and further showed that TSHR and IGF1R co-localize to orbital cell membranes [222]. TSH induced ERK phosphorylation can be blocked by an IGF-1R-blocking monoclonal antibody suggesting that IGF-1R might mediate some TSH-provoked signalling. This group are conducting a large scale trial to evaluate a monoclonal antibody which blocks IGF1R in GO

(https://clinicaltrials.gov/ct2/show/NCT01868997).

Efforts to demonstrate autoantibodies to the IGF1R have had mixed success. Minich et al used GO patients sera and purified IgG for IGF1R binding and concluded that IGF1R autoantibodies exist but with similar prevalence (approximately 10%) between normal and GO [223]. They also found that this IgG are antagonist in nature and concluded that anti-IGF-IR antibodies are uninvolved in the pathogenesis of GO. Whilst Varewijck et al [224] suggested that in subset of GO patients with high TBII, IGF-IR stimulating activity is increased with age. Neumann & Gershengorn propose that cross-talk between the TSHR and IGF1R, rather than direct IGF1R activation, might stimulate the tissue remodelling [225].

1.10.6.3 Thyroglobulin

Thyroglobulin (TG) is produced by thyroid follicular cells, is the substrate for thyroid hormones and the first thyroid autoantigen described. Rodents immunized with TG develop thyroiditis and sera from some patients with thyroid disease contain antibodies which bind to TG in immunohistochemical analysis using thyroid slices. TG is a 660 kDa, dimeric protein encoded by a gene located on the long arm of chromosome 8 [226]. TG production is controlled by TSH, it is secreted and stored in the follicular lumen as colloid.

In the 1970's, Joseph P. Kriss postulated that thyroidal TG is transported to the orbital tissues through the lymphatic system via veins in the inferior orbital fissure and then initiates the inflammatory processes leading to GO [227]. The same group also provided evidence for TG/anti-TG immune complexes in the orbit [228].The TG hypothesis was modified by reports that it shares antigenic epitopes with acetylcholinesterase – an abundant enzyme in the highly innervated orbital muscles [229]. More recently, Marino et al. demonstrated that TG is present in the orbit;

furthermore it is iodinated suggesting that it is the product of the thyroid gland [230, 231]. The significance of these findings is unclear since GO patients do not have particularly elevated anti-TG antibody titres and patients with Hashimoto's thyroiditis generally do not have evidence of GO.

1.10.6.4 Thyroid peroxidase

Thyroid peroxidase (TPO) is the second major thyroid autoantigen, previously known as the microsomal antigen, with TPO antibodies being a feature of destructive thyroiditis [232]. The 110kD protein is encoded by a gene on chromosome 2 comprising 17 exons, its expression is controlled by TSH; TPO has similarity with myeloperoxidase. TPO antibodies are present in almost all Hashimoto's patients but only in 50% of those with GD. Lai et al. have demonstrated significantly higher levels of TPO messenger ribonucleic acid (mRNA) and protein in orbital fat tissue of GO compared to normal subjects [233]. As far as we are aware, this is the only evidence to suggest that TPO has a role in GO, in fact the absence of TPO autoantibodies has been reported in various studies in GO.

1.10.6.5 Other candidate antigens

Other potential candidate antigens are G2S proteins (55 kDa fragment of the FOX-P1 transcription factor), non-tissue-specific membrane protein called D1 (64 kDa) and calsequestrin (63 kDa), a calcium-binding protein localized in the sarcoplasmic reticulum of the skeletal muscle fibre [234-236]. Skeletal muscle and cardiac calsequestrins are encoded by *CASQ1* and *CASQ2* gene respectively [237]. It is interesting to see from microarray data, that *CASQ2* gene is up-regulated (confirmed with QPCR) in the GD thyroid from patients with GO (relative to those without eye disease) while genes encoding TG, TPO and TSHR were not differentially expressed

[238]. It is proposed that *CASQ2* gene upregulation may generate production of autoantibodies in the thyroid and sensitized T-lymphocytes, which cross-react with calsequestrin in the extraocular muscle of patients who develop orbitopathy.

1.10.7 Tissue Remodelling in GO

As mentioned above, expansion of tissues in the orbit causes proptosis; the two main mechanisms in operation are overproduction of extracellular matrix (ECM) components, especially hyaluronan (HA) and excess adipogenesis.

Adipogenesis is a process in which preadipocytes differentiate into mature adipose tissues (see Figure 8). Most of our current understanding of adipogenesis has been derived using the murine 3T3L1 cell line. Although 3T3L1 cell lines can spontaneously differentiate into adipocytes when maintained in a high concentration of foetal calf serum, this normally takes weeks but the process can be accelerated by employing adipogenic cocktails containing high concentrations of insulin, glucocorticoids and 3-isobutyl-1-methylxanthine (IBMX). Additional components may also be included in the differentiation mix including PPARγ agonists such as pioglitazone, triiodothyronine, biotin, pantothenate and indomethacin. Insulin is known to mimic insulin-like growth factor-1 and activates MAP (mitogen-activated protein kinase pathways) [239] and PI3 kinase pathways [240]. Phosphorylation of Akt in turn phosphorylates the inhibitory transcription factor FOXO1 causing it to exit from the nucleus leading to increase adipogenic genes transcription. Glucocorticoids induce expression of C/EBP-δ (early adipogenic gene) which in turn contributes to an increase in PPAR-γ expression and production of prostacyclin which increases intracellular cAMP [241, 242]. IBMX is a nonselective phosphodiesterase inhibitor which raises intracellular cAMP and protein kinase A (PKA) which is required for transcriptional activation of PPARγ [243]. PPARγ transcript levels then increase followed by heterodimer complex

formation with the retinoic X receptor (RXR) with subsequent increase in adipogenesis related genes transcription. PPARγ is known as the master regulator of adipogenesis. It is a transcription factor and encoded by the PPARγ gene. The human PPARγ gene has nine exons. Alternate splicing and alternate transcription start sites generate the PPARγ1 and PPARγ2 mRNAs, which differ at their 5'-ends. PPARγ1 is encoded by eight exons, and PPARγ2 is encoded by seven exons with six common exons 1 to 6 [244]. The two isoforms of PPARγ are detected in the human: PPARγ1 (found in nearly all tissues except muscle) and PPARγ2 (mostly found in adipose tissue and the intestine).

Primary cells are more challenging to differentiate but the information gathered is more relevant. In the orbit, Thy-1 negative [245] fibroblasts can be induced to differentiate when cultured in appropriate adipogenic medium [246] whereas Thy1 positive cells are more likely to undergo differentiation to myofibroblasts and cause fibrosis. Adipogenesis contributes to orbital expansion because a fibroblast has a diameter of 30 microns but that of a mature adipocyte is 150 microns, as mentioned above, during differentiation expression of the target antigen TSHR is increased.

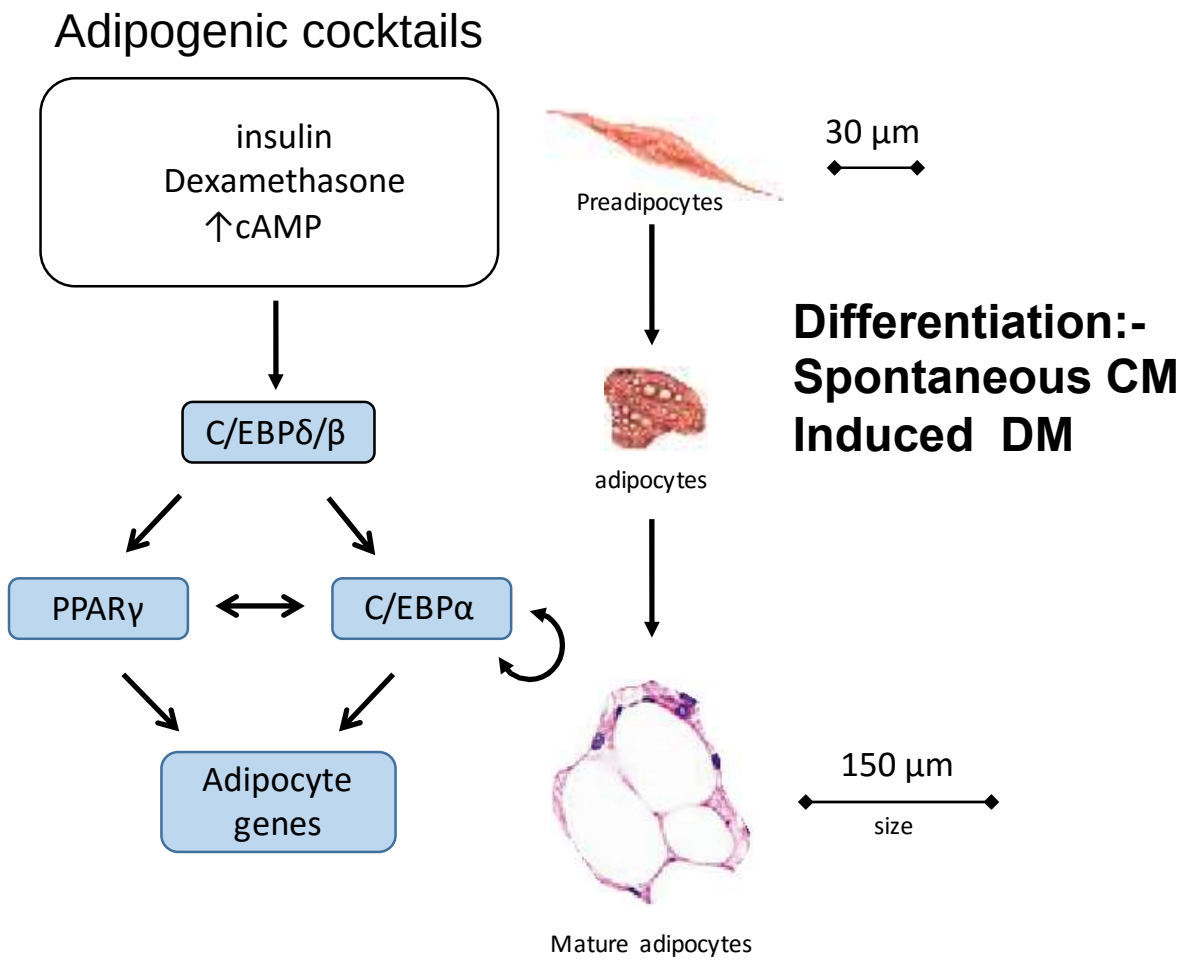

Figure 8: Stages of adipocyte differentiation. Preadipocytes can undergo spontaneous differentiation in culture medium (CM) or the process can be accelerated by differentiation medium (DM) containing insulin, dexamethasone and cyclic adenosine monophosphate (cAMP). The process contributes to orbital expansion as a fibroblast has a diameter of 30 microns but a mature adipocyte is 150 microns. The Transcription factor cascade is depicted on the left side of the diagram. The initial adipogenic induction rapidly induces expression of the CAAT/enhancer-binding proteins (C/EBPs) C/EBPδ and β. These in turn induces peroxisome proliferator-activated receptor-γ (PPAR-γ) and C/EBPα genes activation which are the key transcriptional regulators of adipocyte differentiation. PPARγ activates the promoter of C/EBPα and vice versa. Also C/EBPα has a stimulatory effect on itself creating a positive-feedback loop which in turn feeds into adipocytes related gene induction (see text for more detail).

1.10.7.1 Adipogenesis regulation by TSAB

Several research groups have addressed this issue but with varying responses because 1) they have not studied the same cell populations 2) have employed different culture conditions 3) used a variety of methods to activate the TSHR.

Zhang et al have shown that activation of TSHR in human orbital OF can stimulate the early stages of adipogenesis [247]. The studies were performed by introducing an activating mutant TSHR into OF using viral vectors. The mutants used were L629F and M453T, which previously have been reported in two newborns with non-autoimmune hyperthyroidism and proptosis [248, 249] and are similar (but not identical) to TSAB activation. Using cultured mouse embryonic stem cells, Lu et al showed that TSH can stimulate adipogenesis, even in the absence of adipogenic factors, suggesting that TSHR activation can initiate the early lineage commitment process [250]. The same study also showed that TSH can enhance adipogenesis in the presence of adipogenic cocktails (Insulin, T3 and PPARγ). Human monoclonal TSAB (M22) is able to interact with TSHR via both cAMP/pI3K pathways in Fisher Rat Thyroid cell Line (FRTL-5) [38]. Rebecca Bahn's group have investigated M22 effects in human OF and reported that they are able to enhance their differentiation into adipocytes partly via the PI3K signalling cascade, i.e. it mimics the action of insulin [251]. Of interest the patient from whom M22 was derived did not have GO.

1.10.7.2 Over-production of ECM

In GO, the over-production the GAGs particularly HA in the orbital adipose tissue and extraocular muscle leads to oedema with consequent proptosis and diplopia respectively. Several extracellular matrix (ECM) components are overproduced in GO including collagens and glycosaminoglycans (GAGs). GAGs can be classified into four groups: chondroitin/dermatan, heparin/heparan, keratan and hyaluronic acid

(HA) (Table 7).

Table 7: Classes of GAGs and their disaccharide building blocks

Class	Disaccharide	U	H	Modifications
Hyaluronic acid	$GlcA_{(\beta1,3)}$ $H_{NAc\ (\beta1,4)}$	GlcA	Glucosamine	None
Heparin/heparan	$U_{2X\ (\alpha/\beta1,4)}$ $H_{NY,3X,6X\ (\alpha1,4)}$	IdoA/GlcA	Glucosamine	X – sulfated Y – acetylated/ sulfated
Chondroitin/ dermatan	$U_{2X\ (\alpha/\beta1,3)}$ $H_{NAc,4X,6X\ (\beta1,4)}$	IdoA/GlcA	Galactosamine	X – sulfated
Keratan	$Gal_{6X\ (\beta1,4)}$ $H_{NAc,6X\ (\beta1,3)}$	Gal	Glucosamine	X – sulfated

The abbreviations used: α-l-iduronic acid, IdoA or I; α-d-glucuronic acid, GlcA or G; U is uronic sugars, H is either α/β-d-glucosamine (GlcNAc) or β-d-galactosamine (GalNAc) depending on the GAG class; β-d-galactose, Gal; Acetylation (COCH3) is indicated using Ac and sulfation (SO3) using S. Adapted from Sasisekharan et al [252].

These differ in their disaccharide building blocks; uronic sugars (glucuronic acid or iduronic acid) or galactose; sulfation and/or acetylation. The GAGs are synthesised by the Golgi apparatus except HA which is produced by integral membrane synthases and immediately secreted as the disaccharide chain elongates. HA is the only non-sulfated form of the GAGs and is a major contributor to GO orbital expansion as it is able to absorb up to 1000x its weight in water. HA is generated by 3 HA synthetase (HAS) enzymes and broken down by hyaluronidases. The 3 HAS isoforms each

possess distinct activities and produce HA molecules of differing length [253]; HAS1 (has tissue specific expression [254]), HAS2 (proinflammatory and inducible [255]) and HAS3 isoform which is associated with a resting, non-pathological phenotype and present in most cell types [256].

Hyaluronidases break down HA via degradation of the β-N-acetyl-D-glucosaminidic linkages in the HA polymer. There are currently six hyaluronidases genes known to be present in the human genome in 2 clusters of triplicates (Figure 9): *HYAL-1, -2* and *-3* genes are clustered in the chromosome 3p21.3 locus (found to be expressed in human orbital OFs and increased by the activation of TSHR and hyaluronidase 3 was increased by IGF1R [257]) and *HYAL-4, HYAL-P1* (which is a pseudogene: transcribed but not translated) and *PH20* (encodes sperm hyaluronidases necessary for fertilisation) in the chromosome 7q31.3 locus [258]. HYAL-1, -2 and -3 are considered acidic type as these are maximally active at acidic pH [259] whilst PH20 is has maximal activity at neutral pH [260]. HYAL-1 and HYAL-2 are the two major hyaluronidases for the degradation of HA. HYAL-1 can degrade high molecular weight HA down to small oligomers (tetrasaccharides) whilst HYAL-2 able to degrade HA to an approximately 20 kDa product (approximately 25 disaccharide units) [261]. Little is known about HYAL-3 and 4.

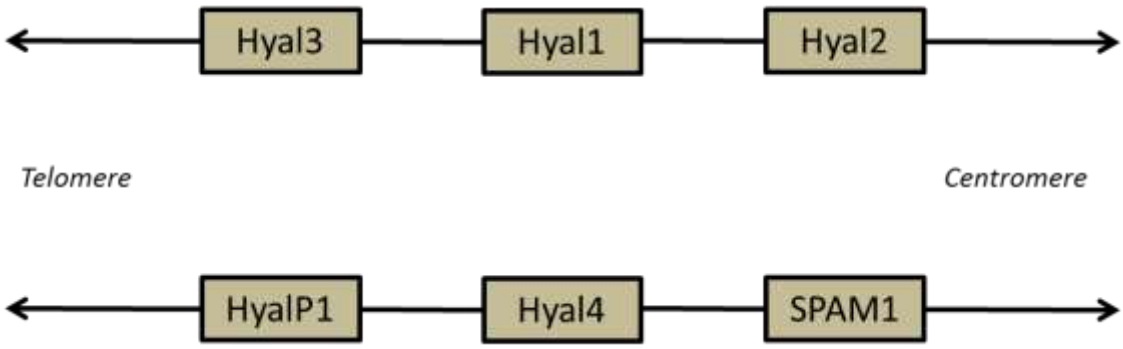

Figure 9: Chromosomal orientation of the six hyaluronidase genes at their two respective chromosomal sites in triplicates. Modified from Csoka et al [258].

1.10.7.3 ECM regulation by TSAB

Various immune and endocrine factors have been implicated in the upregulation of HA production. Since TSAB causes GD, it is logical that these antibodies have been investigated but with conflicting results. The difference may be due to the differing ligands used to activate the TSHR. The group of Terry Smith reported that although Graves' IgGs are able to increase HA production, the effect is not mediated via the TSHR (using recombinant TSHR) but the IGF1R [222].

In contrast, our own data indicate that TSHR activation (cAMP) in preadipocyte/fibroblasts (PF) does increase HA production. Comparison of gene expression profiles of PF experiencing TSHR activation (L629F or M453T as described above) or not revealed significant upregulation of HAS1 and HAS2 in the former. Furthermore, a monoclonal antibody devoid of TSAB activity also produced the same effect – suggesting that signalling cascades other than cAMP might be involved [262].

van Ziejl et al found contradictory results [263] using different ligands; recombinant TSH (rhTSH) and GD-IgG, they reported that the former increased cAMP by 25-50% but GD-IgG had no effect. Accordingly, no HAS mRNA and HA synthesis were detected. The same author tested the same theory in differentiated OF and found that both rhTSH and GD-IgG induced a cAMP response. Only some samples showed HAS1 upregulation but not HAS2 and 3. There was no measurable HA in rhTSH but marked HA response in GD-IgG [264]. These studies suggest that TSAB are more likely to regulate HA production via cAMP in orbital cells undergoing adipogenesis.

Zhang and colleagues also demonstrated that adipogenesis and HA production are linked in the orbit; they went on to dissect the signalling pathways implicated, major depot specific differences which might explain why orbital fat expands when other depots in GD/GO patients tend to shrink [265]. In this study, adipogenesis in orbital preadipocytes was accompanied by HA accumulation and significantly increased *HAS2* transcripts (but not *HAS 1* and *3*) and in contrast to subcutaneous cells, differentiation significantly decreased secreted HA and *HAS2* transcript levels. IGF-I alone did not increase *HAS2* levels, but inhibition of Akt increased orbital *HAS2* transcripts but not subcutaneous preadipocytes. In subcutaneous preadipocytes inhibition of mTOR leads to an increase in IGF-1 mediated *HAS2* production in contrast by a MAPK kinase inhibitor in orbital fibroblasts.

Studies from Smith's group indicate that immunoglobulins from GO patients are able to stimulate ECM production, also production of cytokines from orbital fibroblasts [266, 267]. Their explanation is IGF1R autoantibodies but others invoke TSHR/IGF1R cross-talk.

Most in vitro models use 2D cultures, a major advance proposed by Ezra and Bailly who cultured orbital fibroblasts in a 3D collagen matrix to study both processes [268]. Traditional 2D cell cultures lack the metabolic and proliferative gradients that are

present in the human body. 3D extracellular environments are the way our cells routinely operate in vivo. In theory 3D cultures should provide more physiological environments for cell adhesions, mechanical force and diffusible factors interactions than the conventional 2D models. The major finding from Ezra and Bailly's work was that in both thy-1 positive and negative orbital fibroblast (further discussed below), adipogenesis can be induced in 3D culture without the need for chemical stimulation and under pressure stress although slightly lower potential in Thy-1 positive [268]. In this 3D model Thy-1 expression has some impact but not all on adipogenic differentiation potential. However, it has no impact on the contractile phenotype potential.

1.10.7.4 Fibrocyte or Fibroblast

Smith and colleagues have suggested that TSHR expressing cells in the orbit might be fibrocytes rather than in situ mesenchymal stem cells [269]. Fibrocytes are circulating bone marrow derived cells which express unique CD34, CD13, CD45 and CXCR4 surface markers. These cells synthesize collagen I and are involved in inflammation, tissue remodelling and fibrosis [269-271]. The same group have shown that GD patients have increased fibrocyte numbers in their peripheral blood which spontaneously express TSHR at levels comparable to those found on thyroid epithelial cells and respond to TSH by producing IL-6 and TNF-α. These cells also can differentiate into adipocytes and myofibroblasts when treated with PPAR-γ ligands and TGF-β respectively [272].

Even though many people have studied orbital fibroblasts in vitro, very few have assessed their surface markers to indicate what cell types are present. Orbital fibroblasts display heterogeneous phenotypes in culture. As mentioned previously, this includes expression of cell surface marker of Thy-1 (CD90) in approximately 65%

of the orbital fat cell population but nearly all fibroblast within extraocular muscles [273]. Thy-1 is a 25-kilodalton glycoprotein and involved in the transduction of extracellular signals. Thy-1 function in orbital fibroblast is currently unknown. Thy-1 orbital population has been shown capable of producing hyaluronan, prostaglandin E2, IL-6 [274, 275] and are capable of myofibroblast differentiation [276] which can participate in inflammation, repair, and fibrosis. Whilst Thy-1 negative population is capable of differentiation into mature fat cells. Within the orbit, relative proportions of Thy-1+ and Thy-1− fibroblasts and their degree of exposure to TGF-β may affect disease expression, including whether muscle or fat expansion predominates and the extent of fibrosis that develops. Recently Eckstein group has shown that orbital fibroblasts possess surface markers of pluripotent mesenchymal stem cells (MSC) that are CD29, CD44, CD71, CD73, CD90, CD105, and CD166 with capability of adipogenic, osteogenic, chondrogenic, myogenic, and neuronal differentiation [277].

1.11 Study objectives

As discussed, the main pathological features of GO include expansion of orbital fat, mononuclear cell infiltration of orbital connective tissue and muscle, and tissue remodelling, which culminate in fibrosis and diminished eye motility [278]. The key mechanisms are excessive adipogenesis and secretion of glycosaminoglycans in the orbit, which increase volume and cause exophthalmos [279]. The opposite effect, enophthalmos (recession of the eye into the orbit), has been described in patients with glaucoma (intraocular hypertension) treated topically with Bimatoprost ($PGF_{2\alpha}$), a prostaglandin analogue [280-282]. This side effect is more noticeable if only one eye is exposed to treatment as the treated eye is easily comparable with the unexposed eye. However, since most patients receive treatment to both eyes it is possible that the incidence of enophthalmos in Bimatoprost treated patients has been underestimated. I hypothesised that the enophthalmos in glaucoma patients treated

with Bimatoprost is secondary to reductions in orbital tissue proliferation, adipogenesis and/or increased lipolysis. Since these processes underpin the tissue remodelling in GO, prostaglandin analogue therapy could be useful in this disease.

There is close clinical and temporal association between GD and GO suggesting an autoimmune response to common antigen/s in the orbit and thyroid gland. Since the TSHR is expressed in fat [118] and virtually all patients with hyperthyroid GO have TSAB, the receptor is the most logical candidate. Apart from TSH and TSAB, novel ligands for the TSHR have been described including thyrostimulin, which comprises novel α2 and β5 subunits [283]. It has high TSHR affinity but very little is known about its location and function; it has not been detected in the circulation suggesting paracrine effects. Transgenic mice over-expressing the α2 subunit had no overt phenotype but overexpression of β5 in mice is associated with hyperthyroidism, weight loss and proptosis [284]. These facts suggest it is a potential major contributor to the GD and GO disease processes. In contrast, several TSHR variants have been described which lack the transmembrane domain leading to soluble receptor products which could serve as TSH/TSAB/thyrostimulin binding proteins. Potentially these variants could promote pathogenesis of GO by inducing further production of TSAB or protect against GO by either 'neutralizing' TSAB or inducing immune tolerance. I hypothesised that variation in expression of TSHR binding protein (truncated TSHR variants) and/or novel ligands such as thyrostimulin, might provide a mechanism to protect against or exacerbate GO.

Another difficult problem for GD patients (who lose weight during active disease) is weight gain following treatment. Increases of up to 10kg in weight from baseline [285, 286] have been recorded. Whilst this may reflect at least in part; excessive treatment with anti-thyroid measures and subsequent alteration of a patient's baseline thyroid axis; it may also arise due to changes in peripheral fat. There are two types of adipose

tissue; white adipose tissue (WAT) mainly responsible for fat storage and brown adipose tissue (BAT) responsible for heat dissipation (GD patients are heat intolerant). GD weight loss has been attributed to the lipolytic effects of thyroid hormone [287] but the TSHR is expressed in fat and our lab has reported that TSHR activation (by TSAB) leads to a 'browning' of fat from various depots in vitro (15). Analysis has suggested that a diagnosis of GD (as opposed to other causes of thyroid over-activity such as toxic goitre), is an independent predictor of weight gain [288], raising the possibility that TSAB, not only modify orbital fat, but also have long-term effects on peripheral adipose tissue. I hypothesised that TSAB which alter fat biology in the orbit, might also have long-term effects on peripheral adipose tissue composition and TSHR activation per se may contribute to changes in body composition separately from the effects of thyroid hormone levels.

The first aim of my thesis was to investigate the effects of Bimatoprost eye drops in vitro on proliferation, adipogenesis and lipolysis to determine whether it might be of benefit in GO. (Chapter 2). This was followed by randomised controlled double blind crossover trial on the effect of Bimatoprost on GO (Chapter 3). My second aim was to measure the relative expression of TSHR variants, TSHR full-length and thyrostimulin transcripts and protein in GO orbits compared with non-GO in ex vivo samples and how this compares with the level of adipogenesis. This aspect was investigated using the in vitro model (Chapter 4). Finally, I would hope to delineate the effect of TSAB and thyroid hormone on adipogenesis by studying GD neck fat samples (experienced TSAB stimulation and hyperthyroid state) with 2 different controls: toxic multinodular goitre - the tissues experienced hyperthyroid state without TSAB stimulation and normal who were euthyroid with negative TSAB. My aim was to investigate the effect of TSHR activation on brown, beige and white adipose tissue formation in ex vivo human neck fat tissues (Chapter 5).

Chapter Two

2 PROSTAGLANDIN $F_{2\alpha}$ ($PGF_{2\alpha}$) EFFECTS ON ADIPOCYTE BIOLOGY RELEVANT TO GRAVES' ORBITOPATHY

2.1 INTRODUCTION

The prostaglandins (PG) are a group of active lipid molecules having multiple hormone-like effects in humans. They are different from hormones as there is no specific organ producing it or organ target but they are present in most cells and act either via autocrine (acting on the source cell itself) or paracrine (acting on the adjacent cells) routes. They are synthesized from the essential fatty acids which form part of the plasma membrane. An intermediate arachidonic acid is created from diacylglycerol via phospholipase-A2 which proceeds to either the cyclooxygenase or the lipoxygenase pathway to form either prostaglandin and thromboxane or leukotriene respectively. Prostaglandin $F_{2\alpha}$ ($PGF_{2\alpha}$) is produced following the sequential oxidation of arachidonic acid by cyclooxygenases 1 and 2 followed by terminal prostaglandin F synthase (See Figure 10).

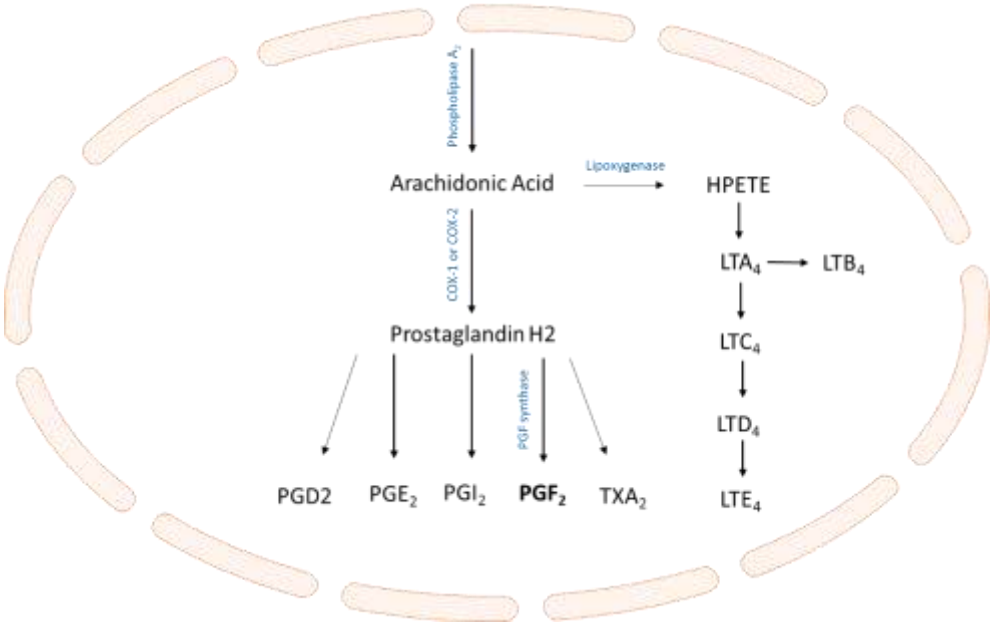

Figure 10: Prostaglandins biosynthesis. Modified from Ricciotti et al 2011 [289]. PGD2, prostaglandin D2; PGE2, prostaglandin E2; PGI2, prostaglandin I2 or prostacyclin; TXA2, Thromboxane; HPETE, hydroperoxyeicosatetraenoic acid; LTA4-E4, Leukotriene A4-E4.

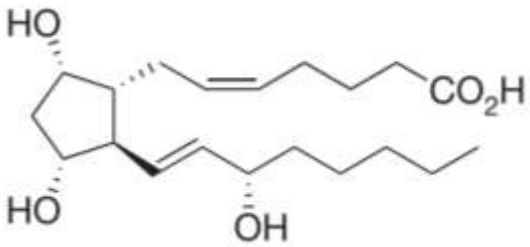

Figure 11: Molecular structure of $PGF_{2\alpha}$ depicting 20 carbon atoms including a 5-carbon ring. Adapted from Coulthard et al 2012 [290].

Studies into $PGF_{2\alpha}$ function have led to the generation of analogues, including Latanoprost, Travoprost, Carboprost and Bimatoprost. These have proven efficacy, when used topically during glaucoma therapy, to lower intraocular pressure (IOP). It

is believed that $PGF_{2\alpha}$ lowers IOP by increasing aqueous humour outflow through both the uveoscleral and trabecular meshwork routes by mimicking the action of naturally occurring prostamides [291] which stimulate production of matrix metalloproteinases (MMPs). MMPs are a family of neutral, zinc-dependent enzymes that can hydrolyze extracellular matrix proteins and proteoglycans [292]. These molecules are secreted as inactive proenzymes also known as zymogens and become activated by proteolytic truncation. There are multiple types of MMP and each MMP type targets specific peptide sequences in ECM macromolecules for cleavage. The most commonly used subtypes are the collagenases, the gelatinases, the stromelysins, and the membrane-type MMPs. MMPs have been shown to increase degradation of ciliary muscle ECM which increases uveoscleral flow [293]. Exposure of ciliary smooth muscle cells to $PGF_{2\alpha}$ induces at least four different MMPs including MMP-1, MMP-2, MMP-3, and MMP-9 [294]. Each of these has an Activator protein 1 (AP-1) regulatory element within their promoter [295]. This regulatory element promotes transcription when it is bound by a regulatory complex containing *Fos* and *Jun* family proteins [296]. Treatment of ciliary smooth muscle cells with $PGF_{2\alpha}$ induces *c-fos* expression supporting the view that $PGF_{2\alpha}$ induction of MMPs is mediated by AP-1 activation [297].

These positive effects of $PGF_{2\alpha}$ are not without the balance of some adverse effects. There are emerging case reports worldwide of deepening of the lid sulcus and/or enophthalmos developing in patients treated with Bimatoprost, albeit in small numbers [280-282, 298-300]. This side effect is more noticeable if only one eye is exposed to treatment as the treated eye is easily comparable with the unexposed eye. However, since most patients receive treatment to both eyes it is possible that the incidence of enophthalmos in Bimatoprost treated patients has been underestimated. This effect can be reversed by discontinuation of the prostaglandin analogue therapy. A possible mechanism by which $PGF_{2\alpha}$ agonists might produce

enophthalmos is through reduction of orbital fat volume [301]. A $PGF_{2\alpha}$ receptor agonist has been shown to be a potent inhibitor of adipose differentiation in new-born rat precursor cells [302]. This raises the possibility that $PGF_{2\alpha}$ exerts direct effects on adipose tissue precursors. The inhibition of this adipose tissue differentiation may be mediated via $PGF_{2\alpha}$ binding to a member of the G-protein coupled receptor family known as Prostaglandin F receptor (FP) [303]. This receptor is encoded by the *PTGFR* gene located on chromosome 1 in humans [304] and chromosome 3 in mice [305]. A splice variant has been described as FP(S) which lacks transmembrane-7 and the intracellular carboxyl tail [306]. FP(S) has been suggested to form a heterodimer complex with FP to exert its effects [307]. The FP receptor is a Gq coupled receptor, which once activated leads to release of inositol-1,4,5-trisphosphate and diacylglycerol which in turn increases the Ca^{2+} level [304, 308, 309]. Previous work from others, using the murine preadipocyte 3T3-L1 cell line, reports that $PGF_{2\alpha}$ inhibits adipogenesis via a calcineurin dependent mechanism by blocking expression of critical adipogenic transcription factors *PPARγ* and *C/EBPα* [310]. This mechanism can be negated by calcineurin inhibitors such as Cyclosporine and Tacrolimus (FK506) [311] which might explain inconsistent results in the management of Graves' Orbitopathy (GO) with these agents [312, 313]. Other main effects of the FP receptor are uterine contraction [314], luteolysis [315], and bronchoconstriction [316].

The opposite of enophthalmos, i.e. exophthalmos is a feature of GO. This represents a poorly understood component of Graves' disease (GD) and was described in detail in chapter 1. Graves' disease is caused by thyroid stimulating antibody and there are indirect demonstrations that they might also be important in GO [262]. The main features of GO include orbital connective tissue fat pad expansion, tissue and extraocular muscle infiltration with mononuclear cells, and tissue remodelling that leads to fibrosis and reduced eye motility. GO has an annual adjusted incidence rate

of 3 men and 16 women per 100,000 population [156]. So called subclinical (minimal or no clinical signs or symptoms) involvement is quite common approaching up to 70% of adults with GD detected via MRI or CT scanning [279].

2.1.1 3T3-L1 cell lines

3T3-L1 cell lines have been fundamental in cardiometabolic disease research for over 5 decades. 3T3 cell lines were developed by Todaro and Green in 1962 from Swiss albino mouse embryonic fibroblasts [317]. In their study, the embryos were originally minced and digested with trypsin before being grown in suspension and later forming a monolayer. The cells were then cultured for 3 or 6 days with a fixed amount of cells being inoculated. Lower than 3 x 10^5 cells in the inoculum were associated with poor growth rate whilst the higher inoculums were associated with higher growth rate and multilayer formation before being limited to grow any further by contact inhibition. 3 x 10^5 inoculums after 20-30th passages, the cells started to have constant rate of growth which was described as 'established cell lines'. These cells were sensitive to contact inhibition and able to remain in a resting state for long periods. Green later described the isolation of a clone from 3T3 clones, also known 3T3-L1, which accumulated lipid droplets when they entered a resting state induced by a high concentration of serum up to 30% [318].

The '3T3-L1' abbreviation used refers to "3 x 10^5 cells cultured for 3 days before being trypsinised and transferred to another plate; L1 simply denotes L1 clone. In culture medium, 3T3-L1 exhibits a fibroblast-like morphology and can be induced to differentiate to mature adipocytes by adipogenic cocktail (see below) making it a useful model to study adipocyte differentiation [319, 320]. The adipogenesis process is associated with increase in fatty acid transcription factors including CCAAT/enhancer binding protein alpha (C/EBPα) and peroxisome proliferator-activated receptor gamma (PPARγ) [319]. Although initially thought that the cells need

to undergo mitotic clonal expansion (2-3 cycles of growth after growth arrest) before going into adipogenesis, this later was found not to be a necessary step for 3T3-L1 to differentiate into adipocytes [239].

Primary orbital preadipocytes are the model of choice for the current study but there are limitations because of their scarcity and slow growth. 3T3-L1 on the other hand so far have provided most known knowledge on adipogenesis. It is immortalized and easily managed. They are relatively accurate representations of true preadipocytes, based on ultrastructure and their ability to form fat pads when injected into athymic mice. However, despite their strengths as preadipocyte models, there are differences:

i. Aneuploid rather than diploid
ii. Regulation of cell cycle events are different between cell lines and primary cultures of human preadipocytes
iii. More recently, using gene array technology, similarities and differences in clusters of genes regulated during adipogenesis have been described between the widely used 3T3-L1 cell line and primary mouse preadipocytes

I made use of this cell line because apart from the convenience and short duration of replication, it allows development of the right methods and techniques before embarking on the study on primary orbital preadipocytes.

I hypothesised that the observed enophthalmos in patients treated with $PGF_{2\alpha}$ is secondary to reductions in orbital tissue proliferation, adipogenesis and/or increased lipolysis. The aim was to investigate which of these is affected, using 3T3-L1 cell lines and human orbital fibroblasts, to determine whether the drug might be useful as a treatment for GO.

2.2 MATERIAL AND METHODS

All tissue culture components were obtained from Lonza (Verviers, Belgium) and reagents from Sigma-Aldrich (St. Louis, MO) unless otherwise stated. 17-phenyl trinor Prostaglandin $F_{2\alpha}$ free acid ($PGF_{2\alpha}$) was obtained from Cayman Chemical and diluted in Dimethyl sulfoxide (DMSO) to produce a stock solution of 1 millimolar (10^{-3}M). Working concentrations were from 10^{-6} to 10^{-8} molar concentration. Please see Figure 12 for the summary of the methods used in the study.

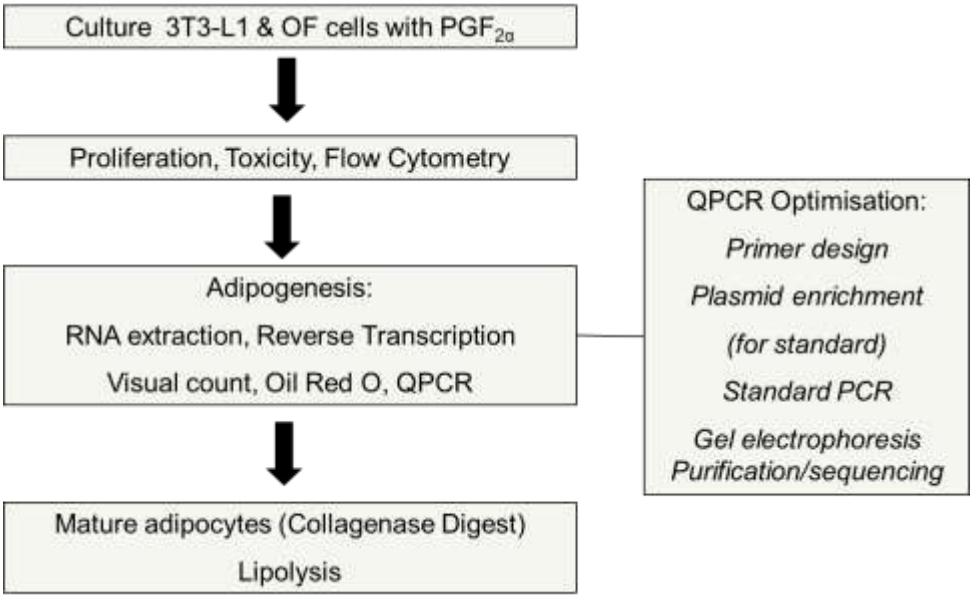

Figure 12: A flow diagram illustrating methods used to study the effect of $PGF_{2\alpha}$ eye drops on orbital adipose tissue remodelling.

2.2.1 Tissue specimen and preparation

The 3T3-L1 preadipocyte cell line was obtained from the American Type Culture Collection (Rockville, MD). They were cultured in complete medium (see Table 8). Orbital tissue samples were collected, with informed consent and local research ethics committee approval. GO patients (n=5; 3 females and 2 males with median age of 50 years of age (range 39-54 years) were diagnosed on clinical grounds based

on the presence of typical clinical features in the context of autoimmune thyroid disease. The GO samples were obtained from patients undergoing decompression surgery and having inactive disease with a clinical activity score below 2. None of these patients had previous orbital radiotherapy. Only one patient had steroid treatment and was on the treatment during orbital decompression. The non-GO samples (n=5; 3 males and 2 females, median age 53 years old (range 52-60 years) were from individuals free of thyroid or other inflammatory eye disease who underwent augmented blepharoplasty. Orbital preadipocyte/fibroblasts (OF) were obtained from explant cultures. Briefly, orbital fat biopsies were diced and placed in 6 well plates in 1.5 ml of complete medium (Table 8) and allowed to attach so that OF migrated out from the tissue. Once OFs were adherent, the plates were washed with culture media and OFs were grown to confluence replacing media every 7 days. The cells were detached with 1.5 ml of trypsin and frozen in liquid nitrogen (please see below) until further use. Cells were used at low passage number (≤3) thus not every sample was used for each experiment.

Table 8: Complete medium containing 10% foetal calf serum

Component	Volume in millilitres to make 200 millilitres of complete medium.
Dulbecco's Modified Eagle Medium (Cat no. BE12-741F)	85
Ham's F12 (Cat no. BE12-615F)	85
Foetal Calf Serum (Cat no.DE14-802F)	20
Penicillin/Streptomycin (10 000iu penicillin/ml 10 000iu streptomycin/ml) (Cat no. DE17-602E)	4
Pyruvate (Cat no. BE13-115E)	2
Bicarbonate 7.5% (Cat no. BE17-613E)	2

2.2.2 Passaging cells

Both types of cells were thawed rapidly at 37°C and then cultured in 10 ml CM in 75 cm^2 flasks .CM medium were replaced every 3rd day for 3T3-L1 and once a week for OF. Once the cells reached 75% confluence, they were trypsinised and counted for subsequent experiments. A proportion of the cells were frozen using freezing mixture (90% FCS 10% DMSO) in a cryo vial at 1°C/hour using a Nalgene cryo container with 100% isopropyl alcohol before being transferred into liquid nitrogen for long term

storage.

2.2.3 Preadipocyte/fibroblast culture and cell counting

Five thousand cells (3T3-L1 or OF) were plated in CM and allowed to attach for 1 day; $PGF_{2\alpha}$ at 10^{-8}M concentration was then added only on day 0 to test for reversibility or daily to mimic current topical application in clinical practice. $PGF_{2\alpha}$ at 10^{-8}M concentration was chosen as this is physiological concentration. In some experiments 10^{-6}M concentration was chosen to replicate pharmacological concentrations of the drug. Control cells were cultured in CM containing 0.02% v/v DMSO. Due to the very short half-life of the product and rapid proliferation rate of the 3T3-L1 cell line, direct cell counting (Cellometer®) was performed on days 1, 2 and 3. In contrast, the low population doubling time (PDT) of primary OF required that cell counts were performed on day 5. Individual experiments were done in triplicate and repeated at least twice. Results are expressed as mean ± SD.

2.2.4 Trypan blue exclusion

Trypan blue analysis (0.1%) was carried out after 24 hours exposure to 10^{-6} to 10^{-8} molar of $PGF_{2\alpha}$. To make 0.2% for use with cellometer; trypan 0.4% (stock solution) was diluted with PBS or complete media 1:1 volume i.e. 1 ml of trypan blue 0.4% with 1 ml of PBS or CM. To stain cells equal volumes of cell suspension and trypan blue were mixed.

2.2.5 In vitro adipogenesis

The various cell populations were plated in 6 well plates in CM. Adipogenesis was induced in confluent cells by replacing with differentiation medium (DM) (see Table 9) for 7 (3T3-L1) or 15 (OF) days. Prostaglandin $F_{2\alpha}$ was introduced together with DM on day 0 at 10^{-8}M, 10^{-7}M and 10^{-6}M concentration; DM ± $PGF_{2\alpha}$ was changed every 3

days. Reversibility was tested by applying $PGF_{2\alpha}$ (10^{-6}M) for a limited number of days (3, 6, 9, 12 or 15 days) to allow cell recovery. Adipogenesis was assessed microscopically to detect the accumulation of lipid droplets and also by oil red O staining and QPCR analysis of markers of differentiation.

Table 9: Differentiation medium (DM). 100 millilitres of 2X DM was prepared as below. An equal volume of CM was added to give a 10% FCS for human primary culture and 5% FCS for 3T3-L1.

Component	Volume	Final Concentration
DMEM (Lonza)	44.5 ml	
Ham's F12 (Lonza)	44.5 ml	
FCS (Lonza)	10/20 ml	10% (human), 5% (3T3-L1)
Biotin (Sigma B-4639)	64ul µl	33 µM
Pantothenate (Sigma P-5155)	200 µl	17 µM
T3 (Sigma T-5516)	1.4 µl	1 nM
Hydrocortisone (Sigma H-2270)	20 µl	1 µM
Pioglitazone (Takeda)	20 µl	1 µM
Insulin (Sigma I-1882)	570 µl	500 nM

2.2.6 Oil red O staining/Absorption

Saturated (0.25-0.5% in isopropanol) oil red O stock solution can be stored for up to 1 month. Prior to use, 12 ml saturated solution were mixed with 8 ml distilled water, left at room temp for 5-10 minutes. This was filtered using Whatman filter paper and used within 2 hours.

For cells to be stained, the medium was removed and washed with 1 ml PBS or

HBSS. The cells then fixed in 500 µl 60% isopropanol for 10 minutes then washed x 1 with 1 ml PBS and 100 µl Oil red O was added per well and left for 15 minutes at room temperature. Oil red O was then removed carefully. If the cells were going to be photographed, they were rinsed with 1 ml 60% isopropanol and washed with 1 ml water. If oil red O staining was to be quantified, they were washed at least x 4 with 1 ml water until all precipitate was removed and 200 ul 100% isopropanol was added per well. The extracted Oil red O was then transferred to a 96 well plate and read at OD490.

2.2.7 Lipolysis

Adipogenesis was induced in vitro using DM (as above) in 3T3-L1; on day 7 the DM was replaced by serum free medium (SFM). Mature human orbital adipocytes were obtained by collagenase digest and centrifugation on a phthalic acid dinonyl ester gradient (see Figure 13) and resuspended in SFM. In both cases, varying concentrations of $PGF_{2\alpha}$ were introduced alone (unstimulated lipolysis) or combined with 10^{-8}M to10^{-6}M L-Norepinephrine (stimulated lipolysis) for 4 hours. Cell suspensions/supernatants were extracted and free glycerol assays (Cayman Chemical) were performed according to the manufacturer's instructions, after 15-minute incubation with the assay reagents the OD was read at 490nm.

2.2.8 Collagenase digest

Collagenase Type 2 was prepared by dissolving 300 mg in 10 ml of DMEM and filter-sterilization. This was frozen in 1 ml aliquots and stored at -20°C. 7.5% BSA was prepared by adding 7.5 g in 100 ml of distilled water, dissolved at 37°C in a water bath and filter-sterilised. The fat then was cut into small pieces and transferred into a 20 ml universal container (UC). Three ml tissue was used per UC to which was added 7 ml HBSS, 2 ml BSA, 1 ml collagenase. This was incubated at 37°C in a water bath

for 1 hour and shaken every 5 minutes to facilitate the digestion. The sample was then spun at 4°C for 5 minutes at 1500 rpm (see Figure 13). The mature adipocytes and preadipocytes were removed and resuspended in culture medium.

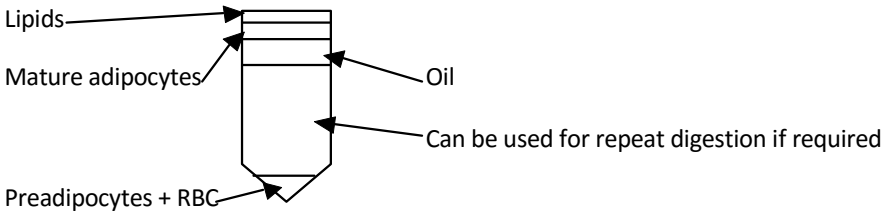

Figure 13: Showing disaggregated layers which separate after centrifugation.

2.2.9 Cell cycle analysis using flow cytometry

3T3-L1 cells and OFs were plated in 75 cm^2 flask, allowed to attach for 24 hours and then treated with 10^{-6}M $PGF_{2\alpha}$ for 48 hours and 5 days respectively. The cells were detached with 5 ml of trypsin and neutralised with 5 ml of CM. These were then washed twice with 5 ml of PBS. Each time the cells were spun at 1000 rpm for 5 minutes. They then were fixed in 1 ml ice cold 70% ethanol and stored at -20°C before analysis. At this temperature, the fixed cells can be stored for a few weeks prior to PI staining. Before analysis, ethanol was removed by centrifugation at 2000 rpm for 5 minutes and washed twice with 1 ml PBS. Finally, samples were resuspended in 468.75 µl PBS with propidium iodide 25 µl of 1 mg/ml stock (final concentration 50 µg/ml) and RNAse A 6.25 µl of 4 mg/ml stock (50 ug/ml) to a final volume of 500 µl. The tube was then wrapped in aluminium foil to protect it from light and left to incubate overnight at 4°C. Flow cytometry was performed on BD FACS Canto II using

FACSDiva 6.0 software from Becton Dickinson and Co. (Mountain View, CA). Propidium iodide was detected using the 575/26nm channel. Forward light scatter, side light scatter, and fluorescence emissions were collected for 10000 cells. Results were analysed using FlowJo software version 10.0.5 (Tree Star, Inc).

2.2.10 RNA extraction

This was performed using Tri Reagent (Sigma Catalogue Number T9424). “This product, a mixture of guanidine thiocyanate and phenol in a monophase solution, effectively dissolves DNA, RNA, and protein on homogenization or lysis of tissue sample. After adding chloroform and centrifuging, the mixture separates into 3 phases: top layer; an aqueous phase containing the RNA, the interphase containing DNA, and an organic phase containing proteins”.

For 6 well plates, medium was aspirated and cells were washed using 1 ml/well PBS followed by 1 ml/well Tri reagent. The cells were resuspended in the Tri reagent and when lysis was complete, were transferred to a 1.5 ml Eppendorf tube. This could be processed immediately or frozen at -80°C for future processing. For each 1 ml of Tri Reagent, 200 µl of chloroform was added and centrifuged at 13000 rpm at 4°C for 15 minutes. Centrifugation separates the mixture into 3 phases: a colourless upper aqueous phase (containing RNA), an interphase (containing DNA), and a red organic phase (containing protein).

The aqueous phase was then transferred into a new 1.5 ml vial. 500 µl of isopropanolol was added to each 1 ml of clear supernatant to precipitate RNA. This was gently mixed by turning the vial upside down several times and allowed to rest at room temperature for 10 minutes. The mixture then was spun at 13000 rpm at 4°C for 10 minutes. The RNA precipitate would form a pellet on the side and bottom of the tube. The supernatant was then carefully removed. 1 ml of 75% ethanol was

added to the RNA pellet to purify the RNA from excess salts, followed by a quick vortex then spun at 8000 rpm at 4°C for 5 minutes. The alcohol was removed and the remaining drops were carefully removed with a 200 µl pipette tip. The pellet was allowed to dry at room temperature for 10-15 minutes. The pellet was dissolved with 6 µl of RNAse free water followed by a quick vortex and spun twice. The RNA concentration was then measured using NanoDrop™ Lite Spectrophotometer - Thermo Scientific. An absorbance A260/280 ratio of 1.8 or more was considered acceptable.

2.2.11 Reverse transcription (First-strand synthesis of cDNA)

All the components are from Promega supplier.

Components	Volume (µl)
dNTPs (C1141)	4
oligodT 500 µg/ml (C1101)	4
5X Buffer (M531A)	4
M-MLV Reverse Transcriptase 200 u/µl (M1705)	1
RNAse inhibitor 40 u/µl (N2511)	1
Total (Master mix)	14
RNA 1 µg	6
TOTAL VOLUME	20

1 µg RNA was made up to 6 µl with RNAse free water in a 500 µl vial. This was heated in a heat block at 60°C for 10 minutes to denature secondary structures within the template. Meanwhile the master mix was prepared, all components except the Moloney Murine Leukaemia Virus (M-MLV) reverse transcriptase enzyme. After 10 minutes, the RNA was transferred immediately onto ice for 5 minutes to prevent secondary structure from reforming. The reverse transcriptase enzyme was finally added to the master mix and 14 µl was then added into each RNA sample. The reaction mix was placed in a thermocycler machine with the following settings: 37°C for 1 hour (Reverse Transcription step), 95°C for 5 minutes (Destroyed RT enzyme) and hold at 4°C. The resultant cDNA was stored at -20°C.

2.2.12 Primer design

The primers were designed using primer 3 software (http://primer3.ut.ee/). As far as

possible the primer pairs were designed to cross exons in order to reduce the chance of amplifying contaminating genomic DNA. The primers were ordered at 25 nmol scale and desalted for purity. Please see Table 10 for primer pairs used in these experiments.

Table 10: PCR primers used indicating exon location and size of amplicon.

	Accession number	**Forward**	**Reverse**	**Amplicon size (bp)**
Arp (mouse)	NM_018853.3.	GAGGAATCAGATGAGGATATGGGA (Exon 7)	AAGCAGGCTGACTTGGTTGC (Exon 7)	72
Gapdh (mouse)	NM_001289726.1.	ATGCTCGCCACAGAATCCACAC (Exon 8)	AACCGGCAGCCCTTGACTTG (Exon 8)	124
Ptgfr (mouse)	NM_008966.3	ATGTTTGCTGTGTTCGTGGC (Exon 2)	GGCCATTGTTACCAGAAAGGG (Exon 3)	330
APRT (human)	NM_001030018.1	GCTGCGTGCTCATCCGAAAG (Exon 3)	CCTTAAGCGAGGTCAGCTCC (Exon 5)	247
LPL (human)	NC_000008.11	GAGATTTCTCTGTATGGACC (Exon 7)	CCTTAAGCGAGGTCAGCTCC (Exon 9)	275
PTGFR (human)	NM_000959.3	GCCCATCCTTGGACATCGAG (Exon 2)	GGCCATTGTAACCAGAAATGGG (Exon 3)	304

Primers were reconstituted using RNAse free water to produce stock solutions of 100 uM. For QPCR, an optimization step was performed using forward and reverse primers at 100, 300 and 500 nM final concentration, a total of 9 combinations (see Table 11).

Table 11: Primer concentrations grid

Final concentration in 25 µl volume by using 0.5 µl of primer mix	Volume of primer stock used (µl)
100 nM	10
300 nM	30
500 nM	50
+ H_2O	100

For example, in order to get 100 nM of forward and 300 nM of reverse primers in the final reaction mix, the primer mix was prepared by adding 10 µl of forward and 30 µl of reverse primers 100 µM stock with 60 µl of RNAse free water.

2.2.13 Standard polymerase reaction

The following programme was used to amplify the gene of interest: Initial denaturation - 95°C for 5 minutes; amplification steps - 94°C 30 sec, 60°C 30 sec, 72°C 30 sec (35 cycles); final extension - 72°C for 10 minutes and hold at 4°C. Please see Table 12.

.

Table 12: Standard PCR reaction components

Component	Volume (µl)
Primer mix	1
dNTPs	1
10X Buffer	2.5
H_2O	19
Taq polymerase	0.5
DNA template	1
TOTAL	25

2.2.14 Agarose gel electrophoresis analysis of PCR product

PCR products were analysed in a 2% agarose gel containing 400 ng/ml ethidium bromide (Promega). 10 µl of PCR samples or DNA ladder mixed with 2 µl 6X loading dye (Promega 6190A) before being loaded onto the gel. The gel was then run at 100V for 45 minutes. The DNA was then visualised on an UV transilluminator, and photographed using Alpha Innotech MultiImage II, Alpha Imager HP, and wave length of 365 nm.

2.2.15 DNA purification

PCR purity was achieved using Wizard SV gel and PCR clean-up system (Promega A98281) according to the manufacturer's instructions. Briefly following electrophoresis, the DNA band was excised from the gel, placed in a 1.5 ml Eppendorf tube with 10 µl membrane binding solution per 10 mg of gel slice and incubated at 50–65°C until the gel slice was completely dissolved. An equal volume of membrane binding solution was added to the PCR amplification. Meanwhile SV minicolumn was inserted into collection tube. The dissolved gel mixture was added to the minicolumn

assembly. This was incubated at room temperature for 1 minute followed by centrifugation at 13000 rpm for 1 minute. Flow-through was discarded and the minicolumn was reinserted into the collection tube. 700 µl membrane wash solution (ethanol added) was added then centrifuged at 1300 rpm for 1 minute. Flow-through was discarded again and this time 500 µl membrane wash solution was added and centrifuge for 5 minutes. The collection tube was emptied and the column assembly was recentrifuged for 1 minute with the Eppendorf tube lid open (or off) to allow evaporation of any residual ethanol. Minicolumn was carefully transferred to a clean 1.5 ml microcentrifuge tube where 20 µl of RNAse free water was added and incubated at room temperature for 1 minute. Finally, this was centrifuged at 13000 rpm for 1 minute to elute the DNA which was stored at –20°C.

2.2.16 DNA sequencing

To confirm that the PCR amplicon was the intended product, the DNA sample was sequenced. Each sequence reaction contained 2 µl Big Dye Terminator V3.1 Sequence Reaction mix (Life Technologies, Grand Island, NY, USA), 2 µl forward primer (10 pmol/µl) and approximately 50 ng (typically 5 µl) of purified PCR made up to 10 µl with H_2O. Sequencing reactions were run on a PCR machine (see Table 13).

Table 13: Programme used for sequencing

Number of cycles	Temperature °C	Time
28	96	10 sec
	50	5 sec
	60	4 min

Prior to sequencing, PCR products were precipitated using sodium acetate. 1.5 µl of 3 M sodium acetate (pH 5.4), 7 µl of water and 31.5 µl of absolute ethanol were added to each 10 µl sample to be sequenced then vortexed and incubated at room temperature for 15 minutes. Samples were centrifuged for 20 minutes at 4°C at 13,000 rpm, the supernatant was carefully discarded and the DNA pellet was washed with 250 µl of 70% ethanol (vortexed and spun for 10 minutes). Supernatant was removed and the samples were dried in a heat block at 95 °C for 1 minute – lid open to evaporate the ethanol - before re-suspension and analysis on an ABI 3100 Genetic Analyser.

2.2.17 Quantitative polymerase chain reaction

Quantitative polymerase chain reaction was performed using Sybr Green QPCR mastermix (Stratagene Cat no 600548) and a Stratagene (La Jolla, CA) MX3000P light cycler. QPCR master mix was prepared as per Table 14. Negative template control was prepared with 24 µl master mix along with 1 µl distilled water, while remaining wells were filled with 24 µl of master mix and 1 µl cDNA. To avoid contamination, negative template control was prepared first and capped, followed by cDNAs and finally the standards.

Table 14: Quantitative PCR components

Components	Volume (µl)
Sybr green	12.5
H_2O	11
Primer mix	0.5
Master mix subtotal	24
cDNA	1

The QPCR plate was spun at 1500 rpm for 3 minutes. The following programme setting was used:

Table 15: QPCR programme - 2 Steps amplification with dissociation curve setting

Segment	Temperature (°C)	Duration	Number of cycle
1 Enzyme Activation	50	2 min	1
	95	2 min	
2 PCR	95	15 secs	40
	60	30 secs	
3 Dissociation curve	95	1 minute	1
	55	30 secs	
	95	30 secs	

To allow quantification of the transcript copy numbers (TCN) per microgram input RNA of the gene product, standard curves were used; these comprised either the target gene cloned into a plasmid or serial dilutions of the target PCR amplicon. In

addition, transcripts for a housekeeping gene were measured so that values could be expressed relative to this (transcripts per 1000 housekeeping gene). In a single Q-PCR experiment, all measurements were made in duplicate.

The estimation of the TCN of the standard was based on the assumption that the average weight of a base pair (bp) is 650 Daltons. This means that one mole of a bp weighs 650 g and that the molecular weight of any double stranded DNA template can be estimated by taking the product of its length (in bp) and 650. The inverse of the molecular weight is the number of moles of template present in one gram of material. Using Avogadro's number, $6.022x10^{23}$ molecules/mole, the number of molecules of the template per gram can be calculated: mol/g x molecules/mol = molecules/g. Finally, the number of molecules or number of copies of template in the sample can be estimated by multiplying by $1x10^{9}$ to convert to ng and then multiplying by the amount of template (in ng). The formula used was: number of copies = (amount x 6.022x1023) / (length x $1x10^{9}$ x 650). This was done using an online tool at http://cels.uri.edu/gsc/cndna.html.

2.2.18 Bacterial transformation

Bacterial plasmid glycerol stocks are important for long-term storage of plasmids. The preparation of plasmid constructs will be described in details in chapter 5. The addition of glycerol stabilizes the frozen bacteria, preventing damage to the cell membranes and keeping the cells alive. The bacterial plasmids were used to generate standard curves for QPCR or as positive control in standard PCR. Once the bacterial glycerol stock is made, the process of generating plasmid DNA would be a lot easier without the need for bacterial transformation. Experimental plasmids DNA used in the experiment (mouse *Arp/ Gpdh* and human *APRT/ LPL*) were stored at -20°C and glycerol stocks were stored at -80°C which could last for many years.

The first process to amplify plasmid stocks is via bacterial transformation. Luria Bertani (LB) Agar (Sigma L3147) 40 g/L was prepared by suspending 40 g of the agar powder in 1 L of distilled water. This was boiled in the microwave to dissolve it then autoclaved for 15 minutes at 121°C. It was cooled to 50°C prior to addition of 400 µl of ampicillin (stock 100 mg/ml) to give a final concentration of 100 µg/ml and dispensed into sterile petri dishes. Once solidified, the plate was dried further by turning upside down in a sterile laminar flow hood.

LB broth (USB Affymetrix Luria Broth 758541) 25 g/L was prepared by adding 12.5 g of the powder with 500 ml distilled water. This was autoclaved and allowed to cool to 55°C prior to addition of antibiotic if needed.

This bacteria transformation was achieved by using One Shot® TOP10 Chemically Competent *E.coli* (Thermo Fisher C4040-10). For blue/white screening selection, 40 µl of 40 mg/mL X-Gal in dimethylformamide was spread on top of the agar and left to diffuse into the agar for approximately 1 hour. This was done on the principle that if β-galactosidase is produced, X-gal is hydrolysed to form 5-bromo-4-chloro-indoxyl, which spontaneously dimerizes to produce an insoluble blue pigment called 5,5'-dibromo-4,4'-dichloro-indigo. The colonies formed by non-recombinant cells, therefore appear blue in colour while the recombinant ones appear white. The desired recombinant colonies then can be easily picked and cultured.

The vial(s) containing the plasmid/ligation reaction(s) was centrifuged briefly and placed on ice. The cloning process will be described in details in chapter 5. On ice, one 50 µl vial of One Shot® cells was thawed. This can be divided into 2X25 µl in 1.5 ml Eppendorf. 2 µl of each plasmid/ligation reaction was added directly into the vial of competent cells and mixed by tapping gently. The vial(s) was incubated on ice for 30 minutes. Then this was further incubated for exactly 30 seconds in the 42°C water bath before placing them back on ice. 250 µl of pre-warmed 37°C Super Optimal broth

with Catabolite repression (SOC) medium was added to each vial. SOC is a rich medium (see Table 16). The vial(s) was then placed in a microcentrifuge rack on its side, secured with tape to avoid loss of the vial(s) at 37°C for exactly 1 hour at 225 rpm in a shaking incubator. 70 µl from each transformation vial was spread on separate, labelled LB agar plates. The remaining transformation mix may be stored at 4°C and plated out the next day, if desired. The plate(s) was inverted and incubated at 37°C overnight. Approximately 5-10 colonies were selected and each transferred into 5 ml of LB broth. This was then cultured overnight again prior to miniprep. The remaining cultures then stored at 4°C.

Table 16: SOC medium components

SOC medium components
2% tryptone
0.5% yeast extract
10 mM NaCl
2.5 mM KCl
10 mM MgCl2
10 mM MgSO4
20 mM glucose

2.2.18.1 Miniprep

The miniprep was performed using GenElute™ Plasmid Miniprep Kit (Sigma PLN70) according to the manufacturer's instructions. Two ml of LB Broth were harvested and centrifuged at 13000 rpm for 1 minute. The supernatant was discarded. The pellet was then resuspended with 200 µl of resuspension solution. The cells then lysed with

200 µl lysis solution by gentle inversion 6-8 times. This was neutralised with 350 µl of neutralising solution by inverting 5 times and centrifuged at 13000 rpm for 10 minutes. The column was then prepared by adding 500 µl column preparation solution and centrifuged at 13000 rpm for 1 minute. The lysate was then loaded into the column and centrifuged at 1300 rpm for 1 minute. The column was then washed with 750 µl of wash solution, centrifuged as before and the DNA was eluted into new vial with 100 µl elution solution.

2.2.18.2 Plasmid digestion

To confirm the identity of the amplified plasmid, the plasmid was digested by using the following digestion reaction mix (see Table 17*)***:**

Table 17: Component of enzyme digestion

Components	Volume (µl)
Plasmid	1
Xbal1 (restriction enzyme)	0.5
10X Buffer	1.5
H_2O	12
Final volume	15

Xba1 enzyme was an example of the restriction enzyme used. Initially master mix was prepared, vortexed and centrifuged. Fourteen µl of the master mix was added to each vial containing 1 µl of plasmid and was again vortexed and centrifuged. The reaction was incubated 1-4 hour in the shaking incubator (37°C) and analysed by agarose gel electrophoresis. If the digest generated restriction fragments of the expected sizes, the plasmid was also verified by sequencing as described in section

2.2.16)

2.2.19 Statistical analysis

For statistical analysis, we used SPSS 18.0 software. Where appropriate, data were analysed using Student's t test for parametric and Mann-Whitney for non-parametric; in all cases, $p<0.05$ was considered significant. Multiple comparisons of group means were analysed using one-way ANOVA with post hoc Tukey HSD. The statistical analysis applied is indicated in the tables and figure legends. All parametric data are presented as mean ± standard deviations and median ± interquartile range for non-parametric.

2.3 RESULTS

2.3.1 Morphology of 3T3-L1 in complete and differentiation medium

Upon plating after a rapid thawing process from liquid nitrogen, 3T3-L1 cells in complete medium had a round appearance and would attach to the plate in approximately 10-15 minutes. The higher the cell numbers being plated the more likely they would be to clump in the centre of the well. Therefore, the culture had to be shaken sideways to encourage the cells to spread out in the well. By the next day, it would adopt a phenotypic appearance of fibroblast-like cells with an elongated shape (see Figure 14A). It grew rapidly with doubling time of 1 day. Once subjected to adipogenic medium, by day 7 the cells turn into a very rounded adipocyte-like cell with multiple lipid droplets in each cell (see Figure 14B). Some of these cells' lipid droplets coalesce to form slightly larger size droplets but none have a large single droplet typical of mature adipocytes (see Figure 15). These cells were easily detachable and float easily. Approximately 70-90% of the 3T3-L1 cells could be induced into adipocyte-like cells.

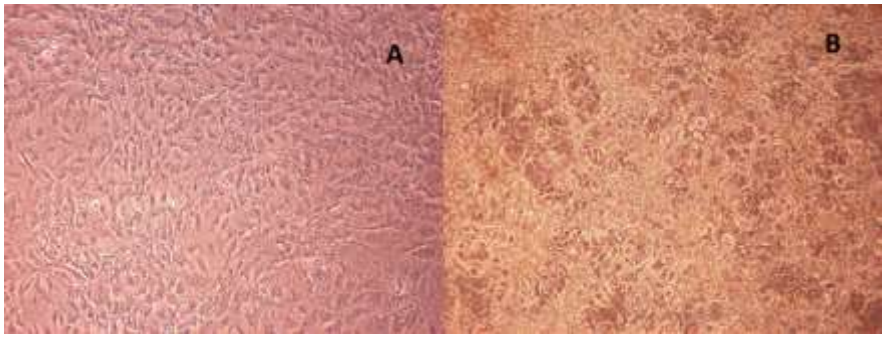

Figure 14: Phase contrast photomicrograph of undifferentiated 3T3-L1 in complete medium (A) and differentiation medium (B). After 7 days, lipid droplet accumulation in differentiated cells is clearly visible in 70-90% of the cells. Magnification 100x.

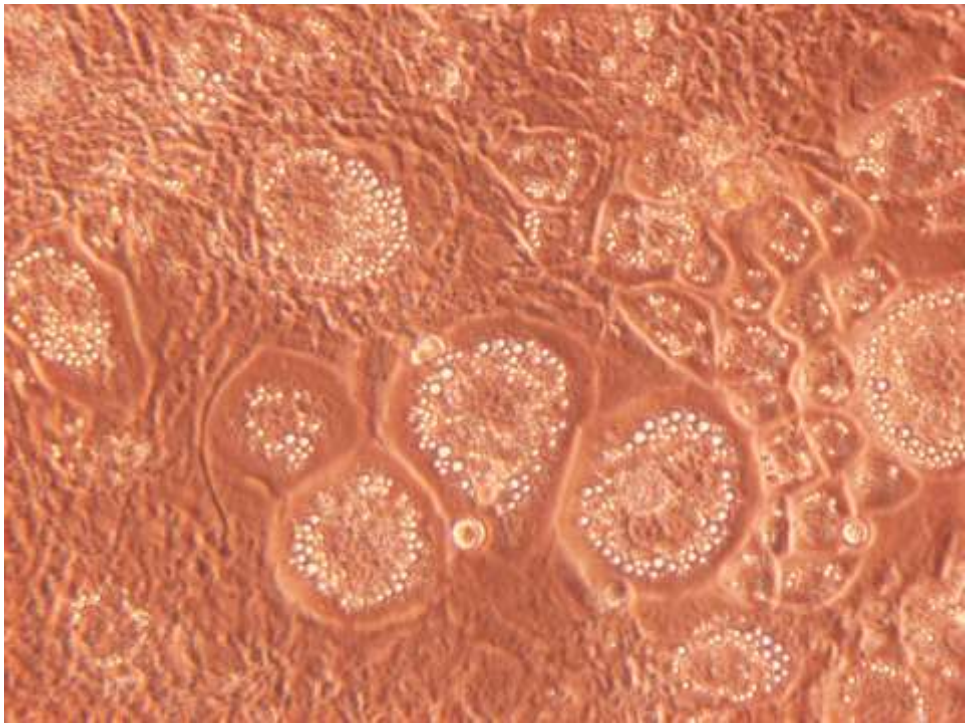

Figure 15: Higher magnification (400x) of phase contrast photomicrograph of differentiating 3T3-L1 in differentiation medium showing ring formation of lipid droplets.

2.3.2 Validation of the QPCR assay

In order to confirm that the QPCR assays generated the intended products with high efficiency, the experimental data was validated by confirming that:

(a) A single peak for the melting curve indicating single product has been amplified.

(b) High PCR reaction efficiency.

(c) A single band of the appropriate size on gel electrophoresis.

(d) Identity of the intended DNA sequence.

The reaction efficiency was calculated by running a standard curve using a serial 10-fold dilution of plasmid DNA. I normally performed a standard curve having 10^8 copies in the highest and then 10-fold dilutions to 10^1. Example of optimization of *Arp* QPCR showing agarose gel electrophoresis (see Figure 16) and melt curve analysis (see Figure 17B) confirming that the *Arp* QPCR assay produced a single product of the correct size which was 72bp and correct sequence on Sanger sequencing analysis. Analysis of serial dilutions of *Arp* plasmid DNA (see Figure 17) was used to determine the efficiency of the assay. This can be calculated from Efficiency (E) formula, $E = 10^{(-1/slope)}$. The slope was obtained by plotting the Ct values against serial plasmid DNA concentration using the MxPro software (Stratagene). This showed that the reaction has linear standard curve ($r^2>0.999$), consistency across replicates and high amplification efficiency of 111.3%.

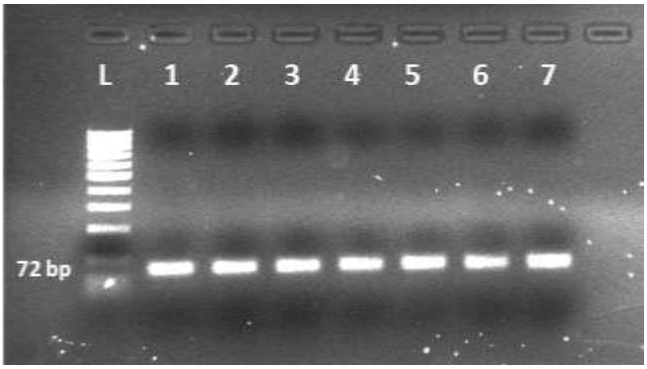

Figure 16: Agarose gel (2%) in 1xTris-acetate-EDTA confirming the size of the *Arp* QPCR product of 72bp. Lanes (L) DNA 100bp ladder and samples tested lane 1-7. Lane 1-7 represents day 0, 1, 2, 3, 5, 8 and 10 during differentiation protocol of the 3T3-L1 cell line.

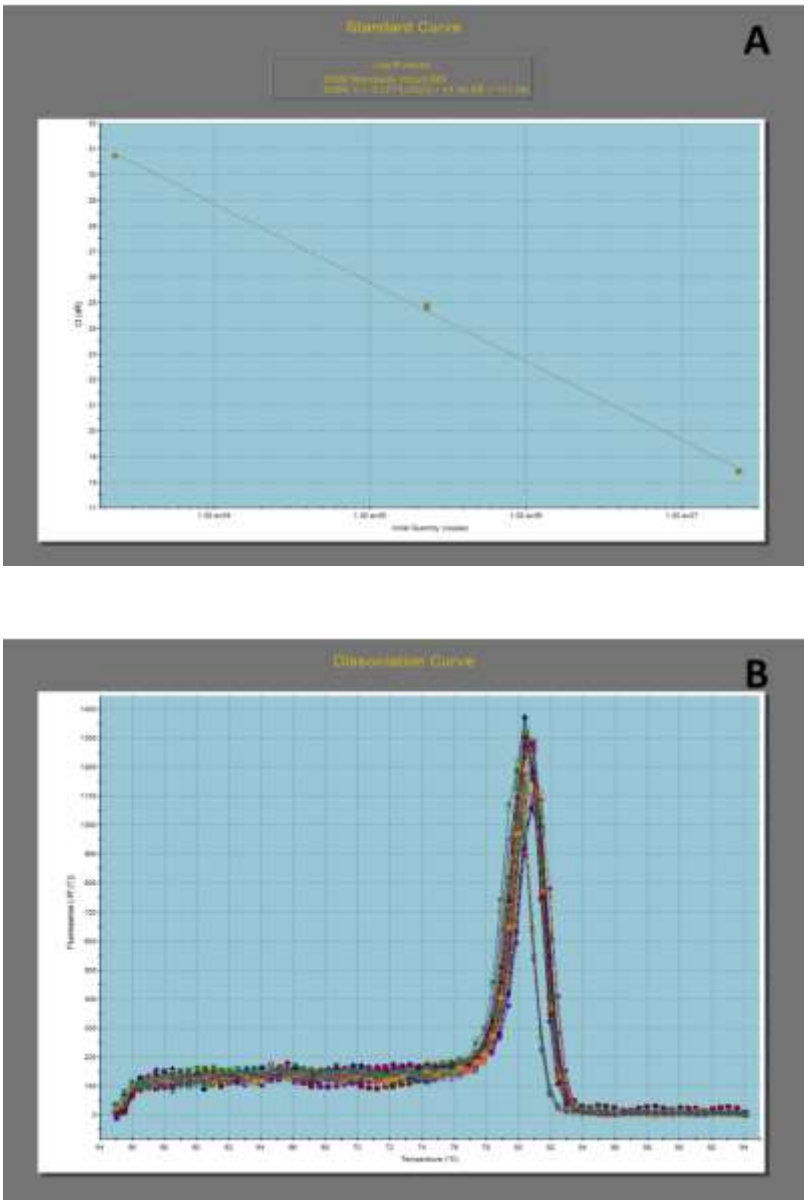

Figure 17: Validation of *Arp* QPCR assay performed on serial dilutions of plasmid DNA producing the standard curve (A) and single melting peak curve analysis (B).

2.3.3 $PGF_{2\alpha}$ reduces 3T3-L1 cell proliferation by prolonging the G2/M phase

In the 3T3-L1 cell line, the population doubling time (PDT) of untreated cells was 27.3 ± 4.4 (mean ± standard deviations) hours. The DMSO control at 0.02% significantly increased the PDT to a mean of 44.6 ± 14.4 hours (p=0.007 compared to the untreated cells). $PGF_{2\alpha}$ at 10^{-8} M concentration significantly reduced 3T3-L1 cell proliferation with PDT of 93.6 ± 15.0 hours (p=0.049 compared to DMSO control). However, the limited half-life of the compound resulted in recovery of cell proliferation, with cell numbers returning towards untreated levels by day 3. In contrast, daily administration of $PGF_{2\alpha}$ produced a sustained significant reduction in proliferation (see Figure 18).

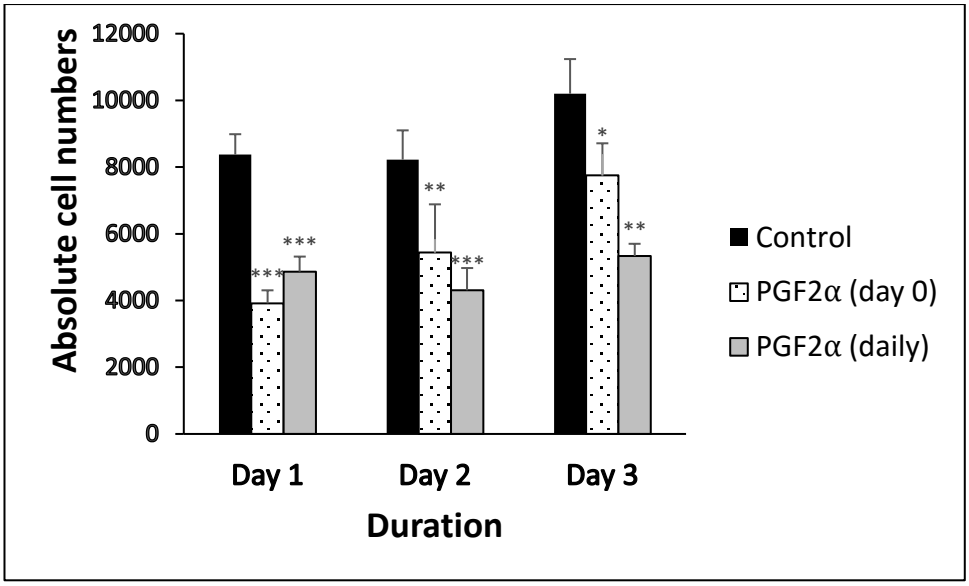

Figure 18: Direct cell counting to assess the effects of $PGF_{2\alpha}$ on proliferation of 3T3-L1 cells cultured alone (black bars, DMSO control), with addition of 10^{-8}M $PGF_{2\alpha}$ on day 0 (stippled bars) or with daily addition of $PGF_{2\alpha}$ (grey bars). Results are expressed as the mean ± SD of 2 individual experiments all performed in triplicate. *p<0.05, **p<0.01 and ***p<0.001 compared with the control on the respective days.

To exclude simple toxicity as the cause of reduced growth, trypan blue exclusion was performed and indicated >90% survival across three concentration of $PGF_{2\alpha}$ (10^{-8}M to 10^{-6}M), suggesting that this is not the case (see Figure 19). In the same experiment, we also obtained a dose-dependent decrease in proliferation.

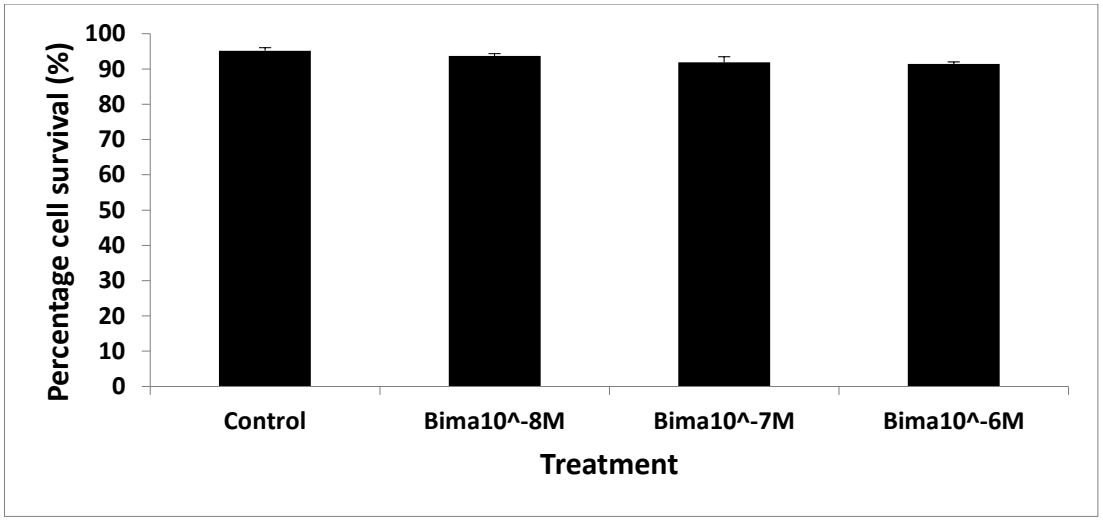

Figure 19: Trypan blue exclusion study on 3T3-L1 showing more than 90% survival across three concentration of $PGF_{2\alpha}$ (10^{-8}M to 10^{-6}M). Results are expressed as the mean ± SD of individual experiments (n=3) all performed in triplicate.

To determine whether an increase in apoptosis or cell cycle disruption was responsible for the increased PDT, cell cycle analysis was undertaken. Our results illustrate that $PGF_{2\alpha}$ significantly increased the percentage of cells in the G2/M phase from 23.97 ± 2.87% in untreated to 35.65 ± 1.29% in treated cells, p = 0.04 (see Figure 20), indicating prolongation of this stage, but did not increase the proportion of cells undergoing apoptosis (as defined by the pre-G1 peak). The cell cycle analysis histogram reports DNA content with the G1 peak representing normal diploid DNA content and the G2+M peak representing double this amount as the cells prepare for mitosis. Therefore, the pre-G1 peak indicates less than the diploid DNA content as occurs in cells undergoing apoptosis.

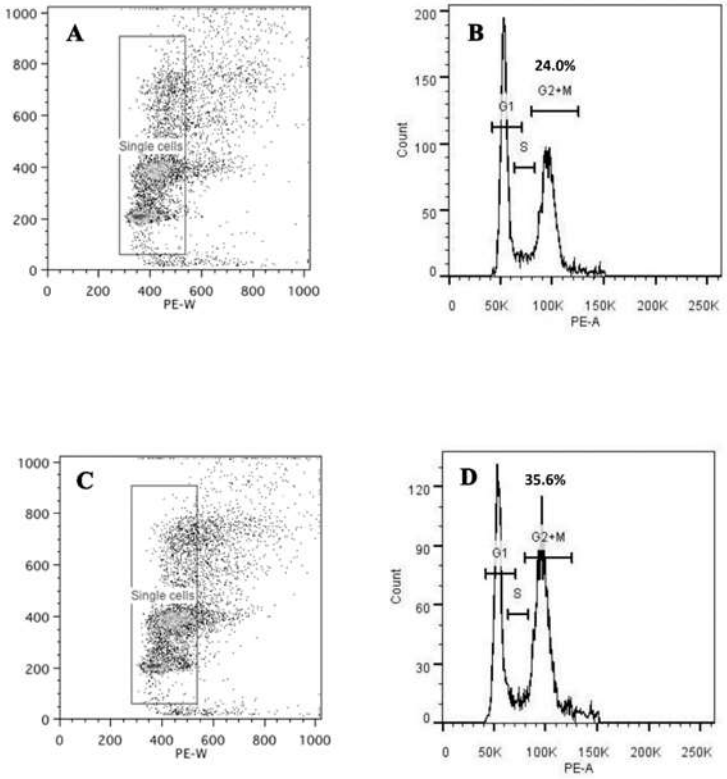

Figure 20: Cell cycle analysis of 3T3-L1, to assess $PGF_{2\alpha}$ effects, presented as scatter plots (A & C) and histograms (B & D) in control (A & B) and 10^{-6}M $PGF_{2\alpha}$ (C & D) treated cells. The x axis on the scatter plot represents cell size where the arbitrary box was drawn to gate single cells and the y axis represents fluorescence intensity of DNA dye (propidium iodide). The histograms show the G1, S and G2/M phases (figures above = percentage of cells) in (B) control (+ DMSO) medium or (D) treated with $PGF_{2\alpha}$. The histogram report DNA content (x axis) and cell number (y axis). The figure is a representative experiment of 2 performed, both in duplicate.

2.3.4 $PGF_{2\alpha}$ reduced in vitro-induced adipogenesis in 3T3-L1

In DM 3T3-L1 cells were induced to undergo adipogenesis with more than 70% of the cells acquiring a rounded appearance and intracellular lipid droplet accumulation. In our system, we managed to induce an approximately 14-fold increase in the terminal marker of differentiation, Glycerol-3-phosphate-dehydrogenase (*Gpdh*) transcript by day 7 as compared to day 0 (p=0.002). To hypothesise that the effect observed in this experiment was mediated by $PGF_{2\alpha}$ via its receptor (PTGFR), we have to show that

Ptgfr transcript is present. *Ptgfr* transcripts were detected in the 3T3-L1 at baseline and after differentiation with no apparent change during adipogenesis (Figure 21). In view of the proliferation results, which indicated that $PGF_{2\alpha}$ has a short half-life, the drug was added at every medium change throughout the period of differentiation. When assessing adipogenesis morphologically, in both treated and control groups, by day 3, adipogenic changes were seen but with no difference in the number of adipogenic foci. At day 7, the increase in numbers of lipid droplets was similar in $PGF_{2\alpha}$ treated cells and controls. I found that the adipogenesis process in 3T3-L1 was very rapid and diffuse hence difficult for us to show the morphological difference between treated and untreated cells. When using QPCR measurement of markers of differentiation, the presence of 10^{-8}M $PGF_{2\alpha}$ reduced transcripts for *Gpdh* by about 12-fold (p=0.01) with a dose dependent response (see Figure 22).

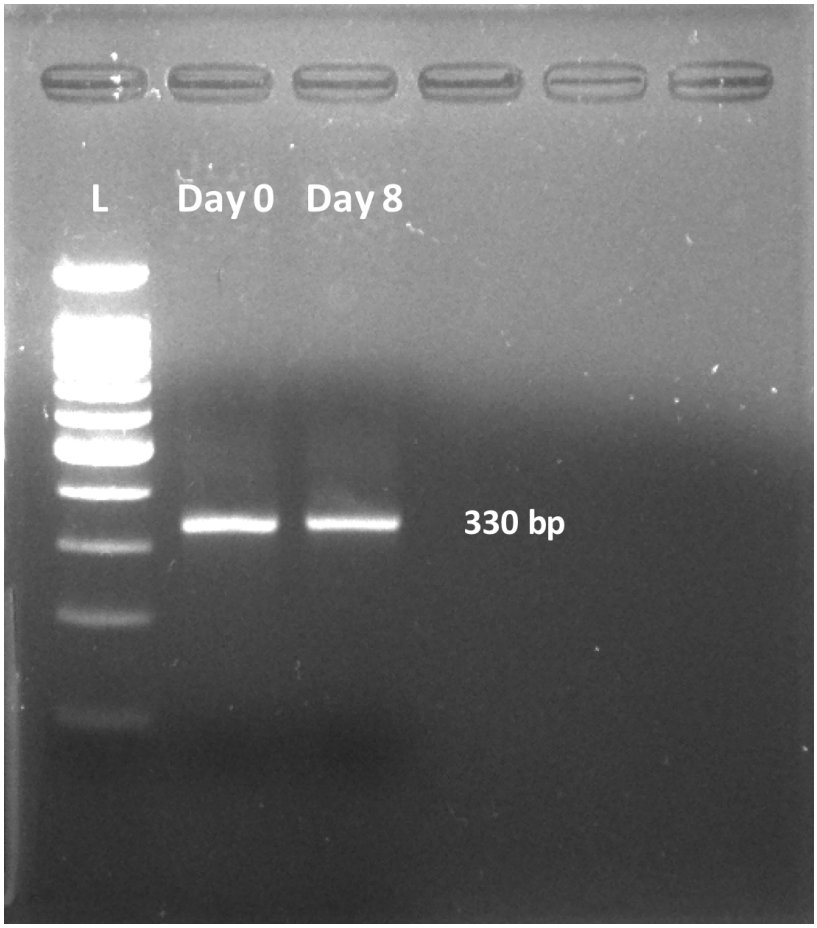

Figure 21: Agarose gel (2%) in 1xTris-acetate-EDTA confirming the size of the *Ptgfr* QPCR product of 330bp. Lanes (L) DNA 100bp ladder and samples tested on day 0 and 8 during differentiation protocol of the 3T3-L1 cell line.

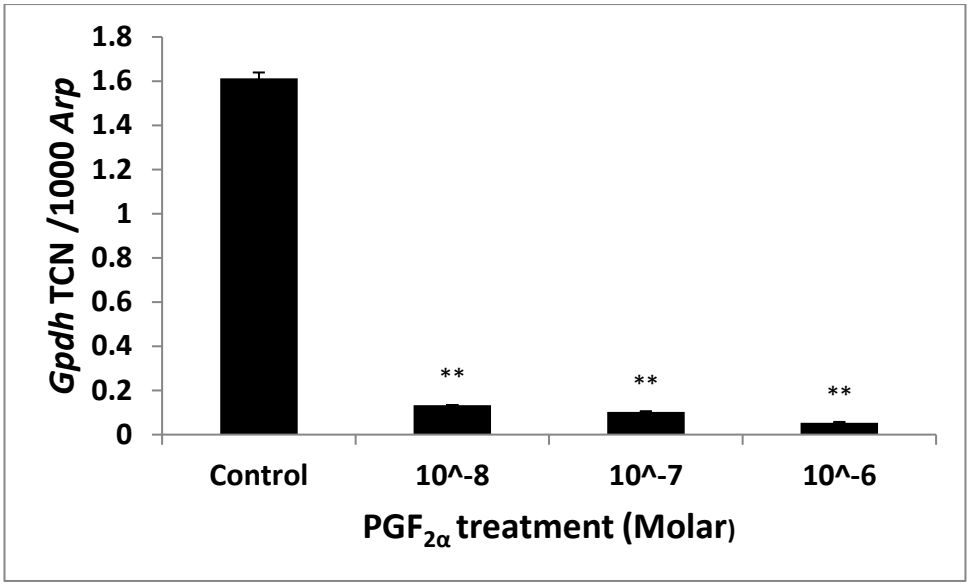

Figure 22: In vitro induced adipogenesis of 3T3-L1 cells assessed by QPCR measurement of glycerol-3-phosphate dehydrogenase (*Gpdh*) transcripts expressed as transcript copy number (TCN) per 1000 copies of acidic ribophosphoprotein (*Arp*) housekeeper gene following 7 days exposure to control (DM+DMSO) and treatment (DM+$PGF_{2\alpha}$). Data shown (mean ± SD) are from a representative experiment of two performed in duplicate. Error bar represents ± SD; **p< 0.01.

2.3.5 $PGF_{2\alpha}$ had no effect on lipolysis on differentiating 3T3-L1

In order to study the effects of $PGF_{2\alpha}$ on 3T3-L1 lipolysis, we induced adipogenesis by culturing confluent cells in DM for 7 days. As noted above, at this point >70% of the cells had undergone differentiation and contained large lipid droplets although none were fully mature adipocytes with a single lipid vacuole, since these cells are not adherent and are removed during manipulations.

The effects of 10^{-8}M to 10^{-6}M $PGF_{2\alpha}$ on lipolysis were assessed in unstimulated in vitro differentiated cells and also in cells in which lipolysis was induced using 10^{-8}M to10^{-6}M norepinephrine (produced a dose-dependent increase in free glycerol peaking at 300%). $PGF_{2\alpha}$ alone did not induce lipolysis and had no effect on norepinephrine mediated lipolysis (see Figure 23).

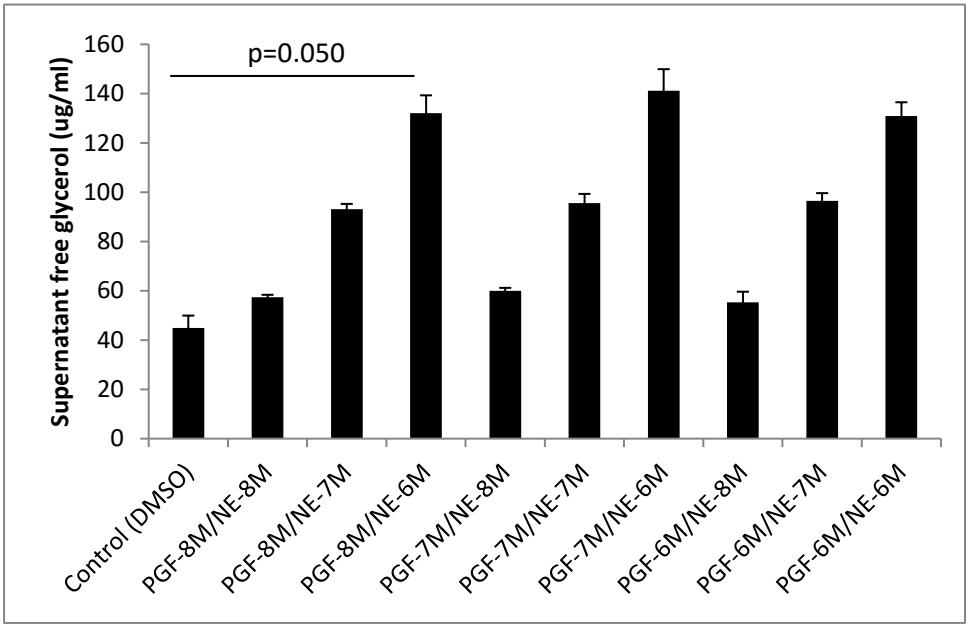

Figure 23: The lipolysis effect of $PGF_{2\alpha}$ was studied by inducing 3T3-L1 into adipogenesis for 7 days in unstimulated and stimulated conditions. The control contained DSMO 0.02% only whilst the stimulated contains $PGF_{2\alpha}$ at the concentrations of 10^{-8}M to 10^{-6}M and Norepinephrine at similar concentration ranges. The experiments were performed twice. Norepinephrine showed dose dependent effect on lipolysis but not $PGF_{2\alpha}$. Error bar represents median ± IQR.

2.3.6 Morphology of primary orbital fibroblast in complete and differentiation medium

After a few days in complete medium, primary human orbital fibroblasts (OF) proliferated out from explanted orbital fat piece as a very elongated cell with very long string like processes at both ends (see Figure 24). It would take approximately 1 month to obtain confluent cells in 6 well plates and few weeks longer if it was from normal/non-GO orbital fat explant. Similar duration was noted upon thawing and re-inoculating in the 75 ml flask. As the OFs became more confluent, they realign along themselves with their long processes interlacing with each other (see Figure 25 A and C). After 2-3 weeks in differentiation medium primary human OFs underwent

morphological changes characteristic of conversion from a fibroblast to adipocyte morphology. They appeared more rounded in shape filled with lipid droplets. These observations only happened in 30-40% of the primary OFs from GO samples and to a lesser degree (<5%) in normal OFs (see Figure 25 B and D).

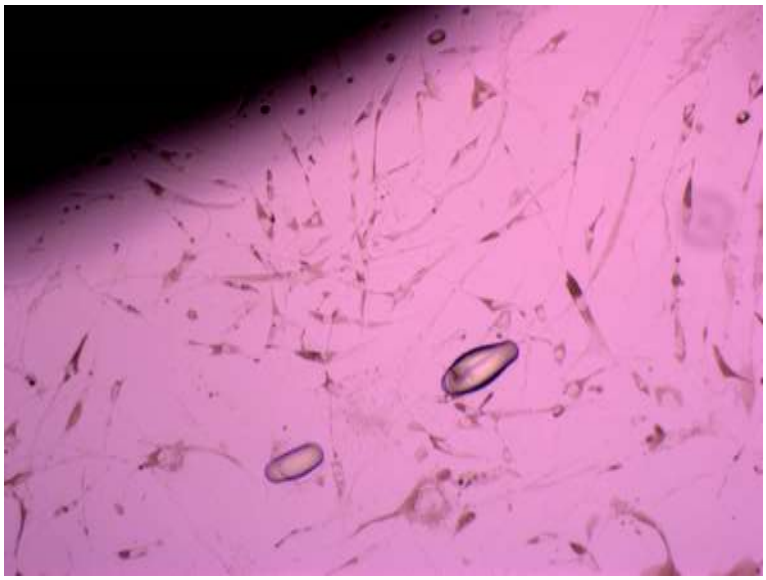

Figure 24: Orbital fat explant culture showing very narrow and elongated fibroblasts proliferated out from the fat (black shadow on the top left corner) after 3 days.

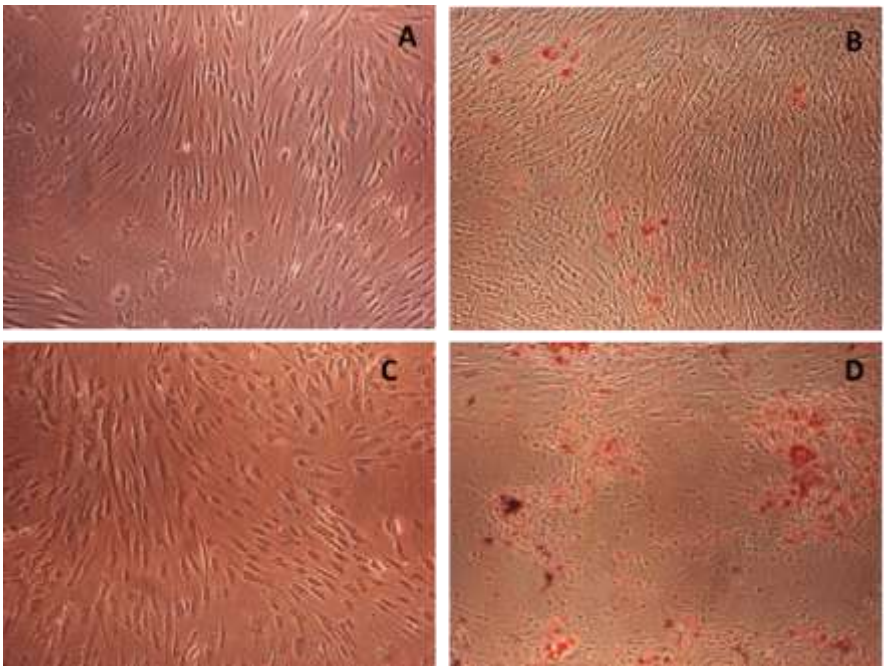

Figure 25: Phase contrast photomicrographs show various stages of adipocyte differentiation. Undifferentiated normal human orbital OFs at day 0 (A) and after 15 days in differentiation medium (B) stained with Oil Red O. Figure C (day 0) and D (day 15) representing OFs from GO patients indicating higher degree of lipid droplet accumulation. Magnification 100x.

2.3.7 Validation of the QPCR assay

Example of optimization of *APRT* genes showing agarose gel electrophoresis (see Figure 26) and melt curve analysis (see Figure 27B) confirming that the *APRT* QPCR assay produced a single product of the correct size which was 247bp and had the correct sequence. Analysis of serial dilutions of *APRT* plasmid DNA (see Figure 27) was used to determine the efficiency of the assay. The slope was obtained by plotting the Ct values against serial plasmid DNA concentration dilutions using the MxPro software (Stratagene). This showed that the reaction has linear standard curve (r^2>0.999), consistency across replicates and amplification efficiency of 83.9%.

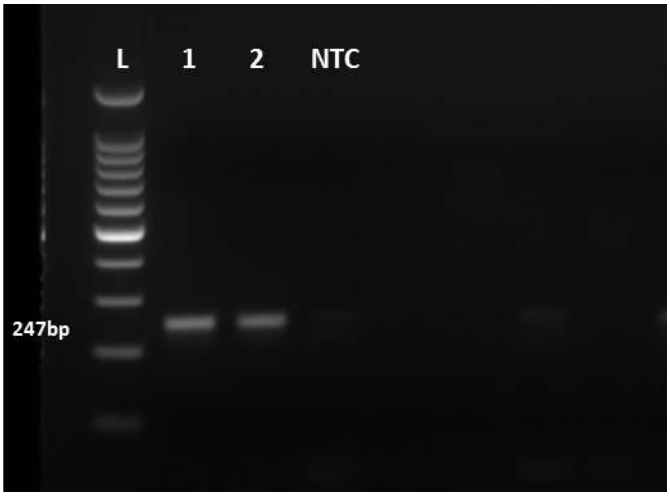

Figure 26: Example of agarose gel (2%) in 1xTAE confirming the size of the *APRT* QPCR product of 247bp. Lanes (L) DNA 100bp ladder, samples tested lane 1 & 2 and negative template control (NTC).

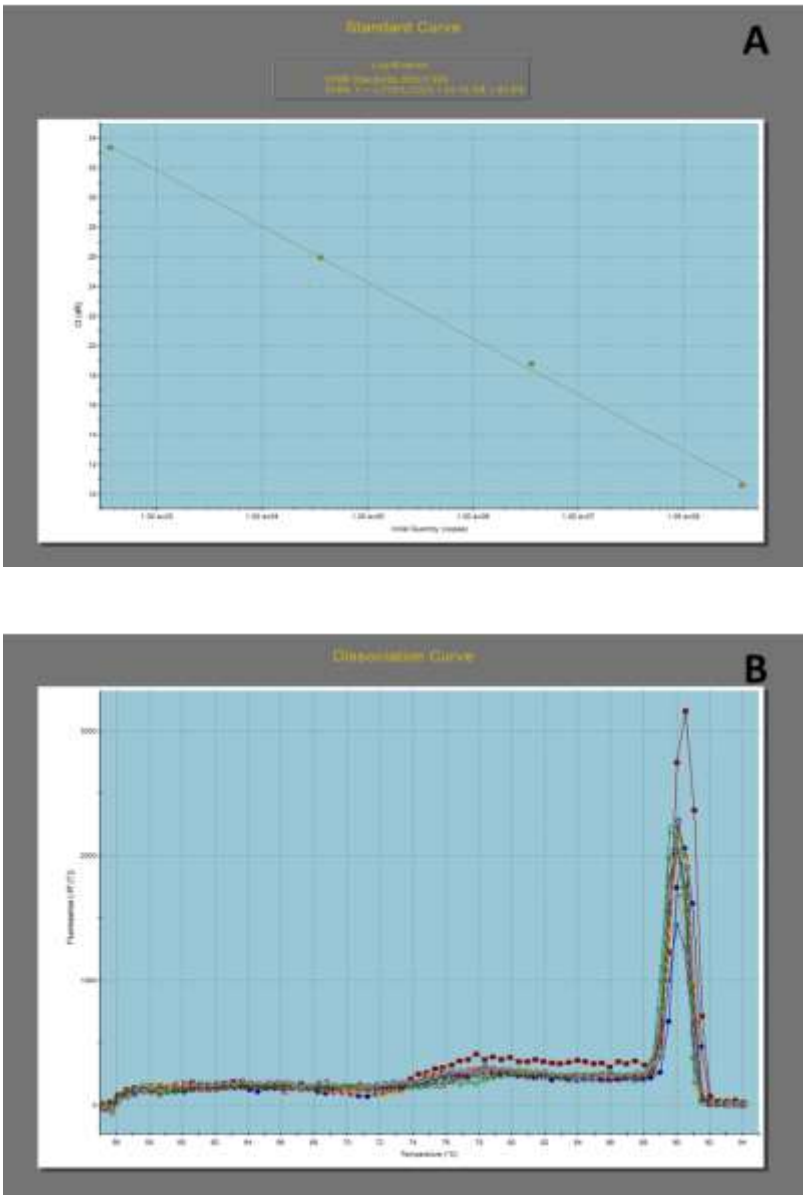

Figure 27: Validation of *APRT* QPCR assay performed on serial dilutions of plasmid DNA resulting the standard curve (A) and single melting peak curve analysis (B).

2.3.8 $PGF_{2\alpha}$ reduced cell proliferation in GO and non-GO orbital preadipocytes

We subsequently performed the experiments in primary OF obtained from patients with GO and individuals free of thyroid or other inflammatory eye disease. The average PDT for orbital cells from GO patients (n=3) was 5.36 ± 0.88 days but for

non-GO orbits (n=3) was 6.63 ± 0.69 days, the difference was significant (p=0.035) with GO orbital cells proliferating more rapidly. In view of the longer PDT of primary orbital cells, the effects of $PGF_{2\alpha}$ on proliferation were assessed by cell counting 5 days after plating in CM. Similar results to those for 3T3-L1 were obtained, in that $PGF_{2\alpha}$ reduced orbital cell proliferation both in GO and non-GO patients compared to control (Figure 28). Cell-cycle analysis of the primary OF also demonstrated G2/M phase arrest in both GO and non-GO populations. In non-GO OF the percentage of cells in G2/M in control was 17.14 ± 0.72 and increased to 22.43 ± 0.89 (p=0.003); whilst in GO OF, $PGF_{2\alpha}$ increased the percentage to 18.57 ± 0.17 from 12.49 ± 0.30 in the DMSO control (p<0.001) (Figure 29).

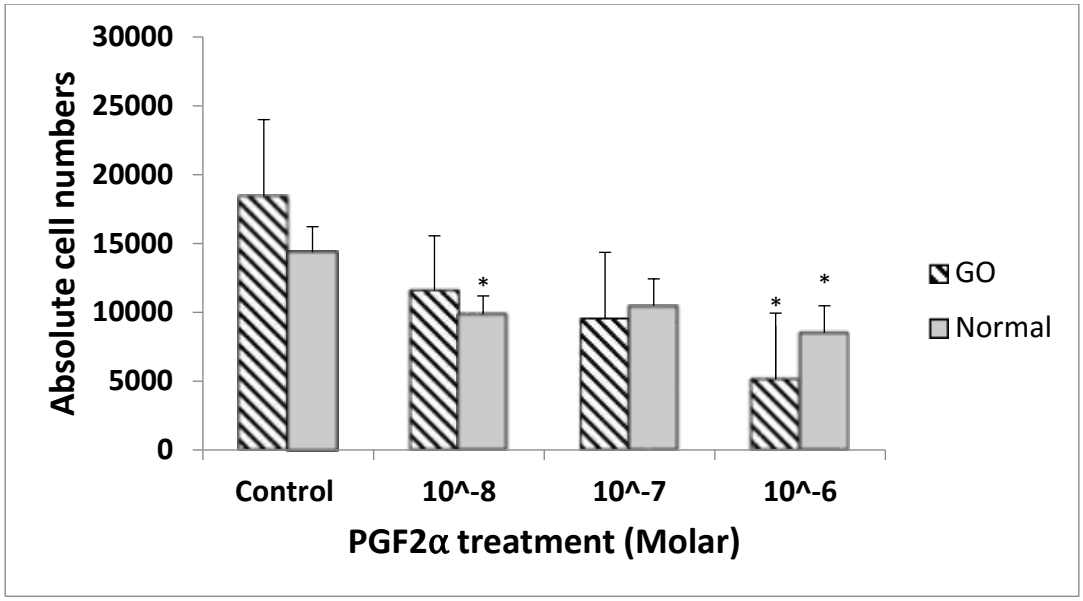

Figure 28: Direct cell counting to assess the effects of $PGF_{2\alpha}$ on proliferation of human orbital fibroblasts (OF) cultured for 5 days alone (DMSO control) or with 10^{-8}M to 10^{-6}M $PGF_{2\alpha}$ added on day 1 and 3. Stippled bars are Graves' OF (n=3) and grey bars non-GO (n=3). Results are presented as mean ± SD; *p value <0.05 compared to control on each respective day.

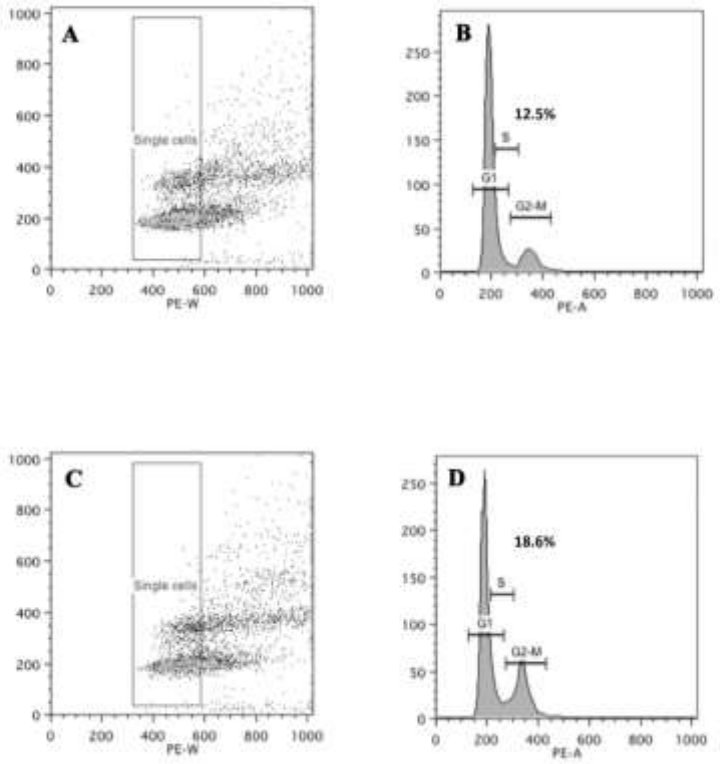

Figure 29: Cell cycle analysis was performed in orbital fibroblasts, to assess $PGF_{2\alpha}$ effects, presented as scatter plots (A & C) and histograms (B & D) in control (A & B) and 10^{-6} M $PGF_{2\alpha}$ (C & D) treated cells. The x axis on the scatter plot represents cell size where the arbitrary box was drawn to gate single cells and the y axis represents fluorescence intensity of DNA dye (propidium iodide). The histograms show the G1, S and G2/M (figures above = percent of cells) phases in (B) control (+ DMSO) medium or (D) treated with $PGF_{2\alpha}$. The histogram report DNA content (x axis) and cell number (y axis). The figure presents data from Graves' OF and is a representative experiment of 2 performed (using OF from different donors), both in duplicate.

2.3.9 $PGF_{2\alpha}$ reduced in vitro-induced adipogenesis in GO and non-GO preadipocytes

After 15 days incubation in DM, preadipocytes from GO and non-GO orbits were seen to be undergoing adipogenesis. Compared with the 3T3-L1 cell line, only a small proportion (up to 30-40%) of the primary cells differentiate by assuming a rounded appearance and forming lipid vacuoles. In our in vitro model, the addition of DM

induced at least a 500-fold increase in the terminal marker of differentiation *LPL* transcripts in GO orbital cells and an approximately 150-fold increase in those from non-GO orbits compared to day 0 ($p<0.001$). The increased adipogenic potential of the GO cells was further supported by their significantly higher colony count ($p=0.013$) and Oil Red O absorbance data ($p=0.008$), shown Figure 31.

$PGF_{2\alpha}$ receptor transcripts (*PTGFR*) were present in both normal and GO OF at baseline and after differentiation protocol with no apparent change during adipogenesis. (Figure 30). The addition of $PGF_{2\alpha}$ significantly inhibited adipogenesis in GO and non-GO OF when assessed by all 3 measures of differentiation (Figure 31 A-C). The drug produced visible signs of reduced adipocyte colony formation and Oil Red O staining, but its effects on adipogenesis were most apparent when comparing transcript levels for *LPL*. I have used *LPL* transcript marker in human study and *Gpdh* transcript marker for the mouse as the primers for both genes have been fully optimised in our lab for PCR use and also we have cloned the respective gene into a plasmid to allow absolute gene number quantification. A significant reduction in *LPL* transcripts was observed in cells from GO and non-GO orbits at all concentrations of $PGF_{2\alpha}$ from 10^{-8}M to 10^{-6}M, $p<0.01$. The effects were partly reversible as illustrated in Figure 32, in which OF exposed to the drug for 3 days had no significant reduction in adipogenesis, cells exposed for 6, 9, 12 or 15 days all demonstrated a significant reduction in differentiation but with no significant difference when comparing cells exposed for 15 days with those for 6, 9 or 12.

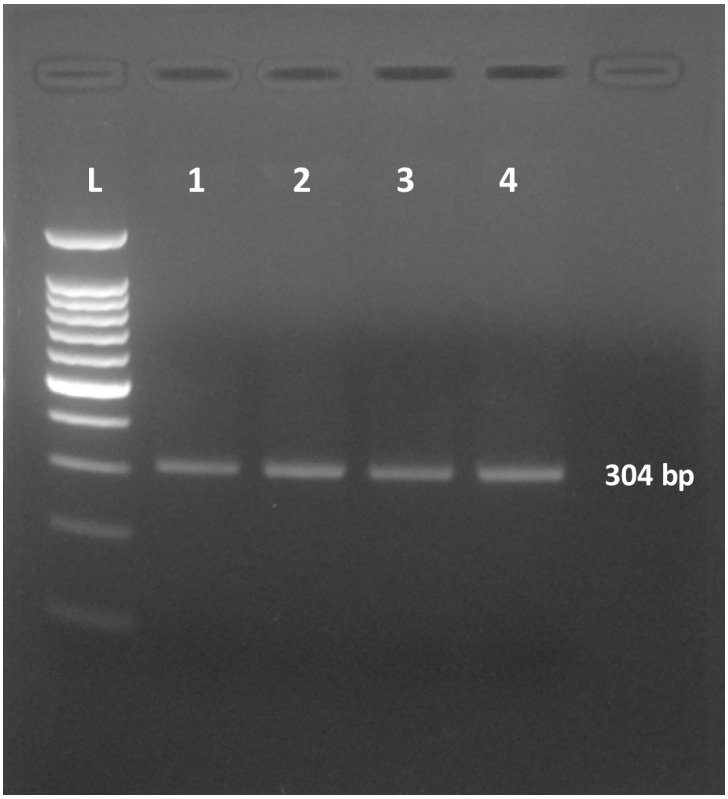

Figure 30: Agarose gel (2%) in 1xTAE confirming the size of the *PTGFR* QPCR product of 304bp. Lanes (L) DNA 100bp ladder, samples tested lane 1 & 2 were from normal OF on day 0 and after 15 days differentiation respectively and lane 3 and 4 were from GO OF on day 0 and after 15 days differentiation respectively.

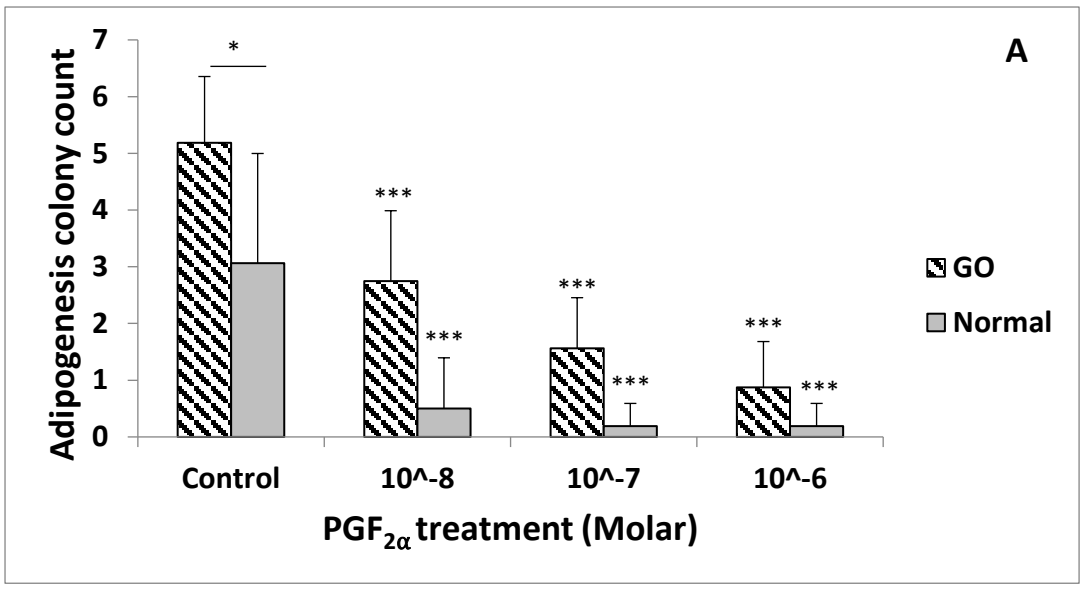

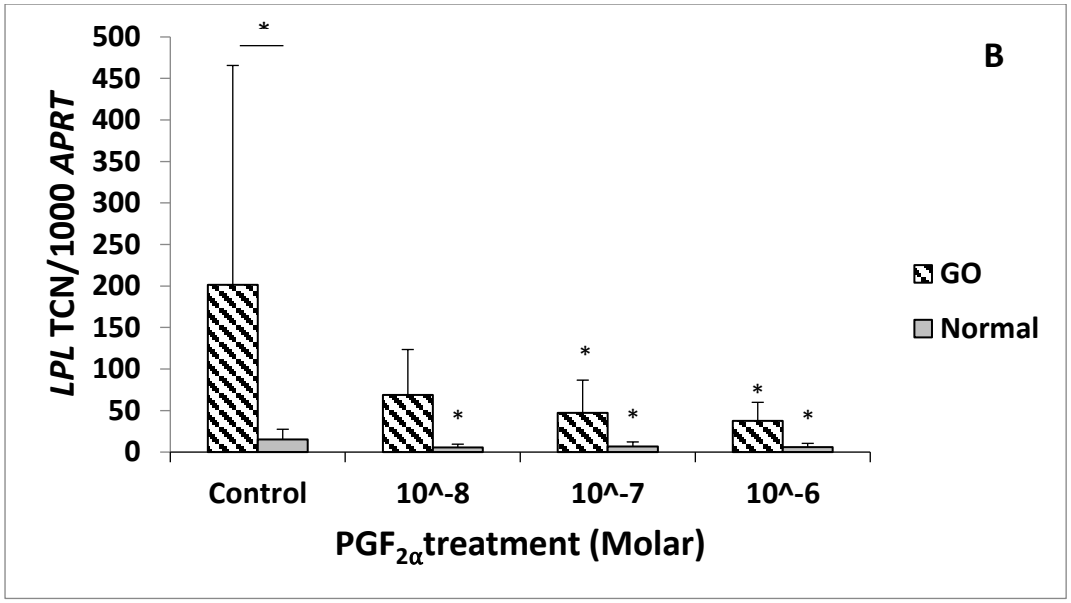

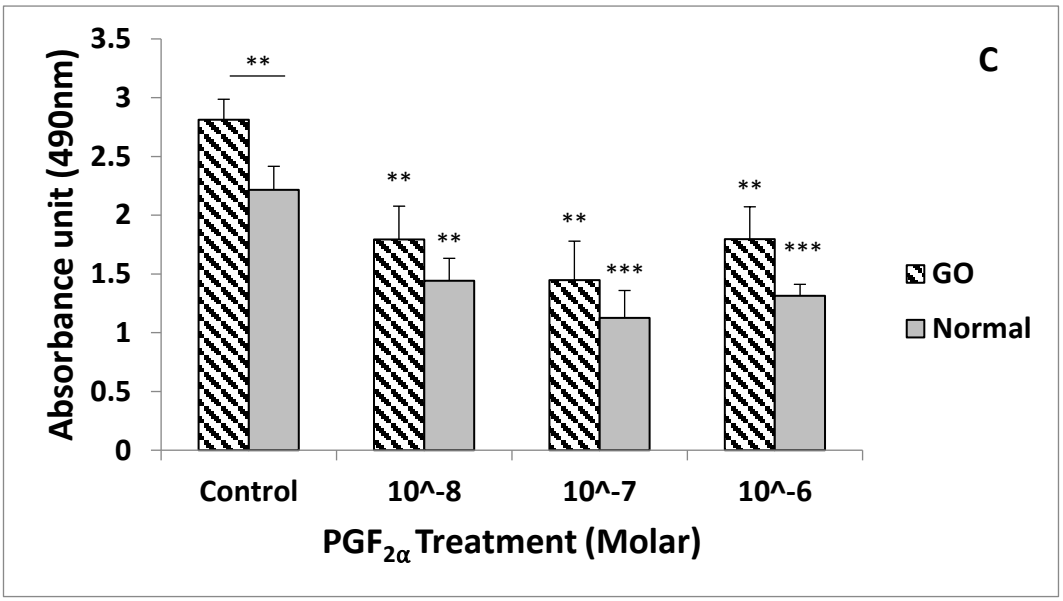

Figure 31: In vitro induced adipogenesis (15 days in DM) in orbital preadipocytes in control (DMSO) and $PGF_{2\alpha}$ treated cells was assessed by (A) counting foci of differentiation, (B) QPCR measurement of *LPL* transcripts and (C) quantification of Oil Red O staining. (A) Colony counts (n=3) are expressed as the mean ± SD from 4 representative quadrants of the well. (B) QPCR results (n=5) expressed as mean ± SD of transcript copy number (TCN) per 1000 copies of housekeeper gene (adenosine phosphoribosyl transferase, *APRT*). (C) Oil Red O staining (n=2) expressed as the mean ± SD of the OD490 absorbance. Stippled bars are Graves' OF and grey bars non-GO. In all cases, the bar above the control represents statistical comparison between GO and non-GO orbital cells, other comparisons are between treated and control, *p<0.05; **p<0.01; ***p<0.001.

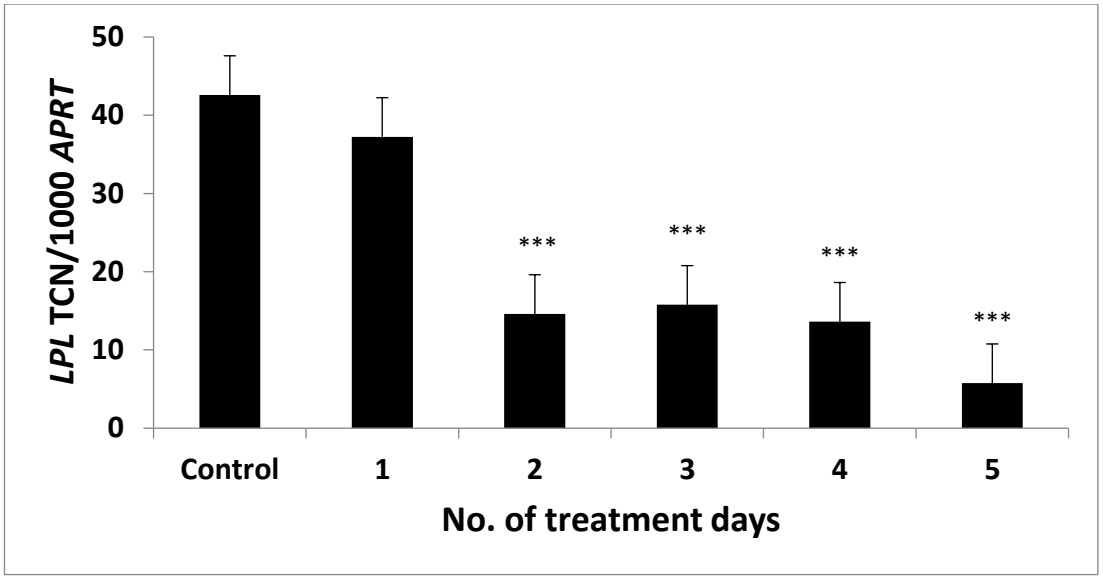

Figure 32: The effects of $PGF_{2\alpha}$ on adipogenesis are reversible; confluent Graves' OF (n=2) were treated with differentiation medium alone or supplemented with $PGF_{2\alpha}$ 10^{-6}M for varying periods during differentiation as indicated in the graph. Lipoprotein Lipase transcripts were measured on day 15 expressed as mean ± SD of transcript copy number (TCN) per 1000 copies of housekeeper gene (adenosine phosphoribosyl transferase, *APRT*). OF exposed to the drug for 3 days had no significant reduction in adipogenesis when LPL was measured 15 days later, indicating cell recovery; cells exposed for 6, 9, 12 or 15 days all demonstrated a significant reduction in adipogenesis. In all cases, comparisons are between treated and control, **p<0.01; ***p<0.001.

2.3.10 $PGF_{2\alpha}$ had no effect on lipolysis on mature orbital adipocytes

We obtained mature adipocytes from 2 GO patients and treated them with $PGF_{2\alpha}$ alone or in the presence of norepinephrine, as described above for the 3T3-L1 cell line. No concentration of $PGF_{2\alpha}$ induced lipolysis in basal conditions. Norepinephrine produced a dose-dependent increase in glycerol with a maximum of 260% of unstimulated, but as with the cell-line, this was not altered by $PGF_{2\alpha}$ (Figure 33).

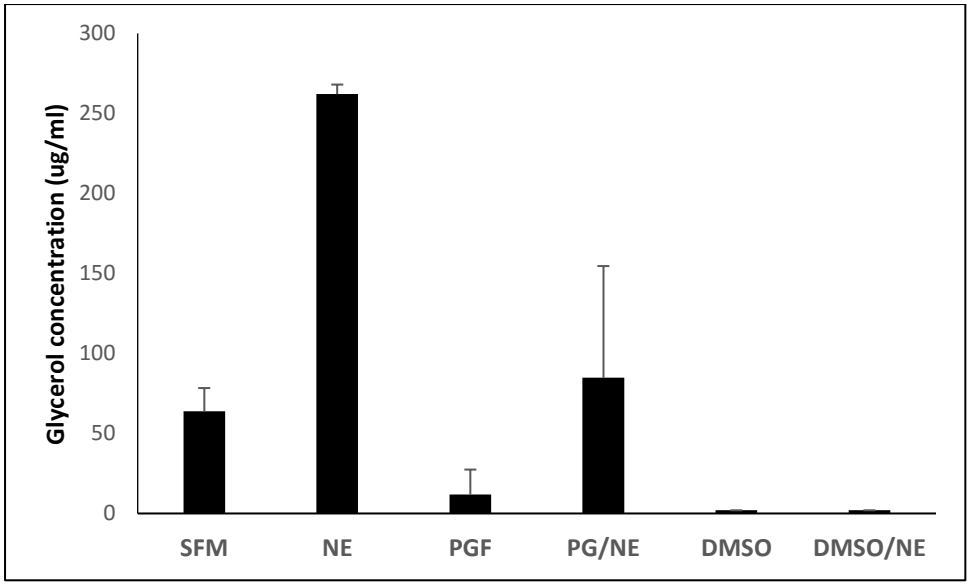

Figure 33: Mature adipocytes obtained from GO patients (n=2) via collagenase digest of orbital fat tissue tested in varying conditions. SFM: serum free media, NE: Norepinephrine (10^{-6}M), PGF: Prostaglandin $F_{2\alpha}$ (10^{-6}M), DMSO: Dimethyl sulfoxide (0.02% v/v). Experiments were performed in triplicates. Results were expressed as median ± interquartile range.

2.4 DISCUSSION

The study was designed to find out whether the observed enophthalmos in patients treated with $PGF_{2\alpha}$ is secondary to reductions in orbital tissue proliferation, adipogenesis and/or increased lipolysis using the well-established 3T3-L1 cell line and also human primary orbital fibroblasts from normal and patients with GO. The results presented in this study demonstrate that $PGF_{2\alpha}$ agonists could be a potential treatment for GO.

In the 3T3-L1 cell-line, proliferation was inhibited by $PGF_{2\alpha}$ in a dose-dependent manner, from 10^{-8}M (physiological concentration) to 10^{-6}M (pharmaceutical concentration). We are unaware of any studies investigating whether proliferation of 3T3-L1 is modified by $PGF_{2\alpha}$. The process appears to be mediated by prolongation of the G2/M phase of the cell cycle and not by cytotoxicity. This could potentially be mediated by downstream pathways of phospholipase C either via IP_3 or diacylglycerol-PKC route but would require further investigation [305]. Direct cell counting and toxicity was performed by using an automatic counter (Cellometer®) which is based on image analysis of the disposable counting chamber. Even though it is an automated counter, the process itself was labour intensive and highly variable especially at low cell numbers. This was mainly due to loss of cells during preparation and the presence of remaining volume of media on the cell pellet. As the resuspension volume is small (50 µl), any remaining media can potentially dilute the sample. To overcome this, the cells were centrifuged at 2000 rpm instead at 1000 rpm without causing cell rupture and each vial of the cells has to be manually aspirated to ensure that minimal residual media before resuspension in HBSS. Trypan blue analysis at 0.2% and 0.4% was found to be too concentrated for Cellometer® to read hence this was performed at 0.1% final concentration. For further reassurance, each set of experiments was performed in triplicates. The automated

counter is easy to use and reduces the amount of effort required to count cells compared to a traditional haemocytometer. Despite this, we found the technique has difficulty obtaining accurate measurements of cells that are extremely small (unable to distinguish the debris) or extremely dilute. We were surprised to note that the vehicle, DMSO, exerted significant inhibition of proliferation, even at very low concentrations. DMSO is a widely used reagent in cell biology. It is commonly used as a solvent due to its efficiency as a carrier for a wide range of chemicals. It is also used to differentiate cells and its mode of action includes cell cycle arrest [321] but it should be noted that $PGF_{2\alpha}$ exerted an additional significant reduction in proliferation.

The inhibitory effects of $PGF_{2\alpha}$ on adipogenesis are in agreement with those of several other authors [310, 322, 323]. This is despite using different adipogenic cocktails than us (3-isobutyl-1-methylxanthine instead of pioglitazone and T_3) which might be due to a common inhibitory pathway by the $PGF_{2\alpha}$. Prostaglandins are known to exert their effects either via surface or nuclear receptors (Majority are via surface G-protein coupled receptors) and different prostaglandin molecules have different potency in inhibiting adipogenesis. This suggests that the process might be mediated by binding to FP receptor [324]. Membranes prepared from either undifferentiated or differentiated 3T3-L1 exhibited similar specific binding for [3H] $PGF_{2\alpha}$ suggesting that FP receptors are present throughout differentiation [324]. It is proposed that stimulation of FP receptor leads to increase in intracellular calcium via activation of phospholipase C [305] and the release of calcium. This in turn leads to activation of calmodulin-dependent protein kinase (CaMK) [324], calcineurin-dependent signalling pathway [310] and activation of mitogen-activated protein kinase resulting in phosphorylation of PPARγ [325] which is the main regulator of adipogenesis. Casimir et al [323] reported that endogenous $PGF_{2\alpha}$ production is higher in undifferentiated then differentiated cells and postulated that its release from preadipocytes provides a control mechanism to limit adipogenesis. This could be via

reduction in the substrate arachidonic acid which moves towards eicosatrienoic acid production during adipogenesis process [326].

We were unable to demonstrate any modification of lipolysis, either basal or norepinephrine induced, by $PGF_{2\alpha}$. Other studies using different $PGF_{2\alpha}$ analogues (latanoprost and travoprost) also did not show the effect of $PGF_{2\alpha}$ on lipolysis [322]. We found that DMSO has no effect on lipolysis. We used in vitro differentiated 3T3-L1, which displayed abundant lipid accumulation but these had not coalesced into the single vacuole which typifies a mature adipocyte (MA). Since MA cells are non-adherent, they are lost from the culture well during media changes, but the immaturity of the cells used might provide some explanation for the absence of any effect. Using in vitro differentiated human adipocytes for studying lipolysis was not performed because the adipogenesis process happens in patches, and even remarkably less so in normal OFs cultures, making the comparison even more difficult. However, the fact that we did not observe any effect of $PGF_{2\alpha}$ on lipolysis, when using freshly isolated MA from human orbital adipose tissues, albeit both samples are from GO patients, suggests that this limitation had minimal impact on the interpretation of the results. We were unable to use normal fat sample as the sample received is too small for collagenase digest.

Experiments using OF from human orbits revealed disease-associated differences, e.g. significantly higher proliferation and adipogenic potential in cells from GO patients compared with those from donors free of any inflammatory eye problem or thyroid disease; even though the GO tissues were obtained from patients with apparently inactive disease. The increased proliferation in GO has been reported previously [327] and the enhanced adipogenesis agrees with previous ex vivo data from ourselves [120] and others [328].

$PGF_{2\alpha}$ significantly inhibited the proliferation of OFs, originating in GO and non-GO

orbits and agree with the results of Seibold et al [329] but using human subcutaneous preadipocytes. This is consistent with previous clinical reports and MRI studies regarding $PGF_{2\alpha}$ causing upper eyelid sulcus deepening and reduced infraorbital fat combined with enophthalmos [281, 298, 301]. Similarly, in cell cycle analyses, in common with the 3T3-L1 cell line, there was an accumulation of OFs in the G2/M phase, with GO and non-GO cells being similarly affected.

In agreement with Choi and colleagues [330] we showed that $PGF_{2\alpha}$ also inhibited adipogenesis in OF. Although these authors only investigated cells from normal orbits, our studies illustrate that the GO OFs remain highly responsive to the drug and have not become resistant e.g. by losing FP receptors. This is in contrast with the result from Silvestri et al which suggested that FP receptor is down regulated during adipogenesis using commercially available human subcutaneous preadipocytes [331].

We recognise that this study has limitations, including the use of in vitro models devoid of the inflammatory cytokines and cell-cell interactions operating in GO orbits. The differences observed also could be due to differences of the donors' age and sites of the biopsy (blepharoplasty procedures from controls and orbital decompression from GO). The model of adipogenesis itself is using supraphysiological concentration of dexamethasone, insulin, PPARγ and T_3. However the models have been used by ourselves [332] and others [245, 328] to provide valuable insights into the tissue remodelling leading to GO, and in the absence of a robust animal model is the best currently available. Current case reports of $PGF_{2\alpha}$ causing enophthalmos are small. However, since most patients receive treatment to both eyes it is possible that the incidence of enophthalmos in $PGF_{2\alpha}$ treated patients has been underestimated.

The results obtained are encouraging, since they indicate that several of the

mechanisms which contribute to the expansion of the orbital volume, and responsible for the exophthalmos in GO, are inhibited by $PGF_{2\alpha}$. The inhibitory actions on proliferation and differentiation were obtained in the range of 10^{-8}M to10^{-6}M $PGF_{2\alpha}$ and even the most concentrated is 3 orders of magnitude less than the 0.03% used in eye drops; although this is a prodrug. The prodrug, 17-phenyl trinor $PGF_{2\alpha}$ ethyl amide needs to be converted by an amidase enzyme present in human cornea, to the corresponding free acid, 17-phenyl trinor $PGF_{2\alpha}$ [333, 334]. The latter free acid compound, which we used in these experiments to negate the requirement of the amidase enzyme, is a potent FP receptor agonist but has a short half-life, as illustrated by the rapid recovery of 3T3-L1 proliferation and OF adipogenesis when the agent was withdrawn, and indicates that daily administration would be required.

We would predict that the drug will reach the retro-orbital space to exert its intended effect, since topical ocular administration of $PGF_{2\alpha}$ leads to its detection in the aqueous humor and systemic circulation [335, 336]; the existence of reduced periorbital fat in Bimatoprost treated patients also supports the prediction [301]. Fortunately, drug formulations containing $PGF_{2\alpha}$ have been in regular use for glaucoma for more than a decade, and indeed nowadays $PGF_{2\alpha}$ preparations are available over-the-counter for cosmetic application, thus their safety is well established.

About 1 in 5 of patients with Graves' disease suffer with disfiguring eye disease or GO [149]. The majority of these patients have inactive disease in which the disfigurement persists, but there is no longer active inflammation. Rehabilitative surgery and symptomatic treatment is the mainstay of treatment for the late disease phase. However, surgery is not always successful in reducing proptosis. Here we suggest $PGF_{2\alpha}$ agonists may thus be particularly useful in the late-phase of GO, a disease stage in which disfigurement and impairment of ocular function persists after

resolution of the initial inflammatory process and which affects 5-10 times as many people as the early active phase. Stable inactive patients also mean that the true effect $PGF_{2\alpha}$ can be measured and not due to natural progress of the disease itself. We conclude that randomised clinical trials of $PGF_{2\alpha}$ and/or associated products are warranted in GO.

Chapter Three

3 PROSTAGLANDIN F2-ALPHA EYE DROPS (BIMATOPROST) IN GRAVES' ORBITOPATHY: A RANDOMISED CONTROLLED DOUBLE BLIND CROSSOVER TRIAL

3.1 INTRODUCTION

Graves' orbitopathy (GO) is the commonest extra thyroidal manifestation of Graves' hyperthyroidism. A key mechanism underlying GO is an increase in adipogenesis in the orbit resulting in orbital volume expansion and proptosis (eye protrusion). Proptosis may persist after inflammation has subsided in the late "burnt out" phase of GO and the persistent disfigured appearance of the eyes is a source of significant psychological distress and impaired quality of life for sufferers. Despite the negative impact of the condition, however, there are no specific medical treatments that target orbital volume reduction in late stage disease. Furthermore, a UK nationwide survey of patients with GO revealed low satisfaction levels with existing therapies [337]. In this study, we propose to take advantage of the observation that enophthalmos (recession of the eye into the orbit) occurs in some patients treated with prostaglandin analogue eye drops like Bimatoprost ($PGF_{2\alpha}$) for glaucoma as well as our in vitro findings reported in Chapter 2, that prostaglandin analogues reduce fat expansion. We hypothesise that topical treatment with Bimatoprost may reduce orbital tissue volume in non-inflamed orbits and thereby improve quality of life in patients with GO.

3.1.1 Current management

The natural history of GO comprises an early active inflammatory phase followed by a late or “burnt out” disease phase. For the majority of patients these treatments are supportive but in 5-10% of cases the disease is severe enough to merit major immunosuppressive therapy (e.g. high dose steroids or ciclosporin) and orbital radiotherapy during the inflamed "active" phase of the disease, or surgical decompression and rehabilitative surgery at a later stage [338]. Each of these treatment modalities has significant drawbacks in terms of side effects. Surgical decompression carries the risk of worsening double vision and local complications, while high dose steroid therapy may be complicated by weight gain, diabetes mellitus, depression, or life threatening liver dysfunction and is not effective in "burnt-out" disease; orbital radiotherapy is not always effective and carries the potential risk of a tumour developing at the treatment site [339].

As mentioned above, most available non-surgical treatments are targeted towards control of inflammation during the active stage whereas rehabilitative surgery is the mainstay of treatment for the late disease phase. However, surgery is not always successful in reducing proptosis and carries the attendant risks of anaesthesia and local complications, (decompression surgery is highly skilled and involves removal of one, two or three orbital walls). $PGF_{2\alpha}$ agonists may thus be particularly useful in the late-phase of GO, a disease stage in which disfigurement and impairment of ocular function persists after resolution of the initial inflammatory process and which affects 5-10 times as many people as the early active phase. If $PGF_{2\alpha}$ is confirmed to be effective in reducing proptosis in this study, it would indicate that $PGF_{2\alpha}$ could represent a safe, locally acting agent in the management of GO, reducing the need for potentially high risk therapies such as surgical rehabilitation.

3.1.2 Pathophysiology

The main pathological features of GO include expansion of orbital tissue fat, mononuclear cell infiltration of orbital connective tissue and extra ocular muscle, and tissue remodelling, a process that can culminate in fibrosis and diminished eye motility [278]. A key mechanism underlying GO is an increase in adipogenesis and associated secretion of glycosaminoglycans in the orbit, resulting in an increase in orbital volume and exophthalmos (protrusion of the eye) [247, 262]. The opposite effect, enophthalmos (recession of the eye into the orbit), has been described in patients with glaucoma treated with daily Bimatoprost ($PGF_{2\alpha}$), a prostaglandin analogue used topically in the management of intraocular hypertension (glaucoma). Cases of enophthalmos developing in patients treated with Bimatoprost have been reported worldwide, albeit in small numbers [280-282]. This side effect is more noticeable if only one eye is exposed to treatment as the treated eye is easily comparable with the unexposed eye. However, since most patients receive treatment to both eyes it is possible that the incidence of enophthalmos in Bimatoprost treated patients has been underestimated.

3.1.3 Mechanism of action and trial rationale

A possible mechanism by which $PGF_{2\alpha}$ agonists might produce enophthalmos is through reduction of orbital fat volume [280]. A $PGF_{2\alpha}$ receptor agonist has been shown to be a potent inhibitor of adipose differentiation in new-born rat precursor cells [340]. This raises the possibility that $PGF_{2\alpha}$ exerts direct effects on adipose tissue precursors. We have confirmed this finding in in-vitro studies in our laboratory using 3T3-L1 cell lines and human primary orbital fibroblast cultures. Thus, $PGF_{2\alpha}$ agonists may be effective in reducing orbital fat expansion, ameliorating proptosis, and thus improving quality of life in patients with GO. There has been no clinical trial of $PGF_{2\alpha}$

agonists in patients with GO. We hypothesize that in order for Bimatoprost to work, patients must have active adipogenesis in vivo. In our in vitro model, most GO samples were from inactive or burnt out GO who underwent orbital decompression. Despite this, the tissues still have higher proliferation and adipogenesis potential than cells from normal orbits. This was shown in Chapter 2.

3.2 METHODS

3.2.1 Conduct of trial

The trial was conducted according to the protocol and in compliance with the principles of the Declaration of Helsinki (1996), the principles of Good Clinical Practice (GCP) and in accordance with Medicines for Human Use (Clinical Trials) Regulations 2004, as amended in 2006, the Research Governance Framework for Health and Social Care, the Data Protection Act 1998 and other regulatory requirements as appropriate. The trial has been approved by a local NHS Research Ethics Committee (REC, registration number: 14/WA/0081), the Medicines and Healthcare Products Regulatory Agency (MHRA, registration number: 21323/0043/001-0001) and is registered with ClinicalTrials.gov (registration number: NCT02059655) and International standard randomized controlled trial network (ISRCTN, registration number: ISRCTN46696624).

3.2.2 Trial design

3.2.2.1 Cross-over design

The study was a randomised placebo controlled double blind cross over design, which was chosen for several reasons. First each participant serves as his or her own control thus reducing the influence of confounding variables (e.g. smoking status).

Second, each patient is exposed to both control and treatment and thus the design is highly efficient in that it reduces the actual number of participants required for the study. This is particularly useful for conditions like GO in which the prevalence of the condition is relatively low. Lastly the quick onset and short duration of action of Bimatoprost eye drops (reversible in 3 days in vitro cell cultures [18]) makes this a feasible design to study its effects. The drawback of this study design was that the long term effect of the treatment on patient outcomes, side effects and costs cannot be estimated, however short term efficacy could be assessed with good value for money.

We had carefully considered the risk of carry over and discussed this with our advisory statisticians. As a result, we had extended the wash-out period from 1 month in our initial plans to 2 months, since the evidence suggested that carryover effect is likely to be negligible with the 2 months wash out period, allowing us to take advantage of the crossover design. In human studies, the elimination half-life of topical Bimatoprost is 45 minutes and the intra ocular pharmacological effect is not known to exceed 24 hours [17]. By one month the drug is completely washed out and we have allowed an extra one month of recovery period for any tissue changes to stabilise. Clinical case reports [13-15] suggest that effects wear off in 4-6 weeks so that a 2-month washout period will allow subjects to experience both treatment and placebo equally. Therefore, the two-month washout period should be adequate for complete elimination of the drug and for its biological effect to have worn off. Analysis of any treatment order effect will confirm this was the case at the end of the study.

3.2.2.2 Patients recruitment

This was a randomised controlled double blind crossover trial of Bimatoprost in GO. Thirty-one patients with stable late inactive disease were enrolled. Patients was

allocated either Bimatoprost or placebo for 3 months, followed by 2 months wash out period before crossing over to the opposite treatment. Follow-up continued for 10 months' duration. The key eligibility criteria were patients with stable proptosis of at least 6 months' duration.

Patients were recruited from the multidisciplinary thyroid eye disease clinic at University Hospital of Wales. There is a database of 200 patients with inactive (previously treated) thyroid eye disease of which we expected 60% to be ineligible such as due to patient refusal, current treatment with glaucoma eye drops, recent steroid usage or disease reactivation. This would leave 80 patients available for recruitment in the 6 months available; assuming a 60% recruitment rate we should achieve the target of 31 by contacting 50 patients. We intended to consent 31 patients with a diagnosis of GO in the late inactive disease stage and meeting the inclusion and exclusion criteria. The diagnosis of GO was made by a consultant ophthalmologist on the basis of clinical assessment. ***GO was diagnosed clinically in the presence of one or more of the following features: soft tissue changes in the eye, proptosis, extra ocular muscle dysfunction, corneal abnormalities, and optic nerve involvement.*** Allocation of subjects was by randomisation and minimisation to ensure balance between the 2 trial arms. This service was provided by remote computerised web-based allocation of treatment arm (https://trials.cardiff.ac.uk/BIMA) and was supported by telephone service during working hours should network failure occur.

Figure 34: Expected participant flow

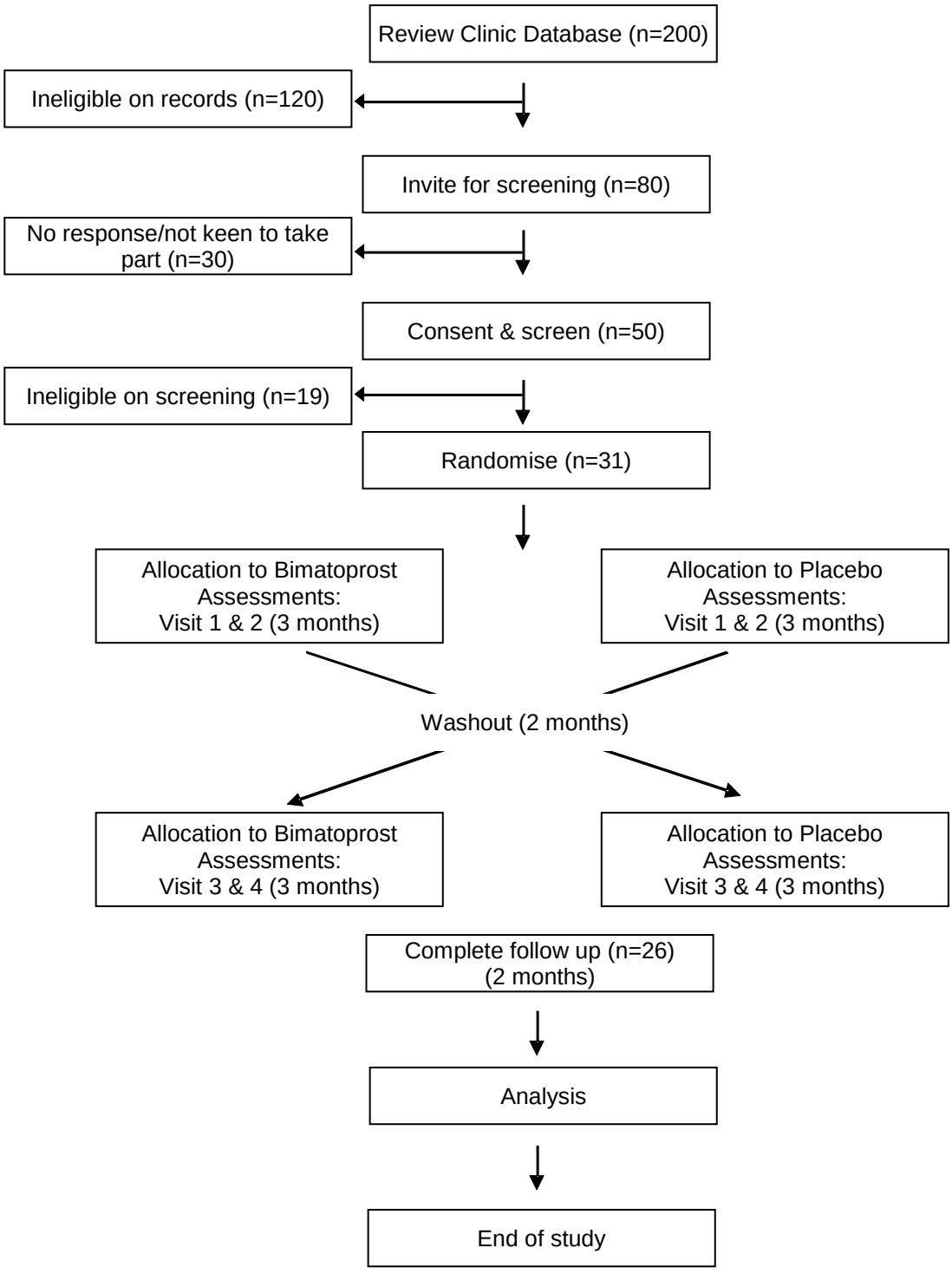

Trial participants were randomised to receive Bimatoprost or placebo (illustrated above (n=expected number of participants)).

3.2.3 Selection of subjects

3.2.3.1 Inclusion criteria

1. Stable GO with no reported change in proptosis for at least 6 months. See section 3.2.2.2 for GO definition;
2. Clinical activity score <3 (Appendix 4);
3. Proptosis (subjective unilateral proptosis confirmed by asymmetry in exophthalmometry of >2mm OR greater than 20 mm on exophthalmometry measurement in one eye);
4. Euthyroid (FT3 and FT4 in the reference range);
5. If female, must be using a reliable form of contraception during the trial, e.g. oral contraceptive and condom, intra-uterine device (IUD) and condom, diaphragm with spermicide and condom.

3.2.3.2 Exclusion criteria

1. Age <18 yrs;
2. Dysthyroid optic neuropathy unless previously treated;
3. Pregnancy or lactation;
4. Previous Corneal Herpes Simplex infection;
5. On therapy for glaucoma or intraocular hypertension;
6. Less than 6 months from prior systemic steroid use;
7. Aphakia, pseudophakia with torn posterior lens capsule or anterior chamber lenses;
8. Patient with risk factors for cystoid macular oedema, iritis or uveitis;
9. Severe Asthma (risk of severe allergic reaction to medication);
10. Previous allergy to Bimatoprost or preservative.

3.2.3.3 Baseline assessment

Potentially eligible patients were assessed by one of the Clinical Investigators. Patients received a patient information sheet at least 24 hours before this visit. Any questions related to the trial was answered prior to signing informed consent. Subjects fitting the clinical eligibility criteria were invited to enter the trial.

The purpose of the baseline visit was to confirm eligibility, further discuss the pros and cons of taking part in the study, obtain consent in patient agreeing to participate and conduct the trial baseline assessments. A case record form (CRF) was used to record the information and a modified version of the Initial Assessment Proforma published in 2002 by the European Group on Graves Orbitopathy (EUGOGO) was used. The key components of the baseline visit were to document:

<u>Medical History</u>

a. Duration and severity of GO symptoms
b. GO treatment to date
c. Prior and current thyroid status and treatments
d. Ocular Co-morbidity
e. General Past Medical History
f. Current medications
g. Smoking History
h. Weight and Height

<u>Ophthalmological assessment</u>

a. Proptosis (using an Oculus© exophthalmometer)
b. Intraocular pressure in primary position and up gaze

c. logMAR Visual Acuity

d. Clinical activity score (CAS)*

e. Palpebral aperture*

f. Gorman's diplopia score

g. Corneal integrity (Defined as healthy/dry (staining)/ulcerated) *

*(*Please see appendix 4)*

Photographs

Colour photographs of the eye in the lateral and anterior views according to standard operating procedure.

Blood tests

Thyroid Function Tests (TSH, FT3, FT4). These was analysed in endocrinology laboratory University Hospital of Wales, as per standard practice. See appendix 4 or management of abnormal thyroid function test.

3.2.4 Trial treatments

3.2.4.1 Bimatoprost 0.03%

Bimatoprost (Lumigan®) was administered at a strength of 0.03%. This was purchased from the manufacturer (Allergan) and is the strength used in the treatment of intraocular hypertension and glaucoma. It was administered at a dose of one drop in the eye once daily between 6:00 - 00:00 pm starting from the day of allocation. It was self-applied to the affected eye in unilateral involvement or in case of bilateral involvement, to both eyes.

3.2.4.2 Placebo

The placebo was an artificial tear purchased from the manufacturer (Blumont Healthcare). To enhance masking the placebo contained artificial tears with similar preservative (Benzalkonium chloride) which replicated any mild stinging sensation experienced with Bimatoprost. It was administered at a dose of one drop in the eye once daily between 6:00 - 00:00 pm starting from the day of allocation. It was self-applied as per Bimatoprost eye drops.

3.2.4.3 Concomitant medication

Patients were allowed to use preservative free eye drops during the trial which had to be applied at least 30 minutes before/after IMP application. No other eye drops were allowed during the trial period. Patients were asked during each visit regarding any change in their regular medication especially recent steroid exposure.

3.2.5 Follow up assessment

The primary outcome measure for the trial was based on exophthalmometry readings of proptosis measured using a Hertel exophthalmometer, according to a standard operating procedure. This was assessed by the lead ophthalmology investigator at each follow-up visit and their measurement recorded on the trial's Clinical Report Form. Please refer to visit schedule in Appendix 4 for more details.

The key components of the follow-up visits were:

1. Ophthalmological assessments
2. Adverse events
3. Any Changes in medications (including thyroid treatments)
4. Any Changes in smoking habit
5. Weight
6. Colour photographs of the eye in the lateral and anterior views according to standard operating procedure
7. GO-QOL (Appendix 4) done at clinic visits
8. EQ-5D-5L (Appendix 4 done at clinic visits
9. Review of clinical blood tests

3.2.6 Objectives

The overall objective was to determine whether Bimatoprost eye drops can reduce proptosis in inactive thyroid eye disease.

3.2.6.1 Primary endpoint

The primary endpoint of the study was to compare the change in exophthalmometry readings over the two 3-month treatment periods. A treatment effect of reducing

proptosis by 2 mm for treatment compared to placebo would be considered clinically relevant.

3.2.6.2 Secondary endpoints

1. Change in quality of life scores on the GO quality of life questionnaire (GO-QOL). The GO-QOL measures two different aspects of health related quality of life: (1) visual functioning as a consequence of double vision and decreased visual acuity (question 1-7) and (2) psychosocial functioning as a consequence of a changed appearance (question 8-15). A score of 1, 2, or 3 was assigned to each of the questions in each subscale to indicate whether the limitation was marked, mild, or absent, respectively. The scores were added to obtain a raw score. The final score was calculated as follows: [(raw score-7)/14x100]. In case one item has to be excluded (no answer to one question) the final score is calculated as follows: [(raw score-6)/12x100. The scores range from a minimum of 0 (marked limitation) to 100 (no limitation). A change of at least 6 points was considered a minimal clinically important difference (MCID). This cut-off value was derived from a previous study in which the MCID, defined as the smallest difference in score on the domain of interest which patients perceived as of benefit and which would mandate, in the absence of troublesome side effects and costs, a change in the patient's management in either GO-QOL subscales appeared to be 6 points. The change was measured during the 2 treatment periods and 2 two-month wash out periods (between treatment and at the end of the trial). This would indicate whether QOL is improved or worsened once the effect of medication wears off during the washout phase.

2. Change in intraocular pressures (IOP)

IOP during primary gaze and chin forward position:

a) Treatment versus placebo and

b) Primary gaze versus chin forward pressure.

3. Side effect profiles of Bimatoprost in GO patients during the study.

Safety was evaluated with a summary of adverse events. All trial subjects were asked about co-morbidities, medications and new or unexpected symptoms at each follow-up visit (collected via patient's diary), as well as an ophthalmic and general examination. Patient's photographic assessment by a blinded assessor also was performed.

Common side effects

I. Conjunctival redness

II. Lengthening of eyelashes

III. Darkening of eye lashes

IV. Peri-ocular skin pigmentation

V. Darkening of the iris

Rare side effects

I. Iris cysts

II. Cystoid macular oedema

III. Anterior uveitis

IV. Reactivation of herpes simplex virus infection.

4. Health economic evaluation

The primary intention of the economic evaluation was to explore the cost associated with GO treatment. It was measured from the perspective of the NHS, the patient and society using the client service receipt inventory

(CSRI) which had been modified under the guidance of a health economist to capture the cost associated with Graves' disease and GO. In theory, Bimatoprost intervention would lead to the net cost savings to NHS in comparison to surgical rehabilitation that the patient otherwise would go through. We were aware of limitations in the trial design as its primary intention is to evaluate efficacy of Bimatoprost in GO, not to follow up patients until they might need surgery. However, it would be useful to collect the resource use and quality of life data during this trial period on a pilot basis which may lead to a larger health economic focus study in the future. It was not envisaged that the crossover design would yield data that could allow a meaningful incremental cost-effectiveness ratio (ICER) to be calculated for Bimatoprost against placebo, as the duration of effects on perceived quality of life cannot be predicted in advance.

3.2.6.3 Other outcomes

1. Generic (EQ-5D-5L) Health Questionnaire
2. Clinical activity score
3. Total eye score
4. Palpebral aperture
5. Subjective eye changes
6. Patients' satisfaction with the treatments
7. Blinding success (assessor and patient)
8. Photographic assessments

3.2.7 Statistical analysis

3.2.7.1 Determination of sample size

The primary outcome of interest was the change in proptosis with Bimatoprost treatment and a reduction of 2 mm or more was regarded as clinically relevant. Previous studies have shown a standard deviation of 2.5 mm in proptosis measurements in patients with GO [19, 20]. We calculated that 16 participants would be needed to be able to identify a treatment effect of 2 mm as statistically different (p=0.05, two-sided, power 0.84) and 26 participants would be needed to be able to identify a treatment effect of 1.6 mm as statistically significant (p=0.05, two-sided, power 0.88) (Figure 35). We have opted for the latter which meant we would have more data (26 participants) but a smaller treatment effect than originally intended. Allowing for a 15% dropout rate and/or incomplete datasets, we intended to recruit 31 participants. If the number of participants with incomplete datasets reached 30% there would still be 80% power to detect an effect of this size.

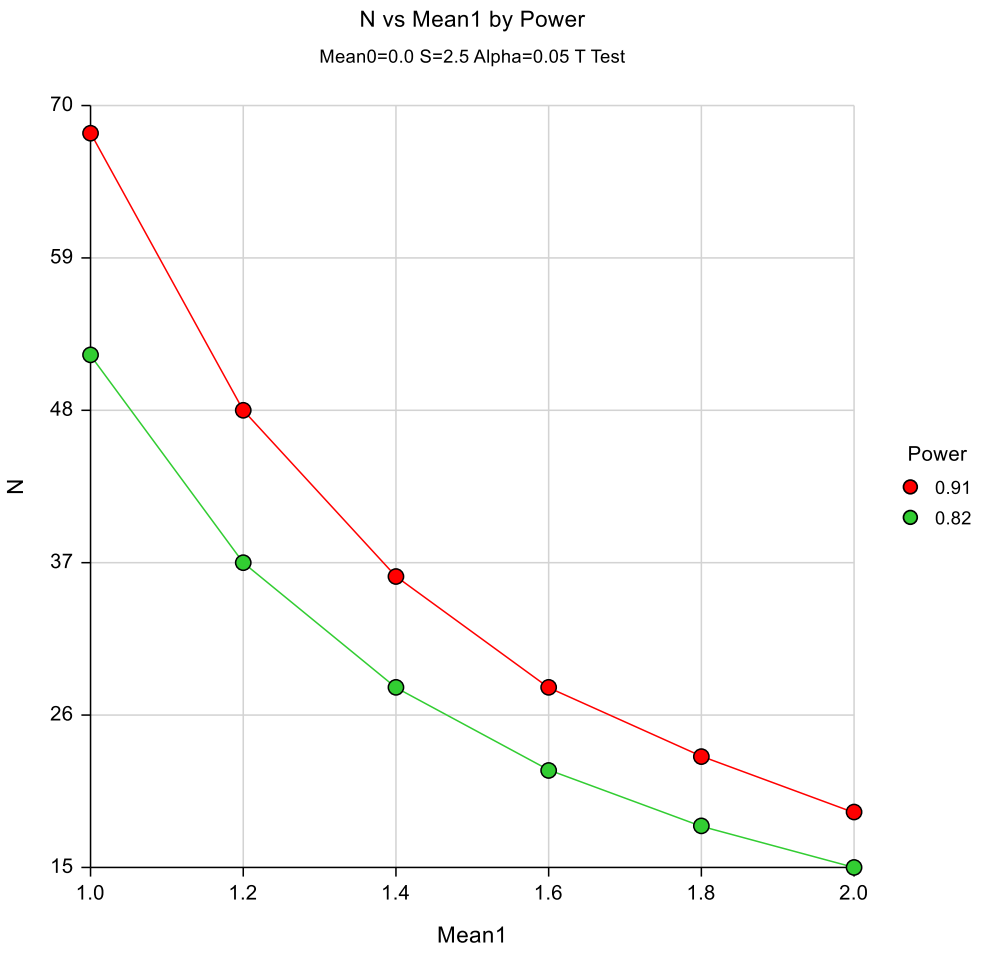

Figure 35: Graph plot of power calculation. Total sample size (N) was plotted against size effect in millimetres (Mean1) with standard deviation of the differences is 2.5 mm using a significance level (alpha) of 0.05 and two-sided paired t-test. It shows that that sample size drops as effect size increases. Red dot indicates power of approximately 91% and green dot indicates power of 82%.

3.2.7.2 Data preparation

Data cleaning and preparation were carried out prior to analysis. The process involved monitoring the following:

1. Naming and labelling of all variables and values
2. Presence of duplicates in the file;
3. Presence of non-existent patients;
4. Compulsory completion of a variable;

5. Out-of-range values;
6. Logical inconsistencies between variables;
7. Missing data investigated and data imputation considered where missing is not considered to be at random;
8. Data set preparation for multilevel modelling to include both eyes and both phases where appropriate;
9. Normality of outcome variables investigated.

Data analysis was proceeded according to CONSORT guidelines for randomised controlled trials.

3.2.7.3 Demographic and Baseline Characteristics

Descriptive statistics were used to describe the group of individuals recruited to the trial in relation to those eligible, and to investigate comparability of the trial arms at baseline. A tabulation of demographic and clinical variables was carried out to identify any chance imbalances at baseline between the two treatment groups.

3.2.7.4 Primary outcome analysis

1. The mean change in proptosis measurement in the treated phase and control phase was compared with a paired t-test and displayed visually using Box plots. This was carried out using the mean improvement of the two eyes where both have been treated.

2. Proptosis for patients with both eyes treated and the one eye for patients with only one treated eye was analysed using a multilevel

model in STATA. This would also enable us to use one data point for those patients who were unwilling or unable to proceed to the second phase of the protocol, thus using all available data as efficiently as possible.

Demographic and clinical variables (including baseline, the order of treatment and carryover effects) were used in this multilevel model regression model to reduce the unexplained variance and obtain better estimates of effect size with tighter confidence intervals. The results were expressed as millimetres effect from the treatment arm controlling for the placebo effect with 95% confidence intervals and p-values.

3. Phase effects and carry over effects were also reported in this way, but the study had not been designed to be powered to detect these effects as statistically significant unless they are as large as the treatment effect.

3.2.7.5 Secondary outcome and other analysis

Secondary and other outcomes were summarized with descriptive statistics. Continuous variables were summarized with n, mean and standard deviation for normally distributed data and with n, median and interquartile range for non-parametric data. Frequency counts and percentage of subjects within each category were provided for categorical data.

These secondary outcome variables were tested for differences by treatment phase using Wilcoxon signed rank tests and McNemar's tests for non-normally distributed data and categorical data respectively for significance testing. To provide statistics on the strength of differences between the two phases, mean differences with 95%

confidence intervals were produced for normally distributed variables, and similar 95% confidence intervals were provided where possible for other types of statistic.

The frequency of adverse effects was compared in the treatment and control phases by observation of data tables and where appropriate use of the McNemar X2 for paired samples.

3.3 RESULTS

3.3.1 Trial process

Seventy-two patients were invited initially of which 33 agreed for the trial enrolment. One patient was ineligible on screening and one patient chose not to take part due to fear that Bimatoprost might change her pupil colour. Thirty-one patients were subsequently randomised and underwent the first phase of the trial successfully. Unfortunately, one patient died at the end of wash out period due to pulmonary embolism which was not considered to be related to the investigational product. Therefore, 30 patients were entered into the second phase of the trial. One patient did not return for visit 4 (end of second phase assessment) due to withdrawal of consent. Twenty-nine patients entered second washout phase and completed the trial.

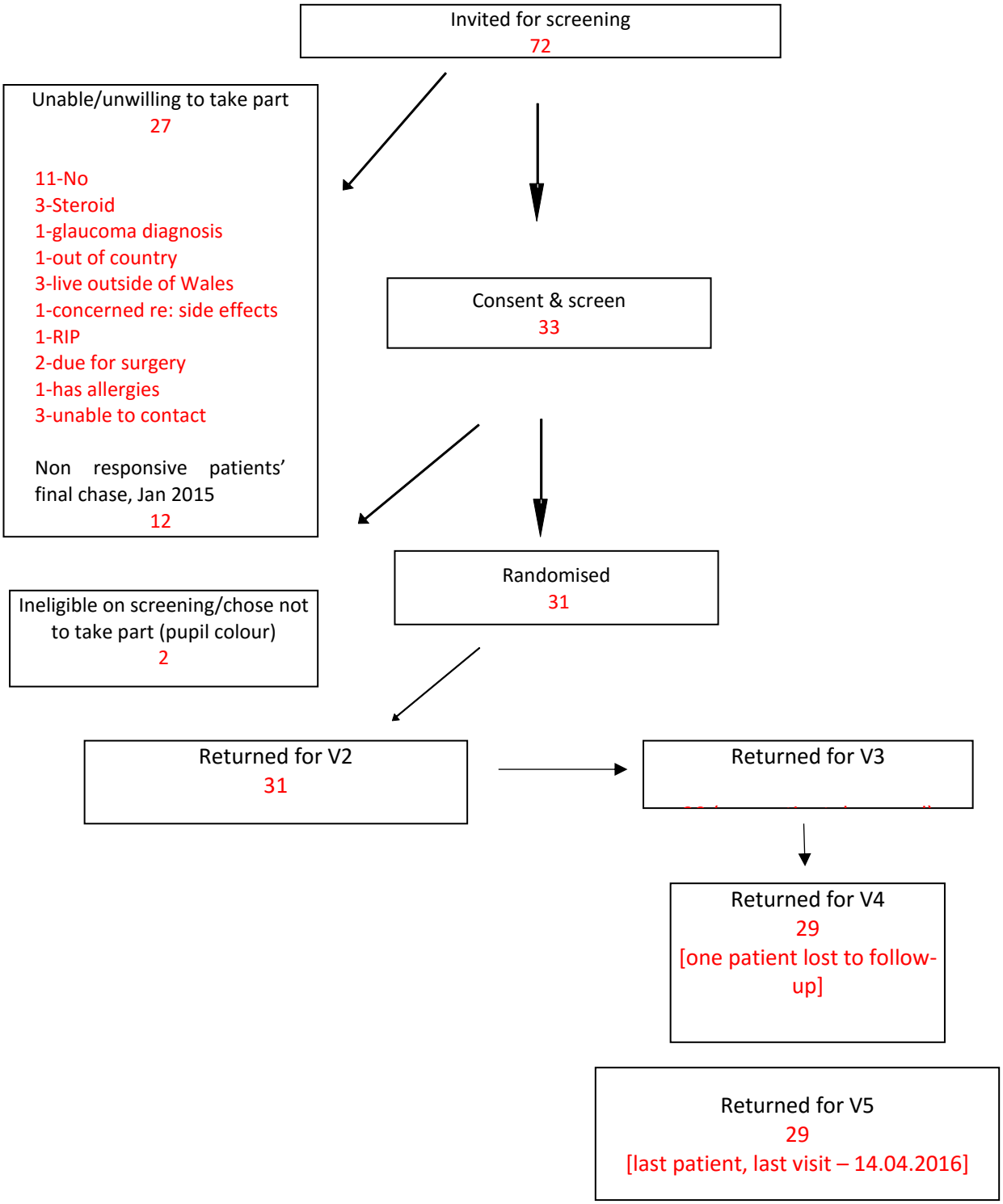

Figure 36: Study consort diagram

3.3.2 Demographic and baseline characteristics

Out of 31 patients, we have female preponderance with 5:1 ratio and mean age of 55 (SD 11). Patients had a median symptom duration of 4.0 (IQR 5.0) months before the diagnosis was made. As we were looking at late phase ‘burnt out’ GO, the median duration of GO was 7.6 (IQR 8.7) years. As expected the majority were smokers at diagnosis (74.2%) but this reduced to 38.7% after the diagnosis. The majority are still suffering from diplopia (61.3%) with bilateral involvement (61.3%). There was a good balance between the 2 treatment allocations with some differences on smoking history but not at trial entry and more patients with constant diplopia (Table 18).

Table 18: Demographics of all the trial patients and then split into treated with Bimatoprost first or placebo first phases. Data presented as means (standard deviation or range) unless stated otherwise or % (patient number/total).

Treatment allocations	**All patients**	**Bimatoprost**	**Placebo**
F:M (ratio)	26:5	14:2	12:3
Caucasian: Others (ratio)	29:2	14:2	15
Age (years)	55 (11)	55 (9)	55 (12)
BMI (kg/m2)	29.0 (6.5)	28.8 (6.3)	29.2 (7.0)
Symptom duration before diagnosis (months), median (IQR)	4.0 (5.0)	3.5 (4.5)	4.0 (5.0)
GO Duration (years), median (IQR)	7.6 (8.7)	8.8 (10.9)	7.1 (8.0)
Smokers at diagnosis (%)	74.2 (23/31)	81.2 (13/16)	66.7 (10/15)
Current smoking (%)	38.7 (12/31)	37.5 (6/16)	40.0 (6/15)
No. cigarettes/week	84 (0-280)	82 (0-280)	86 (5-210)
FT4 (pmol/L)	16.1 (3.5)	17.2 (3.4)	14.8 (3.4)
TSH (mU/L), median (IQR)	0.87 (2.48)	0.76 (1.07)	1.45 (5.21)
Total Diplopia (%)	61.3 (19/31)	62.5 (10/16)	60.0 (9/15)
Intermittent	25.8 (8/31)	18.8 (3/16)	33.3 (5/15)
Inconstant (gaze-evoked)	16.1 (5/31)	12.5 (2/16)	20.0 (3/15)
Constant	19.4 (6/31)	31.3 (5/16)	6.7 (1/15)
% Eyes treated			
Both	61.3 (19/31)	62.5 (10/16)	60.0 (9/15)
Right or Left	38.7 (12/31)	37.6 (6/16)	40.0(6/15)
Clinical activity score, median (IQR)	0 (1)	0 (1)	0 (1)
GO severity at enrolment			
Mild	31/31	16/16	15/15
Palpebral aperture (mm)	11.1 (2.0)	11.8 (2.0)	10.4 (1.7)

Previous treatments of GO (%)			
Selenium	29.0 (9/31)	25.0 (4/16)	33.3 (5/15)
Steroid	51.6 (16/31)	37.5 (6/16)	66.7 (10/15)
Other immunosuppressant	22.6 (7/31)	31.3 (5/16)	13.3 (2/15)
Radiotherapy	35.5 (11/31)	37.5 (6/16)	33.3 (5/15)
Decompression	19.4 (6/31)	18.8 (3/16)	20.0 (3/15)
Blepharoplasty	35.5 (11/31)	25.0 (4/16)	46.7 (7/15)

The diplopia severity was assessed by Gorman score and GO severity according to EUGOGO. GO, Graves' orbitopathy; BMI, body mass index; IQR, interquartile range; FT4 (9.0-19.1 pmol/l); TSH (0.30-4.4 mU/l).

3.3.3 Primary outcome analysis

The mean exophthalmometer readings of the treated eyes throughout the trial was around 23 mm (range 18 – 31.5) (see Table 19 and Figure 37).

Table 19: The mean exophthalmometer readings of the treated eyes throughout trial visits. “Obs” indicates number of observations.

Visit	Obs	Mean (mm)	Std. Dev.	Min	Max
1	31	23.6	2.5	20	30.5
2	31	23.4	2.7	18	30
3	30	23.1	2.7	19	29
4	29	23.7	2.9	19	31
5	29	23.9	2.6	20	31.5

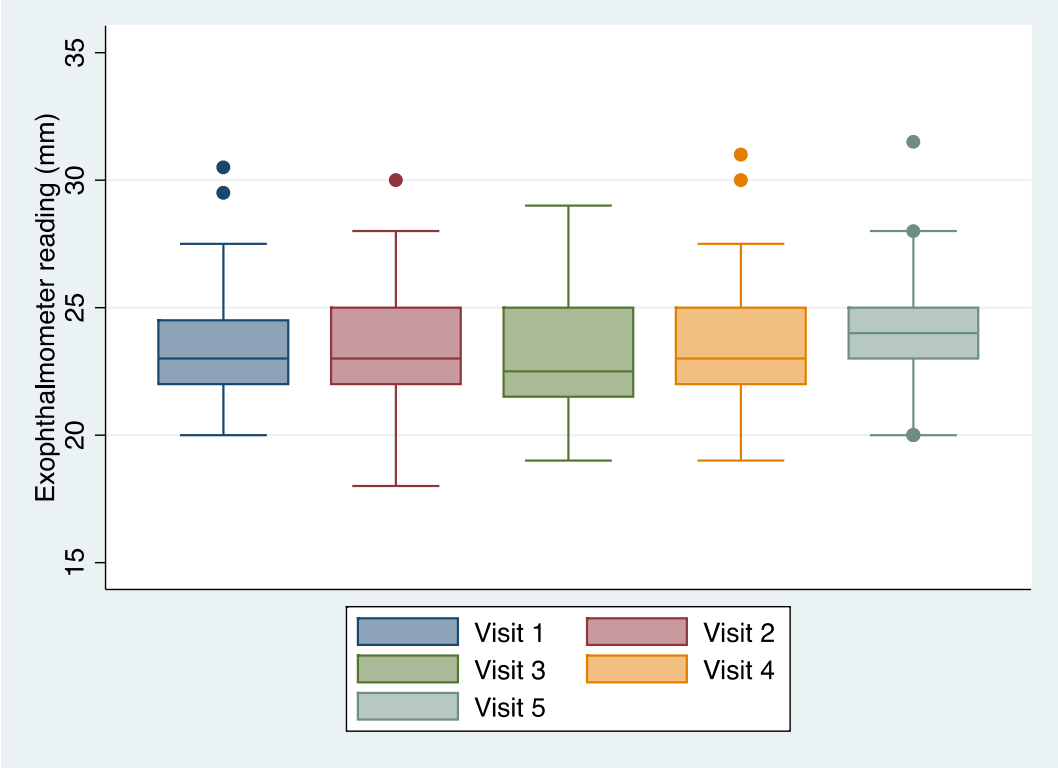

Figure 37: The mean exophthalmometer readings of all treated eyes throughout the trial. The box represents interquartile range (IQR) with median line and the whiskers represent all data points within 1.5 IQR.

The mean change in measurement was calculated by subtracting the baseline measurement from that following treatment. Therefore, negative values indicate an improvement in the treatment. The mean change in proptosis measurement in the placebo phase and Bimatoprost phase was compared with a paired t-test and displayed using dot plots (Figure 38). This was carried out using the mean improvement of the two eyes where both have been treated. The mean changes in Bimatoprost phase were 0.17 mm (95% CI -0.35 to 0.69) versus 0.26 mm (95% CI -0.51 to 1.03) in the placebo phase. These were not statistically different with p value = 0.8455.

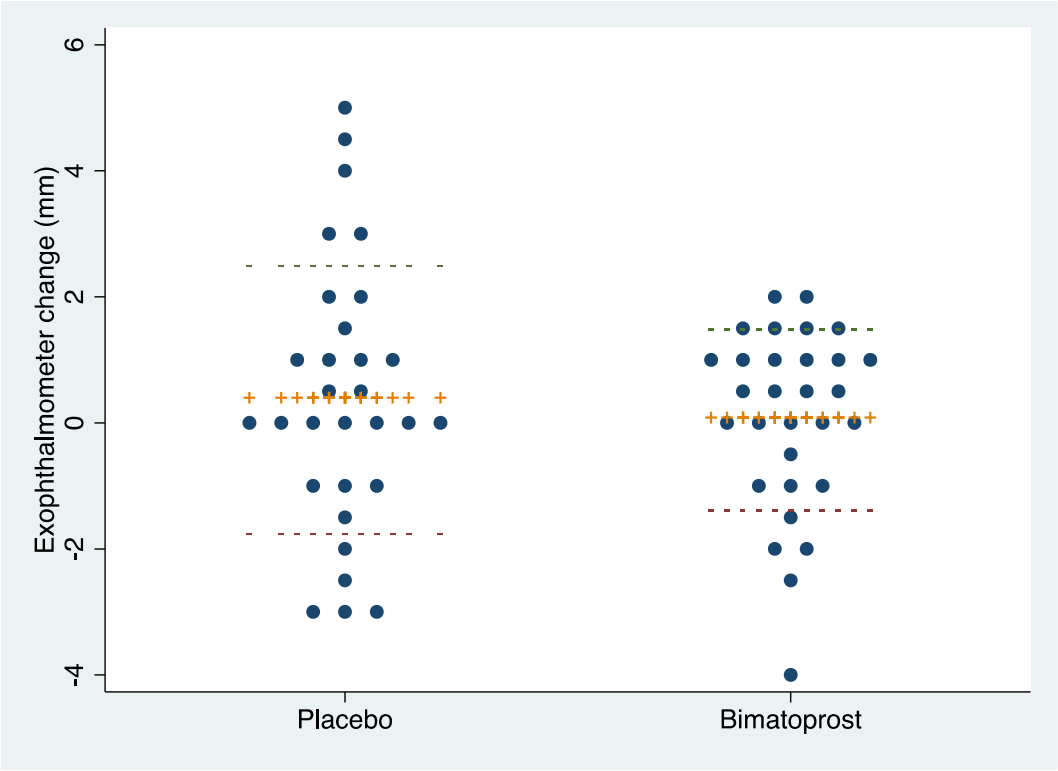

Figure 38: Dot plot of the mean change in proptosis measurement in the placebo phase and Bimatoprost phase expressed in millimetres. The mean change in measurement was calculated by subtracting the baseline measurement from that following treatment. Therefore, negative value indicates an improvement in the treatment. The ++ represents mean and the -- represents standard deviation. Paired t-test p value=0.8455.

There were 3 patients who were deemed to be protocol non-compliant with inclusion criteria who had FT4 levels above the reference range with normal FT3 during the screening period. This was due to missed interpretation of the inclusion criteria: Euthyroid (FT3 **and** FT4 in the reference range), instead FT3 **or** FT4 results were used. It should be stressed that all of these patients were clinically euthyroid during randomisation. A sensitivity analysis was done after exclusion of these three subjects to determine any effect on the study conclusions. There was no difference between the 2 groups with Bimatoprost mean change of 0.17 mm (95% CI -0.40 to 0.75) versus placebo mean change 0.02 mm (95% CI -0.75 to 0.79) p=0.727 (Figure 39).

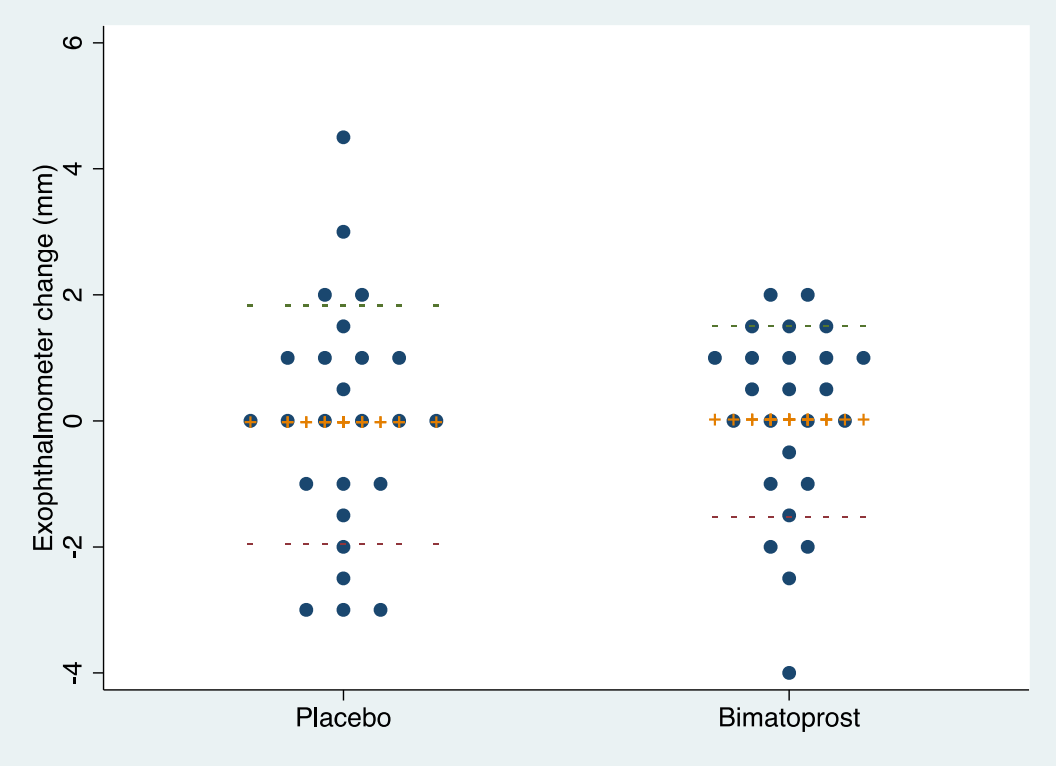

Figure 39: Dot plot of the mean change in proptosis measurement in the placebo phase and Bimatoprost phase expressed in millimetres excluding 3 patients with protocol non-compliance. The mean change in measurement was calculated by subtracting the baseline measurement from that following treatment. Therefore, negative value indicates an improvement in the treatment. The ++ represents mean and the -- represents standard deviation. Paired t-test p value=0.727.

Using pkcross function on the STATA version 12 program, there were no period (p=0.38) or carryover (p=0.46) effects observed.

3.3.3.1 Multilevel modelling

Data from patients with both eyes affected/treated and patients with one eye affected/treated were analysed using a multilevel model in STATA which will also give us the ability to use one data point for those patients who were unwilling or unable to proceed to the second phase of the protocol thus using all available data as efficiently

as possible. In this process, each patient's eye outcome measured was nested within each individual patient.

Crude analysis (model 1) did not show any treatment effect on the exophthalmometer readings with coefficient of -0.27 mm (95% CI -1.43 to 0.89, p=0.648). Adding multilevel modelling correcting for baseline and phase of treatment (model 2) improved the model with treatment coefficient of -0.17 mm (95% CI -0.67 to 0.32) but not statistically significant p=0.490. Carryover adjustment was omitted because of collinearity with the phase of treatment. Adding the assessors to the model did not improve the model with treatment effect of -0.16 mm (95% CI -0.65 to 0.33, p=0.531) and assessor coefficient of -0.34 (95% CI -0.96 to 0.27, p= 0.274). Removing 3 patients with protocol deviation to the model 2 and 3 resulted in a worsening of treatment effect with model 2 treatment coefficient of -0.06 mm (905% CI -0.56 to 0.45, p=0.827) and model 3 treatment coefficient of -0.04 mm (95% CI -0.55 to 0.46, p= 0.861). Using response to any drop in IOP as a surrogate marker for compliance improved the model but with no statistically significant treatment effect on proptosis as measured on the exophthalmometer (Table 20).

Table 20: Beta coefficient of Bimatoprost effect on exophthalmometer readings using multilevel modelling with each treated patient's eye within the patient. Minus protocol deviation indicated 3 patients removed from the analysis due to the stated reason. Minus IOP non-responder indicated removal of eyes with no reduction in intraocular pressure (surrogate marker to compliance).

Model	N	β coefficient	95% CI	p value
All patients				
Model 1	96	-0.27	-1.43, 0.89	0.648
Model 2	96	-0.17	-0.67, 0.32	0.490
Model 3	96	-0.16	-0.64, 0.33	0.531
Minus protocol deviation				
Model 1	88	-0.20	-1.44, 1.03	0.745
Model 2	88	-0.05	-0.56, 0.45	0.827
Model 3	88	-0.04	-0.55, 0.46	0.861
Minus IOP non-responder				
Model 1	88	-0.34	-1.59, 0.91	0.593
Model 2	88	-0.29	-0.81, 0.24	0.283
Model 3	88	-0.26	-0.78, 0.25	0.313

Model 1 Crude.
Model 2 Adjusted for baseline, phase and carryover.
Model 3 Adjusted for baseline phase, carryover and assessors.

3.3.4 Exophthalmometer change in patients with unilateral proptosis

There were 12 patients with unilateral proptosis. In these patients, only the eye with proptosis was treated whilst the other untreated eye served as a control. Analysis of the exophthalmometer reading revealed predicted baseline exophthalmometer difference with higher exophthalmometer mean of 22.17 mm in the treated (95% CI 21.16 to 23.17) compared with 20.33 mm (95% CI 19.14 to 21.52) p=0.0032 in the untreated eye (Figure 40). Interestingly, treatment with Bimatoprost produced a statistically significant reduction in exophthalmometry in treated eyes, with a mean change of -1.17 mm (95% CI -2.62 to 0.29) compared to the untreated eye of 1.92 mm (95% CI 0.60 to 3.23) p=0.0067 (Figure 41). In this case 9 patients had a reduction in their exophthalmometer reading whilst 3 patients did not.

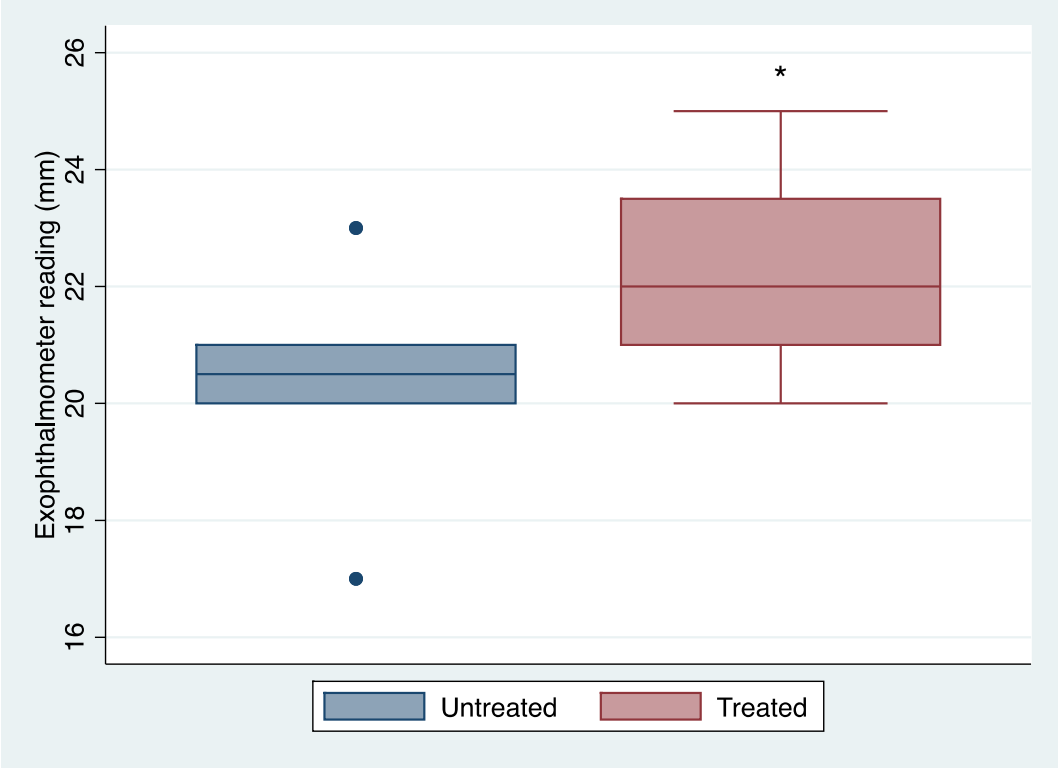

Figure 40: Box plot of the baseline proptosis measurement in the untreated and treated eyes expressed in millimetres in patients with unilateral proptosis (n=12). Paired t-test p value=0.0032.

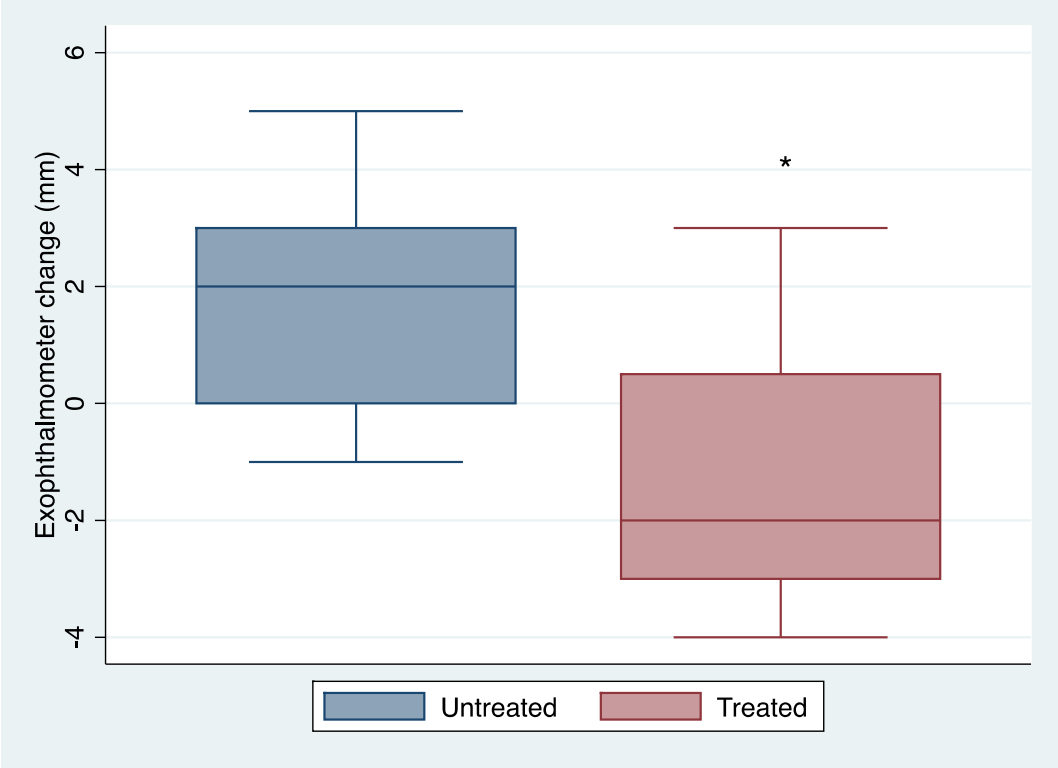

Figure 41: Box plot of the mean change in proptosis measurement in the untreated and treated eyes expressed in millimetres in patients with unilateral proptosis (n=12). The mean change in measurement was calculated by subtracting the baseline measurement from that treatment. Therefore, negative value indicates an improvement in the treatment. Paired t-test p value=0.0067.

3.3.5 Secondary outcome analysis

3.3.5.1 Change in quality of life scores on the GO quality of life questionnaire (GO-QOL) [341]

3.3.5.1.1 Total visual score

In general patients scored highly on total visual score throughout trial visits with the range of mean total visual scores of 79 to 85 (see Table 21 and Figure 42). Test for downward trend for total visual score mean with time was not significant (p=0.2816).

Table 21: Total visual score of GO-QOL throughout trial visits. “Obs” indicates observation numbers.

Visit	Obs	Mean	Std. Dev.	Min	Max
1	31	84.5	20.6	8.3	100
2	31	85.0	24.6	0	100
3	30	81.3	24.9	8.3	100
4	29	79.4	24.9	14.3	100
5	29	79.4	24.9	14.3	100

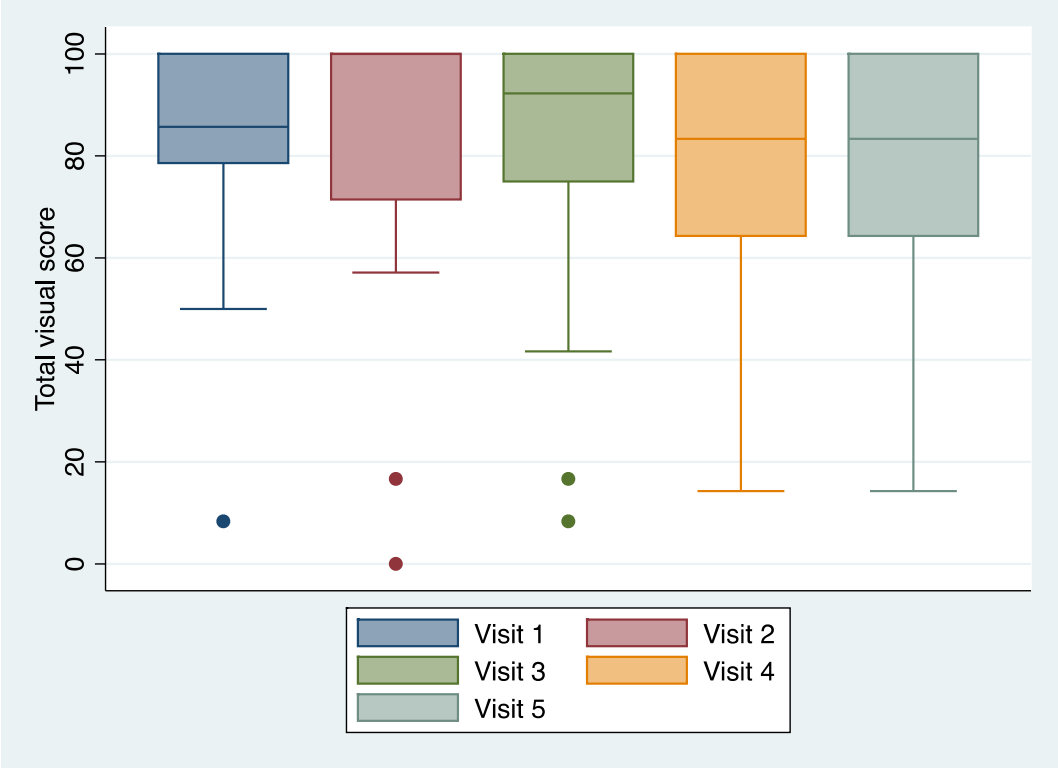

Figure 42: Box plot of total visual score of GO-QOL throughout trial visits. The box represents interquartile range (IQR) with median line and the whiskers represent all data points within 1.5 IQR.

With regard to treatment, we did not see any change in total visual scores using GO-QOL questionnaire. The change was calculated by subtracting post treatment score

against baseline score. A positive value would indicate an improvement in quality of life and a change of at least 6 points was considered a minimal clinically important difference. The mean changes for Bimatoprost was 0.8 (95% -7.1 to 8.7) versus placebo -0.6 (95% CI -6.5 to 5.2) p=0.7933. There was a moderate negative correlation between Gorman diplopia score and total visual score (Spearman's rho -0.5118, p<0.0001). This negative correlation persisted even after removing patients treated with prism (Spearman rho -0.5111, p<0.0001).

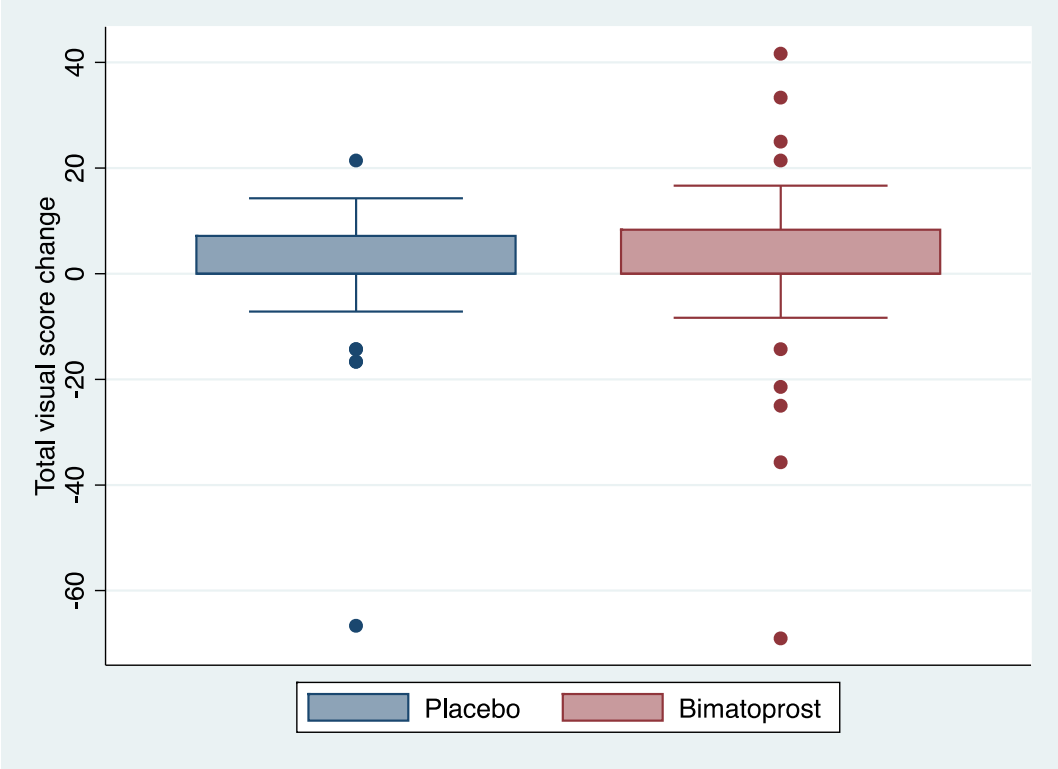

Figure 43: Total visual score change of GO-QOL 3 months after each treatment. The change was calculated by subtracting post treatment score against baseline score. A positive value would indicate an improvement in quality of life and a change of at least 6 points was considered a minimal clinically important difference. Paired t-test p=0.7933.

3.3.5.1.2 Total appearance score

Patients scored moderately throughout trial visits with regard to total appearance score with the mean ranging from 52 to 58 (see Table 22 and Figure 44).

Table 22: Total appearance score of GO-QOL throughout trial visits. “Obs” indicates observation numbers.

Visit	Obs	Mean	Std. Dev.	Min	Max
1	31	52.2	26.2	0	100
2	31	55.6	28.7	0	100
3	30	57.9	30.1	0	100
4	29	55.4	29.7	0	100
5	29	55.0	29.8	0	100

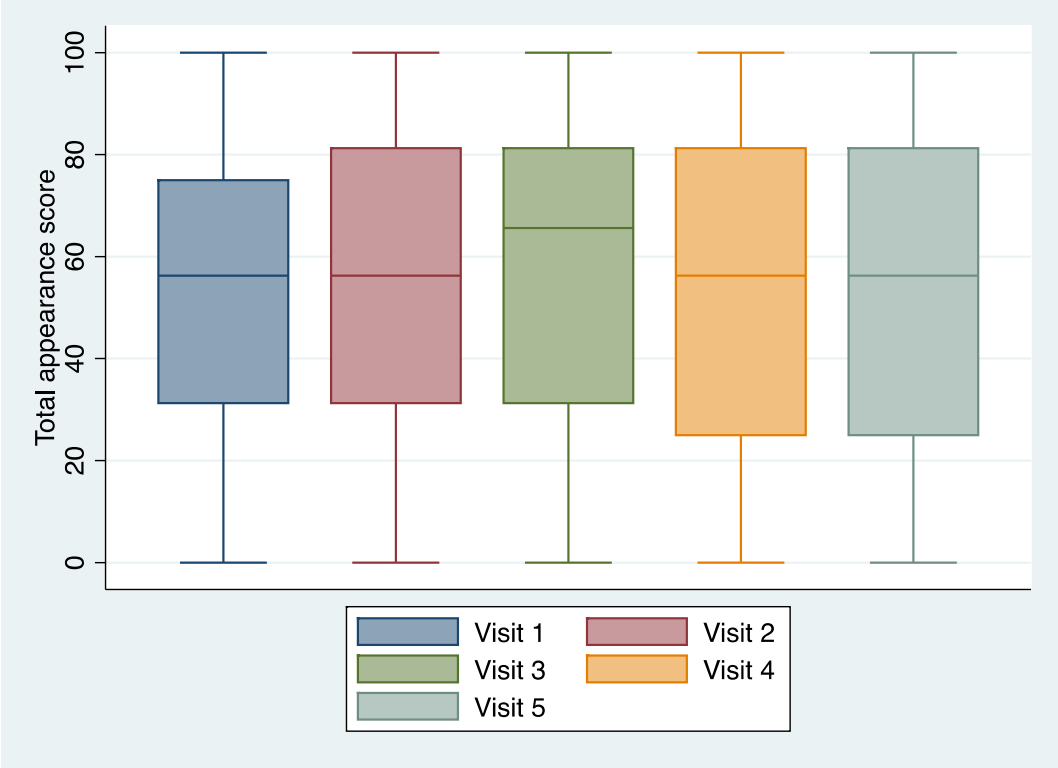

Figure 44: Box plot of total appearance score of GO-QOL throughout trial visits. The box represents interquartile range (IQR) with median line and the whiskers represent all data points within 1.5 IQR.

Similarly, we did not see any change in total appearance score at 3 months after Bimatoprost treatment with the mean of 0.4 (95% CI -3.6 to 4.5) versus placebo 2.2 (95% CI -5.2 to 9.5) p=0.6897 (Figure 45). There was no correlation between Gorman diplopia score and total appearance score (Spearman's rho –0.0785, p=0.3396). This negative correlation became significant after removing patients treated with prism albeit rather weak association (Spearman rho -0.2282, p<0.0115).

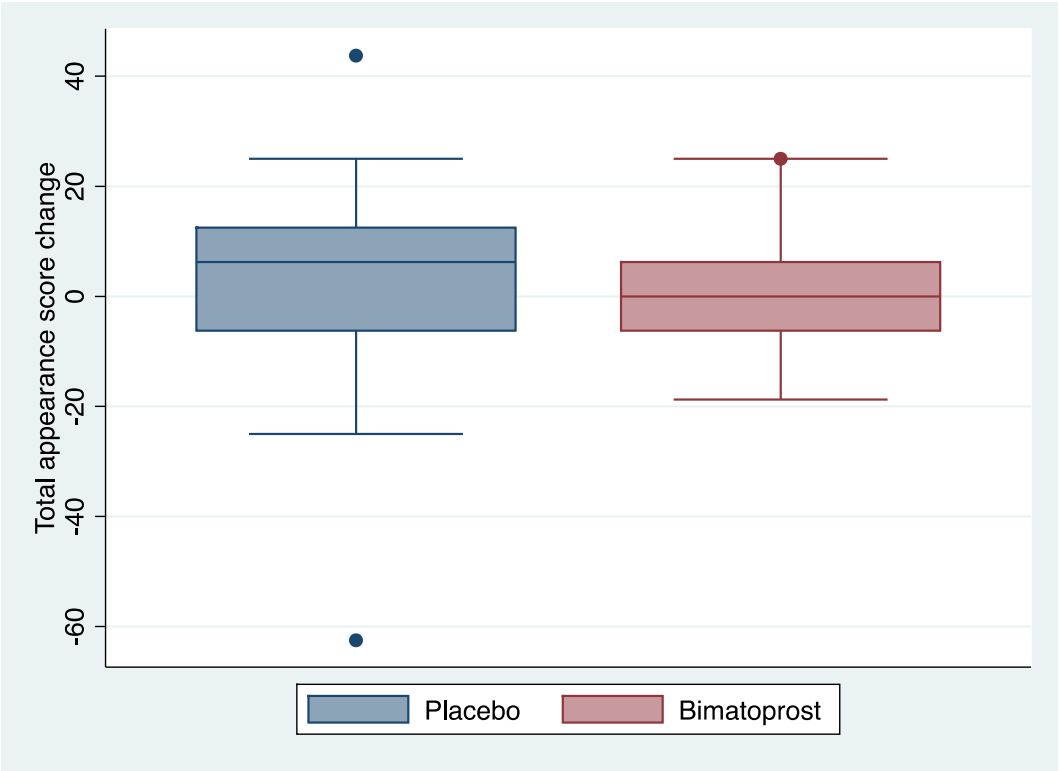

Figure 45: Total appearance score change of GO-QOL 3 months after each treatment. The change was calculated by subtracting post treatment score against baseline score. A positive value would indicate an improvement in quality of life and a change of at least 6 points was considered a minimal clinically important difference. The box represents interquartile range (IQR) with median line and the whiskers represent all data points within 1.5 IQR. Paired t-test p=0.6897.

3.3.5.2 Change in intraocular pressures (IOP)

3.3.5.2.1 IOP during trial visits

During trial visits, the mean intraocular pressures measured in primary position were between 16-18 mmHg (Table 23 and Figure 46).

Table 23: Intraocular pressure measurements (mmHg) during trial visits.

Visit	Obs	Mean (mmHg)	Std. Dev.	Min	Max
1	31	18.2	4.0	10	25
2	31	17.3	3.6	11.5	25
3	30	17.8	3.5	11	24
4	29	16.2	3.5	10.5	22
5	29	17.3	3.6	11.5	22.5

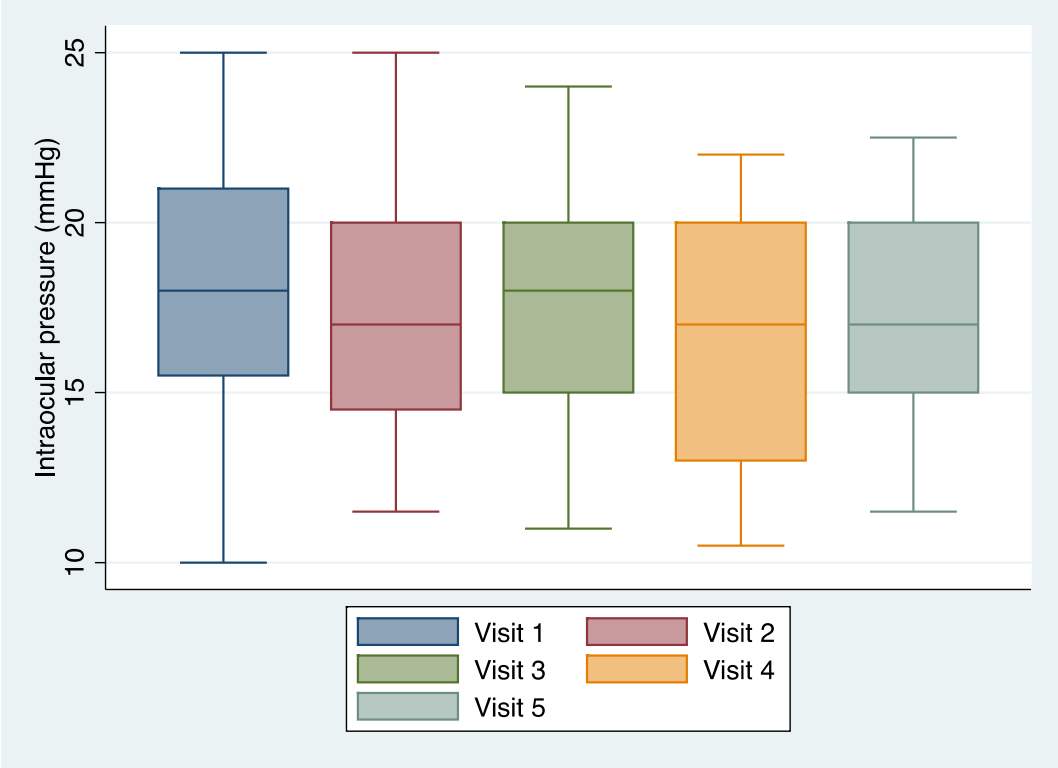

Figure 46: Box plot of intraocular pressure measurements (mmHg) during trial visits. The box represents interquartile range (IQR) with median line and the whiskers represent all data points within 1.5 IQR.

3.3.5.2.2 IOP Treatment versus placebo in primary position

As expected Bimatoprost caused reduction in IOP pressure by the mean change of -2.7 mmHg (95% CI -4.0 to -1.4) compared to placebo with the mean change of 0.3 mmHg (95% CI -1.4 to 2.1) p=0.0070 (Figure 47).

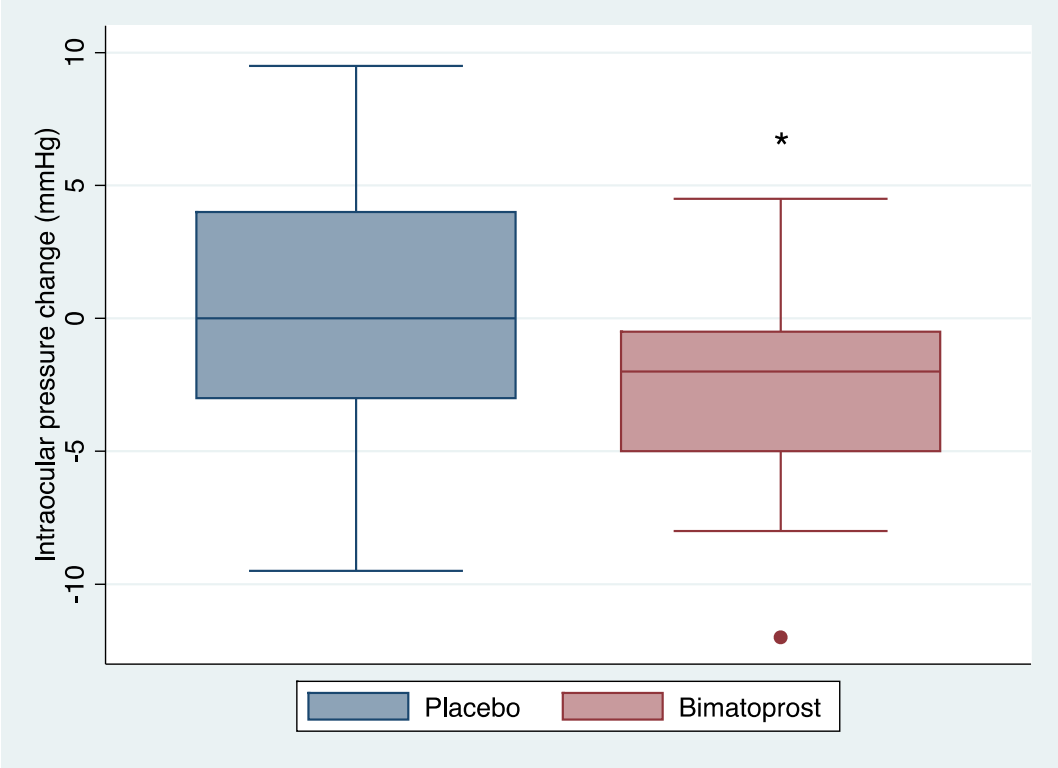

Figure 47: Mean change of intraocular pressure (mmHg) in placebo compared to Bimatoprost (*Paired t-test p=0.0070). The box represents interquartile range (IQR) with median line and the whiskers represent all data points within 1.5 IQR.

3.3.5.2.3 IOP in primary versus chin forward position

We found chin forward position did not alter intraocular pressure significantly. On Bimatoprost the mean change in primary position was -2.7 mmHg (95% CI -3.9 to -1.4) compared to chin forward position mean -2.2 mmHg (95% CI -3.8 to -0.9) p=0.5208. The mean change in primary position in placebo group was 0.4 mmHg (95% CI -1.3 to 2.1) compared to chin forward position 1.4 mmHg (95% CI -0.5 to 3.3) p=0.1249 (Figure 48).

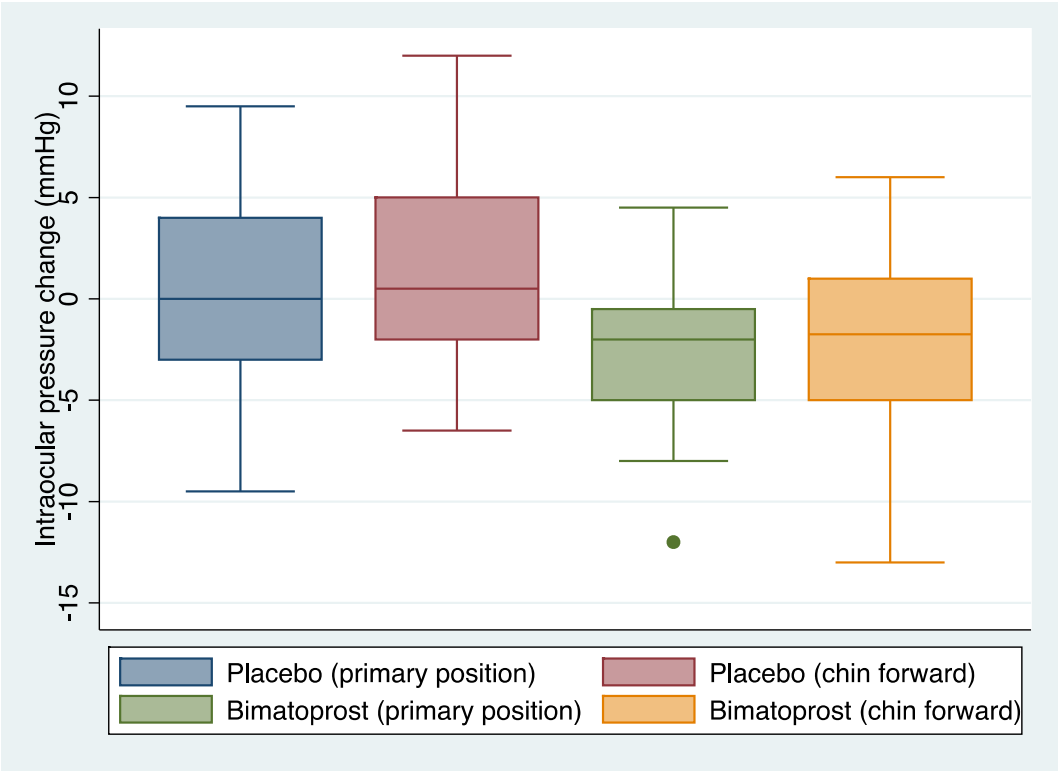

Figure 48: Box plot of intraocular pressure change in placebo and Bimatoprost in primary position versus chin forward position. The box represents interquartile range (IQR) with median line and the whiskers represent all data points within 1.5 IQR.

3.3.5.3 Side effect profiles of Bimatoprost in GO patients during the study

Bimatoprost was associated with more patient reported ocular side effects in particular conjunctival hyperaemia in 10 patients (32.3%) versus 3 patients (9.7%) in placebo and eye pruritus 4 patients (12.9%) versus 1 patients (3.2%) in placebo (Table 24). There was also higher incidence of headache in Bimatoprost group 9 patients (29%) compared to 2 patients (6.5%) in placebo (Table 25).

Table 24: Patient reported ocular side effects.

Ocular side effects			
	Bimatoprost n (%)	Placebo n (%)	Trial total n (%)
Conjunctival hyperaemia	10 (32.3)	3 (9.7)	16 (51.6)
Eye pruritus	4 (12.9)	1 (3.2)	5 (16.1)
Eyelid swelling	3 (9.7)	2 (6.5)	5 (16.1)
Visual disturbance	2 (6.5)	0	2 (6.5)
Meibomian cyst	2 (6.5)	2 (6.5)	5 (16.5)
Burning sensation	1 (3.2)	1 (3.2)	3 (9.7)
Eye dryness	1 (3.2)	1 (3.2)	2 (6.5)
Eyelid pigmentation	1 (3.2)	0	1 (3.2)
Conjunctivitis	1 (3.2)	0	2 (6.5)
Foreign body sensation	0	1 (3.2)	1 (3.2)
Eye pain	0	1 (3.2)	1 (3.2)
Ptosis	0	1 (3.2)	1 (3.2)
Difficulty eye opening	0	1 (3.2)	2 (6.5)
Sub total	25 (80.6)	14 (45.2)	46 (148.4)

Table 25: Patient reported non-ocular side effects.

Non-ocular side effects			
	Bimatoprost n (%)	Placebo n (%)	Trial total n (%)
Pain (total)	16 (51.6)	2 (6.5)	22 (71.0)
Pain headache	9 (29.0)	2 (6.5)	11 (35.5)
Infection	3 (9.7)	1 (3.2)	6 (19.4)
Sinus	3 (9.7)	4 (12.9)	9 (29.0)
Flu-like syndrome	1 (3.2)	1 (3.2)	6 (19.4)
Urticarial	1 (3.2)	1 (3.2)	4 (12.9)
Bronchospasm	1 (3.2)	0	1 (3.2)
Osteoarthritis	1 (3.2)	0	1 (3.2)
Dizziness	0	1 (3.2)	1 (3.2)
Heartburn	2 (6.5)	0	2 (6.5)
Musculoskeletal	1 (3.2)	0	1 (3.2)
Polydipsia	0	1 (3.2)	1 (3.2)
Tooth ache	1 (3.2)	0	1 (3.2)
Urine colour change	0	1 (3.2)	1 (3.2)
D&V	1 (3.2)	0	2 (6.5)
Joint function	0	2 (6.5)	2 (6.5)
Ear wax	0	0	1 (3.2)
Pulmonary Embolism	0	0	1 (3.2)
Osteoporosis	0	0	1 (3.2)
Middle ear surgery	0	0	1 (3.2)
Total	31 (100.0)	16 (45.2)	64 (206.5)

3.3.5.4 Health economics consumption

The primary intention of health economic evaluation was to explore the cost associated with GO treatment. In theory, Bimatoprost intervention would lead to the net cost savings to NHS in comparison to surgical rehabilitation that the patient otherwise will go through. However it would be useful to collect the resource use on a pilot basis which may lead to a larger health economic focus study in the future. As expected there was no difference in NHS health economics consumption between Bimatoprost and placebo period. The median thyroid and GO related drugs cost 4 months' post Bimatoprost treatment was £12.36 (range £0.00-£136.04) compared to placebo treatment £10.85 (£0.00-£131.84) and the NHS encounter median cost during similar period was £86.60 (£0.00-£528.80) compared to placebo £67.80 (£0.00-£995.40) (Table 26).

Table 26: Health economics consumption comparison

	2 months period		2 months period		All (4 months period)	
Post	Bimatoprost	Placebo	Bimatoprost washout	Placebo washout	Bimatoprost	Placebo
Total drug cost Median/mean (range)	£6.14/£9.71 (0.00-70.12)	£5.68/£11.81 (0.00-65.92)	£6.14/£12.93 (0.00- 65.92)	£6.02/£9.42 (0.00-65.92)	£12.36/£22.41 (0.00-136.04)	£10.85/£21.24 (0.00-131.84)
Total NHS encounter cost Median/mean (range)	£0.00/£57.49 (0.00-253.20)	£7.80/£79.12 (0.00-567.00)	£7.80/£66.93 (0.00-275.60)	£4.30/£75.09 (0.00-428.40)	£86.60/£124.59 (0.00-528.80)	£67.80/£154.21 (0.00-995.40)

3.3.6 Other outcomes

3.3.6.1 Generic (EQ-5D-5L) Health Questionnaire

There was no change with regard to generic EQ-5D-5L general well-being questionnaires with median total utility score 0.796 (IQR 0.479-0.837) in Bimatoprost versus placebo 0.826 (IQR 0.696 to 1.000) p=0.9652 (Figure 49). There was a positive correlation between EQ-5D-5L utility score and GO-QOL total visual score (Figure 50, Spearman rho 0.6515, p<0.0001). Similar but weaker correlation was found between EQ-5D-5L utility score and total appearance score (Figure 51, Spearman rho 0.1997, p=0.0143).

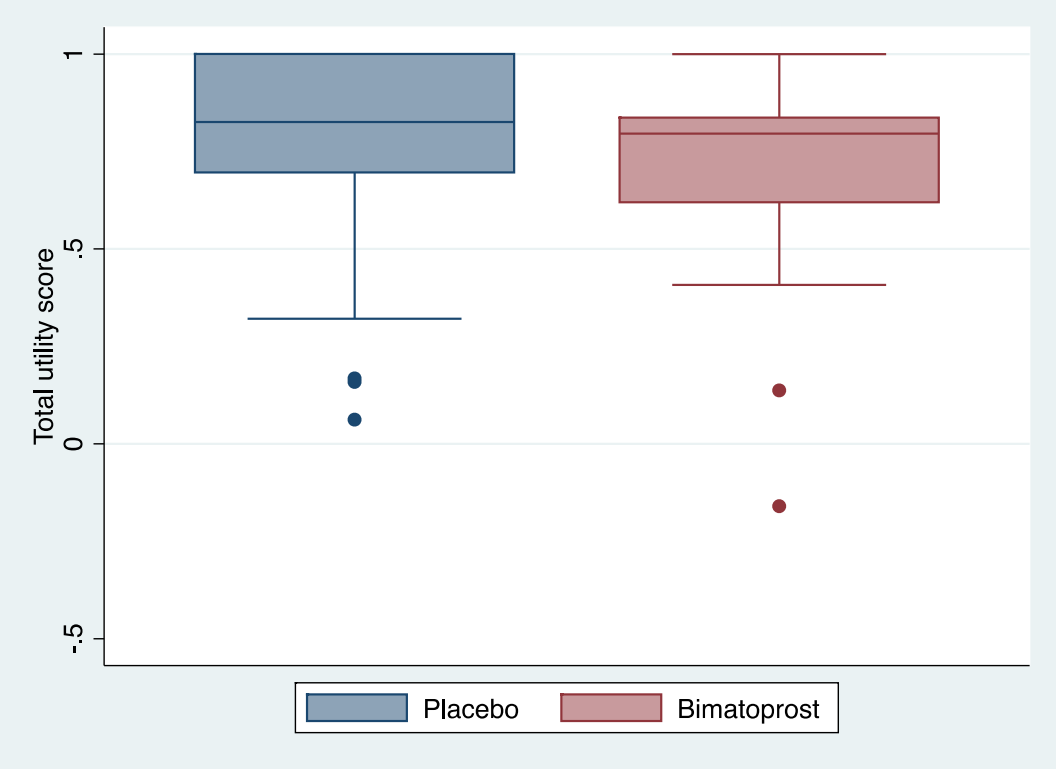

Figure 49: EQ5D-5L total utility score in placebo compared to Bimatoprost. The box represents interquartile range (IQR) with median line and the whiskers represent all data points within 1.5 IQR. Wilcoxon signed-rank test p=0.9652.

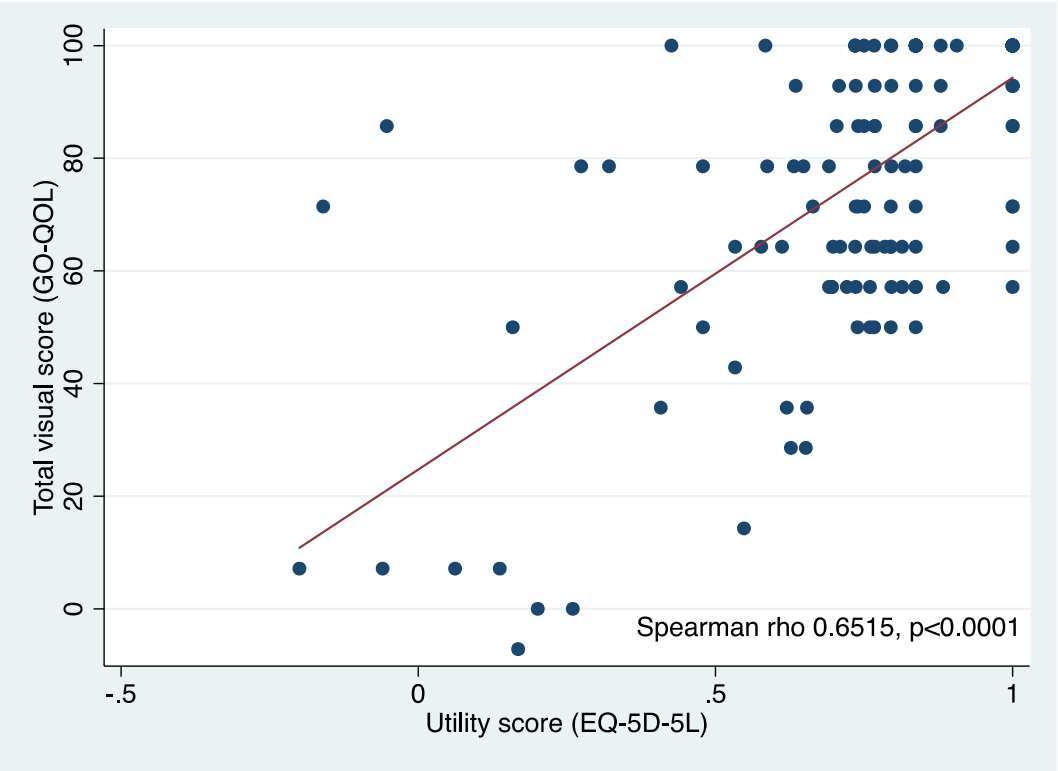

Figure 50: Scatter plot of total visual score (GO-QOL) against utility score questionnaires with fitted values (red line) showing a positive correlation with Spearman rho 0.6515, p<0.0001.

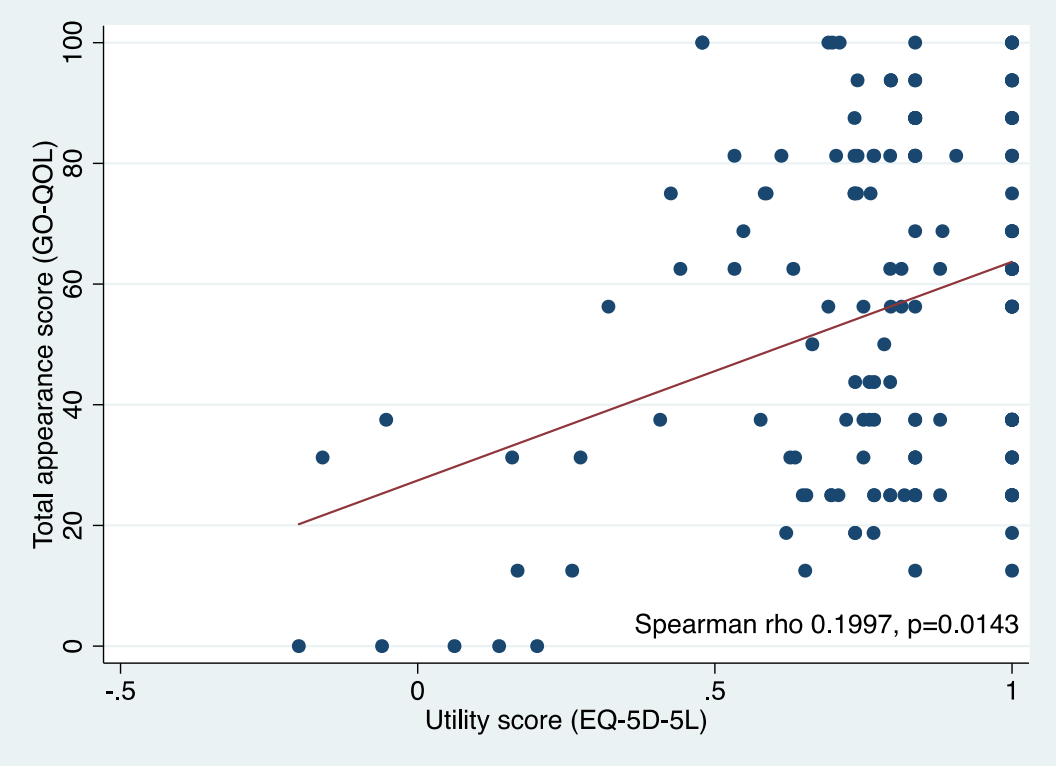

Figure 51: Scatter plot of total appearance score (GO-QOL) against utility score questionnaires with fitted values (red line) showing a positive correlation with Spearman rho 0.1997, p=0.0143.

3.3.6.2 Clinical activity score (CAS)

Patient thyroid eye disease remained inactive throughout trial period with median CAS score of 0 as depicted in Figure 52.

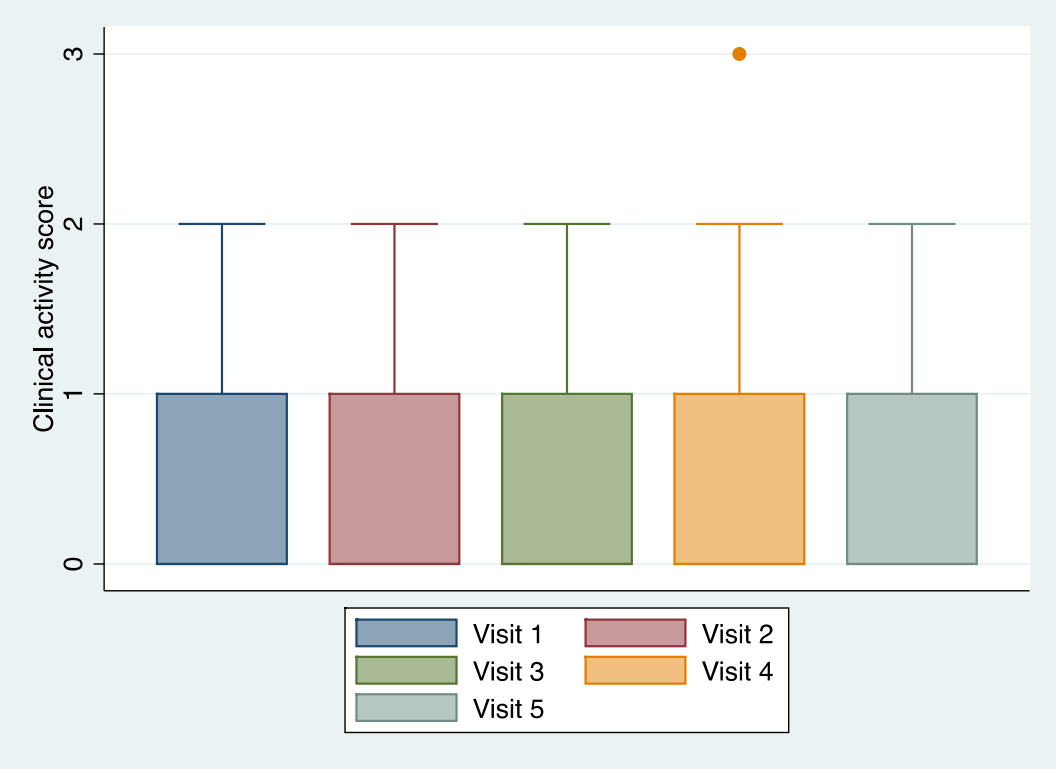

Figure 52: Clinical activity score during trial visits. The box represents interquartile range (IQR) with median line and the whiskers represent all data points within 1.5 IQR.

There was no evidence that Bimatoprost can induce GO disease activity in this patient group (p=0.7179) (Figure 53).

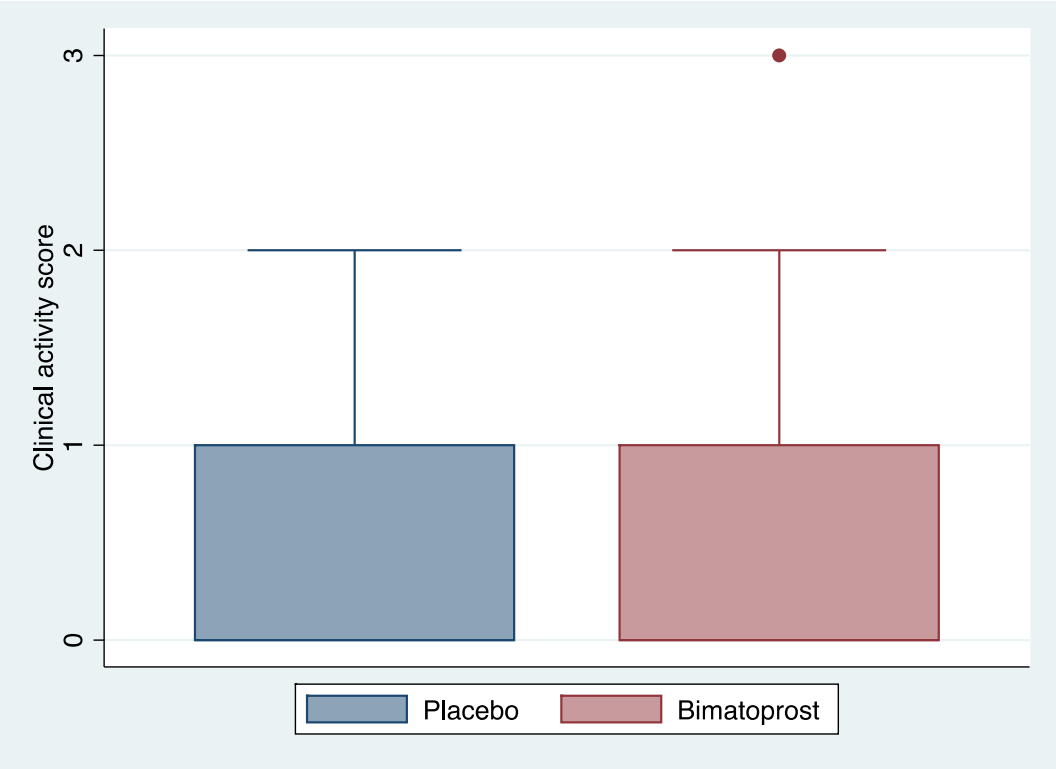

Figure 53: Clinical activity score in placebo versus Bimatoprost. The box represents interquartile range (IQR) with median line and the whiskers represent all data points within 1.5 IQR. Wilcoxon signed-rank test p=0.7179.

3.3.6.3 Total eye score (TES)

There was no change with regard to total eye score. Bimatoprost median TES was 6 (IQR 2-11) compared to placebo median TES of 8 (IQR 5-11) p=0.2089 (Figure 54).

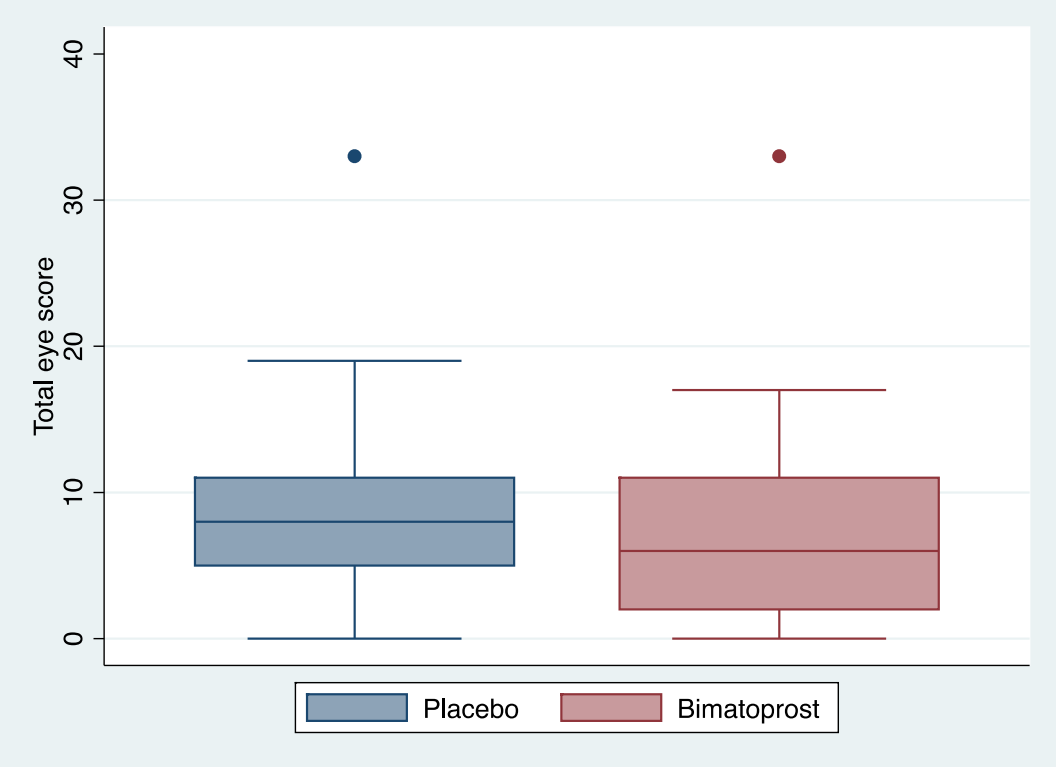

Figure 54: Box plot of total eye score at the end of each treatment period. The box represents interquartile range (IQR) with median line and the whiskers represent all data points within 1.5 IQR. Wilcoxon signed-rank test p=0.2089.

3.3.6.4 Palpebral aperture

There was no change with regard to palpebral aperture measurements with Bimatoprost mean change of 0.16 mm (95% CI -0.36 to 0.67) compared to placebo -0.60 (95% CI -1.27 to 0.06) p=0.1043 (Figure 55).

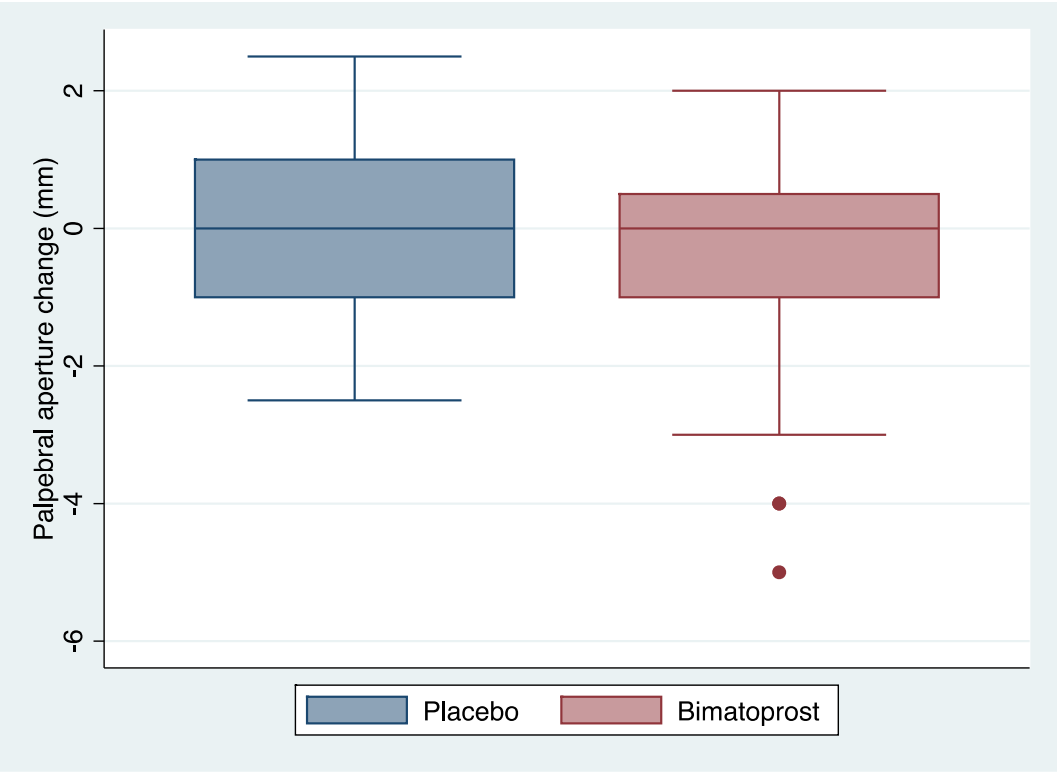

Figure 55: Box plot palpebral aperture change in placebo compared to Bimatoprost. The box represents interquartile range (IQR) with median line and the whiskers represent all data points within 1.5 IQR. Paired t-test p=0.1043.

3.3.6.5 Subjective eye changes

There were 13 patients (41.94%) who thought that their eye prominence had changed with the Bimatoprost and 8 patients (26.67%) in the placebo group (Table 27). Remarkably in both groups, if there was a change this was most likely to be an improvement (less prominence) (Table 28).

Table 27: Patients' response to question 'As the result of last 3 months treatment, has the prominence of your eyes changed?' in placebo and Bimatoprost.

Response	Placebo n (%)	Bimatoprost n (%)
Yes	8 (26.67)	13 (41.94)
No	22 (73.33)	18 (58.06)

Table 28: Patients' response to question 'If so, is the prominence more or less?'.

Response	Placebo n (%)	Bimatoprost n (%)
More	1 (12.50)	3 (23.08)
Less	7 (87.50)	10 (76.92)

3.3.6.6 Patients' satisfaction with the treatment

Only 13 patients (41.94%) preferred Bimatoprost treatment. Fourteen (46.47%) patients preferred placebo eye drops (Table 29).

Table 29: Patients' preference with the treatment.

Response	Placebo n (%)	Bimatoprost n (%)
Yes	14 (46.67)	13 (41.94)
No	12 (40.00)	10 (32.26)
Not sure	4 (13.33)	8 (25.81)

3.3.6.7 Treatment masking success (assessor and patient)

Sixteen patients (53.33%) in placebo group thought that either they are on Bimatoprost or unsure of their treatment allocation. Nineteen patients (51.29%) in Bimatoprost group thought they either on placebo or unsure of their treatment allocation (Table 30).

Table 30: Patients' treatment masking response. The question asked was 'Do you think you have been on treatment or placebo?'.

Response	Placebo n (%)	Bimatoprost n (%)
Treatment	3 (10.00)	12 (38.71)
Placebo	14 (46.67)	10 (32.26)
Don't know	13 (43.33)	9 (29.03)

Assessors have guessed correctly that patient on placebo in 22 cases (73.33%) but only in 13 cases (43.33%) for Bimatoprost allocation (Table 31).

Table 31: Assessors' treatment masking response. The question asked was 'Do you think patient has been on treatment or placebo?'.

Response	Placebo n (%)	Bimatoprost n (%)
Treatment	7 (23.33)	13 (43.33)
Placebo	22 (73.33)	14 (46.67)
Don't know	1 (3.33)	3 (10.00)

3.3.6.8 Photo assessment

Proptosis measurements were also made by photographic assessment of the patient photos taken during the trial. The measurements were taken either from lateral canthus or nasal bridge to the corneal apex by a masked assessor.

3.3.6.8.1 Lateral canthus to corneal apex measurement

There was no different between placebo and Bimatoprost with placebo mean change of 1.30 mm (95% CI -0.74 to 3.35) compared to Bimatoprost 0.98 mm (95% CI -1.25 to 3.20) p=0.8160 (Figure 56).

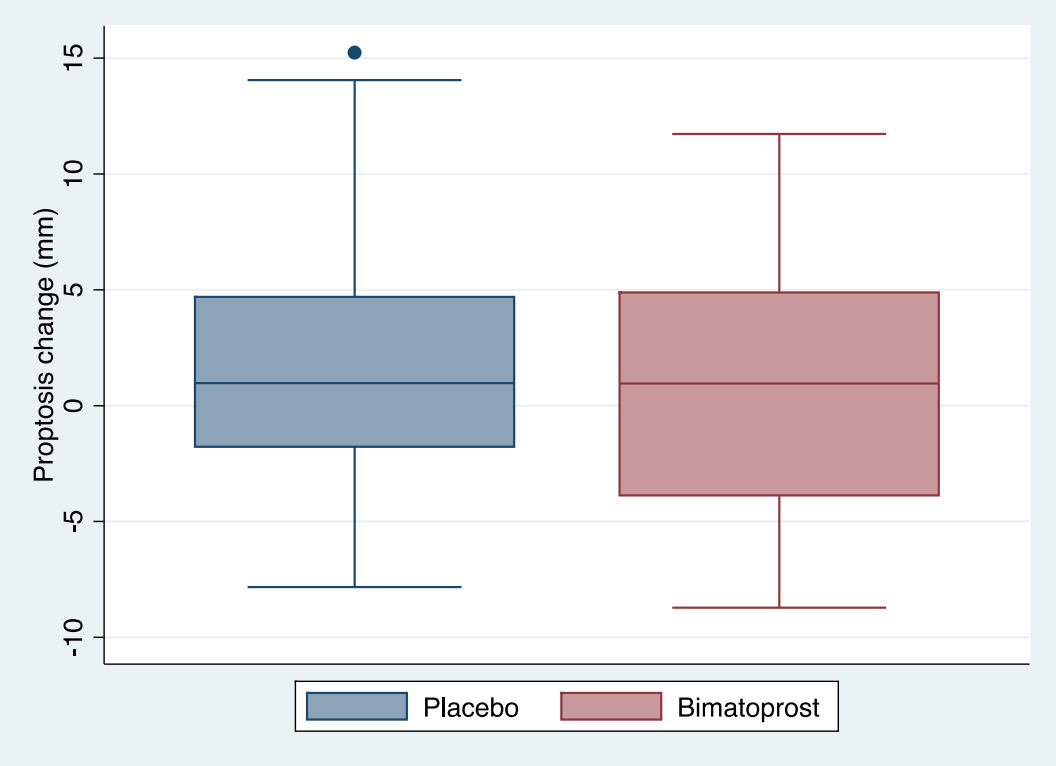

Figure 56: Box plot mean lateral canthus to corneal apex measurement change in placebo compared to Bimatoprost. The box represents interquartile range (IQR) with median line and the whiskers represent all data points within 1.5 IQR. Paired t-test p=0.8160.

3.3.6.8.2 Nasal bridge to corneal apex measurement

There was no different between placebo and Bimatoprost with placebo mean change of -0.50 mm (95% CI -4.18 to 4.08) compared to Bimatoprost 1.30 mm (95% CI -5.65 to 8.25) p=0.6870 (Figure 57).

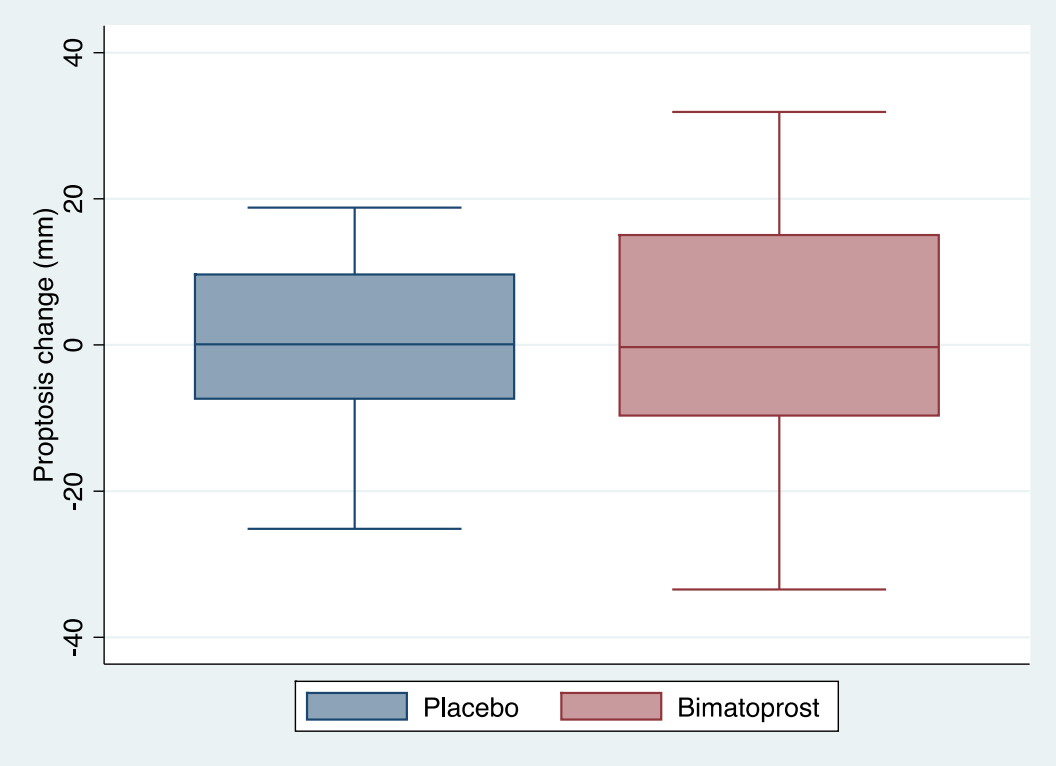

Figure 57: Box plot mean nasal bridge to corneal apex measurement change in placebo compared to Bimatoprost. The box represents interquartile range (IQR) with median line and the whiskers represent all data points within 1.5 IQR. Paired T-test p=0.6870.

3.3.6.8.3 Exophthalmometry and photo assessment correlations

All data from 5 visits were used for this analysis. There was a moderate positive correlation Spearman rho 0.609 p<0.0001 for exophthalmometer and lateral canthus to corneal apex measurement and weaker negative correlation (which was expected negative correlation as the measurement was taken from nasal bridge to corneal apex i.e. the more proptosis the lesser the distance to the nasal bridge) Spearman rho -0.396, p<0.0001. See Figure 58 and Figure 59.

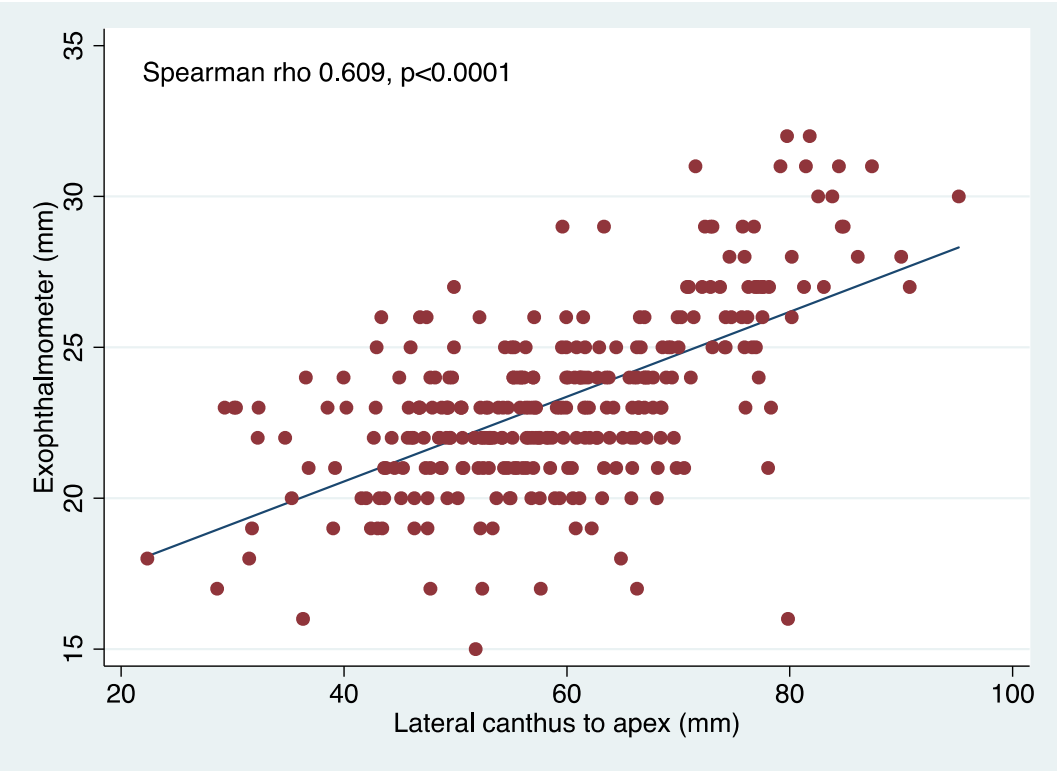

Figure 58: Scatter plot of clinical exophthalmometer against lateral canthus to corneal apex measurements by photograph with fitted values (blue line) showing a positive correlation with Spearman rho 0.609 and p<0.001.

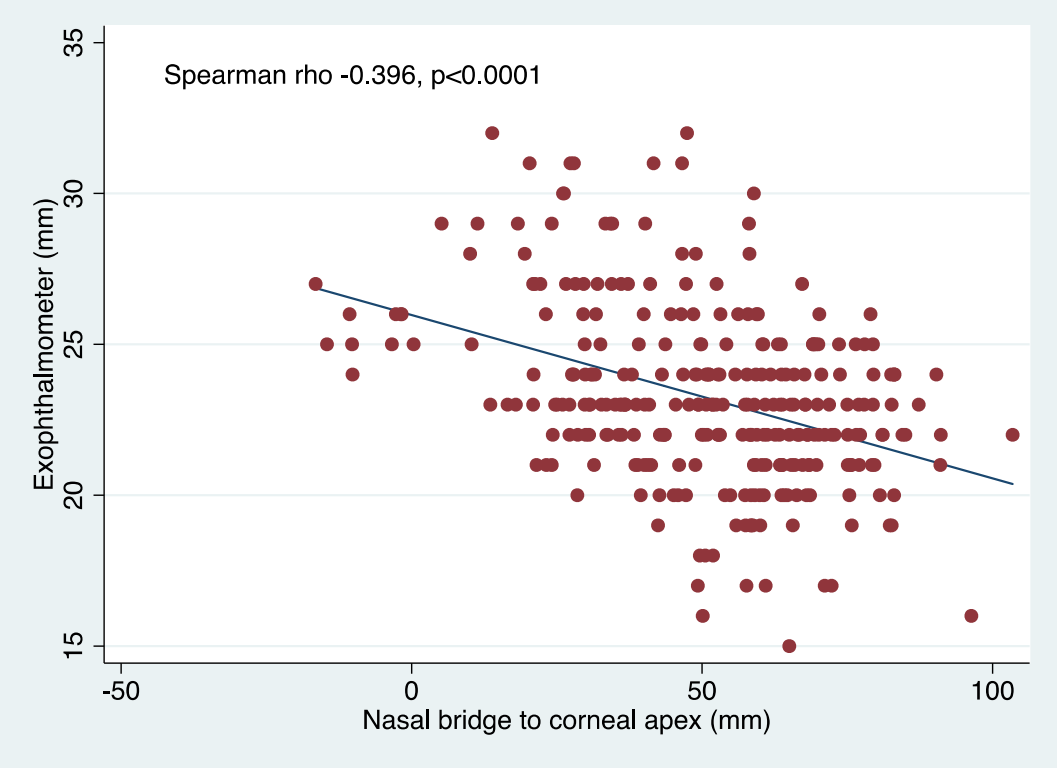

Figure 59: Scatter plot of clinical exophthalmometer against nasal bridge to corneal apex measurements by photograph with fitted values (blue line) showing a negative correlation with Spearman rho -0.396 and p<0.001.

3.3.6.8.4 Detectable side effects

Apart from patients' reported side effects, subjective assessments were also made by an independent masked assessor. Patients treated with Bimatoprost have higher detectable side effects including skin discoloration and eye lashes prolongation (Table 32). Majority 14 /16 (87.50%) of the patients experienced at least 1 side effect compared to placebo 3/15 (20.00%) after the first phase of treatment (Fisher's exact p <0.0001). Only 3 patients (18.75%) developed periorbital fat atrophy which was a desired effect in this trial.

Table 32: Frequency of detectable side effects (percentage) recorded by masked assessor on photographic assessment after 1st phase of treatment

Phase 1		Treatment		Fisher's p value
		Placebo	Bimatoprost	
Iris colour changes		0 (0)	1 (6.25)	1.00
Skin colour changes		0 (0)	7 (43.75)	0.007
Eye lashes elongation		2 (13.33)	11 (68.75)	0.003
Redness	Conjunctival	1 (6.67)	6 (37.50)	0.083
	Upper lid	2 (13.33)	6 (37.50)	0.220
	Lower lid	1 (6.67)	5 (31.25)	0.172
Fat atrophy	Upper lid	0 (0)	1 (6.25)	1.00
	Lower lid	0 (0)	2 (12.50)	0.484

After the second phase of treatment, there were no detectable differences in side effects between the 2 groups (Table 33) and with no statistically different number of patients with any side effects between the 2 groups (Bimatoprost 7/16 (43.75%) versus 8/15 (53.33%), Fisher's exact p=0. 724).

Table 33: Frequency of detectable side effects (percentage) recorded by masked assessor by photographic assessment after 2nd phase of treatment

Phase 2		Treatment		Fisher's p value
		Placebo	Bimatoprost	
Iris colour changes		1 (6.67)	0 (0)	1.00
Skin colour changes		2 (13.33)	2 (16.67)	1.00
Eye lashes elongation		3 (20.00)	7 (58.33)	0.057
Redness	Conjunctival	2 (13.33)	2 (16.67)	1.00
	Upper lid	3 (20.00)	4 (33.33)	0.662
	Lower lid	1 (6.67)	2 (16.67)	0.569
Fat atrophy	Upper lid	1 (6.67)	1 (8.33)	1.00
	Lower lid	0 (0)	0 (0)	na

3.3.6.8.5 Persistent side effects after washout period

Some of side effects persist and some improved after the 2 months' washout period. These include skin colour changes and eye lashes elongation (Table 34 and Table 35).

Table 34: Frequency of detectable side effects (percentage) after 2 months wash out phase 1 period recorded by a masked assessor by photographic assessment

Two months' post Phase 1 persist/improved/new		**Treatment**		**Fisher's p value**
		Placebo	Bimatoprost	
Iris colour changes		0 (0)	1 (6.67)/0/0	1.00
Skin colour changes		0(0)	2 (13.33)/4 (26.67)/0	0.017
Eye lashes elongation		1 (6.67)/1(6.67)/0	8 (53.33)/2(13.33)/0	0.004
Redness	Conjunctival	0 (0)/1(6.67)/1(6.67)	0 (0)/6(40.00)/1(6.67)	0.080
	Upper lid	1 (6.67)/1(6.67)/1(6.67)	3(20.00)/2(13.33)/0	0.577
	Lower lid	1 (6.67)/0/0	2 (13.33)/3(20.00)/1(6.67)	0.115
Fat atrophy	Upper lid	0 (0)	1 (8.33)/0/0	1.00
	Lower lid	0 (0)	2 (13.33)/0/0	0.483

Table 35: Frequency of detectable side effects (percentage) after 2 months wash out phase 2 period recorded by a masked assessor by photographic assessment.

Two months' post Phase 2 persist/improved/new		**Treatment**		**Fisher's p value**
		Placebo	Bimatoprost	
Iris colour changes		1(6.67)/0/0	0/0/1(8.33)	0.701
Skin colour changes		2(13.33)/0/0	1 (8.33)/1(8.33)/1(8.33)	0.543
Eye lashes elongation		2 (13.33)/1(6.67)/2(13.33)	6 (50.00)/1(8.33)/3(25.00)	0.045
Redness	Conjunctival	2 (13.33)/0/0	1 (8.33)/1(8.33)/1(8.33)	0.543
	Upper lid	0/3 (20.00)/0	2(16.67)/2(16.67)/0	0.353
	Lower lid	0/1(6.67)/0	1 (8.33)/1(8.33)/0	0.713
Fat atrophy	Upper lid	1(6.67)/0/1(6.67)	0/1(8.33)/1(8.33)	0.844
	Lower lid	0/0/1(6.67)	0/0/1(8.33)	1.00

3.3.6.8.6 Eyes similarity

As eye symmetry is very important to the patients, we asked the masked assessor: ‘At the end of treatment do the right and left eye looks similar?’ There were no different between the 2 groups (Fisher’s exact p=1.000) (Table 36)

Table 36: Frequency of eyes symmetry by a masked assessor by photographic assessment. Fisher’s exact p=1.00 in both phases.

	Phase 1		Phase 2	
Eyes symmetry	Placebo	Bimatoprost	Placebo	Bimatoprost
Yes	15 (100)	15 (93.75)	14 (93.33)	12(100)
No	0	1 (6.35)	1(6.67)	0

3.3.6.8.7 Treatment masking success (photographic assessment)

The assessor has guessed correctly that patient on placebo in 8 cases (61.54%) and in 10 cases (66.67%) for Bimatoprost allocation. The assessor also has guessed incorrectly or unsure of treatment allocation in 10 patients (35.71%).

Table 37: Assessors' treatment masking response by photographic assessment. The question asked was 'Which phase do you think is the treatment phase?'.

Response	Placebo n (%)	Bimatoprost n (%)
Treatment	1 (7.69)	10 (66.67)
Placebo	8 (61.54)	3 (20.00)
Don't know	4 (30.77)	2 (13.33)

3.4 DISCUSSION

In this study, we showed that treatment with Bimatoprost for 3 months was not effective in reducing proptosis in late phase GO patients. At baseline, we found that up to 75% of our patients were smokers prior to the diagnosis which came down close to 40% after the diagnosis. This is lower than the findings from Prummel et al of in a case control study with prevalence of 81% compared to control of 38% [59] in Netherlands and above that of Bartalena 64.2% in GO and other thyroid conditions of 30% [170] in Italy. Although there was a 35% prevalence reduction after the diagnosis in our trial population, this is still at least double to that of national Wales smoking prevalence which was approximately 20% in 2014 (http://www.ash.org.uk/files/documents/ASH_93.pdf). Our diplopia rate is lower at 61.3% than that of 75% in moderate to severe GO measured by motility assessment [342]. The difference might be explained as the subjective nature of our assessment using Gorman diplopia score which might be more relevant from patient perspective and also the late burnt out stage of the disease process where patients have been treated initially. Our figure includes all types of diplopia from untreated intermittent to constant diplopia inclusive of those treated with prisms (19.35% of total patients). Although there was a high prevalence of diplopia, visual function in GO-QOL was well preserved in our patients with mean total visual scores throughout trial visits between 79 and 85 whilst appearance score was poor with means of 52 to 58. Despite this finding, there was a negative correlation between diplopia score and visual function in GO-QOL but not with appearance score which is consistent with the original finding of Terwee et. al [343]. The findings of persistent high rates of untreated diplopia raise a significant question regarding the management or treatment effectiveness in acute stage in reducing diplopia.

This is the first clinical trial assessing the effects of $PGF_{2\alpha}$ in GO. Using multilevel modelling this trial failed to show that Bimatoprost is capable of reducing proptosis. This is in contrast with the in vitro findings [344, 345] and anecdotal case reports in people without GO [280-282] suggesting adipocytes differentiation inhibition and orbital fat atrophy. Interestingly, we found a statistically significant reduction in proptosis in patients treated for unilateral disease. The

lack of the effects in the primary analysis might be due to several explanations. There was considerable 'noise' in the exophthalmometer measurements with standard deviation between visits ranging from 2.5 mm to 2.9 mm. However, this negative result does not rule out the possibility of Bimatoprost having an effect. This is illustrated by the statistically significant reduction we observed in patients with unilateral disease in which the unaffected (and hence untreated) eye served as a control hence reducing overall 'noise'. Although type 1 error is a possibility, these patients are phenotypically different possibly suggesting a different predominant disease process which might be susceptible to Bimatoprost. Not all glaucoma patients develop enophthalmos. Some patients with GO have predominantly fat excess whilst the others have muscle predominant disease. This suggests a subgroup of subjects that are more susceptible to the effect of Bimatoprost who could be identified by screening using orbital imaging. We did consider orbital imaging in our study but was prohibited by its cost. We are fully aware that the 2 main mechanisms of GO are adipogenesis and hyaluronan accumulation [346]. In the burnt out stage, this will be fibrosis in nature. In the search for stable disease in order to show the effect of $PGF_{2\alpha}$, we might have chosen the wrong stage of the disease where the disease state is predominantly caused by hyaluronan or fibrosis rather than adipogenesis. $PGF_{2\alpha}$ inhibits adipogenesis per se but does not affect lipolysis and hence has no impact on an already fully mature adipocyte [344]. Although the aforementioned case reports described periorbital fat atrophy, our photo assessment showed only 3 patients with this effect which lasted for at least 2 months after treatment had been stopped. There was no prevalence fat available on periorbital fat atrophy. Perhaps 3 months' duration is not long enough to see the intended reduction in proptosis. Compliance also might be an issue although we did not find statistically significant treatment effect after adjustment made for compliance using a reduction in IOP as a surrogate marker (p=0.593).

Exophthalmometer readings are filled with its own caveat in terms of variability of readings with parallax error and pressure of the exophthalmometer against the orbital rim. In experienced hands it will deliver consistent results. For practical reason we did have 2

assessors in order to deliver the project in time. Both assessors were randomly assigned to the trial patients at each trial visit and also pending assessors' availability. Our assessors were calibrated by multiple exophthalmometer readings on the same non trial subjects in the clinic and adjustments were made to ensure their readings were comparable. This negative finding was further supported by our photographic assessment of proptosis conducted by an assessor who was blinded to the treatment phase. We found there were good correlations of proptosis measurement between exophthalmometer and photographic assessments suggesting that the later could be used as an alternative tool for proptosis measurement provided that there is standardisation to its process.

In general, our patient scored reassuringly high on total visual score throughout trial visits with the mean total visual score ranging from 79 to 85 and moderately with regard to total appearance score with the mean ranging from 52 to 58. This is in contrast to the original study of GO-QOL development by Terwee et al with visual means of 54.7 (standard deviation 22.8) and 60.1 (24.8) for appearance [347]. The latter group was from unselected GO patients attending endocrine clinic, 6 years younger than our group (mean 49.1 years old) and shorter duration of the disease (3,7 years) with similar CAS (less than 2) and TES (median of 6) score to our study population. As there was no impact on primary outcome with the Bimatoprost we did not expect to see any improvement with their GO-QOL. Measuring IOP in the clinic is normally performed with the head in primary position. Any deviation from this might stretch the neck muscles which in turns impede the venous return and change the intra ocular pressure. Here we did not show that stretching the head forward alters the IOP. In health economic consumption analysis, we found that there was no difference between Bimatoprost and placebo in terms of total drug and NHS encounter costs for up to 4 months after treatment. Our placebo all-inclusive direct NHS mean cost (including total drug cost) was £526.35 per annum. This was considerably high comparing to Kahaly's group data from Germany quoting £285±736 (€332 ± 857) per annum for their mild GO patients [348].

We found higher rates of visible side effects on photographic assessment skin colour changes (43.7%), eye lashes elongation (68.75%) and conjunctival redness 37.50% compare to what patients were complaining 3.2%, 0 and 32.3% respectively. Other main complaint was eye pruritus at 12.9%. The side effects are comparable to the findings of a 12-month randomized double-blind trial of Bimatoprost in glaucoma with conjunctival redness of 45%, eye lashes elongation (43%), eye pruritus (14.6%) but lower skin colour pigmentation at 5.5% [349]. Interestingly, there were more headaches symptoms in Bimatoprost phase (29%) compared to placebo (6.5%). The rate was higher than of Bimatoprost summary product characteristics which quoted the headache incidence around 1-10%. We found Bimatoprost has no effects on other outcomes measured including palpebral aperture, generic (EQ-5D-5L) Health Questionnaire, clinical activity scores (CAS) and total eye scores (TES).

The success of masking process was analysed by asking patients and assessors directly and also by independent masked assessor on photographic assessment. Approximately 27% of the patients on placebo thought that the prominence of their eyes improved compared to 42% in Bimatoprost. Just above 40% of the patients in both groups preferred the treatment. Majority patients guessed incorrectly or unsure treatment allocation by 53% in placebo group and 61% in Bimatoprost group. The figures were bettered by the assessors, whereby they guessed incorrectly or unsure by 26% in placebo group and 57% in Bimatoprost group. Even though a masked assessor was asked to assess specific side effects on the patients' photograph, these figures improved to 38% in placebo groups and decreased to 33% in Bimatoprost group.

In summary, the questions of whether Bimatoprost can reduced proptosis in inactive thyroid eye disease has been answered in a robust, randomised clinical trial: Bimatoprost does not result in improvement and this information will prevent clinicians trialling this approach and causing side-effects unnecessarily. The BIMA study has demonstrated that crossover studies can be performed reliably in patients with persistent proptosis due to thyroid eye disease and that this study design is acceptable to patients. The BIMA study also has shown that over 60%

of patients with residual proptosis in thyroid eye disease also have double vision (diplopia), confirming the unmet clinical need in this patient group.

Chapter Four

3 MODULATION OF TSHR SIGNALLING BY PUTATIVE LIGAND BINDING PROTEINS

4.1 INTRODUCTION

Graves' orbitopathy (GO) is the commonest extra thyroidal manifestation of Graves' disease (GD) affecting around 30-50% of patients [165, 350-352]. Approximately 5% will have severe disease which may lead to blindness. There is a close clinical and temporal association between GD and GO suggesting an autoimmune response to common antigen/s in the orbit and thyroid gland. Since the thyrotropin receptor (TSHR) is expressed in orbital fat [114, 118, 328, 353] and virtually all patients with hyperthyroid GO have thyroid stimulating antibodies (TSAB), the receptor is the most logical candidate. As with other autoimmune conditions there is female preponderance towards the condition with 6:1 female to male ratio, although in GO the ratio is less skewed. Extensive orbital tissue remodelling (increased adipogenesis & hyaluronan production) produces disfiguring proptosis and underpins all GO signs and symptoms. This was discussed in details in chapter one. In addition most patients with GO have reduced quality of life [153] and suffer long-term psychological distress due to the disfiguring appearance of the proptosis, also known as exophthalmos [154]. Available treatments for GO are unsatisfactory and research is needed to address the pathophysiology of the disease which may lead to early pre-clinical diagnosis promoting preventative/early interventions. This in turn will improve long-term morbidity and socioeconomic impact. As described in the introduction, the TSHR is the target of TSH, a member of the glycoprotein hormone family. In recent years, novel members of this hormone group have been identified the most notable being

thyrostimulin.

4.1.1 Thyrostimulin

The anterior pituitary gland and placenta are known to secrete members of the family of heterodimeric glycoproteins namely thyroid stimulating hormone (TSH), luteinizing hormone (LH), follicular stimulating hormone (FSH) and human choriogonadotropic hormone (HCG). These are composed of a common α subunit and specific β subunits for each hormone type and which thus confer specificity. Thyrostimulin was discovered by Nakabayashi et al in 2002 by the process of GenBank data mining [283]. It was named thyrostimulin because of its ability to stimulate the TSHR and promote thyroid hormone production. It is also known as corticotroph-derived glycoprotein as both subunits are co-localised in corticotroph cells in the anterior pituitary gland [284]. It belongs to the above described heterodimeric glycoprotein hormone family and consists of 2 subunits; α2 subunit (*GPHA2*, accession no. AF403384) - named due to its structural similarity to the common glycoprotein α-subunit and β5 (*GPHB5*, accession no. AF403430) - being the fifth member of the glycoprotein hormone β subunit. The alpha 2 gene is located on chromosome 11q13.1 and β5 is located on chromosome 14q23.2.

4.1.1.1 Thyrostimulin structure

GPHA2 is encoded by 4 exons and *GPHB5* by 3 exons [354]. The 2 subunits form a heterodimer with non-covalent bonds although this assumption was based on SDS-PAGE only after chemical crosslinking of co-expressed recombinant GPHA2 and GPHB5 with disuccinimidyl suberate [283]. The yeast two hybrid assay suggested that GPHA2 can also interact with FSH-β and HCG-β and to a lesser extent with TSH-β and LH-β [283]. Please see Figure 60 and Figure 62 for comparisons of the

sequence and 3D models of human GPHA2 with common α and GPHB5 with TSHβ subunits. GPHB5 sequence lacks the C-Terminal seat belt region but contains all the cysteine residues important for the generation of disulphide bonds and cysteine knot formation [283, 355, 356].

```
α2  1    MPMASPQTLVLYLLVLAVTEAWGQEAVIPGCHLHPFNVTVRSDRQGTCQGSHVAQA
α   1    MDYYRKYAAIFLVTLSVFLHVLHSAPDVQDCPECTLQENPFFSQPGAPILQ
α2  57   CVGHCESSAFP----SRYSVLVASGYRHNITSVSQCCTISGLKKVKVQLQCVGSRREELE
α   52   CMGCCFSRAYPTPLRSKKTMLV----QKNVTSESTCCVAKSYNRVTV----MGGFKVE--
α2  113  IFTARACQCDMCRLSRY
α   102  --NHTACHCSTCYYHKS

β5    1   MKALLLLAGYGCVLGASSGNLRTFVGCAVREFTFLAKKPGCRG-LRITTDACWGRCETWE-K
TSHβ  1   MTALFLMSM---LFGLTCGQAMSF--CIPTEYTMHIERRECAYCLTINTTICAGYCMTRDIN
β5    70  PILEPPYIEAHHRVCTYNETKQVTVKLPNCAPGVDPFYTYPVAIRCDCGACSTATTEC
TSHβ  58  GKLFLPKYALSQDVCTYRDFIYRTVEIPGCPLHVAPYFSYPVALSCKCGKCNTDYSDC
β5    128 ETI
TSHβ  116 IHEAIKTNYCTKPQKSYLVGFSV
```

Figure 60: Protein sequence alignment between (upper panel) human GPHA2 (Refseq NP_570125.1) and common α subunit (Refseq NP_000726.1) (lower panel) GPHB5 subunit (Refseq NP_660154) and TSH-β subunit (Refseq NP_000540). http://blast.ncbi.nlm.nih.gov/Blast.cgi

The consensus sequence for the cysteine knot structure is:

C1-(X)n-C2-X-G-X-C3-(X)n-C4-(X)n-C5-X-C6. G, glycine is the residue most conserved in this polypeptide. In these proteins, three disulphide (SS) bonds are arranged in such a way that one SS bond passes through the ring formed by 8 amino acids completed by the two other SS bridges [357]. The six cysteine residues forming three knotted SS bonds are numbered C1 to C6 from the N to C-terminus along the polypeptide sequence of these proteins. The disulphide bonds between cysteine residues 2 and 5 as well as 3 and 6 form part of the ring whilst cysteine residues 1 and 4 SS penetrates the ring forming a ‘knot’ (Figure 61 and Figure 62).

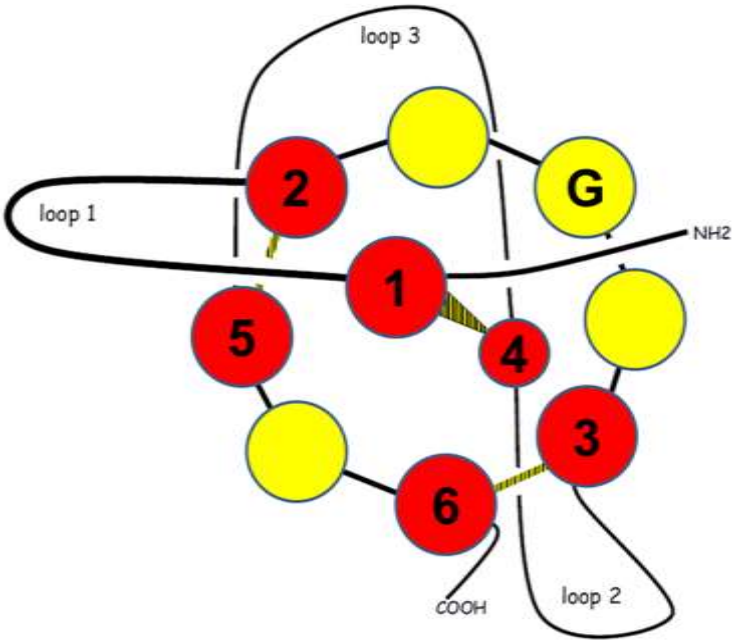

Figure 61: Schematic view of the structure of thyrostimulin protein with six cysteines belonging to the cysteine knot are shown in red with the remaining 4 shown in yellow. The ring is made up of 8 amino acids partly contributed by 2 interconnecting disulphide bridges (SS). G, glycine is the residue that is conserved and typical of an 8 amino-acid ring cysteine knot protein. The yellow lines with black stripes represent SS; yellow triangular with black stripes represents SS bond penetrating through the ring. Adapted from Alvarez et al 2009 [358].

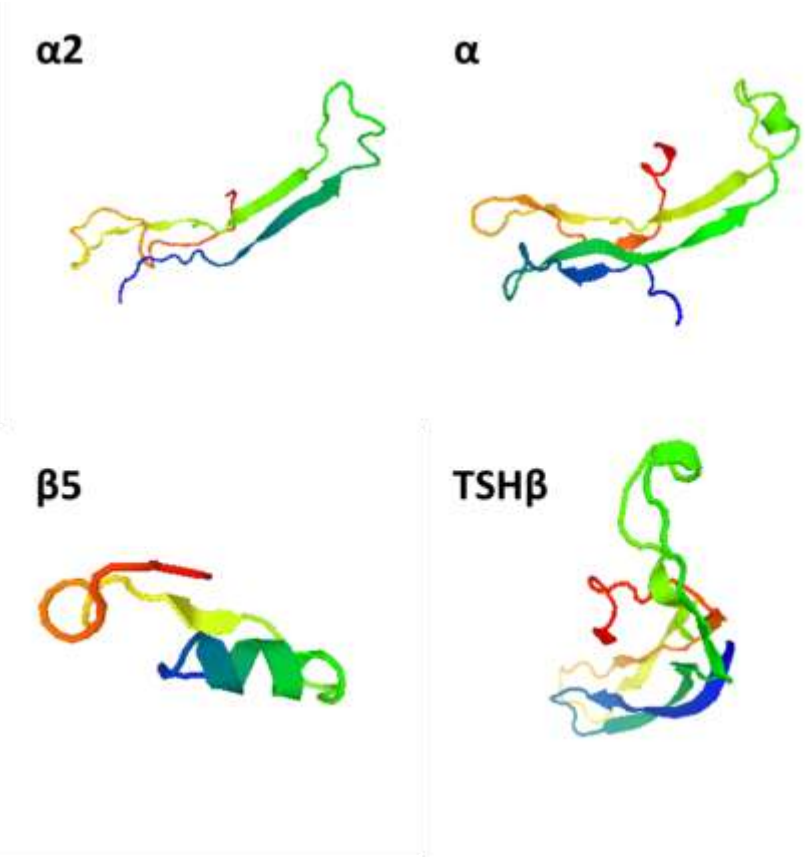

Figure 62: Comparison of protein 3D structures of the GPHA2 (α2), GPHB5 (β5), common α and TSHβ subunits. http://www.proteinmodelportal.org

As the glycoprotein name suggests, thyrostimulin has multiple N-linked glycosylation motifs. GPHA2 glycosylation motifs are located at position 14 and 58 and GPHB5 at location 63. Using site directed mutagenesis, disruption of either of the oligosaccharides in GPHA2 significantly decreased receptor activation. The disruption of either GPHA2 (at both position 14 and 58) or GPHB5 glycosylation motifs are associated with reduced expression and secretion of both subunits in the cell lysate and conditioned medium respectively [355].

4.1.1.2 Human thyrostimulin tissue expression

Similar to other β subunits, *GPHB5* subunit transcripts have restricted tissue

expression, and are found mainly in the pituitary, brain, testes, retina and skin. In contrast, *GPHA2* transcripts are found in diverse tissues [354] [284]. Immunocytochemistry studies have shown that both GPHA2 and GPHB5 are co-localised in the same cell in the pituitary gland [284]. Glycoprotein hormones are normally stabilised by the presence of the seatbelt region. Because of the absence of seatbelt, heterodimerization of GPHA2 and GPHB5 should not require reducing redox potential (to permit opening of the seatbelt SS buckle) but necessitates higher concentrations compatible with a Kd of more than 10^{-7}M [359]. Current evidence would indicate that thyrostimulin would have a short-term paracrine role but not with an endocrine role after dilution in circulation [358] as supported by the recent work of the Williams group in bone [21]. Efforts to find it in the circulation have not succeeded. The only study from human orbital retroorbital fat tissue was from Lantz et al where they were unable to show the present of thyrostimulin GPHB5 subunit but GPHA2 subunit was not tested [360]. Transgenic mice over-expressing the GPHA2 subunit had no overt phenotype but overexpression of GPHB5 in mice is associated with hyperthyroidism, weight loss and proptosis [17]. These facts suggest it is a potential major contributor to the GD and GO disease processes. In order to exert its effects, thyrostimulin or any other ligands have to bind to appropriate receptors-TSHR or potentially to their cognate binding proteins such as TSHR variant.

4.1.2 Thyrotropin receptor variant

As described in Chapter 1, TSHR consists of two subunits. After protein translation, the TSHR is split into two subunits (A and B subunits) which are linked to each other by disulphide bonds. The split results in the loss of an intervening C peptide segment corresponding to approximately 50 amino acids [93, 100]. Of interest, these 50 amino acids segments are found only in the TSHR, not LHR or other glycoprotein receptors. The A subunit is the extracellular domain and encoded by exons 1-9 and the B subunit

is the transmembrane domain responsible for G-protein coupled receptor signalling, mainly via cAMP, and encoded by exon 10 [90].

We and others have shown that activation of the TSHR in orbital preadipocyte-fibroblasts (OF) leads to increase in hyaluronan production and early stages of adipogenesis [247, 262]. TSHR expression has been shown to increase during adipogenesis [118] but little is known about the effects of TSHR activation at various stages during differentiation. G protein signalling will depend on the types and abundance of G proteins available in the cell [219]. Denis-Henriot et al has reported that rat subcutaneous preadipocytes have higher capacity to differentiate than epididymal preadipocytes that seems to be correlated with the decrease in Gq/11 alpha expression and the decreased Gq/11 mediated PKC activation [361].

Several TSHR variants have been described which lack the transmembrane domain and if expressed as protein would lead to soluble receptor products which could serve as TSH/TSAB/Thyrostimulin binding proteins (Figure 63). Variants which have been described are TSHR isoform 2 precursor (*TSHR*_v2) with 1281 base pairs amino acids which codes for amino acid residues 21-253 (NM_001018036.1) [112] and TSHR isoform 3 precursor with 1089 base pairs which code for 21-274 amino acids (NM_001142626.2) [113]. The isoform 3 is similar to isoform 2 with some unknown sequence between the expected exonic sequences. The isoform 2 1.3 kb variant encodes exons 1-8 and has a unique tail sequence (PCR amplification and southern blotting) in the thyroid and also in OF [112] [362]. Paschke et al also found presence of this transcript in the extra ocular muscle, peripheral blood mononuclear cells and cervical fat [362]. Of interest, the exon 1-8 variant is similar in structure to the *TSHR A* subunit which is generated following cleavage of the full length receptor [363, 364]. TSHR variants can potentially act as TSH binding protein, autoantigen or biomarker of GO. The role as potential autoantigen is further supported by success in GD mouse

model using recombinant adenovirus vector expressing TSHR into the muscle by Nagayama et al [365] and GD/GO model by Banga's group using in vivo electroporation of TSHR A-subunit plasmid into female BALB/c mice [80]. The latter has been reproduced successfully in Essen [366].

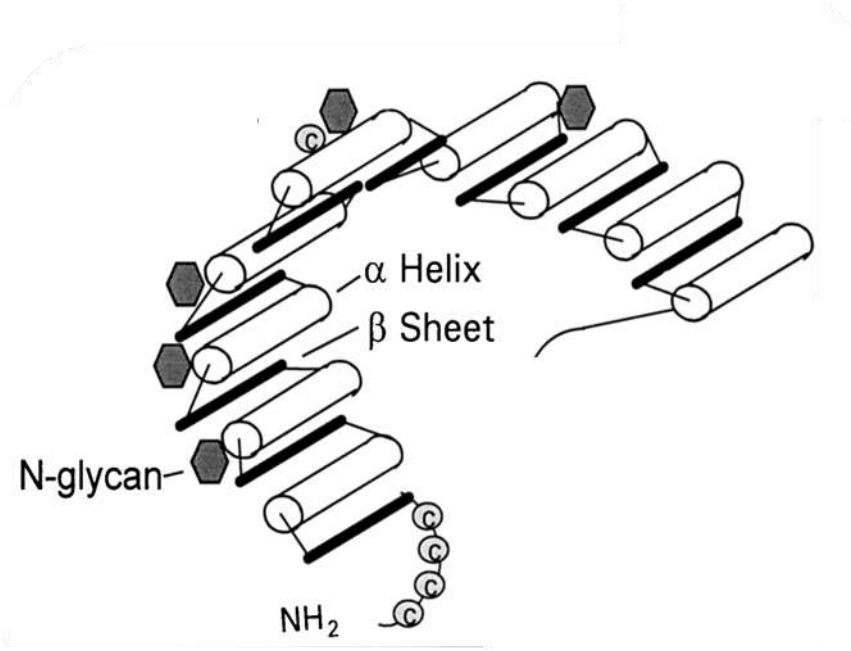

Figure 63: Thyroid binding protein illustration with 2 possible sources: TSHR A subunit shedding and TSHR variant generation. Adapted from Rapoport et al [100].

Taken together and as explained in Chapter 1, the animal models provide evidence that full length TSHR or more likely extra cellular domain TSHR subunit are easily recognisable by immune cells and also that the TSHR is probably the antigen in GO.

We hypothesize that thyrostimulin; probably locally produced, may contribute to TSHR activation and that TSHR_v2 may modulate TSHR activation, whether due to TSH, TSAB or thyrostimulin. We have chosen this variant and not other isoforms as this variant has almost complete extra cellular domain sequence which is needed to exert its function and the most studied variant compares to other isoforms. The aim of this chapter is to apply in vitro models to determine transcript expression levels of

these molecules and to determine whether these are functional using primary human orbital fibroblasts (OF) from GO patients and people free of GO supported by ex vivo analysis of orbital tissues derived from people with GO and unaffected controls. Several laboratory methods are used in this chapter including western blot analysis.

4.1.3 Western blot analysis

Western blotting is a method for detecting specific proteins in a given sample of tissue lysate or supernatant. The technique was developed by Dr W. Neal Burnette at Fred Hutchinson Cancer Research Centre in Seattle in 1979 [48]. The 'Western blot' is a play on the name of Southern blot, a DNA detection technique developed by Edwin Southern [49]. The process uses gel electrophoresis to separate denatured proteins according to molecular weight. The choice of percentage gel concentration depends on the size of protein of interest. A low percentage of acrylamide will allow separation of proteins with high molecular weight, whilst a higher percentage is suitable for the separation of the proteins that have a lower molecular weight. The protein is then transferred to a nitrocellulose membrane and followed by detection using specific antibodies. Details for each step are outlined below in section 4.2.7.

In order to detect meaningful differences in protein expression equal protein loading from each sample must be performed. Several methods exist such as bicinchoninic acid (BCA), Bradford assay and Folin-Lowry. The Bradford reaction is fast and stable for up to an hour but unlike the BCA, it is sensitive to detergents like SDS and Triton X-100. It is using the principle that negatively-charged Coomassie brilliant blue dye binds to positively-charged proteins. When the dye is in solution, it is red (absorbs 465 nm wavelength). Upon binding to basic amino acids in the protein, it becomes blue and absorbs at 595 nm. The absorption in the sample can then be compared to a standard curve. In Lowry assay, copper forms a complex with nitrogen in the protein

followed by reaction of tyrosine and tryptophan with Folin-Ciocalteau phenol reagent to give an intense, blue-green colour which absorbs at 650–750 nm. The downside of this assay is that it is not compatible with lots of common chemicals such as EDTA, Tris and carbohydrates, reducing agents (e.g., DTT, 2-mercaptoethanol). While slower than the Bradford, the BCA assay is an option to choose if the protein samples contain more than 5% detergent. 'This method utilises a known reduction of Cu^{2+} to Cu^{+} by protein in an alkaline medium (the Biuret reaction) with the highly sensitive and selective colorimetric detection of the cuprous cation (Cu^{+}) using a unique reagent containing bicinchoninic acid. The purple-coloured reaction product of this assay is formed by the chelation of two molecules of BCA with one cuprous ion. This water-soluble complex exhibits a strong absorbance at 562nm that is nearly linear with increasing protein concentrations over a broad working range (20-2000 µg/mL)'.

4.2 MATERIALS AND METHODS

All reagents were obtained from Sigma-Aldrich (St. Louis, MO) and tissue culture components were obtained from Lonza (Verviers, Belgium) unless otherwise stated.

4.2.1 Cells and tissues studied; in vitro culture & ex vivo samples

The 3T3-L1 preadipocytes and orbital tissue samples were collected and cultured in complete medium as described in chapter 2, section 2.2.1-2.2.5). Briefly, the orbital samples are from 5 GO patients (2 males and 3 females), median age of 50 years (range 39-54 years) who were diagnosed on clinical grounds based on the presence of typical clinical features and positive TSHR antibody by TBII and luciferase bioassay.

Samples for ex vivo transcript analysis comprised intact samples of orbital fat from 9

GO patients (3 males and 6 females), median age of 45 years (range 32-71 years) and 5 unaffected controls (All females), median age of 66 years (range 52-86 years). The tissue was snap frozen in liquid nitrogen directly following surgical removal.

4.2.2 I*n vitro* adipogenesis

The various cell populations were plated in 6 well plates or 75 cm^2 flasks in CM. Adipogenesis was induced in confluent cells by replacing with differentiation medium (DM) as previously described in chapter 2 section 2.2.5. Adipogenesis was quantified by measuring transcripts for terminal markers of differentiation lipoprotein lipase (*LPL*) for OF and Glyceraldehyde-3-Phosphate Dehydrogenase (*Gpdh*) for 3T3-L1 by quantitative PCR (QPCR).

4.2.3 QPCR

RNA was extracted using Tri Reagent (Sigma) from the OF (See chapter 2, section 2.2.10) and ex vivo samples using RNA easy lipid tissue mini kit (Qiagen cat. no. 74804) and treated with DNAse as described below.

4.2.4 RNA extraction for orbital fat ex vivo samples

Frozen tissues were homogenised using Tissue Ruptor (Qiagen cat. no. 9061273) in 1 ml lysis reagent then incubated for 5 minutes at room temperature. Two hundred microliters of chloroform was added followed by 15 seconds vigorous shaking then left for 3 minutes to settle. This was then centrifuged at 13000 rpm for 15 minutes at 4°C. The upper aqueous layer was transferred to a fresh Eppendorf tube with an equal amount of 70% ethanol, vortexed and transferred to a spin column and centrifuged at 13000 rpm for 15 seconds. Seven hundred microliters of buffer RW1 was added and centrifuged briefly as above to wash the column followed by a further

wash with 500 µl of the same buffer. The column was transferred to a new Eppendorf tube, spun 1 minute to dry any remaining ethanol. Finally, this was transferred into a fresh Eppendorf tube with 30 µl of RNAse free water, centrifuged at 13000 rpm for 1 minute to collect the RNA.

4.2.5 DNAse treatment protocol

For 1 µg RNA, the following were mixed in a 1.5 ml Eppendorf tube on ice:

Table 38: DNase reaction components

Components	Mass or Volume
RNA	1 µg
10X reaction buffer	1 µl
DNase I (1U/µl)	1 µl
H_2O	To 10 µl

This was incubated at 37°C for 15 minutes and terminated by addition of 1 µl 25 mM EDTA for 15 minutes incubation at 65°C. The reaction was subsequently used for reverse transcription.

One µg RNA was reverse transcribed using oligo-dT and M-MLV reverse transcriptase (Promega) (See chapter 2, section 2.2.11-13). cDNA was PCR

amplified using primers in Table 39: for *TSHR*, *TSHR*_v2 and thyrostimulin. *TSHR* (human NM_000369, mouse NM_011648 (*Tshr*)) could be distinguished from *TSHR*_v2 isoforms (human NM_001018036, mouse NM_001113404 (*Tshr*_v2) by using exon 9 & 10 primers that are not present in the truncated isoforms and using the unique sequence in intron 8 of the isoforms that are not present in full length *TSHR*. Sequencing of the amplicons produced confirmed the specificity of the primers for the different types of *TSHR*. QPCR was carried out using Brilliant II SYBR green master mix (Agilent Technologies, Stockport, UK) and a Stratagene (La Jolla, CA) MX3000 light cycler. Levels were normalised against adenosine phosphatylribosome transferase (*APRT*). Standard curves were created using the relevant PCR product cloned into pGEM T-easy (Promega, Southampton, UK) except for human *TSHR*_v2, mouse *Tshr* and *Tshr*_v2 (serial dilutions of quantified PCR amplicon were used) to calculate the copy number/1000 *APRT* copies for human and *Arp* for mouse. *APRT*/*Arp* expression has been previously shown to be unaffected by differentiation). In a single QPCR experiment, all measurements were made in duplicate.

Table 39: Primers for the TSHR isoforms and thyrostimulin subunits

	Accession number	Forward	Reverse	Amplicon size (bp)
Tshr (mouse)	NM_011648	TCTCTTACCCGAGCCACTGC (exon 9)	CCCAACACTGTTGTCACCCG (exon 10)	180
*Tshr*_v2 *(mouse)*	NM_001113404	ACGCATTCCAGGGCCTATGC (exon 6)	TCCTAGATTTGTGCCTGGTGG (exon 8)	232
TSHR	NM_000369	GTGTCACTGCCCTTCCATCCA (exon 9)	GGGGCTATTCAAGGCATTCACAGA (exon 10)	254
*TSHR*_v2	NM_001018036	CCTCCTAAAGTTCCTTGGCATT (exon 7)	AGGACTTTCTTCCAAGAGGTAG (exon 8)	338
GPHA2	NM_130769.3	CTCGGAAGTGATGCCTATGGC (exon 1)	CTAGTAGCGAGAGAGGCGAC (exon 4)	400
GPHB5	NM_145171.3	ATGAAGCTGGCATTCCTCTTC (exon 2)	CAGTTGGGCAGCTTGACAGTC (exon 3)	296

4.2.5 Agarose gel electrophoresis analysis of PCR product

If multiple peaks were observed on the QPCR melting curve (indicating multiple PCR products), the samples were analysed on a 2% agarose gel containing 400 ng/ml ethidium bromide (Promega) and visualised on an UV transilluminator, and photographed using Alpha Innotech MultiImage II (Alpha Imager HP) as previously described in chapter 2 section 2.2.14. To confirm that the PCR amplicon was the intended product, the DNA sample was sequenced as described in chapter 2 section 2.2.16. The confirmed gel bands were analysed using densitometry (AlphaView Software) for semi-quantification and corrected with respective house keeper bands.

4.2.6 Production of antibody specific for *TSHR*_v2

We have used the 21 amino acid sequence (Figure 64) derived from intron 8 of the *TSHR* which is unique to the TSHR_v2 to generate a polyclonal antibody using a commercial company (Generon, Maidenhead, UK). Briefly, the unique peptide

sequence NH2-cLPLGRKSLSFETQKAP-CONH2 (Antigen ID 140626002) was conjugated to highly immunogenic Keyhole limpet hemocyanin (KLH) via terminal Cysteine residues. Two New Zealand rabbits were subjected to a 69-day immunization schedule and bleed production. The rabbits were vaccinated with 200 µg of antigen in Complete Freund's Adjuvant (CFA) twice 2 weeks apart. The injection of antigen in CFA (heat-killed Mycobacterium tuberculosis) induces a Th1-dominated response to create intense inflammatory reaction at the site of antigen deposition. Further two 100 µg of antigen injection in Incomplete Freund's Adjuvant (IFA) 2 weeks apart were given to induce a Th2-dominated response. The rabbits were bled before and after IFA immunizations. The resulting polyclonal antibodies were affinity purified on the immunizing peptide. Using ELISA, approximately 29.73 mg antibodies were produced. We verified the specificity of each antibody using western blots (described below) on the immunizing peptide.

MRPADLLQLVLLLDLPRDLGGMGCSSPPCECHQEEDFRVTCKDIQRIPSLPPSTQTLKLIET

HLRTIPSHAFSNLPNISRIYVSIDVTLQQLESHSFYNLSKVTHIEIRNTRNLTYIDPDALKE

LPLLKFLGIFNTGLKMFPDLTKVYSTDIFFILEITDNPYMTSIPVNAFQGLCNETLTLKLYN

NGFTSVQGYAFNGTKLDAVYLNKNKYLTVIDKDAFGGVYSGPSLL***LPLGRKSLSFETQKAP***R

SSMPS

Figure 64: TSHR_v2 253 amino acid peptide sequence. Peptide sequence used for antibody production is indicated by underlined letters in italics which is where the sequence difference between full length and variant starts. Blue highlighting indicates alternate exons. Red highlighting indicates amino acids encoded across a splice junction. (Adapted from CCDS sequence data, ID number P16473-2).

4.2.7 Western blot analysis

4.2.7.1 Cell lysate and supernatant preparation

OF were cultured in 6 well plates as described previously. Cell lysates from OF at various time points before and during adipogenesis were obtained by scraping the cells with 150 µl of lysis buffer, LB (see Table 40), spun at 13000 rpm for 5 minutes and collection of the supernatant. For culture supernatant preparation, the cells were cultured in 75 cm^2 flask. Following culture medium aspiration, 5 ml serum free media (SFM) without phenol (GIBCO cat no. 11039-021) was added and collected the next day. This was then concentrated by using Amicon Ultra-15 spin columns (Merck Millipore cat no. UFC901024). Twenty ml of SFM was concentrated down to 250 µl (80 fold) by centrifugation at 4°C 3000 rpm for 30 minutes.

Table 40: Lysis buffer component was made to 100 ml and adjusted to pH 7.6. One ml of Complete™ protease inhibitor was added to 10 ml of lysis buffer prior to use.

Component (Final concentration)	Mass or volume
Trizma Base (50 nM)	600 mg
NaCl (150 mM)	875 mg
EGTA (5 mM)	190 mg
Triton x100 (1%)	1 ml
H_2O	Add up to 100 ml

4.2.7.2 Protein concentration determination

Protein concentrations of the cell lysates/supernatants were determined using bicinchoninic acid (BCA) protein assay kit (Pierce cat no. 23225). The protein assay was performed with cell lysate in LB and concentrated supernatant. These were diluted 1: 1000 in PBS before the measurement. The standard curve of 5-250 µg/ml was prepared from supplied bovine serum albumin stock in LB. Twenty-five µl of each standard or unknown sample were pipetted in duplicate into a microplate well. 200 µl of the working reagent was added to each well and mixed thoroughly on a plate shaker for 30 seconds followed by incubation at 37°C for 30 minutes. The protein concentration was measured by reading the absorbance at 562 nm in a plate reader (Dynex Technologies Inc, USA). A standard curve was constructed allowing the

protein concentrations for each cell sample to be calculated. One µg protein from each sample was used for final loading.

4.2.7.3 SDS-PAGE gel preparation

The running gel was prepared as per Table 41. Ten percent running gels were used as it has a separation range of 30-80 kDa. Fifteen percent gel was used to separate the designed TSHR_v2 peptide (1.7 kDa). Seven ml of running gel was added to 1.5 mm gel casting plates. Polymerization of the gel was initiated by ammonium persulphate in the presence of TEMED (N,N,N',N',-tetramethylethylenediamine). One ml water-saturated N-butanol was added on top of gel and the gel was allowed to set. When set, the N-butanol was removed and the gel washed three times with water. Stacking gel mixture (see Table 42) was added to the top of the running gel. Combs were placed to ensure that there are no trapped air bubbles under the comb fingers.

Table 41: Components of running gel

Components	10% Running gel	15% Running gel
30% acrylamide	3.3 ml	9.2 ml
Water	2.92 ml	3.8 ml
1M Tris (pH8.8)	3.75 ml	4.5 ml
10% SDS	100 µl	135 µl
10% ammonium persulfate (APS)*	100 µl	270 µl
TEMED*	5 µl	10 µl

* APS is made up fresh and TEMED added immediately prior to use.

Table 42: Components of stacking gel 4%

Components	Volume
30% acrylamide	1.3 ml
Water	6.1 ml
0.5M Tris (pH 6.8)	2.5 ml
10% SDS	100 µl
10% ammonium persulfate (APS)*	100 µl
TEMED*	10 µl

* APS is made up fresh and TEMED added immediately prior to use

4.2.7.4 Sample loading and gel running

Samples were added to an equal volume of loading buffer (Table 43). Ten µl of molecular weight marker (10-250 kDa) (New England Biolabs cat no. 7703S) was added to 10 µl loading buffer. The samples were boiled for 5 minutes then centrifuged for 5 minutes at 13,000 rpm. The samples which contained 1 µg protein were loaded into each wells and separated at 200v for 30-45 minutes in running buffer (Table 44) until the tracking dye band had reached the bottom of the gel.

Table 43: Loading Buffer

Component	Volume
10% SDS	2 ml
Glycerol	1 ml
0.5M Tris (pH 6.8)	1 ml
cOmplete™, Mini protease inhibitor	0.8 ml
0.2% Pyronin Y	0.1 ml
β-mercaptoethanol	0.1 ml
PMSF (100mM)	10 µl/ml

Table 44: Running buffer

Components	Weight
Tris	15 g
Glycine	72 g
SDS	5 g
H_2O	Made up to 1 litre

4.2.7.5 Electroblotting using PVDF membrane

The resulting SDS-PAGE gel was placed in blotting buffer (Table 45) for 20 minutes on an orbital shaker. PVDF membrane was cut to fit the gel 5.5 cm x 8.5 cm, briefly soaked in 100% methanol and rinsed twice in distilled H_2O. The membrane was then allowed to equilibrate in blotting buffer for 15 minutes by gently shaking. Two pieces of filter paper (cut to similar size to fibre pad) and two fibre pads were soaked in blotting buffer for 10 minutes ensuring no air was trapped in the fibre pad. The gel/membrane sandwich was prepared as depicted in Figure 65.

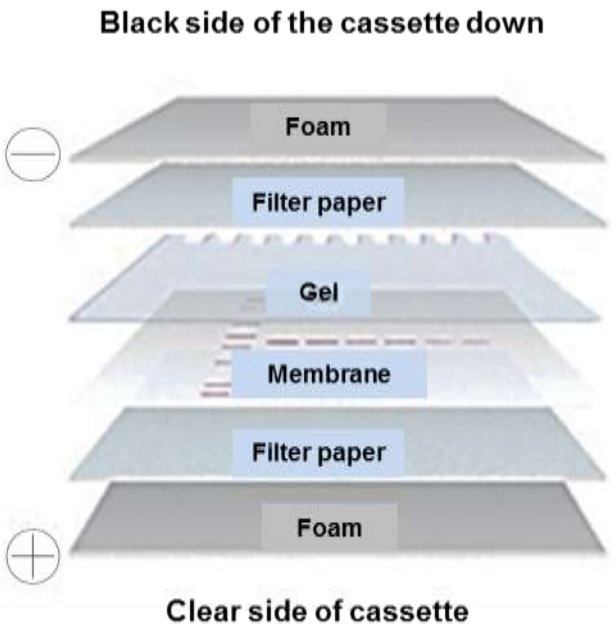

Figure 65: Electroblotting using gel/PVDF membrane sandwich illustration. The figure was adapted from http://www.bio-rad.com/en-uk/category/western-blotting-membranes-filter-paper.

After the second piece of filter was placed on the gel, a Pasteur pipette was rolled over the stack to remove any air bubbles. The cassette was inserted into the tank containing blotting buffer and an ice pack. Protein transfer was achieved by running at 350 mA for one hour while stirring.

Table 45: Components of blotting buffer

Components	Weight/Volume
Tris (0.025M)	3.025 g
Glycine (0.182M)	13.66 g
H_2O	800 ml
Methanol	200 ml

The mixture was cooled at -20°C for an hour prior to use.

4.2.7.6 Blot development

All washes/incubations steps were performed on an orbital shaker. This is to ensure that the blot moves freely and is not stuck to the bottom of the dish. After blotting the membrane was transferred and washed for 5 minutes in TBS-T (see Table 46: and Table 47:). The membrane was blocked with 50 ml blocking buffer (Table 48) overnight at 4°C then placed in a square Petri dish in10 ml blocking buffer containing primary antibody at optimal dilution. The membranes were probed using antibodies to the full length TSHR (2C11, Santa Cruz Biotechnology) and TSHR_v2 antibody, at dilutions of 1:200 and 1:50 respectively at 4°C overnight. After incubation step, primary antibody was removed and membrane washed 3X for 5 minutes with TBS-T. This was followed by a sheep anti-mouse IgG-HRP (1:5000, room temperature for 1 h, GE Healthcare) or donkey anti-rabbit IgG-HRP conjugate (1:5000, room temperature for 1 h, GE Healthcare).

Table 46: TBS (10X)

Components	Weight
Tris (0.2M)	24.2 g
NaCl (0.137M)	80 g
H_2O	Made up to 1 litre

TBS was pH to 7.6 with HCl and stock kept in the fridge

Table 47: TBS-T

Components	Volume
TBS (10X)	100 ml
H_2O	900 ml
Tween 20	1 ml

Table 48: Blocking buffer

Components	Weight/volume
TBS-T	100 ml
Marvel	5 g

4.2.7.7 Stripping and reprobing PVDF membrane

Membranes were re-probed by stripping antibodies off the membrane using stripping buffer (Table 49) which were then probed with housekeeping antibodies. The stripping buffer was prepared and warmed to 60°C in a hybridization oven. If the blot dries out the membrane would be re-wetted with methanol for 30 seconds and washed 3X for 5 minutes with TBS-T, if the membrane still wet this step would be omitted. Blots were then incubated with 50 ml stripping buffer in the hybridization oven (GE Healthcare Life Sciences, UK) at 60˚C 30 minutes with gentle mixing. After stripping blots were washed 3X for 10 minutes with 50 ml of TBS-T. These blots were blocked with blocking buffer for 1 hour at room temperature and re-probed with antibodies to housekeeping protein, actin at dilution of 1:1000 4°C overnight with secondary anti-rabbit as above.

Table 49: Stripping buffer (50 ml)

Components	Volume
Tris 0.5M (pH 6.8)	6.25 ml
10% SDS	10 ml
Mercaptoethanol	0.35 ml
H_2O	33.5 ml

4.2.7.8 TSHR_v2 antibody verification

TSHR_v2 antibodies supplied were verified against the immunization peptide (1.7 kDa). The following adjustments were made- 20 microliters of peptide was diluted with 180 µl SFM and mixed with an equal amount of loading buffer. The comb was taped to give a single well in a 15% gel to accommodate peptide loading. The peptide was run half way down the gel and blotted for 30 minutes instead of 1 hour. The membrane was cut into strips of equal size for immunoblotting.

4.2.7.9 Detection of protein

Membrane-bound proteins labelled with HRP conjugate were detected via chemiluminescence (ECL Plus, GE Healthcare) by exposing PVDF membrane with antigen–antibody complex to film in a dark room. After a series of washings with TBS-T (2X for 30 seconds, 1X for 15 minutes and 3X for 5 minutes), the membrane was removed and excess TBS-T drained. ECL Plus reagent was prepared (1:1 ratio of

solution A: solution B) and 2 ml pipetted onto the protein side of the membrane and incubated at room temperature for 5 minutes. Excess solution was drained before wrapping in saran wrap and placed in a film cassette with the protein side up. A film sheet (HyperflimTM ECL, GE Healthcare, UK) was cut to size and placed on top of the membrane. The film cassette was closed to allow exposure time from 5 seconds to 15 minutes depending on signal strength. Exposed film was placed into the developer solution (Kodak D-19, Kodak, UK) until bands appear and then placed in fixer (Polymax T, Kodak, UK) for a few minutes. The developed film was washed with running water for 15 minutes then dried. Film was aligned with blot in the cassette to mark position of the standards.

4.2.8 Measurement of TSHR activation

TSHR activation was measured in two different contexts. cAMP induced by TSH / TSAB (M22) was measured directly in OF using radioimmunoassay and indirectly using luciferase bioassay to determine whether the TSHR_v2 is secreted as a TSHR-BP (see below).

4.2.8.1 cAMP Radioimmunoassay

4.2.8.1.1 Sample preparation

In the direct assay, 5 x10^4 OF in 1 ml per well were plated in triplicates and cultured in 12 well plates at various time points before and during adipogenesis. Prior to the assay they were switched to 500 µl/well serum free medium for 24 hour and then treated with IBMX 10^{-4}M alone or combined with bovine TSH 5 mu/ml or monoclonal TSAB (m22, RSR) 0.2 ng/µl 37°C for 4 hours. These were then washed with 1ml PBS/well. The cAMP was extracted using 500 µl 0.1M HCl and frozen until further analysis. The day prior to performing RIA, the HCl extracts were evaporated to

dryness using speedvac. The residue was resuspended in 300 µl of acetate buffer and 100 µl was used to measure cAMP.

4.2.8.1.2 Sample analysis

cAMP in the lysate was measured using cAMP [125I] RIA Kit (PerkinElmer Life Sciences). The cAMP stock standard reagent (50,000 pmol/ml) was diluted by fifty-fold by adding 100 µl of the stock solution to 4.9 ml of assay buffer resulting 1,000 pmol/ml standard solution. Further dilution was made down to 40 pmol/ml (by adding 0.1 ml of the 1,000 pmol/ml solution to 2.4 ml of assay buffer). The samples were prepared for acetylation as follows: 100 µl of the sample was pipetted into 400 µl of assay buffer (1:5 dilutions). 150 µl of acetylation reagent was prepared by mixing together in a glass test tube 100 µl of Triethylamine and 50 µl of Acetic Anhydride and vortexed. 10 ml of modified assay buffer was prepared by adding 50 µl of the acetylation reagent to 10 mL of assay buffer. The modified assay buffer was used for the preparation of the cAMP standards and in the “blank” and “zero standard” tubes. The 40 pmol/ml standard was acetylated by adding to it 10 µL of the freshly prepared acetylation reagent and 1.8 ml of assay buffer and further diluted to create a range of concentration from 0.05 to 4 pmol/ml. The samples were acetylated by adding 5 µl of acetylation reagent to each 100 µl diluted samples and vortexed, followed by an addition of 900 µl of assay buffer to each tube (Final sample dilution of 1:50). The working tracer solution was prepared by adding one volume of diluted cAMP [125I]-Tracer to one volume of the reconstituted cAMP carrier serum. 100 µl of working tracer and antiserum complex were added to all tubes and vortexed. These were incubated overnight at 4°C. The following day 500 µl of 4°C cAMP precipitator was added, centrifuged at 4°C for 15 minutes 1,200 x g and decanted before counting in a gamma counter for 50 seconds. The average net counts for each standard and sample were expressed as a percentage of the average net counts for the zero

standard (termed “normalized” percent bound or % B/Bo).

$$\% \text{ B/Bo} = \frac{\text{Average Net Counts of Standard or Sample} \times 100}{\text{Average Net Counts of Zero Standard}}$$

4.2.8.2 Luciferase bioassay

In the indirect assay, culture supernatants from OF before and at various time points during adipogenesis were collected as described above. The supernatants were then added to TSH or M22 whilst they were assayed using an in-house luciferase bioassay as previously described [367]. Clone lulu* cells are CHO cells expressing the full-length human TSHR and a cAMP-responsive luciferase reporter and clone zulu cells are CHO cells expressing cAMP-responsive luciferase reporter without the full-length human TSHR. Initially lulu* cells have been shown to display a dose dependent TSH response detectable from 10 µU/ml and maximal at 10 mU/ml when a >25 fold increase in light output was obtained [367]. Zulu cell serves as control for non-specific binding.

4.2.8.2.1 Maintenance of lulu* and zulu cell line.

Lulu*/zulu cells were maintained in 75 cm^2 flasks at 37°C in 5% CO_2 in Ham’s F12 medium containing 10% FCS and G418 antibiotic (see Table 50). The cells were found to be very sensitive needing medium replacement every second day.

Table 50: Hams F12 medium components

Component	Volume (ml)
Hams F12	171
Sodium Bicarbonate	5
FCS	20
Penicillin/Streptomycin	4
G418 (40mg/ml)	2
TOTAL	200

Once confluent cells were trypsinised and resuspended in fresh medium and aliquotted into new culture vessels at a split ratio of 1:10. The cell stocks were frozen in the liquid nitrogen as described in chapter 2 section 2.2.2.

4.2.8.2.2 Preparation of bioassay

A confluent 75 cm^2 flask of cells were trypsinised and resuspended in 20 ml of Hams F12 medium. 2 x 10^4 lulu* and zulu 200 µl/well were plated in triplicates in 96 well plates in Hams F12 medium for 24 hours. The next day the medium was replaced with Hams F12 containing 10% charcoal stripped serum. On the second day of assay, the cells were washed with 100 µl serum free media and 100 µl culture supernatants added with or without (control) TSH or M22. These were incubated at 37°C for 5 hours

prior to 100 µl saline wash and addition of 55 µl passive lysis buffer (Promega) and frozen at -80°C prior to analysis. The analysis was performed using 50 µl of the cell extracts with luciferase assay reagent (Promega) using Glomax Multidetection System (Promega). Stimulation index was calculated by dividing the mean of stimulated/unstimulated lulu* light unit ratio for each sample by the mean of stimulated/unstimulated zulu light unit ratio.

4.3 STATISTICAL ANALYSIS

For statistical analysis, we used SPSS 18.0 software. Where appropriate, data were analysed using Student's *t* test for parametric and Mann-Whitney for non-parametric. A paired t-test and One- way ANOVA with post-hoc Tukey analysis were carried out where indicated. In all cases, $p<0.05$ was considered significant. The statistical analysis applied is indicated in the tables and figure legends. All parametric data are presented as mean ± standard deviation and median ± interquartile range for non-parametric.

4.4 RESULTS

4.4.1 3T3-L1 in vitro adipogenesis

3T3-L1 was successfully induced to undergo adipogenesis. This was confirmed morphologically and by terminal marker of differentiation glycerol-3-phosphate dehydrogenase (*Gpdh*) transcript levels. Morphologically, the maximum adipogenesis process was noted by day 6-7 but by *Gpdh* transcripts the maximum adipogenesis was achieved by day 8 (Figure 66).

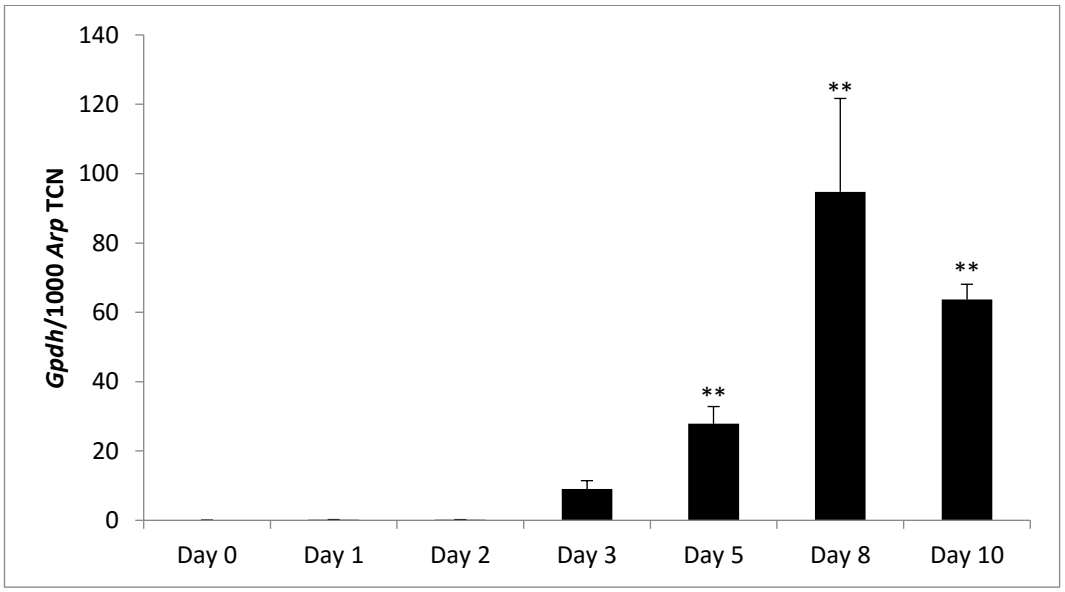

Figure 66: In vitro induced adipogenesis of 3T3-L1 cells assessed by QPCR measurement of glycerol-3-phosphate dehydrogenase (*Gpdh*) transcripts expressed as transcript copy number (TCN) per 1000 copies of acidic ribophosphoprotein (*Arp*) housekeeper gene. Data shown (mean ± SD) are from a representative experiment of two performed in duplicate. **p< 0.01.

4.4.2 3T3-L1 *Tshr/Tshr*_v2 transcripts increase with adipogenesis

Similar to *Gpdh* data, 3T3-L1 *Tshr* full length and *Tshr*_v2 transcript levels were highest on day 8 for *Tshr* and day 10 for *Tshr*_v2 (Figure 67). Despite multiple attempts to optimize primers for *Tshr*_v2, we were unable to produce primer pair that works for QPCR reaction. The designed primers produced multiple peaks on dissociation curve (Figure 68). These were separated on electrophoresis gel to reveal 2 bands, *Tshr*_v2 (232bp) and additional bands around 75bp which might represent primer dimer (Figure 69). Therefore, the results for *Tshr*_v2 were obtained by densitometry and not QPCR.

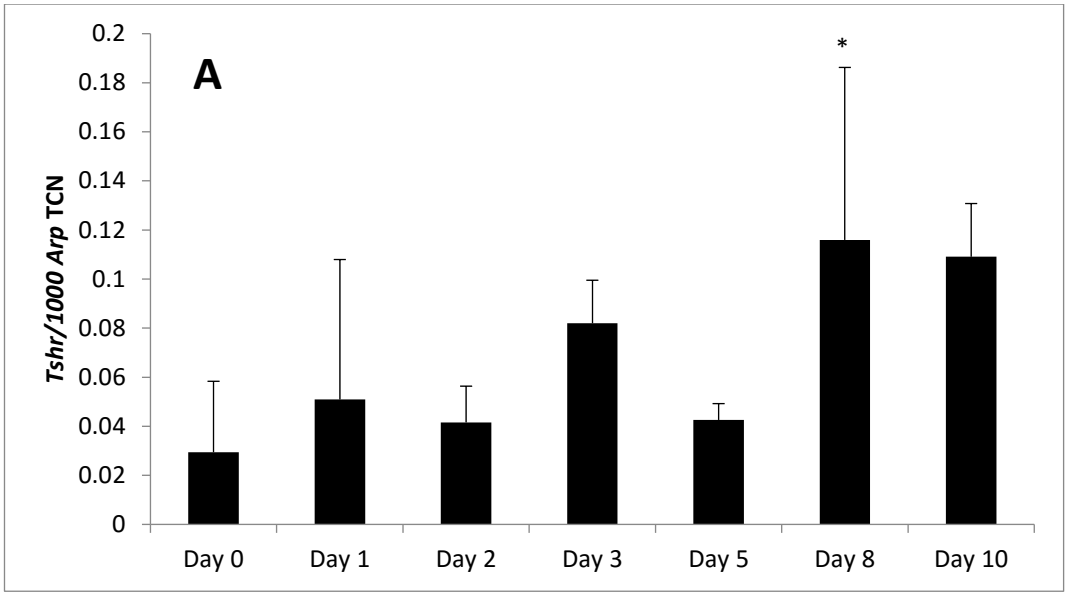

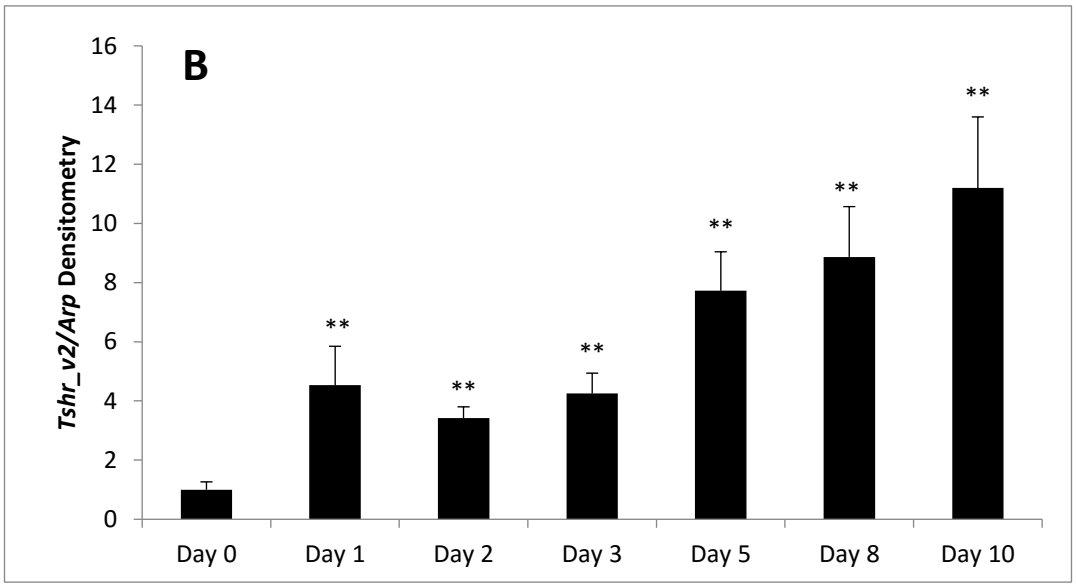

Figure 67: Transcripts for A; the full length *Tshr* and B; the *Tshr*_v2 were measured in 3T3-L1 by densitometry of QPCR products at various time points before (Day 0) and during adipogenesis (Day 1-10). Results are expressed as transcript copy number of *Tshr* per 1000 copies of the housekeeper *Arp* (A) and *Tshr*_v2 corrected to *Arp* by densitometry. Results are presented as mean ± SD. p value ** <0.01 compared to day 0 on each respective day.

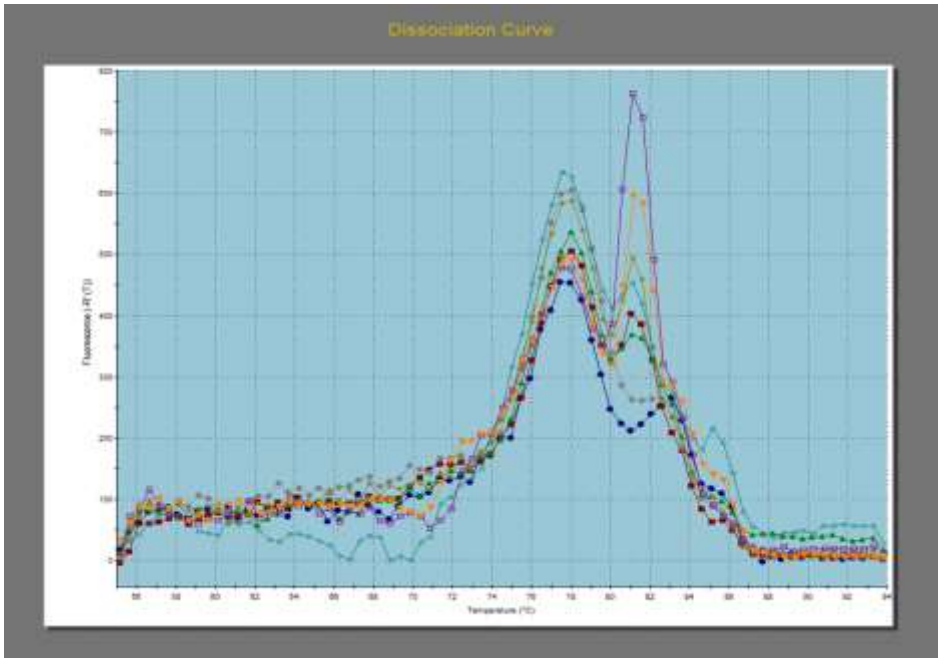

Figure 68: Dissociation curve for *Tshr*_v2 QPCR showing multiple peaks suggesting multiple band sizes.

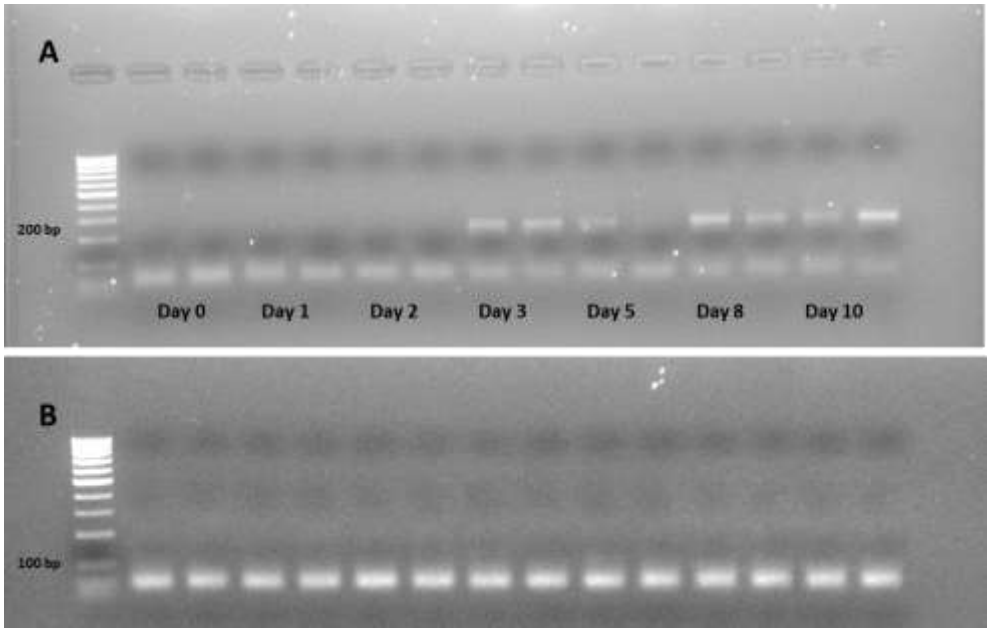

Figure 69: Representative densitometry of *Tshr*_v2 QPCR showing *Tshr*_v2 bands (232bp) and additional bands around 75bp (A) and corresponding to housekeeping *Arp* bands (72bp) (B).

4.4.3 GO orbital fibroblast had higher adipogenic potential than normal

Human OF adipogenesis was induced in about 30% of cells and we noted that cells obtained from GO patients had higher adipogenic potential than those from unaffected orbits (Figure 70).

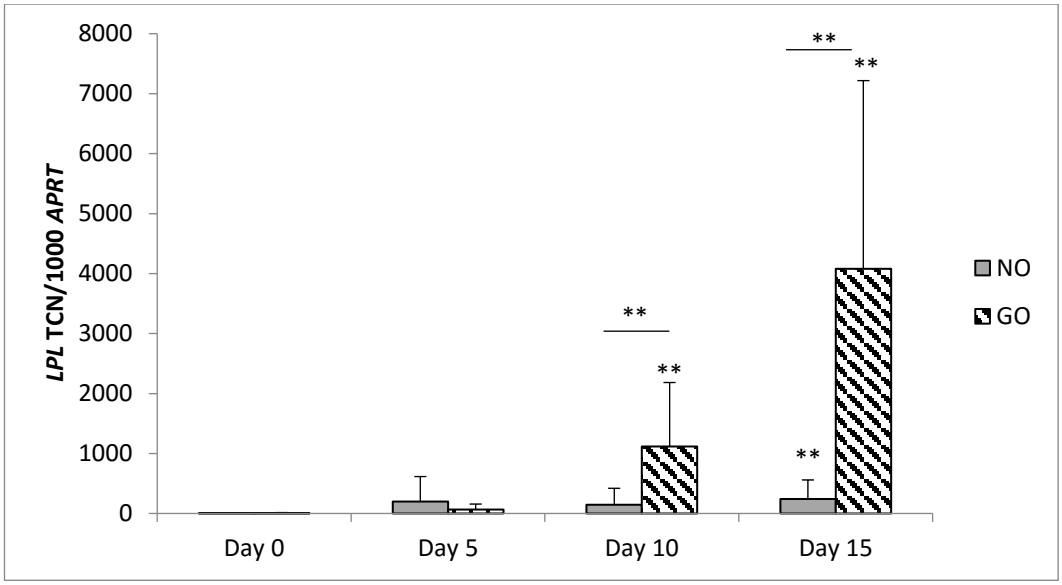

Figure 70: Transcripts for the terminal marker of adipogenesis Lipoprotein lipase (*LPL*) were measured in orbital preadipocyte-fibroblasts from patients with Graves' orbitopathy, GO (Stippled bar, n=5) and unaffected (Grey bar, n=5) at various time points before (Day 0) and during adipogenesis (Day 5, 10, 15). Results are expressed as transcript copy number of *LPL* per 1000 copies of the housekeeper *APRT*. Results are presented as mean ± SD; **p value <0.01 compared to day 0 on each respective day. Horizontal bar represent comparison between normal and GO.

4.4.4 Thyrostimulin is unlikely to have a role in GO

We measured transcripts for both thyrostimulin subunits. As shown in Figure 71, *GPHA2* transcripts were present at baseline but a significant reduction in transcript levels was observed during adipogenesis ($p<0.05$) but with some recovery by day 15. This might suggest some factor(s) secreted during early adipogenesis, but not later in differentiation, which inhibits GPHA2 transcription. No difference was observed between normal and GO OF. In contrast *GPHB5* transcripts were at the limit of detection at all-time points (data not shown).

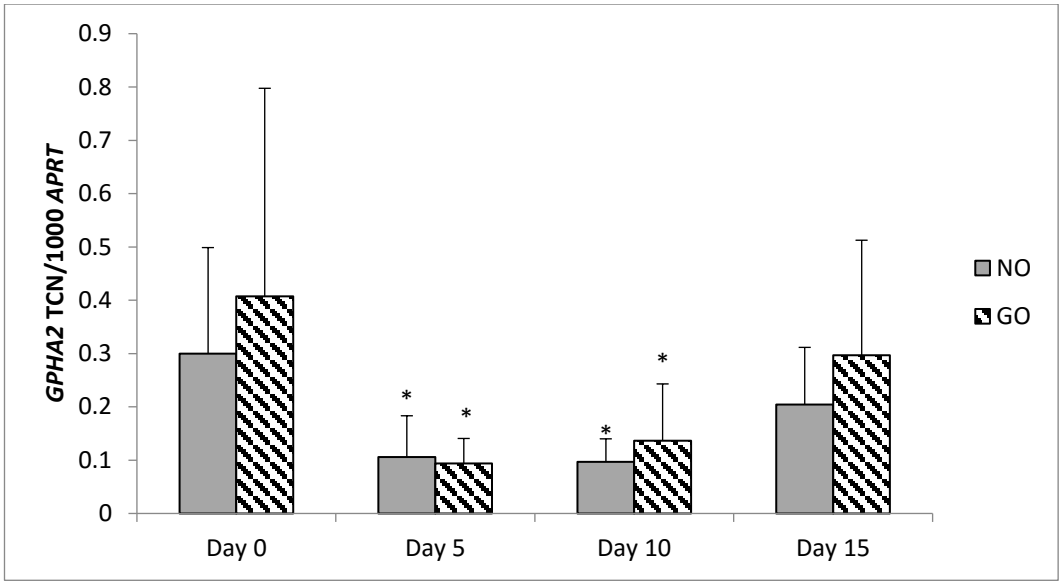

Figure 71: Transcripts for the thyrostimulin *GPHA2* subunit were measured in orbital preadipocyte-fibroblasts from patients with Graves' orbitopathy (Stippled bar, n=5) and unaffected (Grey bar, n=5) at various time points before (Day 0) and during adipogenesis (Day 5, 10, 15). Results are expressed as transcript copy number of α2 per 1000 copies of the housekeeper *APRT*). Results are presented as mean ± SD; *p value <0.05 compared to day 0 on each respective day for GO and non-GO.

4.4.5 *TSHR*_v2 transcripts are more abundant than full-length *TSHR*

We confirmed others and our previous finding that expression of full-length *TSHR* increases during adipogenesis. In this experiment we found there was no significant difference noted between GO and unaffected cells as shown in Figure 72A. The *TSHR*_v2 was more abundant than the complete receptor and again its expression increased during differentiation, as shown in Figure 72B. However, the *TSHR*_v2 was significantly more abundant in GO than unaffected, possibly reflecting the higher adipogenic potential of these cells. Consequently, the ratio of *TSHR*_v2 to *TSHR* differed significantly at various time points when comparing GO and unaffected, as shown in Figure 72C. The fact that *TSHR*_v2 upregulation was no longer shown when corrected with *TSHR* might suggest that *TSHR*_v2 expression regulation is related to *TSHR* expression.

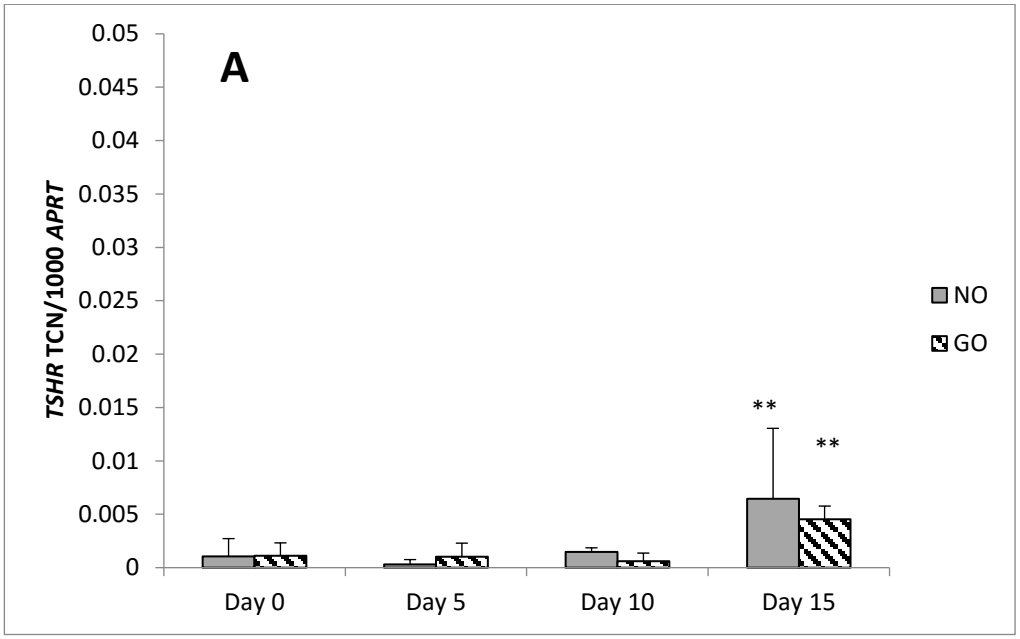
A
0.05
0.045
0.04
0.035
0.03
0.025
0.02
0.015
0.01
0.005
0
TSHR TCN/1000 APRT
**
**
NO
GO
Day 0
Day 5
Day 10
Day 15

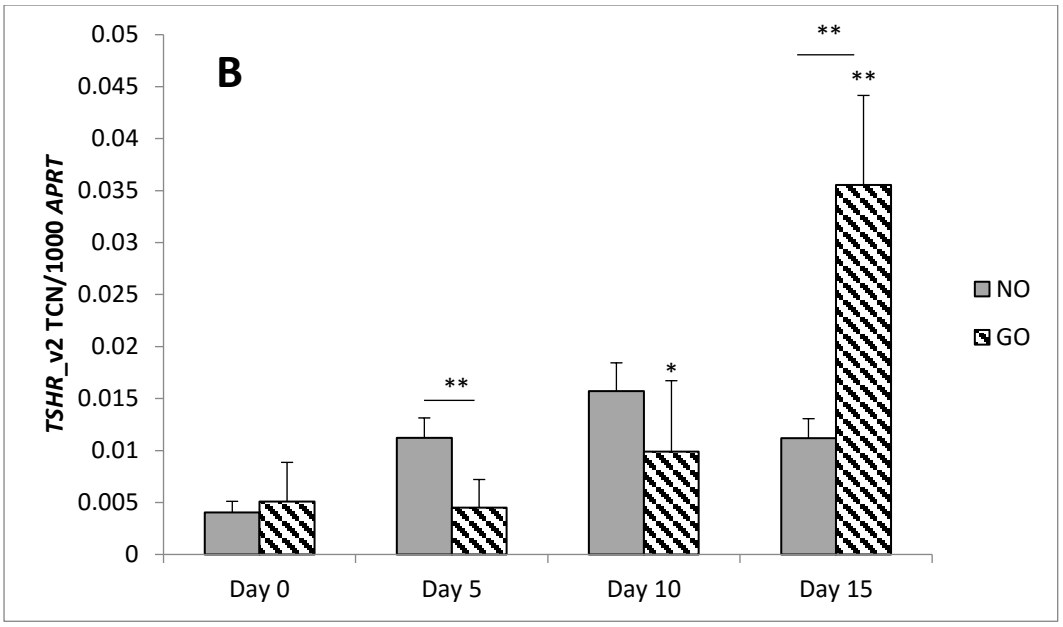
B
0.05
0.045
0.04
0.035
0.03
0.025
0.02
0.015
0.01
0.005
0
TSHR_v2 TCN/1000 APRT
**
**
**
*
NO
GO
Day 0
Day 5
Day 10
Day 15

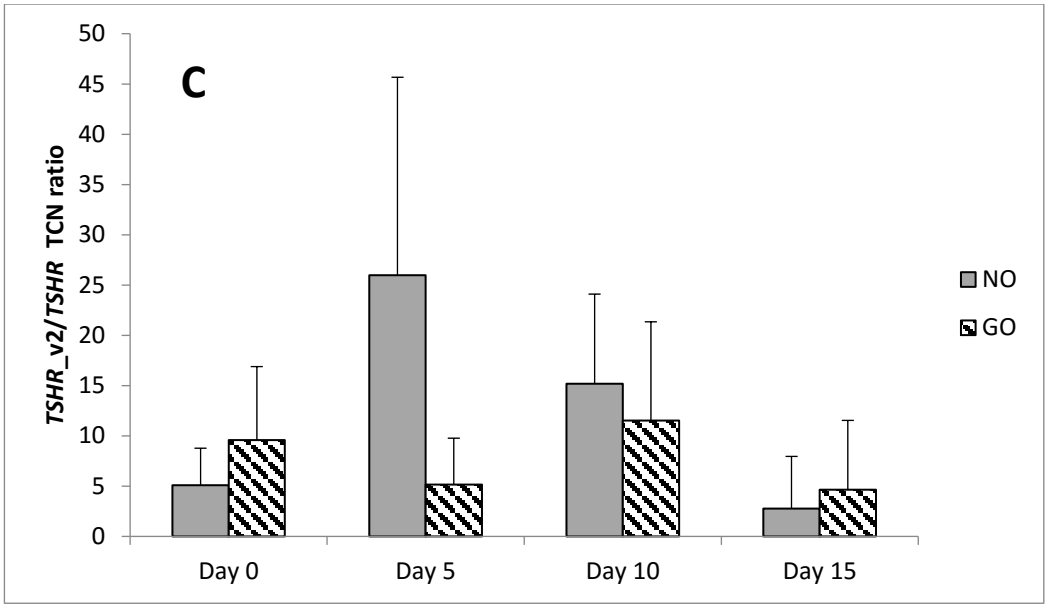

Figure 72: Transcripts for A; the full length *TSHR* and B; the *TSHR*_v2 were measured in orbital preadipocyte-fibroblasts from patients with Graves' orbitopathy, GO (Stippled bar, n=5) and unaffected (Grey bar, n=5) at various time points before (Day 0) and during adipogenesis (Day 5, 10, 15). Results are expressed as transcript copy number of *TSHR* or *TSHR*_v2 per 1000 copies of the housekeeper *APRT*. C; the ratio of *TSHR*_v2*:TSHR* in GO patients (Stippled bar, n=5) and in unaffected orbits (Grey bar, n=5).). Results are presented as mean ± SD except C presented as median ± interquartile range; *p value <0.05, ** <0.01 compared to day 0 on each respective day. Horizontal bars represent comparison between normal and GO.

4.4.6 Thyrostimulin & *TSHR*_v2 in ex vivo samples

Analysis of orbital fat directly after surgical removal and without any modification due to in vitro culture was also performed. As the sample sizes are small, the results are presented as dot plots instead of histograms to show the value for each patient. We confirmed results of in vitro cultures in that *GPHA2* transcripts of the thyrostimulin was present in the ex vivo samples with no difference between GO and unaffected. *GPHB5* were undetectable. Transcripts for the *TSHR*_v2 were also present but we did not observe differential effect between GO and unaffected. We did however confirm results in vitro cultures that *TSHR*_v2 was more abundant than full length *TSHR* (Figure 73). Similar to in vitro transcripts data the *TSHR*_v2*:TSHR* ratio was

no different.

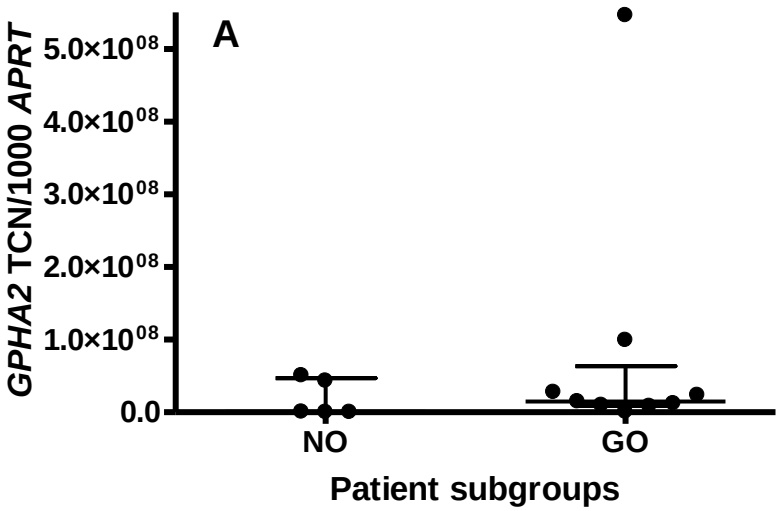

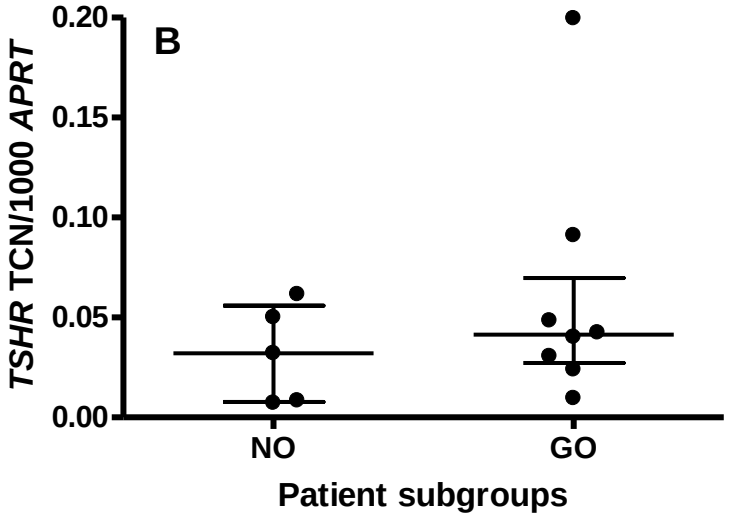

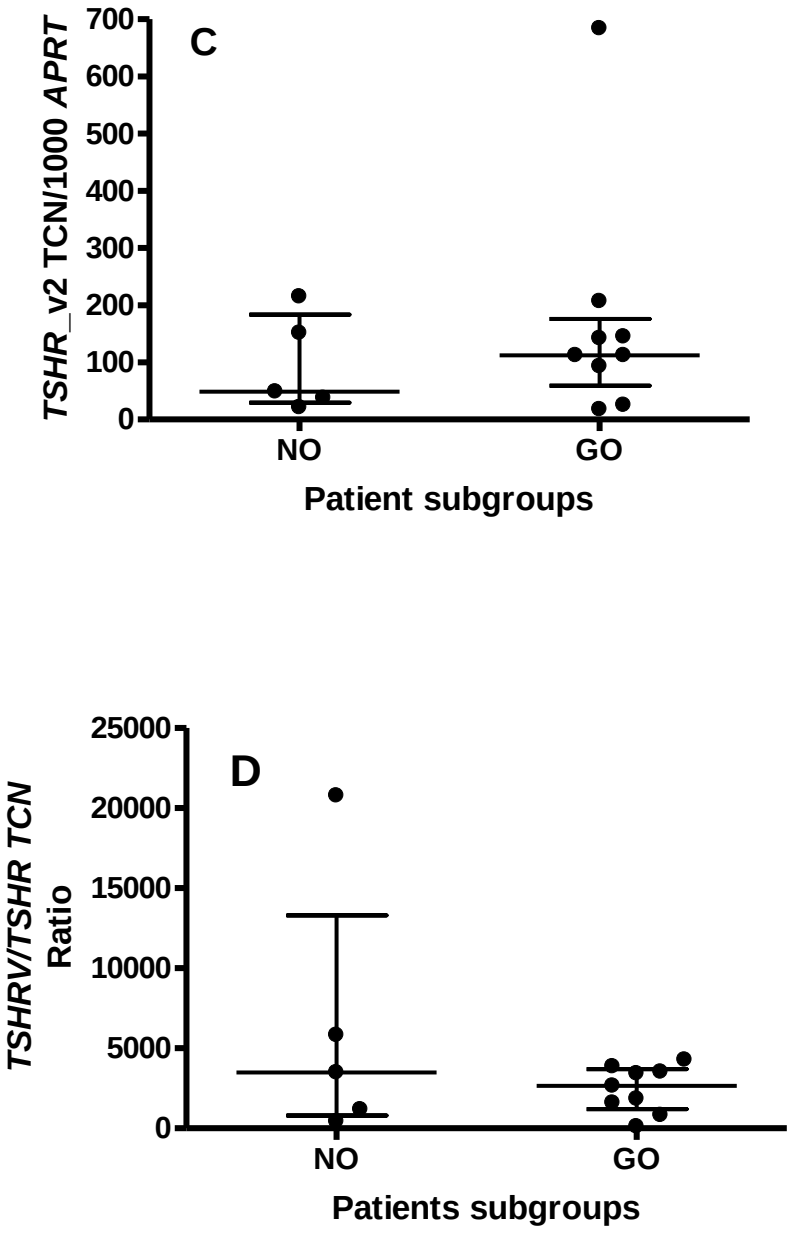

Figure 73: Ex vivo analysis of orbital preadipocyte-fibroblasts from unaffected individuals (NO, n=5) and patients with Graves' orbitopathy, (GO, n=9 except figure B and C n=8) for transcripts of A; *GPHA2* subunit, B; *TSHR*, C; the *TSHR*_v2, D; the *TSHR*_v2:*TSHR* transcripts ratio. Results are expressed as transcript copy number per 1000 copies of the housekeeper *APRT*. Results are presented as median ± interquartile range.

4.4.7 Human TSHR_v2 antibodies were successfully generated

The TSHR_v2 antibodies were successfully generated to detect the intended peptide sequence as shown in Figure 74 as dark bands on the lower part of the figure with calculated molecular weight of 1.7 kDa. Higher titre antibodies were produced from rabbit 1 (Figure 74).

Figure 74: Western blot analysis of immunizing peptide showing stronger band from rabbit 1 sera than rabbit 2. Second immunisation produced a stronger band with higher specificity than 1st immunisation. Pre: Pre immune serum; 1st and 2nd: first and second immunisation; P1 and P2: post affinity column purification.

The antibody was then blotted against GO and normal OF lysates and unconcentrated supernatants. Using 1:50 TSHR_v2 antibodies dilution in PBS resulted stronger signal at an apparent molecular mass of 46 kDa than 1:200 dilutions but at the expense of some other higher molecular mass bands. The TSHR_v2 was not detectable in unconcentrated supernatants either from GO or normal OF (Figure 75). As previously discussed, to ensure the specificity of TSHR_v2 antibodies, the immunisation peptide was designed based on 8th intronic sequence of full length TSHR which was unique to TSHR_v2. This was supported by the absence of TSHR band (expected molecular weight 62 kDa) on the blot indicating specificity of the TSHR_v2 antibodies (Figure 75).

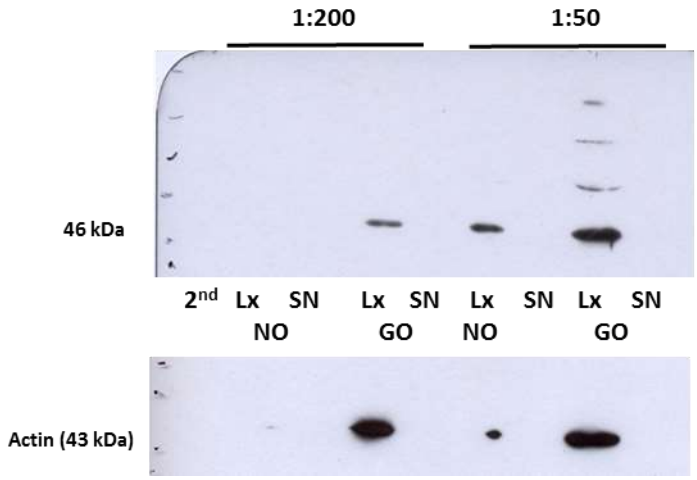

Figure 75: Western blot analysis of preadipocyte-fibroblast lysates and unconcentrated supernatants 15 days after adipogenesis from a patient affected (GO) and not (NO) with Graves' orbitopathy showing protein with an apparent molecular mass of 46 kDa. There were other bands detected at 56, 80 and in between 80-175 kDa by using 1:50 anti TSHR_v2 antibodies dilution. 2nd: secondary antibody only; Lx: lysate; SN: supernatant.

4.4.8 TSHR_v2 and TSHR protein are detectable in orbital preadipocyte-fibroblasts

We then performed western blots on cell lysates and concentrated culture supernatants from GO and unaffected OF. One µg protein was loaded into each well. This was calculated from standard curve of bovine serum albumin by BCA assay (Figure 76). Equal loading was confirmed on western blot of housekeeping protein actin (Figure 77). As shown in Figure 77A, a protein with an apparent molecular mass of 46 kDa was present in the cell lysates and culture supernatants from OF. This is consistent with the TSHR_v2, which comprises 253 amino acids and retains 5 of the 6 putative N-linked glycosylation sites present in the full-length TSHR. The doublet may reflect differing amounts of glycosylation. Its presence in the conditioned culture medium indicates that it can be secreted from cells which express it.

Of note, the protein levels increased when comparing cells before and after adipogenesis and there was a substantially stronger signal in the GO samples, when compared with unaffected, both in the cell lysates and conditioned culture medium (n=3 GO and 3 Normal). Using 2C11 antibody, we also showed that TSHR protein with an apparent molecular mass of 62 kDa was present in the lysates after adipogenesis and higher in GO than normal. This is consistent with the shed TSHR A subunit (Figure 77B).

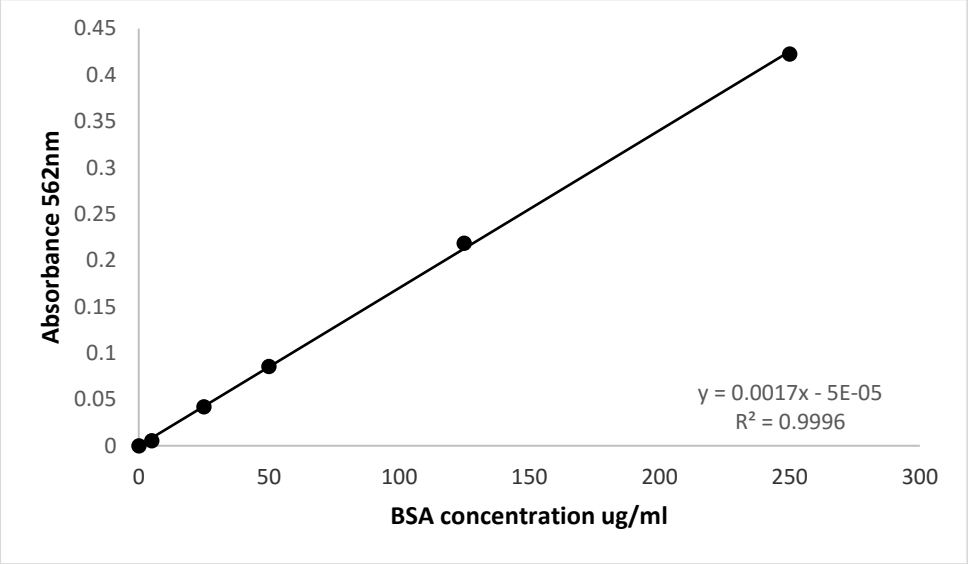

Figure 76: BCA assay standard curve for protein quantifications.

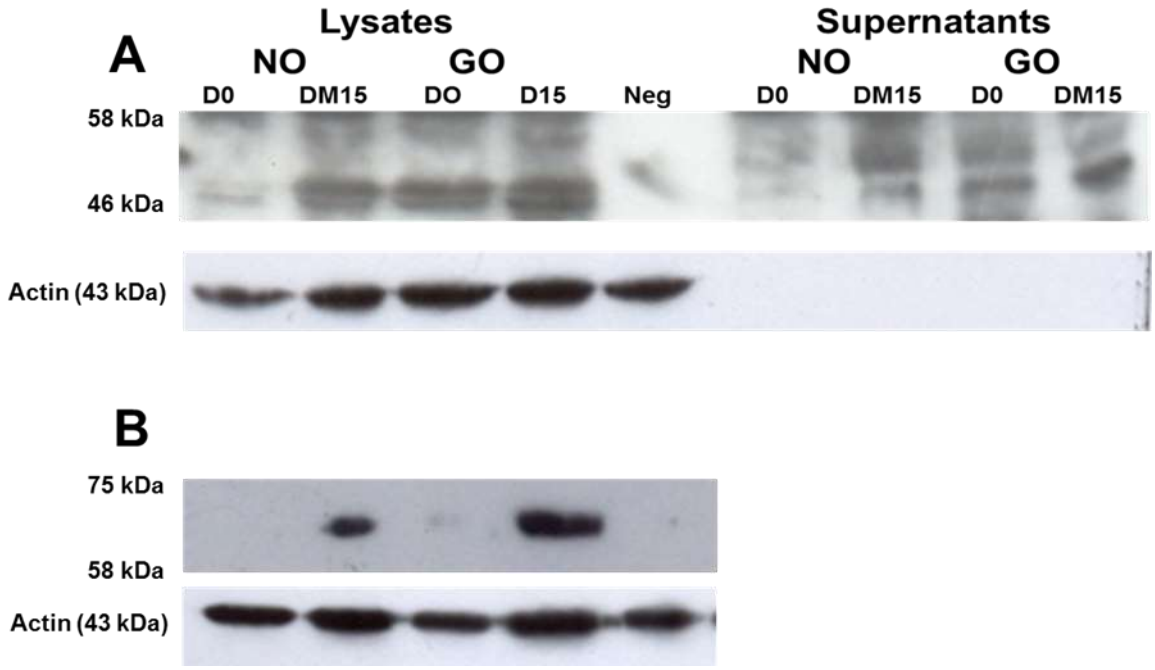

Figure 77: Representative western blot analysis of preadipocyte-fibroblast lysates and supernatants before (D0) and after adipogenesis (DM15) from a patient affected (GO) and not (NO) with Graves' orbitopathy showing higher TSHR_v2 protein concentration (A) as the cells undergoing adipogenesis and higher TSHR protein (B) using 2C11 antibody. Neg; negative control.

4.4.9 Is the TSHR_v2 functional?

We measured cAMP production in response to TSH or a human monoclonal TSAB (M22) at various time points before and after differentiation of OF. This was calculated from a standard curve of acetylated cAMP by radioimmunoassay (Figure 78). We observed a decrease in cAMP from basal levels when OF were stimulated with TSH or M22 before differentiation compared to unstimulated (p value <0.05). In contrast a robust increase in cAMP was induced by both agents in differentiated cells, as shown in Figure 79 and Figure 80. The difference between GO and NO was not significant.

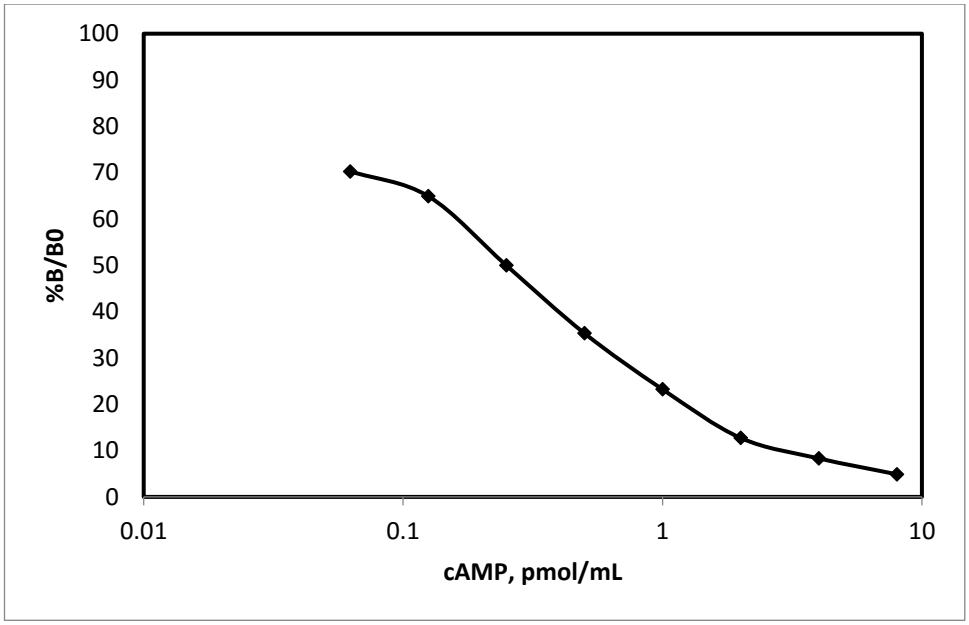

Figure 78: Acetylated cAMP radioimmunoassay standard curve expressed as “normalized” percent bound or % B/Bo plotted against cAMP concentration.

		Net count		"Normalized" percent bound/% B/Bo		cAMP concentration (pmol/ml)	
		GO	NO	GO	NO	GO	NO
Day 0	unstimulated	1765 (349)	1664 (104)	28.4 (5.6)	26.7 (1.6)	0.52 (0.20)	0.57 (0.06)
	TSH	3524** (1041)	1739 (284)	56.6** (16.7)	27.9 (4.6)	0.17** (0.08)	0.53 (0.12)
	M22	2004 (29)	2229* (119)	32.2 (0.5)	35.8* (1.9)	0.42 (0.01)	0.35* (0.03)
Day 5	unstimulated	2001 (283)	791 (283)	32.2 (4.5)	12.7 (4.5)	0.42 (0.11)	2.03 (1.65)
	TSH	1475 (290)	567 (168)	23.7 (4.6)	9.1 (2.7)	0.70 (0.21)	3.53 (1.41)
	M22	1234** (24)	914 (727)	19.8** (0.4)	14.7 (11.6)	0.95** (0.03)	1.58 (1.49)
Day 15	unstimulated	506 (205)	337 (81)	8.1 (3.3)	5.4 (1.3)	4.35 (2.94)	8.46 (4.69)
	TSH	391 (230)	140 (136)	6.3 (3.6)	2.2 (2.1)	6.63 (5.41)	39.49 (32.65)
	M22	446 (241)	259 (134)	6.5 (3.6)	4.2 (2.1)	5.26 (4.44)	13.16 (16.91)
CM 15	unstimulated	1190 (349)	799 (212)	19.1 (5.6)	12.8 (3.4)	1.01 (0.38)	1.98 (0.81)
	TSH	1817 (448)	734 (99)	29.2 (7.2)	11.8 (1.6)	0.50 (0.28)	2.28 (0.56)
	M22	927φφ (145)	742 (122)	14.9φφ (2.3)	11.9 (1.9)	1.54φφ (0.43)	2.24 (0.61)

Figure 79: Radioimmunoassay results of cAMP response in Graves' orbitopathy (GO) and normal (NO) OF pre and post-adipogenesis in response to TSH 5 mU/ml and M22 0.2 ng/µl presented as normalised percentage bound and converted cAMP concentration (n=2). The concentrations of TSH and M22 chosen were shown to stimulate the most cAMP in our luciferase assay. CM 15; undifferentiated OF in CM on day 15. The results presented were median (interquartile values) of duplicate readings from experiment performed in triplicate. Kruskal–Wallis one way ANOVA with post hoc Dunns test within each day comparing to unstimulated*, TSHφ; p value */φ<0.05, **/φφ<0.01.

Day of culture	Treatment	cAMP Stimulation Index (SI)	
		GO	NO
Day 0	TSH	0.29 ± 0.08*	1.30 ± 0.22
	M22	0.75 ± 0.02*	0.84 ± 0.05
Day 5	TSH	1.58 ± 0.40	1.19 ± 0.11
	M22	2.00 ± 0.05*	0.63 ± 0.40
Day 15	TSH	1.55 ± 0.90	2.61 ± 1.31
	M22	1.05 ± 0.57	1.89 ± 0.30
CM 15	TSH	0.52 ± 0.24*	1.20 ± 0.03
	M22	1.63 ± 0.46	1.19 ± 0.22

Figure 80: cAMP response (expressed in fold changes from unstimulated samples, Stimulation Index (SI)) in OF pre and post-adipogenesis in response to TSH 5 mU/ml and M22 0.2 ng/µl. Noted that there were reductions in TSH and M22 stimulated cAMP responses in day 0. Results are expressed as median ± interquartile range. NO, Normal; GO, Graves' Orbitopathy. *Mann-Whitney p value <0.05 compared to normal.

Of note, there was a strong negative association in the amount of cAMP generated and the *TSHR*_v2*:TSHR* transcripts ratio, as demonstrated in Figure 81 but this achieved significance only for M22 (Spearman correlation: TSH r=-0.55, p=0.23, M22 r=-0.87, p=0.03).

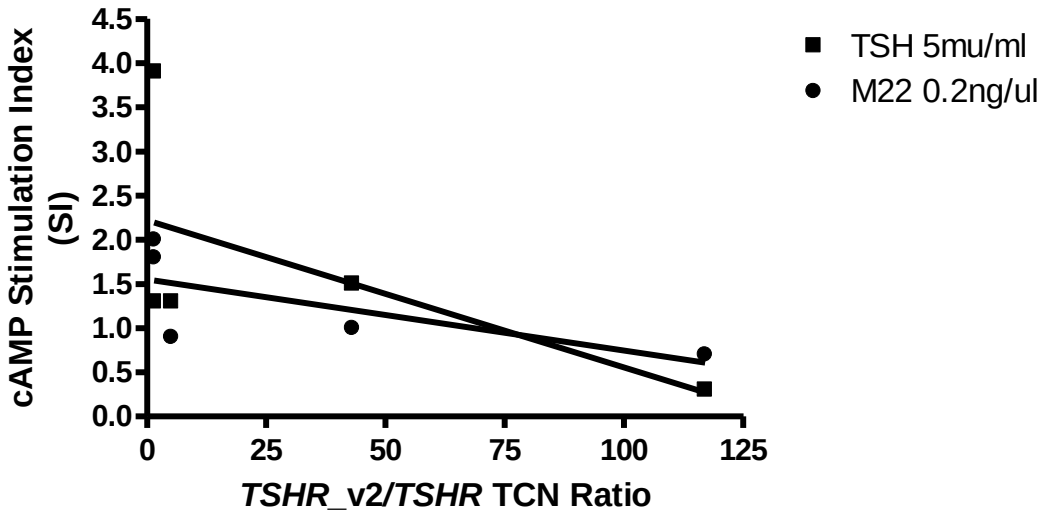

Figure 81: Negative association between cAMP, expressed as a stimulation index (SI) on the x axis and the ratio of *TSHR*_v2*:TSHR* transcripts on the y axis.

We also assessed the ability of conditioned medium from OF before and after differentiation to interfere with TSH or M22 induced TSHR activation in a luminescent bioassay. In the standard assay performed in serum-free medium, both TSH and M22 induce a dose-responsive stimulation index (S.I.); e.g. TSH 5 mU/ml S.I. = 8.1, 0.5 mU/ml S.I. = 4.4; M22, 0.2 ng/µl S.I. = 9.5, 0.01 ng/ µl S.I. =1.1 (Figure 82).

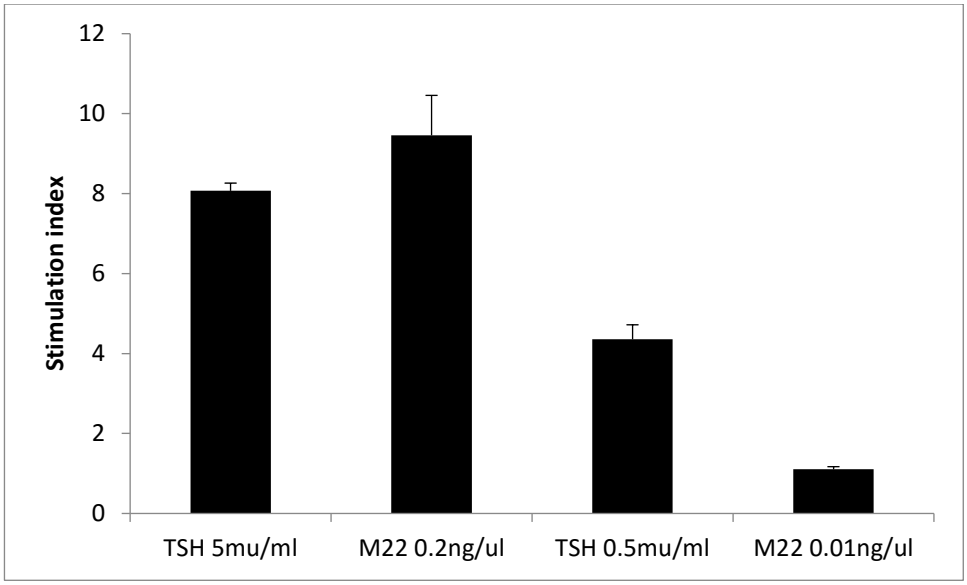

Figure 82: Dose-responsive stimulation index (SI) of TSH and M22 in serum free media.

We used unconcentrated conditioned medium (serum-free) from confluent cells just prior to addition of differentiation medium as the baseline S.I. The value was decreased relative to non-conditioned medium but we observed no significant difference in S.I. between GO and unaffected conditioned medium. At the end of differentiation, the TSH-induced S.I. was significantly lower in GO conditioned medium but not in unaffected, in keeping with the abundance of *TSHR*_v2 in GO. In M22 experiment we observed that S.I was lower in GO than unaffected at day 0 and after differentiation (Figure 83).

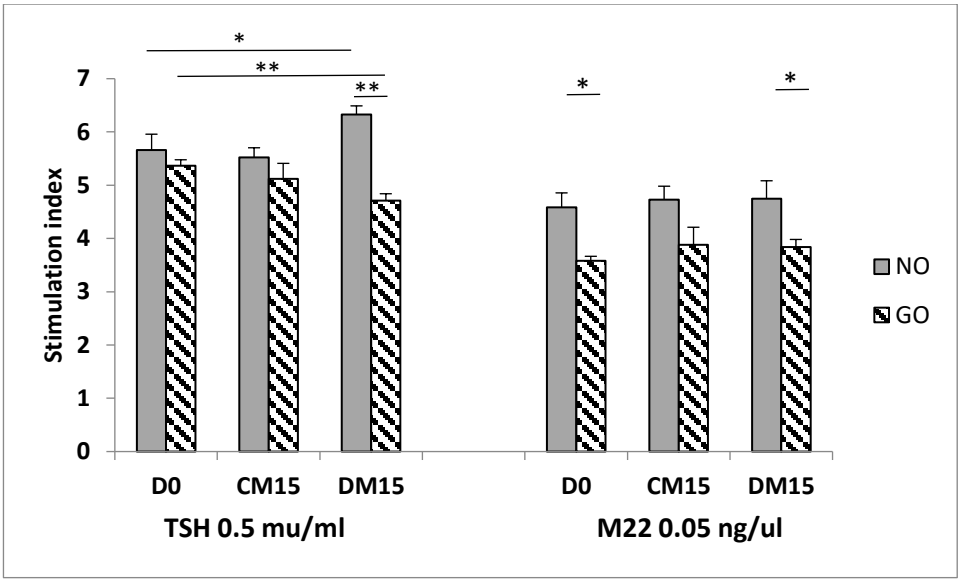

Figure 83: Indirect assays were performed using conditioned medium from OF at various stages of differentiation in the presence of TSH/M22 in a TSHR/cAMP luciferase bioassay. Grey bar represents normal and stripped bar are of Graves' OF. Results are presented as mean ± SD; *p value <0.05, ** <0.01. Horizontal bars represent comparison between normal and GO

4.5 DISCUSSION

Our results do not confirm a role for thyrostimulin in the orbit although we cannot rule out production of this high-affinity TSHR ligand [283] by other orbital components not studied. We did find difficulties in designing GPHA2 primers as these were picking up genomic DNA. Electrophoretic band analysis and sequencing revealed that our forward and reverse primer sequences were also found to be present in the intronic region i.e. we were amplifying the intronic region. Despite careful attention in designing the second set of the primers, we were still picking up genomic DNA which was resolved by treating the RNA with DNAse. We found cDNAs obtained from RNAs extracted using standard Tri-reagent for our orbital fat ex vivo analyses were producing poor CT values for the house keeping genes despite good A260/A280 ratio. The problem was overcome by using commercial specific RNA extraction kit which was optimized for use with fatty tissues.

Our results confirm those of Lantz et al who also investigated orbital tissues [360]. Both orbital studies contrast with the work of Sun et al who identified thyrostimulin as a paracrine regulator in the ovary [368] and also of Bassett and colleagues who reported that thyrostimulin regulates osteoblast formation in bone but only in early life [369]. Analysis of tissue distributions showed that *GPHA2* subunit exhibits a wider distribution than *GPHB5* subunit but both transcripts have been found to be expressed in human pituitary, retina, testis and skin [284, 370]. Here we show that *GPHA2* is present in abundance in the retroorbital adipose tissue but not *GPHB5* which is needed to form the functional heterodimer thyrostimulin. Whilst it is still possible that GPHA2 can act as monomer or heteromerize with unknown partner, current animal model data does not support this is the case [284, 371].

We confirmed our previous findings and that of others that TSHR expression was very low in undifferentiated OF and increased with adipogenesis. We did not find any

differential expression of TSHR between GO and normal in contrast to previous findings [118, 120, 328, 372]. This discrepancy might be explained by different techniques and housekeeping gene used to quantify TSHR. We used QPCR in which absolute numbers of TSHR transcripts are reported per APRT housekeeping gene; this contrasts with Kumar et al who applied relative quantification of the TSHR compared to the 18S RNA [328]. It is well known that different housekeeping gene used will affect the results of gene expressed. However our protein expression analysis of TSHR using 2C11 antibodies by western blot were in agreement with others albeit different techniques used (immunocytochemistry and flow cytometry methods) to show the presence of TSHR protein [118, 120, 372, 373].

Our data suggest that TSHR activation may be further regulated by a variant isoform which can be secreted from cells which express it. Early northern blot analysis of thyroid tissue identified the expected full-length transcript plus 2 additional transcripts at 1.3 and 1.7 kb [362]. We have demonstrated that the more abundant of these isoforms is also present in extra-thyroidal locations where TSHR activation contributes to pathology, i.e. Graves' orbitopathy.

We observed that TSHR activation of non-differentiated orbital fibroblasts, i.e. prior to adipogenesis, leads to a reduction in cAMP suggesting that the receptor is coupled to Gi in these cells. Others have reported that TSHR activation of orbital fibroblasts signals via p70s6 kinase [374], which may result from Gq or Gs-beta/gamma signalling, but to our knowledge this is the first report of the receptor coupling to an inhibitory G protein. The finding may explain our lack of success when using gain-of-function mutants of the TSHR to stimulate adipogenesis [247] and concurs with the study from van Ziejl et al who investigated TSH/TSAB induced hyaluronan production [264].

The TSHR_v2 we have studied comprises 253 amino acids and is predicted to retain

5 of the 6 N-linked glycosylation sites. Previous work by Rapoport and colleagues demonstrated that a TSHR truncated to 229 amino acids was unable to bind TSH. The holoreceptor contains 9 leucine rich repeats (LRR) which have been reported to act as the binding site for both TSH and TSAB [375]. Two of the LRR reside in exon 9 but the unique sequence of 22 amino acids contributed by intron 8 are likely to be sufficient to complete the 8th LRR and thus enable this variant to bind TSH and TSAB.

The variant could function in several ways; (i) A TSH or TSAB binding protein would neutralize their effects and thus prevent the consequences of TSHR activation in the orbit (ii) A potent autoantigenic stimulus could have a positive influence on T cell homing to the orbit and thus exacerbate GO pathology. Studying TSH binding protein/s possess their own challenges. We found cAMP radioimmunoassay was a cumbersome, protracted and expensive assay to perform. With luciferase assays, we were unable to find perfect negative control for the experiment. We tried conditioned medium from HEK293 cells and HCA2 but later found these cells also express TSHR_v2. Adsorption tests of TSH and M22 using CHO cells with TSHR extra cellular domain were not successful for unexplained reasons. In fact the S.I. indexes in these cells were much higher than empty CHO cells. It is possible that these GPI cells were secreting TSH ECD forming a complex with TSH and M22 which enhanced TSHR stimulation in the assay.

Relatively little is known about the regulation of alternative splicing of the *TSHR*. Some single-nucleotide polymorphisms in the proximal *TSHR* promoter or intron 1 have been associated with increased levels of the variant in thyroid tissue and also of receptor expression in the thymus with consequent impact on central tolerance mechanisms [376]. However, GD patients who develop GO do not have a higher prevalence of the disease-associated *TSHR* intronic SNP than GD patients who do not develop GO.

In conclusion, we found no evidence that thyrostimulin presents in the orbital adipose tissue. Both TSHR and TSHR_v2 are present in the orbit. In vitro data supports that TSHR_v2 are more abundant than full length TSHR in OF and during adipogenesis are significantly higher in GO than non-GO. TSHR_v2 is secreted and may alter intracellular TSHR signalling.

Chapter Five

4 DISSECTING THE ROLES OF TSHR ACTIVATION AND THYROID HORMONE IN REGULATING ADIPOSE PHENOTYPE

5.1 INTRODUCTION

Excess thyrotropin receptor (TSHR) activation occurs in two common conditions, Graves' disease (GD) in which thyroid stimulating antibodies (TSAB) mimic thyroid stimulating hormone (TSH) causing hyperthyroidism, and primary hypothyroidism when elevated circulating TSH compensates for low thyroid hormone (T4/T3) levels resulting from the failing gland [377]. Both confer alterations in body composition e.g. more than 90% of people with GD lose weight, mainly muscle mass and fat [378] whilst hypothyroidism increases fat and bone mineral density (BMD). The opposing differences of thyroid hormone levels have been traditionally suggested for these changes of body compositions, e.g. impact on white adipose tissue (WAT) or brown adipose tissue (BAT) metabolism which will be discussed later in this chapter [379, 380].

There is still considerable controversy regarding the best modality of treatment for hyperthyroidism in Graves' disease. Treatment options include thionamide drugs that block thyroid hormone biosynthesis, radioiodine therapy or thyroidectomy. Radioiodine and/or thyroidectomy might be associated with more weight gain compared to those on anti-thyroid drugs and patients who underwent ablative therapy for thyroid cancer [288, 381, 382]. This suggests that there are some factors

associated with Graves' disease that influence post therapy weight gain. Furthermore analysis has suggested that a diagnosis of Graves' disease (as opposed to another cause of thyroid over-activity), is an independent predictor of weight gain [288] separately from thyroid dysfunction, raising the possibility that the anti-TSH receptor antibodies that alter fat biology in the orbit, might also have long-term effects on peripheral adipose tissue composition; contrary to a study by Rotondi et al which failed to find this association [383].

5.1.1 Adipose tissue

Adipose tissue is a connective tissue system consisting mainly of adipocytes within a structural network of fibres. The main function of the adipose tissue is for fat storage, which could originate from either dietary intakes or intracellular synthesis. The adipose tissue depots are found mainly under the skin (known as subcutaneous fat) but also in the omentum (known as visceral fat), in other locations such as bone marrow, heart, kidneys and elsewhere around the body. It is the largest tissue accounting for about 10-15% of total body weight in the normal population. As mentioned above, adipose tissue is distributed in different anatomical locations and divided into subcutaneous and visceral fat. This division is largely based on the fact that they both have different cellular properties and association with insulin resistance and cardiovascular diseases [384]. There is also different distribution of adipose tissue according to sex. In general, men tend to accumulate adipose tissue around the waist, and women tend to accumulate the adipose tissue around the hips.

Majority of these adipose tissues are consisting of WAT. It is composed of cells containing a single large fat droplet with the nucleus located within a thin rim of cytoplasm at the periphery. Previously believed to be only involved in energy storage, now WAT is thought to be involved in many other functions including glucose

homeostasis, lipid metabolism, vascular homeostasis and inflammatory processes. Many of these roles are achieved via production of signalling proteins also known as adipokines such as adiponectin. Despite being produced solely by adipocytes, its level has been found negatively associated with obesity. In an animal model, the administration of adiponectin has been accompanied by a reduction in plasma glucose and an increase in insulin sensitivity [385]. In contrast to this, a different adipokine called resistin is found positively correlated with obesity. It was named after the discovery that it caused insulin resistance in mice [386]. Other adipokines include leptin, tumour necrosis factor α, interleukin 6, plasminogen activator inhibitor-1, tissue factor angiotensinogen, adipsin, acylation-stimulating protein, and retinol-binding protein. Some of these are also produced by cells other than adipocytes. Mature adipocytes do not divide and new fat cells can be generated only by differentiation of precursor preadipocytes i.e. adipogenesis. Although originally it was thought that all adipocytes originate from a common mesodermal precursor, the origin of these adipocyte precursors is now being questioned [387]. Lineage tracing studies, indicated that WAT originates from a *Myf5*-negative precursors although some subsets of white adipocytes also can arise from *Myf5* expressing precursors [388]. The description of preadipocytes and adipogenesis were described in detail in chapter one.

Until recently, brown adipose tissue was thought to be essentially nonexistent in human adults and only found primarily in infants and young children [389]. With advances in imaging techniques, it is now possible to visualize brown adipose tissue via positron emission tomography (PET) scanning. Work by Cypess and others using a combination of PET scan, ex vivo and in vitro analysis have proven that functional brown fat tissue does exist in human adults [390, 391]. Another interesting finding from Cypess et al in a different study, is that fat tissue becomes more brown (using uncoupling protein1 (*UCP1)* as brown marker) as one moves from subcutaneous to

deeper paravertebral adipose compartment and with the reverse finding with *LEPTIN* (WAT marker) [392].

Two types of brown adipose tissues (BAT) have been identified. They are described as ‘classical’ and ‘inducible (also known as brite/beige)’ BAT and as will be described below, lose energy as heat. Classical BAT is found in the interscapular BAT depot and perirenal regions of rodents. In vivo fate mapping showed that this brown fat arose from precursors that express *Myf5*, a gene previously thought to be expressed only in the myogenic lineage [393]. These *Myf5* derived precursors can differentiate into brown adipocytes through the action of PRDM16 and C/EBP-β although it remains unknown whether the *Myf5* positive cells clonally give rise to brown adipocytes and myocytes [394]. The inducible type of brown adipocytes is found sporadically as clusters in the white adipose of adult animals that have been chronically exposed to cold or to PPARγ ligands. They possess the morphological (multilocular lipid droplets) and biochemical characteristics (e.g. UCP1) of classical brown adipocytes but not of a *Myf5* lineage [393, 395]. Study in mice suggested there is bi-directional interconversion of beige and white adipocytes [396]. Here that the beige adipocyte can be induced by cold temperature into brown fat and conversely can return back into white fat type by heat. Similarly, Lee et al also found that these cells can be turned into brown or white by adrenergic stimulation and high calorie diet, respectively [397].

Human BAT deposits are located in supraclavicular and neck region, but beige adipocytes have been described in WAT and BAT depots including subcutaneous [398, 399]. GD patients display heat intolerance, which has been attributed to excess thyroid hormone increasing metabolic rate. The results from this study indicate that TSHR activation may contribute to this symptom. This concept is supported by studies in the hyt/hyt mouse, which lacks a functional TSHR and deals poorly with low

temperature, a characteristic which can be overcome by transfecting WT TSHR into the animals [400]. High thyroid hormone levels are also known to induce brown fat activity in brown and beige fat [379, 380, 401].

In general, all types of brown fat have specific signature genes (which will be discussed below) such as *UCP1* and peroxisome proliferator-activated receptor gamma coactivator -1 alpha *(PGC1α).* Whilst zinc finger of cerebellum 1 *(ZIC1)* is found selectively in brown adipose tissues and not detectable in white (commonly used gene markers *TCF21* or *LEPTIN*) and beige adipose tissues. On the other hand, Cbp/p300-interacting transactivator, with Glu/Asp-rich carboxy-terminal domain 1 (*CITED1*) was found uniquely in beige fat tissues. One of the unique features of brown fat is that it contains a very high number of mitochondria, which gives its brown appearance. Through its uncoupling proteins, it is responsible for generating heat by non-shivering thermogenesis.

5.1.1.1 Mitochondrial uncoupling proteins

Mitochondria are essential organelles in cells and involved in cell survival and functioning. One of the main functions of the mitochondria is involved in energy production via ATP generation. Historically by studying oxygen consumption (respiration) in mitochondria suspensions, the trace of oxygen can be recorded with an oxygen-sensitive electrode. In the absence of ADP, oxygen consumption of mitochondria is slow but its rate is increased rapidly by addition of ADP, which leads to ATP accumulation in the suspension. The reaction is temporary until another bolus of ADP is added to the mitochondrial suspension. This experiment indicates that respiration of mitochondria is 'coupled' to the oxidative phosphorylation of ADP [402]. In the modern era, this knowledge has been expanded to a process involving a spontaneous electron transfer through complexes I (NADH Dehydrogenase), III (bc_1 complex), and IV (Cytochrome Oxidase) which is coupled to active H^+ ejection from

the mitochondrial matrix into intermembrane space of the mitochondria. H^+ ejection creates a membrane potential and a pH gradient (negative charge and alkaline pH in the inner membrane or matrix). The ATP synthesis is coupled to spontaneous H^+ transport via the ATP-synthase into the matrix compartment driven by the pH and electrical gradients created. The term 'uncoupling' refers to the loss of this coupling process between electron transport in the respiratory chain and ATP production. Compounds capable of stimulating oxygen consumption (respiration) without a concomitant increase in ATP production were termed 'uncouplers'. An uncoupling protein (UCP) is a mitochondrial inner membrane protein that is a proton transporter or a channel thus capable of dissipating the proton gradient generated by the mechanism. This process in turn stimulates respiration, which leads to dissipation of heat. It is estimated that the energy generated by uncoupling constitutes a considerable part of the basal energy expenditure i.e. approximately 20%-50% of total energy expenditure [403].

There are five types of UCP known in mammals namely UCP1 (also known as thermogenin), UCP2, UCP3, UCP4 and UCP5. Although these proteins are similar in their structures, they have different tissue expression in mammals. UCP1, is mainly expressed in BAT, UCP2 is widely distributed, whereas UCP3 is mainly expressed in skeletal muscle, and UCP4 and 5 are mainly expressed in the brain [403, 404]. Thus their roles are also different namely UCP1 is for thermogenesis or energy, UCP 2 and 3 are for regulation of free-fatty acids, all UCPs except 4 are involved in reduction of reactive oxygen species formation. The *UCP1* gene is located on chromosome 4 containing 6 exons [403] and mainly found in BAT. Its expression is increased by adrenergic stimulation, cold temperature, β-agonists, retinoid, non-esterified fatty acids, thyroid hormones, and cAMP [403, 405]. Contrary to the expectation, *UCP1*-knockout mice did not become obese but only sensitive to cold. The transgenic mice

overexpressing *UCP1* expression in WAT were resistant to weight gain by high fat diet [403].

5.1.1.2 PGC1α

The PGC-1 is a family of coactivators consisting of PGC-1α, PGC-1β and PRC (PGC-1-related coactivator). They play a central role in mitochondrial biogenesis and respiratory function. PGC-1α is a protein that in humans is encoded by the *PPARGC1A* gene on chromosome 4 (4p15.2) [406]. As the name suggests, this protein interacts with the nuclear receptor PPAR-γ which is an important regulator of adipocyte differentiation and enhances *UCP1* expression. It is also known to be activated by reactive oxygen species (ROS), cold exposure, cAMP response element-binding (CREB) proteins and AKT pathways [407]. It is expressed in brown adipose tissue, brain, heart, kidney, skeletal muscle [408].

5.1.1.3 ZIC1

The first member of the zinc finger of cerebellum family was identified during a screen for cDNAs enriched in the murine cerebellum [409]. It acts as a transcriptional activator and is mainly involved in neurogenesis. The gene is located on chromosome 3 and contains only 3 exons. There are currently 5 known members namely *ZIC1* to *5*. Samples taken from the interscapular area of mice and human neck (classical brown fat depots) were found to express high levels of *ZIC1* suggesting it to be the gene that best discriminates it as a classical brown fat from other types of fat [395, 399].

5.1.1.4 CITED1

CITED1 was initially identified in a murine melanoma cell line [410]. Its gene is located on chromosome 3 (Xq13.1). This gene encodes a member of the CITED family of proteins. The encoded protein, also known as melanocyte-specific gene 1, may

function as a transcriptional coactivator and may play a role in pigmentation of melanocytes and acts as a transcriptional co-activator for oestrogen receptor [411]. *CITED1* was found selectively expressed in the *UCP1*-positive beige cells in the mice inguinal WAT treated with a β3 agonist and *UCP1*-positive brown adipocytes in human BAT indicating that *CITED1* can serves as a marker for beige cells both in mice as well as in humans [412].

5.1.1.5 HOXC9

This gene belongs to the homeobox family of genes that encode a highly conserved family of transcription factors that play an important role in morphogenesis. It provides cells with specific positional identities on the anterior-posterior axis. Humans possess four similar homeobox gene clusters, *HOXA, HOXB, HOXC* and *HOXD*, which are located on different chromosomes. *HOXC* genes are located on chromosome 12. The transcripts have been found to be expressed mainly in skeletal muscle, adipose tissues, skin, small intestine and fallopian tube. *HOXC9* was originally described as a WAT marker [392] but later was found to be significantly upregulated by PPARγ treatment (suggesting beige quality) [413]. It was found in the beige depots [412], but it was not increased by cold exposure. It was less expressed in white depots and not at all in brown depots [414].

5.1.2 Graves' disease and body composition

TSHR activation occurs in most people with thyroid dysfunction; either due to elevated TSH in hypothyroidism or TSAB in GD. Hypothyroidism is associated with increased body fat and BMD, which revert with treatment – but seldom reach pre-disease levels. Despite restoration of euthyroid status, many GD patients complain of substantial weight gain post treatment [285, 286] with potential negative impact on their future cardiovascular risk. This suggests a role of TSHR activation through the presenting

TSAB after therapeutic treatment of GD [415]. Indeed, the presence of functional extrathyroidal TSHR has been demonstrated in e.g. adipose tissue [117, 247] and bone [416]. This was further supported by Marcus et al, who demonstrated that TSH has a predominant lipolytic effect on isolated neonatal adipose tissue at physiological concentration. Similar but reduced effects were also seen up to adulthood but only at supra-physiological concentrations of TSH [417]. Activation of TSHR in adipose tissues has been shown to be positively correlated with obesity in some recent studies [418-420], and reports using animal models suggest a role for the TSHR in BAT and WAT function [400, 421, 422]. Taken together, there is a clear need for greater understanding of the effect of thyroid auto-antibodies on subcutaneous and visceral fat, which may have key implications for the treatment options offered in managing Graves' disease.

The above evidence led us to hypothesize that TSHR activation per se may contribute to changes in body composition separately from the effects of thyroid hormone levels, e.g. impact on adipose tissues metabolism [423]. We would hope to delineate this by studying GD neck fat samples with 2 different controls. We recognised the limitation that all patients were euthyroid during surgery. However, we would envisage that GD fat samples would experience a period of hyperthyroidism and TSAB stimulation whilst the controls, toxic multinodular goitre - the tissues experienced hyperthyroid state without TSAB stimulation and normal who were euthyroid with negative TSAB. Our aim was to investigate the effect of TSHR activation on brown, beige and white adipose tissue formation in ex vivo human neck fat tissues recognised as a BAT inducible region [390]. Where possible analyses were also extended to investigate the differential expression of these markers between subcutaneous and perithyroidal fat locations.

5.2 MATERIALS AND METHODS

All reagents were obtained from Sigma-Aldrich and tissue culture components from Lonza unless otherwise stated.

5.2.1 Adipose tissue collection

All fat samples were collected with informed consent and local research ethics committee approval. Perithyroidal neck fat samples were obtained from GD (n=14), multinodular goitre (MNG) (n=6) and normal patients (n=11) undergoing thyroid surgery. The perithyroidal fat samples will be referred to as 'deep' fat samples from here on. Where possible paired neck subcutaneous and deep samples were obtained and all patients were euthyroid prior to surgery. Euthyroid is defined as FT4 and/or FT3 in normal reference range. It was acceptable that TSH may remained suppressed many months later after normalisation of thyroid hormones. All GD patients have positive TSHR antibodies measured by thyroid binding inhibiting immunoglobulin (TBII) assays at diagnosis and TSAB luciferase reporter assay [367] measured from serum sample on the day of surgery. There were 2 controls with borderline TSAB. There were kept in their respective groups as none of their TSAB levels reached that of GD TSAB and the cut off TSAB was based on the 97th percentile of normal TSAB levels. One GD patient without TSAB had clinical evidence of GD with marked GO. Furthermore, analysis excluding 2 controls with borderline positive TSAB and the GD patient did not alter the findings of this chapter.

5.2.2 Primer design

Primers were designed using primer3 software as described previously (Chapter 2, section 2.2.12). Please see Table 51 for primer pairs used in this chapter.

Table 51: PCR primers used indicating exon location and size of amplicon.

	Accession number	Forward	Reverse	Amplicon size (bp)
UCP1	NM_021833.4	GGGGCTTCAGCGGCAAATCAG (Exon 2)	TATAAGTCCCCGTGTAGCGAGGTT (Exon 3)	236
PGC1α	NM_013261.3	GAAGAGCGCCGTGTGATTTA (Exon 10-11)	CGCTGTCCCATGAGGTATTC (Exon 13)	433
ZIC1	NM_003412.3	CCCTTCAAGTGCGAGTTTGA (Exon 2)	TGGACCTTCATGTGTTTGCG (Exon 3)	161
CITED1	NM_004143.3	CTCACCTGCGAAGGAGGATG (Exon 2)	CCATTTGAGGCTACCCCAGG (Exon 3)	117
HOXC9	NM_130769.3	CTGGACCCCAGCAACCC (Exon 1-2)	CTCCTTCTCCAGTTCCAGCG (Exon 2)	98

5.2.3 RNA extraction

We used Trizol reagent initially (See chapter 2, section 2.2.10) to extract the RNA from the frozen tissue. Despite having good A260/280 absorbance (e.g. A260/280 of 2.0), the resulting cDNA housekeeping gene was very poor with CT values around 27-39. Subsequently, RNA was extracted as described previously in chapter 4 (section 4.2.4) using RNAeasy lipid tissue minikit (QIAGEN).

5.2.4 PCR analysis of markers for white, beige or brown adipose tissues

Standard PCR was performed for 35 cycles, followed by agarose gel electrophoresis analysis and sequencing to confirm that the PCR amplicon was the intended product (see Chapter 2, section 2.2.12-2.2.16). QPCR was conducted using SYBR Green incorporation measured on a Stratagene MX 3000. As the samples were quite small in amount, only small numbers of PCR studies could be performed on any one sample. The comparative, also known as delta delta CT method was used to calculate

relative gene expression to the same normal control throughout the experiment. This involved comparing the CT values of the samples of interest with average normal control. The CT values of both the calibrator and the samples of interest were normalized to adenine phosphoribosyltransferase (*APRT*) housekeeping gene. The formula used was:

$$\Delta\Delta Ct = \Delta CT \text{ sample} - \Delta CT \text{ reference}$$

If multiple products were detected on the dissociation curve, a densitometry technique was used to express the results. The PCR products were separated on 2% agarose gel for 35 minutes. The confirmed densitometry gel bands were analysed using AlphaView Software for semi-quantification and corrected with respective housekeeper bands as previously described (Chapter 4 section 4.2.6).

5.2.5 Luciferase bioassay

Patients' sera collected on the day of surgery was tested for the presence of TSAB using in-house luciferase bioassay as described in Chapter 4 (section 4.2.9.2). Salt free buffer (Table 52 and Table 53) was used instead of serum free medium due to failure in generating meaningful stimulation index with the latter. The working assay buffer was obtained by diluting sterile PEG (20 ml of pure water added to 5 g) with salt free assay buffer (1 in 5 solution) i.e. 5 ml PEG: 20 ml buffer (sufficient for one full plate).

Table 52: Salt free buffer composition made up to 50 ml with pure water and placed in 37°C water bath for 20 minutes and pH to 7.4 using KOH.

Component	Volume or weight
Solution A	12.5 ml
Glucose	0.05 g
Hepes 20 mM	1 ml
$CaCl_2$ stock	50 μl
BSA	20.75 g
Sucrose 280 mM	4.8 g

$CaCl_2$ stock was made with 1.85 g in 10 ml water.

Table 53: Solution A made up to 250 ml with pure water and stored at 4°C.

Component	Weight
KCL	0.4 g
KH_2PO_4	0.06 g
$MgSO_4$	0.1 g
$NaHCO_3$	0.35 g
Na_2HPO_4	0.48 g

5.2.6 Statistical analysis

Parametric data were analysed using Student's t test, paired t test and one-way ANOVA with post hoc Tukey's test for multiple group comparisons where appropriate. Similarly, Mann-Whitney U test, Wilcoxon signed rank test and Kruskal-Wallis H test with post hoc Dunn's test were used for non-parametric data. Chi-square test was used for categorical variables. All analyses employed 2 tailed tests. Parametric data were presented as mean ± standard deviation and median ± interquartile range for non-parametric data. In all cases $p<0.05$ was considered significant.

5.3 RESULTS

5.3.1 Patient demographics

Please see Table 54 below for demographics of the patients. Patients whose thyroid histology indicated malignancy were excluded. Two patients with histology of multinodular goitre (MNG) but positive TSAB were included in the Graves' disease (GD) group. There was no difference in patients' age (p=0.1322), FT4 (Kruskal-Wallis H p=0.577), TSH (Kruskal-Wallis H p=0.1679) and sex distribution (Chi square p=0.379) between the 3 groups. Patients in GD group had a high level of TSAB compared to TMNG and normal (Kruskal-Wallis H p<0.0001 with Dunn's post hoc test p<0.001 against both TMNG and normal).

Patient ID	Sex	Age	Histology	FT3	FT4	TSH	TRAB	TPO	TSAB
Graves' Disease									
GD1	M	47	GD		13.0	2.06	32		2.6
GD2	F	71	GD	4.7	11.4	6.83	4.7	<2	2.9
GD3	F	23	GD		7.1	7.84	<1	1059	3.0
GD4	M	48	GD	4.3	14.9	0.04	11.7	<2	2.4
GD5	F	63	GD		22.4	<0.02	6.7		2.5
GD6	F	39	GD	5.6	17.5	<0.02			3.1
GD7	F	52	GD	5.6	9.3	0.29	15.8	>1000	3.0
GD8	F	38	GD		13.2	0.43			2.9
GD9	M	31	GD		12.3	2.34			
GD10	F	57	TMNG	4.5	12.9	<0.02	19.3	648	2.7
GD11	F	27	TMNG	4.6	14.1	<0.02			3.3
Toxic MNG									
MNG1	F	43	TMNG	5.3	17.8	<0.02			1.6
MNG2	M	76	TMNG		13.0	0.1	<1		1.1
MNG3	F	61	TMNG		14.3	0.92		50	1.2
MNG4	F	70	TA		13.0	1.22	<1	12.5	1.2
MNG5	M	61	TMNG		13.5	0.21			1.2
MNG6	M	89	TMNG		14.1	0.25			1.1
Normal									
NO1	F	21	CN		13.5	1.56			1.4
NO2	F	78	HN		13.0	3.26			1.1
NO3	F	46	BC		12.6	1.46			1.2
NO4	F	71	EMNG		16.7	1.79			1.3
NO5	M	50	EMNG		12.2	0.61			1.1
NO6	F	27	EMNG		14.0	2.58		<2	1.2
NO7	F	78	EMNG		13.7	0.11			1.8
NO8	F	27	EMNG		14.6	1.09			1.2
NO9	F	61	EMNG		14.0	0.57		<2	1.3
NO10	M	45	EMNG		16.5	0.83		<2	1.4
NO11	F	71	EMNG		13.0	0.65		300	1.2

Table 54: Patients demographic. F=female, M=male, GD=Graves' disease, TMNG=Toxic Multinodular goitre, EMNG=Euthyroid multinodular goitre, TA=Toxic Adenoma, CN=Colloid nodules, HN=Hyperplastic nodules, BC=Benign cyst. Normal reference: FT3 (2.6-5.7 pmol/l), FT4 (9.2-22 pmol/l), TSH (0.30-4.40 mU/l), Thyroid receptor antibodies (TRAB; <1 negative, 1-1.4, borderline >1.4 u/l positive), Thyroid peroxidase antibodies (TPO) (<32 kU/l is negative), Thyroid stimulating antibodies (TSAB; stimulation index 97.5th SD of normal <1.4 is negative).

5.3.2 *TSHR* transcript in the neck adipose tissue

To hypothesise that the browning effect of euthyroid adipose tissue was driven by TSAB, we have to show that *TSHR* transcript is present. *TSHR* transcripts were detected in the neck adipose tissues but at a very low level with a mean CT value of 27.8 (range 23.5 -31.5). There was no difference detected between the 3 patient groups (Kruskal-Wallis test, p=0.1155) (Figure 84).

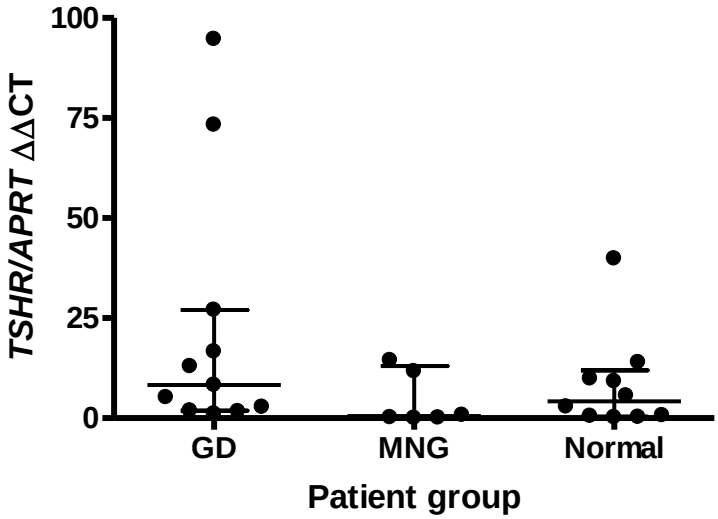

Figure 84: Scatter dot plot showing median ± interquartile range of thyrotropin receptor (*TSHR*) expression in fold change (Normalized against housekeeping gene adenine phosphoribosyltransferase (*APRT*)) to average control normal in ex vivo analysis of deep neck adipose tissues of Graves' disease (GD), multinodular goitre (MNG) and normal subjects. Fold change in expression was calculated using the ΔΔCT method assuming 100% efficiency. There was no difference detected between 3 groups (Kruskal-Wallis test, p=0.1155).

5.3.3 *UCP1* and *PGC1α* - General brown adipose tissue markers

No differences were detected in transcript levels from deep neck adipose tissue for *UCP1* (Figure 85); Kruskal-Wallis test, p=0.7273) and peroxisome proliferator-activated receptor gamma coactivator 1-alpha (*PGC1α*) (Figure 86; Kruskal-Wallis test, p=0.3462) between the 3 groups. The mean of *UCP1* CT value of all samples was 26.5 (range 17.4-29.6) and *PGC1α* was 25.9 (range 20.2-33.0).

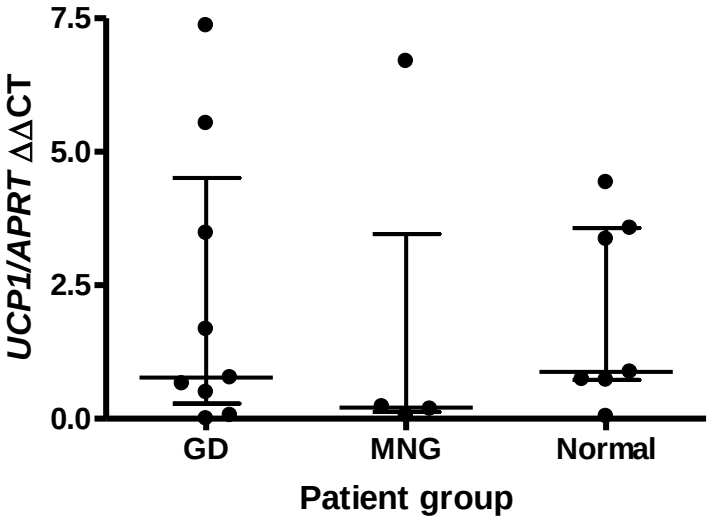

Figure 85: Scatter dot plot showing median ± interquartile range of uncoupling protein 1 (*UCP1*) expression in fold change (Normalized against housekeeping gene adenine phosphoribosyltransferase (*APRT*)) to average control normal in ex vivo analysis of deep neck adipose tissues of Graves' disease (GD), multinodular goitre (MNG) and normal subjects. Fold change in expression was calculated using the ΔΔCT method assuming 100% efficiency. There was no difference detected between 3 groups (Kruskal-Wallis test, p=0.7273).

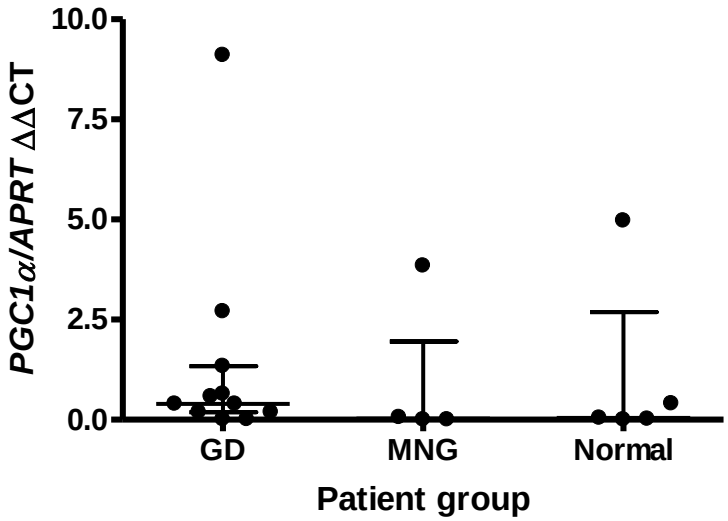

Figure 86: Scatter dot plot showing median ± interquartile range of peroxisome proliferator-activated receptor gamma coactivator 1-alpha (*PGC1α*) expression in fold change (Normalized against housekeeping gene adenine phosphoribosyltransferase (*APRT*)) to average control normal in ex vivo analysis of deep neck adipose tissues of Graves' disease (GD), multinodular goitre (MNG) and normal subjects. Fold change in expression was calculated using the ΔΔCT method assuming 100% efficiency. There was no difference detected between 3 groups (Kruskal-Wallis test, p=0.3462).

5.3.4 *ZIC1* - True brown adipose tissue specific marker

There was no difference in *ZIC1* expression in deep neck fat between the 3 groups (Kruskal Wallis, p=0.4158), lowest levels were present in GD samples but this did not reach significance (Figure 87).

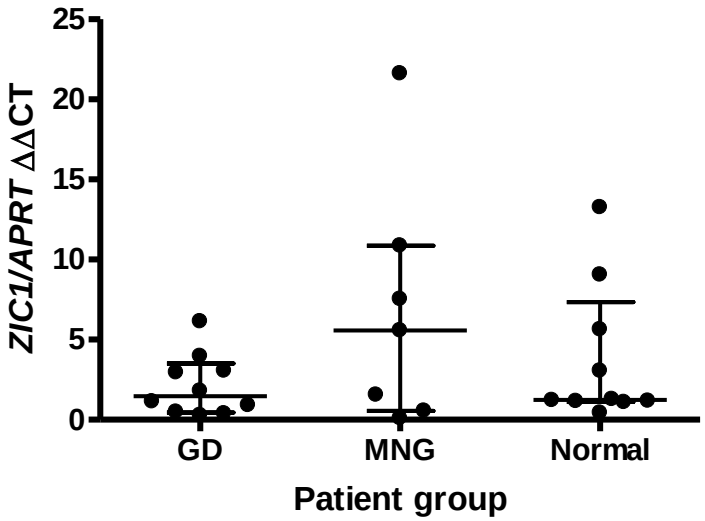

Figure 87: Scatter dot plot showing median ± interquartile range of zinc finger of cerebellum 1 (*ZIC1*) expression in fold change (Normalized against housekeeping gene adenine phosphoribosyltransferase (*APRT*)) to average control normal in ex vivo analysis of deep neck adipose tissues of Graves' disease (GD), multinodular goitre (MNG) and normal subjects. Fold change in expression was calculated using the ΔΔCT method assuming 100% efficiency. There was no difference detected between 3 groups (Kruskal-Wallis test, p=0.4158).

There was no statistical difference in *ZIC1* expression between deep and subcutaneous adipose tissue although 3 out of 5 normal samples showed the expected higher transcript level in deep compared to subcutaneous depot (Wilcoxon signed rank test of all the samples, p=0.4258; normal samples only, p=0.125) (Figure 88).

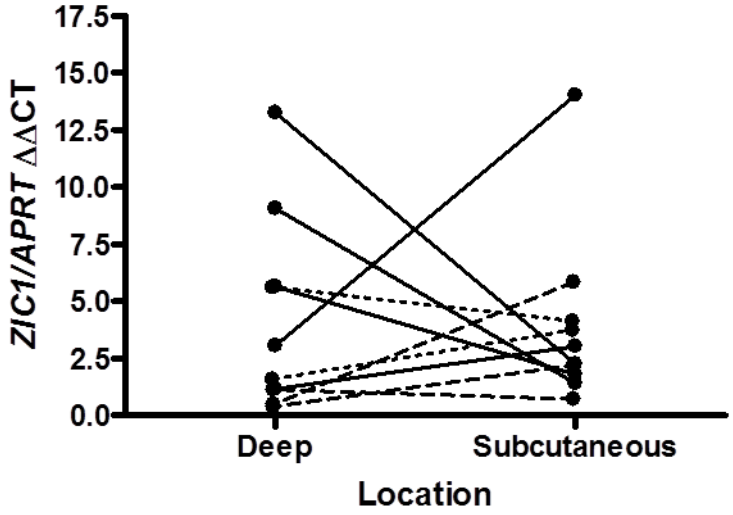

Figure 88: Differential expression of zinc finger of cerebellum 1 (*ZIC1*) in fold change (Normalized against housekeeping gene adenine phosphoribosyltransferase (*APRT*)) to average control normal in ex vivo analysis of deep and subcutaneous neck adipose tissues of Graves' disease (GD-short interrupted line), multinodular goitre (MNG-dotted line) and normal subjects (continuous line). Fold change in expression was calculated using the ΔΔCT assuming 100% efficiency. Wilcoxon signed rank test of all the samples, p=0.4258; normal samples only, p=0.125.

5.3.5 *CITED1* - Beige adipose tissue specific marker

Due to the detection of multiple peaks on the dissociation curve in the QPCR experiment, gene quantifications from here on were analysed semi quantitatively using the densitometry method. In contrast to the prior findings, the beige marker *CITED1* was lower in GD samples compared to normal (ANOVA p=0.0045, post hoc Tukey GD versus normal <0.01, GD versus MNG and MNG versus normal p>0.05) and test for trend p=0.0013 (Figure 89 and Figure 90).

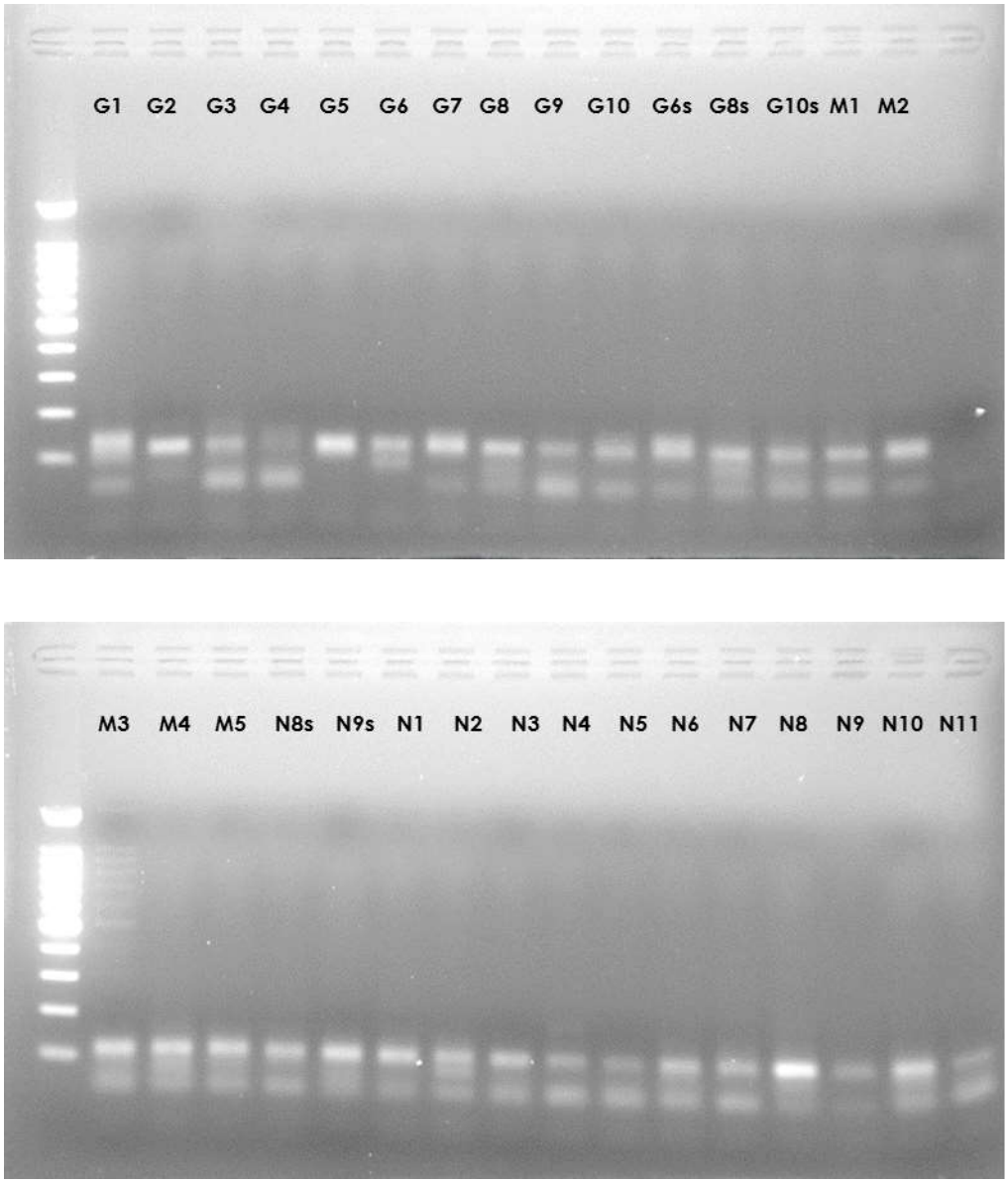

Figure 89: Representative agarose gel (2%) in 1xTAE confirming the size of the *CITED1* PCR product of 117bp with 100bp DNA ladder and primer dimers as the lower bands. Samples tested: G#s represent Graves' disease patient with #=number, s=subcutaneous sample, M represents multinodular goitre and N represent normal individual.

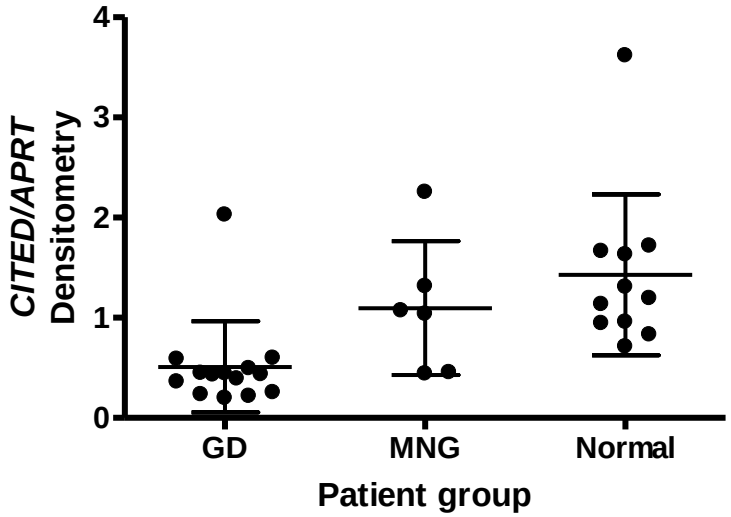

Figure 90: Relative expression of Cbp/p300-interacting transactivator, with Glu/Asp-rich carboxy-terminal domain 1 (*CITED1*) measured by densitometry corrected to housekeeping gene adenine phosphoribosyltransferase (*APRT*) in ex vivo analysis of the deep neck adipose tissues of Graves' disease (GD), multinodular goitre (MNG) and normal subjects. *CITED1* transcripts lower in GD than normal. ANOVA p=0.0045, post hoc Tukey GD versus normal <0.01; GD versus MNG and normal versus MNG p>0.05. Test for trend p=0.0013. Scatter dot plot indicates the standard deviation (lower and upper lines), mean (middle line).

There was no difference between deep and subcutaneous *CITED1* expression (Wilcoxon signed rank test of all the samples, p=0.6953; normal samples only, p=0.6250) (Figure 91).

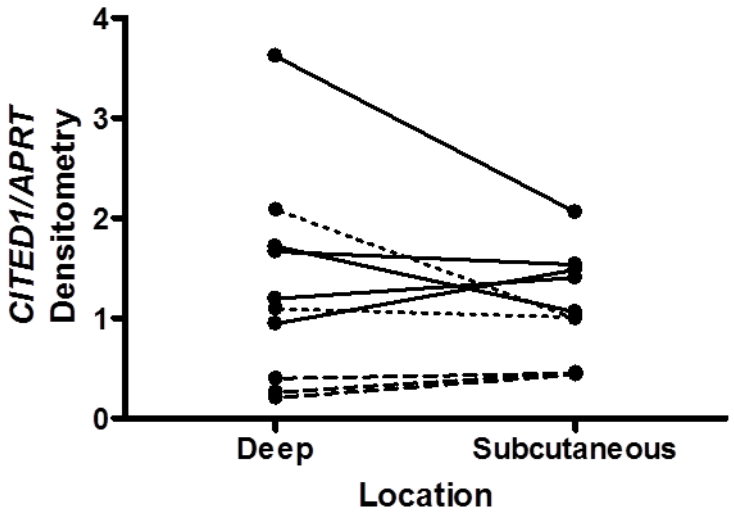

Figure 91: Differential expression between deep and subcutaneous neck adipose tissues of Cbp/p300-interacting transactivator, with Glu/Asp-rich carboxy-terminal domain 1 (*CITED1*) measured by densitometry corrected to housekeeping gene adenine phosphoribosyltransferase (*APRT*) in ex vivo analysis of the neck adipose tissues of Graves' disease (GD-short interrupted line), multinodular goitre (MNG-dotted line) and normal subjects (continuous line). Wilcoxon signed rank test of all the samples, p=0.6953; normal samples only, p=0.6250.

5.3.6 *HOXC9* - Mixed Beige/white adipose tissue marker

There was a reduction in *HOXC9* transcripts in samples from GD patients when compared to MNG and normal subjects (Kruskal-Wallis p=0.0002, Dunn's post hoc GD versus MNG p<0.0001, GD versus normal p<0.01, MNG versus normal p>0.05) (Figure 92 and Figure 93). In normal individuals, *HOXC9* levels were lower in deep compared to subcutaneous adipose tissue samples. The reverse happened in MNG (higher *HOXC9* levels in deep compared to subcutaneous adipose tissue samples). In GD *HOXC9* levels were equally low in both deep and subcutaneous adipose tissues (Wilcoxon signed rank test of all the samples, p=0.4513; normal samples only, p=0.0021) (Figure 94).

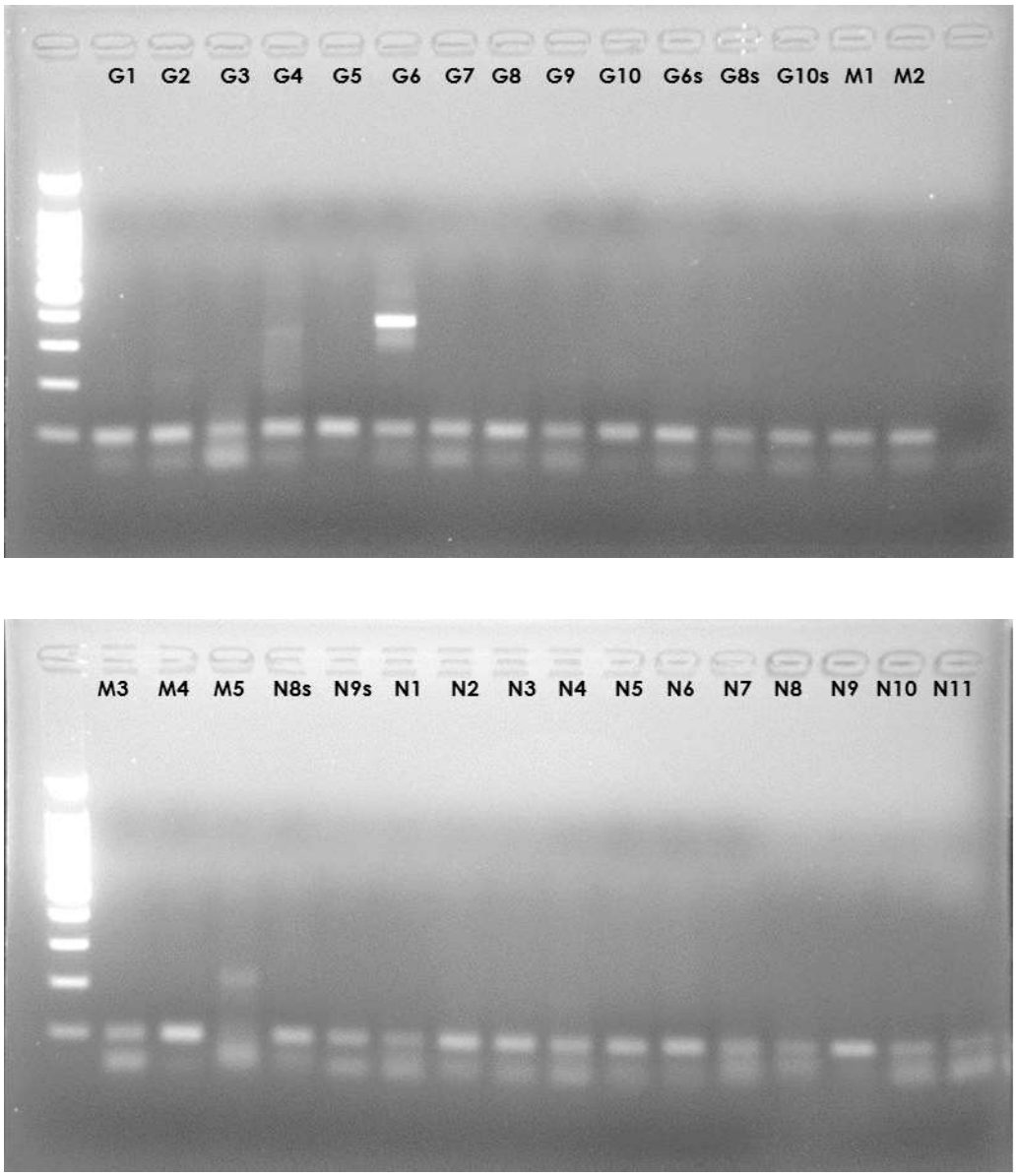

Figure 92: Representative agarose gel (2%) in 1xTAE confirming the size of the *HOXC9* PCR product of 98bp with 100bp DNA ladder and primer dimers as the lower bands. Samples tested: G#s represent Graves' disease patient with #=number, s=subcutaneous sample, M represents multinodular goitre and N represent normal individual.

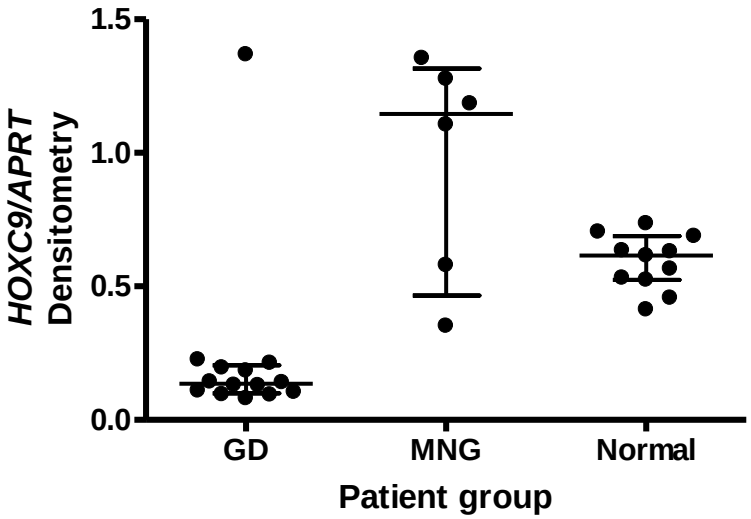

Figure 93: Relative expression of homeobox C9 (*HOXC9*) measured by densitometry corrected to housekeeping adenine phosphoribosyltransferase (*APRT*) in ex vivo analysis of the deep neck adipose tissues of Graves' disease (GD), multinodular goitre (MNG) and normal subjects. *HOXC9* transcripts were more abundant in MNG compared to GD and normal (Kruskal-Wallis $p=0.0002$, Dunn's post hoc GD versus MNG $p<0.0001$, GD versus normal $p<0.01$, MNG versus normal $p>0.05$). Scatter dot plot indicates the interquartile range (lower and upper lines), median (middle line).

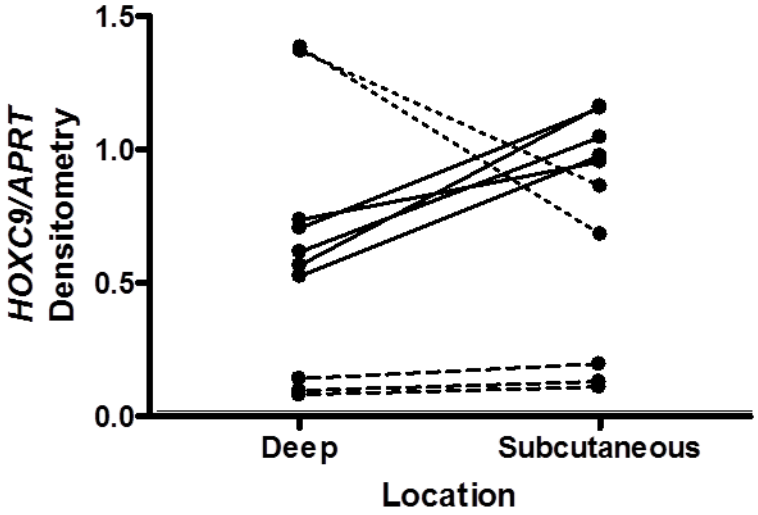

Figure 94: Differential expression between deep and subcutaneous neck adipose tissues of homeobox C9 (*HOXC9*) measured by densitometry corrected to housekeeping gene adenine phosphoribosyltransferase (*APRT*) in ex vivo analysis of the neck adipose tissues of Graves' disease (GD-short interrupted line), multinodular goitre (MNG-dotted line) and normal subjects (continuous line). Wilcoxon signed rank test of all the samples, p=0.4513; normal samples only, p=0.0021.

5.3.7 *LEPTIN* - White adipose tissue specific marker

LEPTIN, a marker of white adipose tissue, was lower in GD samples (Figure 95 and Figure 96) compared to normal (Kruskal Wallis p=0.0031, Dunn's post hoc GD versus normal p<0.01, GD versus MNG and MNG versus normal p>0.05). There was no differential effect on gene expression with regard to location of the fat samples, only 2 out of 5 normal samples indicated the expected higher transcript levels in subcutaneous than deep samples (Wilcoxon signed rank test of all the samples, p=1.0000; normal samples only, p=0.6250).

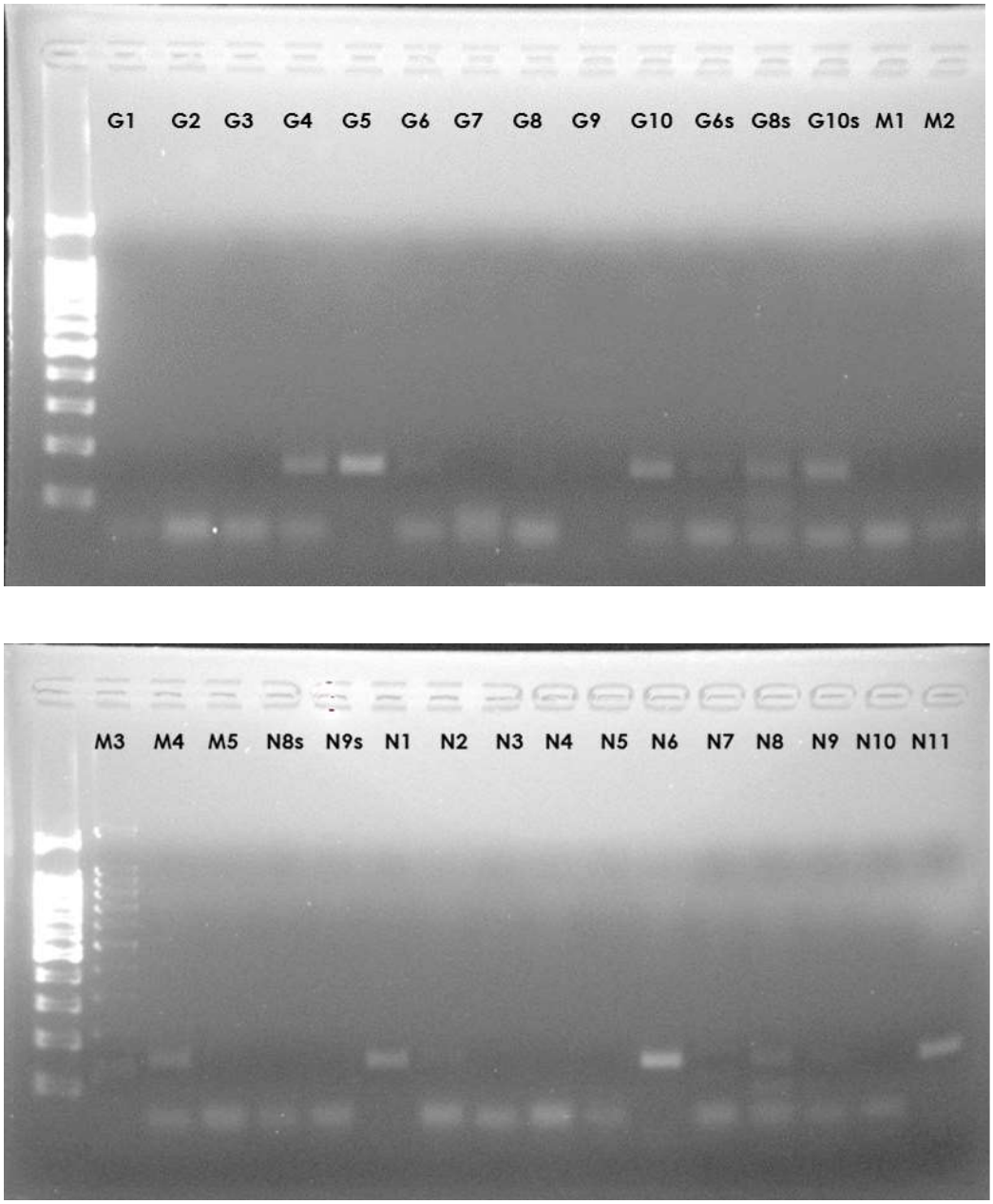

Figure 95: Agarose gel (2%) in 1xTAE confirming the size of the *LEPTIN* PCR product of 158bp with 100bp DNA ladder and primer dimers as the lower bands. Samples tested: G#s represent Graves' disease patient with #=number, s=subcutaneous sample, M represents multinodular goitre and N represent normal individual.

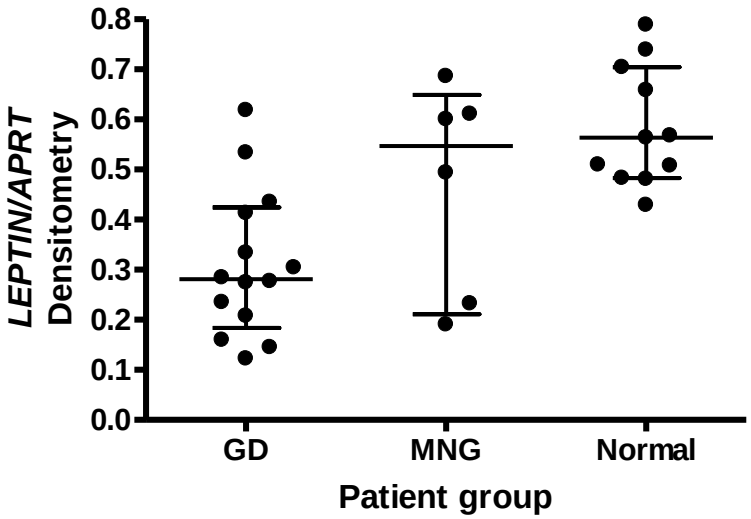

Figure 96: Relative expression of *LEPTIN* transcripts measured by densitometry corrected to housekeeping gene adenine phosphoribosyltransferase (*APRT*) in ex vivo analysis of the deep neck adipose tissues of Graves' disease (GD), multinodular goitre (MNG) and normal subjects. *LEPTIN* transcript levels were lower in GD compared to other normal (Kruskal Wallis $p = 0.0031$, Dunn's post hoc GD versus normal $p<0.01$, GD versus MNG and MNG versus normal $p>0.05$). Scatter dot plot indicates the interquartile range (lower and upper lines), median (middle line).

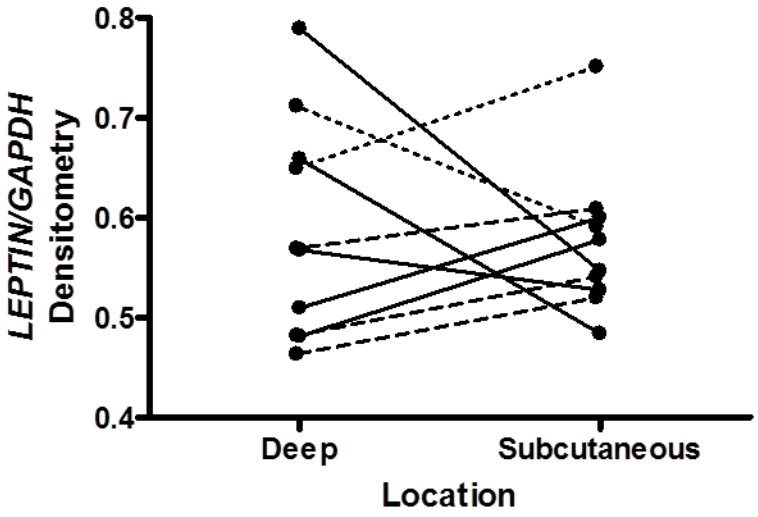

Figure 97: Differential expression between deep and subcutaneous neck adipose tissues of *LEPTIN* measured by densitometry corrected to housekeeping gene adenine phosphoribosyltransferase (*APRT*) in ex vivo analysis of the deep neck adipose tissues of Graves' disease (GD-short interrupted line), multinodular goitre (MNG-dotted line) and normal subjects (continuous line). Wilcoxon signed rank test of all the samples, p=1.0000; normal samples only, p=0.6250.

5.4 DISCUSSION

This pilot study demonstrated that there were lower levels of *CITED1* (beige marker), *HOXC9* (mixed marker) and *LEPTIN* (WAT marker) transcripts in deep neck fat of euthyroid GD patients with positive TSAB compared to MNG and normal individuals. The *ZIC1* (true BAT) expression was low in GD but did not reach statistical significant comparing to other groups. I found that there was no difference in expression of general BAT markers, *UCP1* and *PGC1α* between the 3 groups.

These findings are in contrast to in vitro findings of Zhang et al. using human orbital adipocytes transfected with gain of function mutants of the TSHR, he showed that TSHR activation seems to favour the development of brown adipose tissue in this case *UCP1* expression [247]. TSH also has been shown to increase basal and T3-stimulated *Ucp1* and *Dio2* expression and D2 activity but inhibit *Leptin* expression in the presence of T3 in rat brown adipose tissue but not in the concomitant presence of norepinephrine and T3 [422]. The contrasting findings might be explained by the difference in the in vitro nature of the experiment, fat depot studied, the mechanism of TSHR stimulation and species differences. The general suppression in brown markers suggests that the BAT in GD has reached a 'burnt out' state explaining the lack of difference in general BAT markers (*UCP1* and *PGC1α*). It is possible that the adipose tissue already underwent a 'browning' process during the hyperthyroid phase.

In this study, I was hoping to delineate the effect of TSAB and T3 on adipose tissue using GD and MNG samples. GD patients experienced high T3 and TSAB stimulation and MNG patients experience T3 stimulation only without TSAB. This aspiration was limited by the fact that all patients were euthyroid during the surgery although the GD and TMNG had been hyperthyroid before. Therefore, the changes detected in the adipose tissues only reflect the 'residual' effect of T3, which could be delineated by

comparing TMNG with normal individuals who were always euthyroid and with both groups being negative for TSAB. I found that there was a trend that *CITED1* and *LEPTIN* levels were highest in the normal. The levels were lower in MNG than normal suggesting residual effect of hyperthyroidism on MNG adipose tissue biology. Both levels were lowest in GD suggesting an additive effect of TSAB or other unmeasured factors in GD, above of that T3.

HOXC9 levels were proposed as a brown marker in one study [412] but white marker in other studies [392, 414]. In these analyses, I found *HOXC9* levels were highest in the MNG group, followed by normal samples with GD samples having the lowest transcript levels. This might imply residual T3 positive effect on *HOXC9* expression. This effect was negated in GD adipose tissues suggesting the effect may be mediated by the presence of TSAB. I also found that the level was higher in the subcutaneous compared to deep adipose tissue in normal individuals, which adds weight to its being more of a marker for WAT than BAT. It is interesting to see the reverse was observed in MNG samples and also GD *HOXC9* levels were flat with no gradient at all between subcutaneous and deep samples. It is possible that T3 alone has some effects on converting deep adipose tissue to more WAT phenotype. Again, the low level of both subcutaneous and deep *HOXC9* suggest the 'burnt out' phenomenon experienced by the 2 depots suggesting a role of TSAB in adipocyte biology.

Similar to Cypess' findings [392], I observed a differential gradient of subcutaneous and deep adipose tissue in normal individual samples with regard to *HOXC9* transcripts (higher in subcutaneous compared to deep samples) and ZIC1 transcripts which was higher in deep samples compared to subcutaneous although not reaching statistical significant. However, I could not replicate the *LEPTIN* gradient. This might be due to variability in sample location from different patients. There was no gradient with regard to beige marker again similar to Cypess' finding. I did not analyse *UCP1*

and *PGC1*α in the subcutaneous samples as at the start of the study, I could not get any paired subcutaneous samples from the patients due to lack of patients' consent. Some of the discordant findings might reflect a very small sample size in our study. Despite small sample size, *HOXC9* levels showed 3 distinctive groupings suggesting a differential effect of T3 and TSAB on adipose tissues.

The finding of low *LEPTIN* transcript levels was in agreement with low serum LEPTIN levels reported in treated euthyroid GD patients [424]. Leptin function is to suppress appetite by stimulating its receptor in the arcuate nucleus of the hypothalamus. Although rare, congenital leptin deficiency has been described and presented with morbid obesity, which is reversible with daily recombinant Leptin administration [425]. Patients with severe forms of obesity and metabolic syndrome were also found to have a relatively low levels of leptin [426]. This finding might explain an increase in appetite level leading to the weight gain experienced upon reaching normal thyroid function in GD patients [288, 381].

The study is not without difficulties. The results might be cofounded by the disease process itself i.e. Hyperthyroidism tends to be far greater and of shorter duration in patients with GD than in toxic nodular goitre; also iatrogenic hypothyroidism is commoner in patients treated for GD than other causes, which may have a carryover effect. I found it very hard to recruit MNG patients as most of these patients were having radioactive iodine as a definitive treatment rather than surgery. Although most patients have been shown to have positive TRAB, we were very keen to show that this TRAB was indeed TSAB. We were unable to produce consistent stimulatory index in GD group in order to differentiate it from other groups using serum free media, however the problem was overcame by using salt free buffer in the assay as recommended in the original establishment of the assay [367].

I experienced many problems in generating working primers to amplify the BAT-

specific gene *ZIC1*. This included absence of an amplicon and excessive primer dimer formation, despite multiple optimisation attempts e.g. primer concentration matrix, Q solution and gradient temperature PCR. The primers were successfully generated after the third attempt and cloned into pGEM®-T easy plasmid. However, I experienced issues with inconsistent standard curves between the experiments and double peaks in the dissociation curves in QPCR analysis, forcing me to abandon calculating QPCR by transcript copy numbers. Instead I applied the widely-used ΔΔCT method, which gave me more consistent readings throughout the experiments. The double peaks encountered in some PCR amplifications also meant that I could quantify gene expression only semi quantitatively using densitometry. There was no differential effect noted when *UCP1* and *PGC1α* were analysed based on either *APRT* or *GAPDH* housekeeping genes using transcript copy numbers and ΔΔCT methods. However, by densitometry it appears that GAPDH was expressed in abundance limiting its use in the densitometry calculation. Limited tissue sample size meant that I had to abandon GAPDH as a housekeeping marker.

In conclusion, I found unexpectedly low levels of BAT and WAT markers in GD. I also found unexplained high levels of *HOXC9* in MNG that merits further investigation. Whether the latter finding suggests an effect of the previous hyperthyroid state, whose effect in GD is reversed by TSAB remains purely speculative. The low level of *ZIC, CITED1* and *HOXC9* in euthyroid GD patients with positive TSAB suggests the inhibitory effect of TSAB on beige fat and WAT respectively. But this also can be explained by prior stimulatory effect of TSAB on BAT and WAT in the presence of T3 which is now 'burnt out'. The low level of *LEPTIN* might explain the weight gain experienced upon reaching normal thyroid function in GD patients. Further in vitro study is needed to unravel the mechanistic processes behind these findings.

Chapter Six

6 GENERAL DISCUSSION AND FUTURE WORK

I started my investigation with an in vitro study following clinical observations of enophthalmos in patients treated with $PGF_{2\alpha}$ for glaucoma and trying to dissect the pathophysiology behind it. The work was performed using the well-established 3T3-L1 cell line and also human primary orbital fibroblasts (OF) from normal and patients with GO. The finding was that $PGF_{2\alpha}$ reduced proliferation and adipogenesis of both 3T3-L1 cell line and human OF from normal and GO. I also found that there was higher proliferation rate in GO OF compared to normal and $PGF_{2\alpha}$ has no effect on lipolysis.

Cell counting is essential to evaluate the kinetics of cell growth. In this study, direct cell counting and toxicity was performed by using an automatic counter (Cellometer®) which is based on image analysis of the disposable counting chamber. Even though it is an automated counter, the process itself was labour intensive and highly variable especially at low cell numbers. One way of getting around this issue is perhaps by using a larger number of cells to start with or more dedicated sensitive automated machine such as Beckman Coulter instrument.

Despite the limitations of the method used, the observed increased proliferation in GO deserves more attention as it might shed light on mechanisms central to GO pathophysiology. Further cell cycle analysis is needed to compare any differential process between GO and normal OF. An in vitro analysis of human OF with regard

to local production of $PGF_{2\alpha}$ and cell surface expression of the receptor (FP) or its splice variant (FPS) should help to delineate any differences. Candidate pathways involved such as phospholipase C or other pathways should be investigated using PCR and Western blot analysis with or without relevant pathway inhibitors.

The cell cycle is regulated by 2 key classes of regulatory molecules, cyclins and cyclin-dependent kinases (CDKs). Cell cycle checkpoints are used by the cell to monitor and regulate the progress of the cell cycle [427]. There are 3 main checkpoints namely G1/S checkpoint (rate-limiting step), the G2/M checkpoint and the metaphase (mitotic) checkpoint. These checkpoints consist of a network of regulatory proteins that monitor and dictate the progression of the cell through the different stages of the cell cycle. Studying kinetics of cell cycle in GO OF would be fundamental to better understanding the pathophysiology of GO. This could be achieved by PCR analysis of the relevant genes or using commercially available cell cycle profiler such as Human Cell Cycle RT² Profiler™ PCR Array which profiles the expression of 84 genes key to cell cycle regulation. The array contains genes that both positively and negatively regulate the cell cycle, the transitions between the each of the phases, DNA replication, checkpoints and arrest.

The inhibitory effects of $PGF_{2\alpha}$ on adipogenesis are consistent with those of several other authors [310, 322, 323]. Using 3T3-L1, Casimir et al reported that endogenous $PGF_{2\alpha}$ production is higher in undifferentiated then differentiated cells and postulated that its release from preadipocytes provides a control mechanism to limit adipogenesis [323]. The mechanism could be via reduction in the substrate arachidonic acid which moves towards eicosatrienoic acid production during adipogenesis [326]. It would be interesting to determine whether GO OF are unable or less able to produce endogenous $PGF_{2\alpha}$ and/or experience down-regulated FP receptor expression and hence display enhanced adipogenesis compared with

normal. Measuring arachidonic acids (AA) from OF using mass spectroscopy also would be useful. If there is reduction in AA in OF, the rescue experiment could be performed by supplementing the OF with AA as this could prove one way of treating early-stage GO. Another main mechanism in GO pathophysiology is hyaluronan (HA) production. Understanding the effect of $PGF_{2\alpha}$ on HA and subtypes of HA would be useful. This can be achieved by PCR, western blots and ELISA (enzyme-linked immunosorbent assay) of the products involved. I did consider HA analysis but since Bimatoprost induced enophthalmos seemed due to fat atrophy, it was decided then to focus on this aspect of the investigation.

Based on the in vitro findings, I subsequently conducted a randomised controlled double blind crossover trial clinical trial of $PGF_{2\alpha}$ in late phase GO (BIMA study). The primary outcome was a reduction in proptosis. As mentioned in chapter 3, the choice of late phase or burnt out GO was to ensure that the proptosis was stable and the effect seen was due to the $PGF_{2\alpha}$ and not part of the natural disease recovery itself. The trial showed that treatment with $PGF_{2\alpha}$ in this case Bimatoprost for 3 months was not effective in reducing proptosis in late phase GO patients. At baseline, there was high smoking rate (75%) which reduced close to 40% after the diagnosis. Although there was a 35% prevalence reduction after the diagnosis in our trial population, this is still at least double that of national Wales's smoking prevalence which was approximately 20% in 2014. This finding should lead to more smoking cessation intervention strategies complemented by pre and post intervention audits to measure the effectiveness of the strategy utilised. The observed high diplopia rate (61.3%) many years after initial diagnosis also raises a significant question regarding the management or treatment effectiveness in the acute stage in reducing diplopia. Perhaps greater attention should be placed on diplopia as primary or secondary outcome in any GO related trial, rather than part of a composite outcome which may mask the effect of the intervention on diplopia.

The lack of anticipated $PGF_{2\alpha}$ effects might be due to several explanations. The choice of late stage of the disease where the disease state is predominantly caused by hyaluronan or fibrosis rather than adipogenesis might explain the lack of impact and perhaps 3 months' duration is not long enough to see the intended reduction in proptosis. With 5% drop out rate, the BIMA study has also demonstrated that crossover studies can be performed reliably in patients with persistent proptosis due to GO and that this study design is acceptable to patients. Future trial should be done on early stage GO and active disease. This can be performed on top of standard proven treatment such as selenium for mild GO or IV methylprednisolone in active GO. The issue with lack of trial participants can be negated by multicentre design. Unfortunately, cross over trial cannot be performed for active GO trial due to the natural disease process as per Rundle's curve. The lack of response could also be due to genetic polymorphisms in the FP receptor. Using <10% drop in IOP as a cut off for a low responder, single nuclear polymorphism (SNP) rs12093097 C/T of the FP receptor gene has been associated with lack of IOP response in such trial patients [428].

Exophthalmometer readings have their own caveat in terms of variability of readings with parallax error and pressure of the exophthalmometer against the orbital rim. With the right support, a new device could be invented with a simple pressure sensor to ensure constant pressure is applied to all patients at different visits. To ensure the measurement is parallax free, ultra sound techniques could be used to measure the proptosis distance. There was consistency in terms of clinical exophthalmometer measurement throughout the trial and the negative finding was further supported by photographic assessment of proptosis conducted by an assessor who was masked to the treatment phase. Further analysis should be performed on the data on the correlation and reproducibility of the clinical exophthalmometry measurements versus photo measurements as the data can provide an important basis to design and power

future studies to address the unmet need in this patient group. There is also a possibility to use 3D volumetric assessment analysis of the orbit in particular looking at the fat pad in the eye lid.

The in vitro study of thyrostimulin in OF did not confirm its role in the orbit although I cannot rule out production of this high-affinity TSHR ligand [283] by other orbital components not studied. *GPHB5* was at the limit of detection. *GPHA2* was detected but with no differential effect at baseline and during adipogenesis between GO and normal, limiting its usefulness as GO marker.

The study also suggests that TSHR activation may be further regulated by a variant isoform *TSHR*_v2 which can be secreted from cells which express it. The variant could function in several ways (1) as a TSH or TSAB binding protein it would neutralize their effects and thus prevent the consequences of TSHR activation in the orbit (2) as a potent autoantigenic stimulus it could have a positive influence on T cell homing to the orbit.

The truncated *TSHR*_v2 was detected in both cell layer lysates and medium from orbital fibroblast cultures and appears to increase during adipogenesis. There is also indirect evidence that TSHR_*v2* might modulate TSH and M22 activity from direct cAMP RIA assay and indirectly via bioassay. Detection of the TSHR_v2 protein was achieved using a rabbit polyclonal antibody. To confirm that the protein binding the antibody in the western blot is indeed TSHR_v2 would require targeted proteomic analysis of the band detected in order to confirm its sequence. There was indirect evidence that TSHR_v2 might be binding with TSH and M22 hence reducing its effect. I realised that the effects seen might be due to other unmeasured factors in the medium studied. Even though serum free media was used, other factors could be generated during the overnight incubation period. To prove that the factor is indeed TSHR_v2 further experiments are needed whereby TSHR_v2 is depleted from the

conditioned medium using one of several specific strategies to immune-adsorb or immunoprecipitate out the TSHR_v2.

I observed that TSHR activation of non-differentiated OF, i.e. prior to adipogenesis, leads to a reduction in cAMP suggesting that the receptor is coupled to Gi in these cells. This is in contrast to the situation in differentiating adipocytes in which TSH and TSAB induce an increase in cAMP. If my findings are confirmed it is unknown when and what factors are associated with the conversion to coupling to Gs protein. To confirm the results and investigate further the study could be expanded by measuring cAMP via RIA daily in a bigger sample cohort which should indicate the Gi and Gs switching period. G protein coupled receptors are known to exist in oligomeric structures but whether TSHR abundance dictates the conversion to Gs utilisation is unknown. The fact that TSHR expression increases during adipogenesis which is paralleled by TSHR activation signalling via Gs tends to support this concept. However to address the point I would propose an in vitro model whereby TSHR numbers could be controlled by transfecting increasing amounts of TSHR expression plasmid into OF and measuring cAMP. Furthermore, knock-down using TSHR siRNA could be performed to see if the reverse is true. More sophisticated ways to dissect the issue include fluorescence resonance energy transfer (FRET) and coimmunoprecipitation (COIP) techniques whereby TSHR is tagged with green (GFP) or red fluorescent protein (Myc) as described by Latif et al [107].

If the above study confirmed that TSHR_v2 could modulate TSHR or M22, further study could be performed to understand its regulation. The fact that its production is higher during adipogenesis suggests that it might be a marker for patients who will or will not develop GO. Therefore, TSHR_v2 assay can be tested on serum sample of GO patients, GD patients without GO and MNG patients (control) using ELISA technique. Going forward, one could envisage to use TSHR_v2 in generating mouse

model of GO.

Despite restoration of euthyroid status, many GD patients complain of substantial weight gain post treatment [285, 286] with potential negative impact on their future cardiovascular risk. Indeed, the BIMA study cohort confirmed this finding with an average BMI of 29. I performed a pilot study of brown and white fat markers in GD, MNG and normal ex vivo samples. The study demonstrated that there were lower levels of *CITED1* (beige marker), *HOXC9* (mixed marker) and *LEPTIN* (WAT marker) transcripts in deep neck fat of euthyroid GD patients with positive TSAB compared to MNG and normal individuals. The *ZIC1* (true BAT) expression was low in GD but did not reach statistical significant compared with other groups. There was also no difference in expression of general BAT markers, *UCP1* and *PGC1α* between the 3 groups.

One of the key weaknesses of this ex vivo study is the lack of MNG control samples and paired subcutaneous samples amongst the 3 groups. Therefore, further ex vivo study, with increased numbers and sample size, is needed to confirm the findings. The transcript data also needs to be supported by immunohistological analysis to confirm the presence of the corresponding protein. It could also be useful to analyse different depots such as abdominal, visceral and subcutaneous fat to see whether there are any depot specific differences. Admittedly, it would be difficult to find GD or MNG patients undergoing abdominal surgery although it is possible. Further in vitro experiment is needed in order to understand the mechanism of the difference in BAT and WAT markers in GD. To investigate the role of TSAB and T3 on the BAT and WAT markers, an in vitro model could be performed on OF and also abdominal visceral/subcutaneous fat obtained via collagenase digest. These cells would then be subjected to culture with or without T3 and/or TSH/M22 followed by QPCR measurement of BAT and WAT markers. In this study, I found that *HOXC9* transcripts

behave as a WAT marker; furthermore it displayed 3 unique expression patterns corresponding to the GD, MNG and normal groups suggesting it may be useful in dissecting the role of TRAB above and beyond that of T3.

TSHR signals mainly through Gs, although other cascades may also be involved. One of the main downstream pathways for Gs is cAMP responsive element binding protein (CREB) which binds to its response element (CRE) on the promoter region of the DNA exerting various gene transcription processes, whilst T3 exert its effect via its nuclear receptor which then binds thyroid response elements (TRE). Analysis of promoters for WAT and BAT markers should identify any functional CREs and TREs in this region and gain insight into their influence on adipose tissue marker expression.

The finding of low *LEPTIN* levels was in agreement with low serum LEPTIN levels found in treated euthyroid GD patients [424]. Leptin function is to supress appetite. Patients with metabolic syndrome also found to have a relatively low levels of leptin [426]. It is not known whether hyperphagia experienced by the patient when hyperthyroid is correlated with the LEPTIN level or whether its low concentration post treatment contribute to the weight gain experience by GD patients [288, 381]. Further study of serum LEPTIN level in GD/MNG is needed to confirm this finding and validate previous work by Sera et al [424]. If this is the case, LEPTIN regulation by T3/TSH/M22 is needed to be dissected through in vitro model and whether LEPTIN rescue is beneficial in this condition.

Current data on weight gain in GD post treatment is gathered after clinical diagnosis of hyperthyroidism. It is possible to investigate the GD weight prior to and after the diagnosis by using available database such as Clinical Practice Research Datalink (CPRD) previously known as The General Practice Research Database (GPRD) which contains computerized medical records of over 5,000,000 people from 508

primary care practices throughout the UK (http://www.CRPD.com). This also can be gathered from Secure Anonymised Information linkage (SAIL) databank, which is a nationwide dataset covering the entire population of Welsh residents treated in National Health Service (NHS) hospitals (http://www.saildatabank.com).

7 REFERENCES

1. Van Vliet, G., *Development of the thyroid gland: lessons from congenitally hypothyroid mice and men.* Clin Genet, 2003. **63**(6): p. 445-55.
2. Manley, N.R. and M.R. Capecchi, *The role of Hoxa-3 in mouse thymus and thyroid development.* Development, 1995. **121**(7): p. 1989-2003.
3. Nilsson, M., et al., *Polarized efflux of iodide in porcine thyrocytes occurs via a cAMP-regulated iodide channel in the apical plasma membrane.* Acta Endocrinol (Copenh), 1992. **126**(1): p. 67-74.
4. Wolff, J., *Transport of Iodide and Other Anions in the Thyroid Gland.* Physiol Rev, 1964. **44**: p. 45-90.
5. Bizhanova, A. and P. Kopp, *Minireview: The sodium-iodide symporter NIS and pendrin in iodide homeostasis of the thyroid.* Endocrinology, 2009. **150**(3): p. 1084-90.
6. Brix, K., D. Fuhrer, and H. Biebermann, *Molecules important for thyroid hormone synthesis and action - known facts and future perspectives.* Thyroid Res, 2011. **4 Suppl 1**: p. S9.
7. Kalsbeek, A., et al., *Functional connections between the suprachiasmatic nucleus and the thyroid gland as revealed by lesioning and viral tracing techniques in the rat.* Endocrinology, 2000. **141**(10): p. 3832-41.
8. Itadani, H., et al., *Cloning and characterization of a new subtype of thyrotropin-releasing hormone receptors.* Biochem Biophys Res Commun, 1998. **250**(1): p. 68-71.
9. Patel, Y.C., *Somatostatin and its receptor family.* Front Neuroendocrinol, 1999. **20**(3): p. 157-98.
10. Greenspan, S.L., et al., *Divergent dopaminergic regulation of TSH, free alpha-subunit, and TSH-beta in pituitary cell culture.* Metabolism, 1986. **35**(9): p. 843-6.
11. Sherman, S.I., et al., *Central hypothyroidism associated with retinoid X receptor-selective ligands.* N Engl J Med, 1999. **340**(14): p. 1075-9.
12. Baqui, M., et al., *Human type 3 iodothyronine selenodeiodinase is located in the plasma membrane and undergoes rapid internalization to endosomes.* J Biol Chem, 2003. **278**(2): p. 1206-11.
13. Klebanoff, S.J. and W.L. Green, *Degradation of thyroid hormones by phagocytosing human leukocytes.* J Clin Invest, 1973. **52**(1): p. 60-72.
14. Pittman, C.S., et al., *The nondeiodinative pathways of thyroxine metabolism: 3,5,3',5-tetraiodothyroacetic acid turnover in normal and fasting human subjects.* J Clin Endocrinol Metab, 1980. **50**(4): p. 712-6.
15. Visser, T.J., *Role of sulfation in thyroid hormone metabolism.* Chem Biol Interact, 1994. **92**(1-3): p. 293-303.
16. Bernal, J., *Thyroid hormones and brain development.* Vitam Horm, 2005. **71**: p. 95-122.
17. Yen, P.M., et al., *Thyroid hormone action at the cellular, genomic and target gene levels.* Mol Cell Endocrinol, 2006. **246**(1-2): p. 121-7.
18. Figueira, A.C., et al., *Recognition by the thyroid hormone receptor of canonical DNA response elements.* Biochemistry, 2010. **49**(5): p. 893-904.
19. Adams, M., et al., *Genetic analysis of 29 kindreds with generalized and pituitary resistance to thyroid hormone. Identification of thirteen novel mutations in the thyroid hormone receptor beta gene.* J Clin Invest, 1994. **94**(2): p. 506-15.
20. Collingwood, T.N., et al., *A role for helix 3 of the TRbeta ligand-binding domain in coactivator recruitment identified by characterization of a third cluster of*

mutations in resistance to thyroid hormone. EMBO J, 1998. **17**(16): p. 4760-70.
21. Moran, C., et al., *Resistance to thyroid hormone caused by a mutation in thyroid hormone receptor (TR)alpha1 and TRalpha2: clinical, biochemical, and genetic analyses of three related patients.* Lancet Diabetes Endocrinol, 2014. **2**(8): p. 619-26.
22. Tunbridge, W.M., et al., *The spectrum of thyroid disease in a community: the Whickham survey.* Clin Endocrinol (Oxf), 1977. **7**(6): p. 481-93.
23. Bahn Chair, R.S., et al., *Hyperthyroidism and other causes of thyrotoxicosis: management guidelines of the American Thyroid Association and American Association of Clinical Endocrinologists.* Thyroid, 2011. **21**(6): p. 593-646.
24. Aoki, Y., et al., *Serum TSH and total T4 in the United States population and their association with participant characteristics: National Health and Nutrition Examination Survey (NHANES 1999-2002).* Thyroid, 2007. **17**(12): p. 1211-23.
25. Palos-Paz, F., et al., *Prevalence of mutations in TSHR, GNAS, PRKAR1A and RAS genes in a large series of toxic thyroid adenomas from Galicia, an iodine-deficient area in NW Spain.* Eur J Endocrinol, 2008. **159**(5): p. 623-31.
26. Brent, G.A., *Clinical practice. Graves' disease.* N Engl J Med, 2008. **358**(24): p. 2594-605.
27. Graves, R., *Newly observed affection of the thyroid gland in females.* London Medical and Surgical Journal (Renshaw), 1835. **7**(2): p. 516-517.
28. Parry, C., *Enlargement of thyroid gland in connection with enlargement or palpitations of the heart.* Posthumous, in: Collections from the unpublished medical writings of C. H. Parry, 1825: p. 111-129.
29. Ljunggren, J.G., *[Who was the man behind the syndrome: Ismail al-Jurjani, Testa, Flagani, Parry, Graves or Basedow? Use the term hyperthyreosis instead].* Lakartidningen, 1983. **80**(32-33): p. 2902.
30. Von Basedow, K., *Exophthalmus durch Hypertrophie des Zellgewebes in der Augenhöhle.* [Casper's] Wochenschrift für die gesammte Heilkunde, 1840. **6**: p. 197-204; 220-228.
31. Begbie, J., *Anaemia and its consequences; enlargement of the thyroid gland and eyeballs. Anaemia and goitre, are they related?* Monthly Journal of Medical Science, London, 1849. **9**: p. 496-508.
32. Flajani, G., *Sopra un tumor freddo nell'anterior parte del collo broncocele (Osservazione LXVII).* In Collezione d'osservazioni e riflessioni di chirurgia. Rome, Michele A Ripa Presso Lino Contedini, 1802. **3**: p. 270-273.
33. Ogawa, T., et al., *Thyroid hormone autoantibodies in patients with Graves' disease: effect of anti-thyroid drug treatment.* Clin Chim Acta, 1994. **228**(2): p. 113-22.
34. Saravanan, P. and C.M. Dayan, *Thyroid autoantibodies.* Endocrinol Metab Clin North Am, 2001. **30**(2): p. 315-37, viii.
35. Chiovato, L., et al., *Antibodies producing complement-mediated thyroid cytotoxicity in patients with atrophic or goitrous autoimmune thyroiditis.* J Clin Endocrinol Metab, 1993. **77**(6): p. 1700-5.
36. Adams, D.D. and H.D. Purves, *The assessment of thyroid function by tracer tests with radioactive iodine.* N Z Med J, 1956. **55**(305): p. 36-41.
37. Adams, D.D., *The presence of an abnormal thyroid-stimulating hormone in the serum of some thyrotoxic patients.* J Clin Endocrinol Metab, 1958. **18**(7): p. 699-712.
38. Morshed, S.A., R. Latif, and T.F. Davies, *Characterization of thyrotropin receptor antibody-induced signaling cascades.* Endocrinology, 2009. **150**(1): p. 519-29.

39. Kleinau, G., et al., *Principles and determinants of G-protein coupling by the rhodopsin-like thyrotropin receptor.* PLoS One, 2010. **5**(3): p. e9745.
40. Weetman, A.P., et al., *Thyroid-stimulating antibody activity between different immunoglobulin G subclasses.* J Clin Invest, 1990. **86**(3): p. 723-7.
41. Davies, T.F., et al., *Value of thyroid-stimulating-antibody determinations in predicting short-term thyrotoxic relapse in Graves' disease.* Lancet, 1977. **1**(8023): p. 1181-2.
42. Fairweather, D., S. Frisancho-Kiss, and N.R. Rose, *Sex differences in autoimmune disease from a pathological perspective.* Am J Pathol, 2008. **173**(3): p. 600-9.
43. Zhu, C., et al., *The Tim-3 ligand galectin-9 negatively regulates T helper type 1 immunity.* Nat Immunol, 2005. **6**(12): p. 1245-52.
44. Straub, R.H., *The complex role of estrogens in inflammation.* Endocr Rev, 2007. **28**(5): p. 521-74.
45. Weetman, A.P., *Immunity, thyroid function and pregnancy: molecular mechanisms.* Nat Rev Endocrinol, 2010. **6**(6): p. 311-8.
46. Jansson, R., et al., *The postpartum period constitutes an important risk for the development of clinical Graves' disease in young women.* Acta Endocrinol (Copenh), 1987. **116**(3): p. 321-5.
47. Giron-Gonzalez, J.A., et al., *Consistent production of a higher TH1:TH2 cytokine ratio by stimulated T cells in men compared with women.* Eur J Endocrinol, 2000. **143**(1): p. 31-6.
48. Brix, T.H. and L. Hegedus, *Twin studies as a model for exploring the aetiology of autoimmune thyroid disease.* Clin Endocrinol (Oxf), 2012. **76**(4): p. 457-64.
49. Prabhakar, B.S., R.S. Bahn, and T.J. Smith, *Current perspective on the pathogenesis of Graves' disease and ophthalmopathy.* Endocr Rev, 2003. **24**(6): p. 802-35.
50. Smith, T.J. and L. Hegedus, *Graves' Disease.* N Engl J Med, 2016. **375**(16): p. 1552-1565.
51. Grumet, F.C., et al., *HL-A antigens as markers for disease susceptibility and autoimmunity in Graves' disease.* J Clin Endocrinol Metab, 1974. **39**(6): p. 1115-9.
52. Chen, Q.Y., et al., *HLA-DRB1*08, DRB1*03/DRB3*0101, and DRB3*0202 are susceptibility genes for Graves' disease in North American Caucasians, whereas DRB1*07 is protective.* J Clin Endocrinol Metab, 1999. **84**(9): p. 3182-6.
53. Krummel, M.F. and J.P. Allison, *CD28 and CTLA-4 have opposing effects on the response of T cells to stimulation.* J Exp Med, 1995. **182**(2): p. 459-65.
54. Heward, J.M., et al., *The development of Graves' disease and the CTLA-4 gene on chromosome 2q33.* J Clin Endocrinol Metab, 1999. **84**(7): p. 2398-401.
55. Bossowski, A., et al., *Analysis of chosen polymorphisms in FoxP3 gene in children and adolescents with autoimmune thyroid diseases.* Autoimmunity, 2014. **47**(6): p. 395-400.
56. Zheng, L., et al., *Foxp3 gene polymorphisms and haplotypes associate with susceptibility of Graves' disease in Chinese Han population.* Int Immunopharmacol, 2015. **25**(2): p. 425-31.
57. Yin, X., et al., *Influence of the TSH receptor gene on susceptibility to Graves' disease and Graves' ophthalmopathy.* Thyroid, 2008. **18**(11): p. 1201-6.
58. Holm, I.A., et al., *Smoking and other lifestyle factors and the risk of Graves' hyperthyroidism.* Arch Intern Med, 2005. **165**(14): p. 1606-11.
59. Prummel, M.F. and W.M. Wiersinga, *Smoking and risk of Graves' disease.* Jama, 1993. **269**(4): p. 479-82.

60. Vestergaard, P., *Smoking and thyroid disorders--a meta-analysis.* Eur J Endocrinol, 2002. **146**(2): p. 153-61.
61. Utiger, R.D., *Effects of smoking on thyroid function.* Eur J Endocrinol, 1998. **138**(4): p. 368-9.
62. Hargreaves, C.E., et al., *Yersinia enterocolitica provides the link between thyroid-stimulating antibodies and their germline counterparts in Graves' disease.* J Immunol, 2013. **190**(11): p. 5373-81.
63. Matos-Santos, A., et al., *Relationship between the number and impact of stressful life events and the onset of Graves' disease and toxic nodular goitre.* Clin Endocrinol (Oxf), 2001. **55**(1): p. 15-9.
64. Sonino, N., et al., *Life events in the pathogenesis of Graves' disease. A controlled study.* Acta Endocrinol (Copenh), 1993. **128**(4): p. 293-6.
65. Mandac, J.C., et al., *The clinical and physiological spectrum of interferon-alpha induced thyroiditis: toward a new classification.* Hepatology, 2006. **43**(4): p. 661-72.
66. Coles, A.J., et al., *Pulsed monoclonal antibody treatment and autoimmune thyroid disease in multiple sclerosis.* Lancet, 1999. **354**(9191): p. 1691-5.
67. Aranha, A.A., et al., *Autoimmune thyroid disease in the use of alemtuzumab for multiple sclerosis: a review.* Endocr Pract, 2013. **19**(5): p. 821-8.
68. Hogquist, K.A., T.A. Baldwin, and S.C. Jameson, *Central tolerance: learning self-control in the thymus.* Nat Rev Immunol, 2005. **5**(10): p. 772-82.
69. Mueller, D.L., *Mechanisms maintaining peripheral tolerance.* Nat Immunol, 2010. **11**(1): p. 21-7.
70. Ohashi, P.S. and A.L. DeFranco, *Making and breaking tolerance.* Curr Opin Immunol, 2002. **14**(6): p. 744-59.
71. Wenzel, B.E., et al., *Antibodies to plasmid-encoded proteins of enteropathogenic Yersinia in patients with autoimmune thyroid disease.* Lancet, 1988. **1**(8575-6): p. 56.
72. Brix, T.H., et al., *Too early to dismiss Yersinia enterocolitica infection in the aetiology of Graves' disease: evidence from a twin case-control study.* Clin Endocrinol (Oxf), 2008. **69**(3): p. 491-6.
73. Horwitz, M.S., et al., *Diabetes induced by Coxsackie virus: initiation by bystander damage and not molecular mimicry.* Nat Med, 1998. **4**(7): p. 781-5.
74. Shimojo, N., et al., *Induction of Graves-like disease in mice by immunization with fibroblasts transfected with the thyrotropin receptor and a class II molecule.* Proc Natl Acad Sci U S A, 1996. **93**(20): p. 11074-9.
75. Kikuoka, S., et al., *The formation of thyrotropin receptor (TSHR) antibodies in a Graves' animal model requires the N-terminal segment of the TSHR extracellular domain.* Endocrinology, 1998. **139**(4): p. 1891-8.
76. Kaithamana, S., et al., *Induction of experimental autoimmune Graves' disease in BALB/c mice.* J Immunol, 1999. **163**(9): p. 5157-64.
77. Many, M.C., et al., *Development of an animal model of autoimmune thyroid eye disease.* J Immunol, 1999. **162**(8): p. 4966-74.
78. Costagliola, S., et al., *Transfer of thyroiditis, with syngeneic spleen cells sensitized with the human thyrotropin receptor, to naive BALB/c and NOD mice.* Endocrinology, 1996. **137**(11): p. 4637-43.
79. Baker, G., et al., *Reevaluating thyrotropin receptor-induced mouse models of graves' disease and ophthalmopathy.* Endocrinology, 2005. **146**(2): p. 835-44.
80. Moshkelgosha, S., et al., *Cutting edge: retrobulbar inflammation, adipogenesis, and acute orbital congestion in a preclinical female mouse model of Graves' orbitopathy induced by thyrotropin receptor plasmid-in vivo electroporation.* Endocrinology, 2013. **154**(9): p. 3008-15.
81. Berchner-Pfannschmidt, U., et al., *Comparative Assessment of Female Mouse Model of Graves' Orbitopathy Under Different Environments,*

Accompanied by Proinflammatory Cytokine and T-Cell Responses to Thyrotropin Hormone Receptor Antigen. Endocrinology, 2016. **157**(4): p. 1673-82.
82. Nakahara, M., et al., *Enhanced response to mouse thyroid-stimulating hormone (TSH) receptor immunization in TSH receptor-knockout mice.* Endocrinology, 2010. **151**(8): p. 4047-54.
83. Nakahara, M., et al., *Adoptive transfer of antithyrotropin receptor (TSHR) autoimmunity from TSHR knockout mice to athymic nude mice.* Endocrinology, 2012. **153**(4): p. 2034-42.
84. Gilquin, J., et al., *Delayed occurrence of Graves' disease after immune restoration with HAART. Highly active antiretroviral therapy.* Lancet, 1998. **352**(9144): p. 1907-8.
85. Nagayama, Y., et al., *Molecular cloning, sequence and functional expression of the cDNA for the human thyrotropin receptor.* Biochem Biophys Res Commun, 1989. **165**(3): p. 1184-90.
86. Libert, F., et al., *Cloning, sequencing and expression of the human thyrotropin (TSH) receptor: evidence for binding of autoantibodies.* Biochem Biophys Res Commun, 1989. **165**(3): p. 1250-5.
87. Yokomori, N., et al., *Regulation of the rat thyrotropin receptor gene by the methylation-sensitive transcription factor GA-binding protein.* Mol Endocrinol, 1998. **12**(8): p. 1241-9.
88. Ohe, K., et al., *Interferon-gamma suppresses thyrotropin receptor promoter activity by reducing thyroid transcription factor-1 (TTF-1) binding to its recognition site.* Mol Endocrinol, 1996. **10**(7): p. 826-36.
89. Uyttersprot, N., et al., *Requirement for cAMP-response element (CRE) binding protein/CRE modulator transcription factors in thyrotropin-induced proliferation of dog thyroid cells in primary culture.* Eur J Biochem, 1999. **259**(1-2): p. 370-8.
90. Gross, B., et al., *Composite structure of the human thyrotropin receptor gene.* Biochem Biophys Res Commun, 1991. **177**(2): p. 679-87.
91. Chen, S.T., J.D. Lin, and K.H. Lin, *Characterization of a thyroid hormone-mediated short-loop feedback control of TSH receptor gene in an anaplastic human thyroid cancer cell line.* J Endocrinol, 2002. **175**(2): p. 459-65.
92. Garcia-Jimenez, C. and P. Santisteban, *TSH signalling and cancer.* Arq Bras Endocrinol Metabol, 2007. **51**(5): p. 654-71.
93. de Bernard, S., et al., *Sequential cleavage and excision of a segment of the thyrotropin receptor ectodomain.* J Biol Chem, 1999. **274**(1): p. 101-7.
94. Tanaka, K., et al., *Thyrotropin receptor cleavage at site 1 involves two discontinuous segments at each end of the unique 50-amino acid insertion.* J Biol Chem, 1999. **274**(4): p. 2093-6.
95. Couet, J., et al., *Shedding of human thyrotropin receptor ectodomain. Involvement of a matrix metalloprotease.* J Biol Chem, 1996. **271**(8): p. 4545-52.
96. Misrahi, M., et al., *Processing of the precursors of the human thyroid-stimulating hormone receptor in various eukaryotic cells (human thyrocytes, transfected L cells and baculovirus-infected insect cells).* Eur J Biochem, 1994. **222**(2): p. 711-9.
97. Loosfelt, H., et al., *Two-subunit structure of the human thyrotropin receptor.* Proc Natl Acad Sci U S A, 1992. **89**(9): p. 3765-9.
98. Misrahi, M. and E. Milgrom, *Cleavage and shedding of the TSH receptor.* Eur J Endocrinol, 1997. **137**(6): p. 599-602.
99. Couet, J., et al., *Cell surface protein disulfide-isomerase is involved in the shedding of human thyrotropin receptor ectodomain.* Biochemistry, 1996. **35**(47): p. 14800-5.

100. Rapoport, B., et al., *The thyrotropin (TSH) receptor: interaction with TSH and autoantibodies.* Endocr Rev, 1998. **19**(6): p. 673-716.
101. Zhang, M., et al., *The extracellular domain suppresses constitutive activity of the transmembrane domain of the human TSH receptor: implications for hormone-receptor interaction and antagonist design.* Endocrinology, 2000. **141**(9): p. 3514-7.
102. Neumann, S., M. Claus, and R. Paschke, *Interactions between the extracellular domain and the extracellular loops as well as the 6th transmembrane domain are necessary for TSH receptor activation.* Eur J Endocrinol, 2005. **152**(4): p. 625-34.
103. Jeffreys, J., et al., *Characterization of the thyrotropin binding pocket.* Thyroid, 2002. **12**(12): p. 1051-61.
104. Nunez Miguel, R., et al., *Analysis of the thyrotropin receptor-thyrotropin interaction by comparative modeling.* Thyroid, 2004. **14**(12): p. 991-1011.
105. Smits, G., et al., *Glycoprotein hormone receptors: determinants in leucine-rich repeats responsible for ligand specificity*, in *EMBO J*. 2003. p. 2692-703.
106. Graves, P.N., et al., *Multimeric complex formation by the thyrotropin receptor in solubilized thyroid membranes.* Endocrinology, 1996. **137**(9): p. 3915-20.
107. Latif, R., P. Graves, and T.F. Davies, *Oligomerization of the human thyrotropin receptor: fluorescent protein-tagged hTSHR reveals post-translational complexes.* J Biol Chem, 2001. **276**(48): p. 45217-24.
108. Latif, R., P. Graves, and T.F. Davies, *Ligand-dependent inhibition of oligomerization at the human thyrotropin receptor.* J Biol Chem, 2002. **277**(47): p. 45059-67.
109. Moffett, S., D.A. Brown, and M.E. Linder, *Lipid-dependent targeting of G proteins into rafts.* J Biol Chem, 2000. **275**(3): p. 2191-8.
110. Tenenbaum-Rakover, Y., et al., *Loss-of-function mutations in the thyrotropin receptor gene as a major determinant of hyperthyrotropinemia in a consanguineous community.* J Clin Endocrinol Metab, 2009. **94**(5): p. 1706-12.
111. Gu, W.X., et al., *The thyrotropin (TSH) receptor transmembrane domain mutation (Pro556-Leu) in the hypothyroid hyt/hyt mouse results in plasma membrane targeting but defective TSH binding.* Endocrinology, 1995. **136**(7): p. 3146-53.
112. Graves, P.N., Y. Tomer, and T.F. Davies, *Cloning and sequencing of a 1.3 KB variant of human thyrotropin receptor mRNA lacking the transmembrane domain.* Biochem Biophys Res Commun, 1992. **187**(2): p. 1135-43.
113. Takeshita, A., et al., *Molecular cloning and sequencing of an alternatively spliced form of the human thyrotropin receptor transcript.* Biochem Biophys Res Commun, 1992. **188**(3): p. 1214-9.
114. Roselli-Rehfuss, L., L.S. Robbins, and R.D. Cone, *Thyrotropin receptor messenger ribonucleic acid is expressed in most brown and white adipose tissues in the guinea pig.* Endocrinology, 1992. **130**(4): p. 1857-61.
115. Janson, A., et al., *Presence of thyrotropin receptor in infant adipocytes.* Pediatr Res, 1998. **43**(4 Pt 1): p. 555-8.
116. Feliciello, A., et al., *Expression of thyrotropin-receptor mRNA in healthy and Graves' disease retro-orbital tissue.* Lancet, 1993. **342**(8867): p. 337-8.
117. Crisp, M.S., et al., *Thyrotropin receptor transcripts in human adipose tissue.* J Clin Endocrinol Metab, 1997. **82**(6): p. 2003-5.
118. Crisp, M., et al., *Adipogenesis in thyroid eye disease.* Invest Ophthalmol Vis Sci, 2000. **41**(11): p. 3249-55.
119. Haraguchi, K., et al., *Differentiation of rat preadipocytes is accompanied by expression of thyrotropin receptors.* Endocrinology, 1996. **137**(8): p. 3200-5.

120. Starkey, K.J., et al., *Adipose thyrotrophin receptor expression is elevated in Graves' and thyroid eye diseases ex vivo and indicates adipogenesis in progress in vivo.* J Mol Endocrinol, 2003. **30**(3): p. 369-80.
121. Allgeier, A., et al., *The human thyrotropin receptor activates G-proteins Gs and Gq/11.* J Biol Chem, 1994. **269**(19): p. 13733-5.
122. Laugwitz, K.L., et al., *The human thyrotropin receptor: a heptahelical receptor capable of stimulating members of all four G protein families.* Proc Natl Acad Sci U S A, 1996. **93**(1): p. 116-20.
123. Boutin, A., et al., *beta-Arrestin-1 mediates thyrotropin-enhanced osteoblast differentiation.* Faseb j, 2014. **28**(8): p. 3446-55.
124. Laurent, E., et al., *Dual activation by thyrotropin of the phospholipase C and cyclic AMP cascades in human thyroid.* Mol Cell Endocrinol, 1987. **52**(3): p. 273-8.
125. Büch, T.R.H., et al., *G13-dependent Activation of MAPK by Thyrotropin.* 2008.
126. Postiglione, M.P., et al., *Role of the thyroid-stimulating hormone receptor signaling in development and differentiation of the thyroid gland.* Proc Natl Acad Sci U S A, 2002. **99**(24): p. 15462-7.
127. Vassart, G. and J.E. Dumont, *The thyrotropin receptor and the regulation of thyrocyte function and growth.* Endocr Rev, 1992. **13**(3): p. 596-611.
128. Wang, H.S., et al., *TGF-beta induced hyaluronan synthesis in orbital fibroblasts involves protein kinase C betaII activation in vitro.* J Cell Biochem, 2005. **95**(2): p. 256-67.
129. Wang, J.F., D.J. Hill, and G.P. Becks, *Role of 3', 5' cyclic adenosine monophosphate and protein kinase C in the regulation of insulin-like growth factor-binding protein secretion by thyroid-stimulating hormone in isolated ovine thyroid cells.* J Endocrinol, 1994. **141**(2): p. 231-42.
130. D'Arcangelo, D., et al., *Physiological concentrations of thyrotropin increase cytosolic calcium levels in primary cultures of human thyroid cells.* J Clin Endocrinol Metab, 1995. **80**(4): p. 1136-43.
131. Jhon, D.Y., et al., *Cloning, sequencing, purification, and Gq-dependent activation of phospholipase C-beta 3.* J Biol Chem, 1993. **268**(9): p. 6654-61.
132. Macian, F., *NFAT proteins: key regulators of T-cell development and function.* Nat Rev Immunol, 2005. **5**(6): p. 472-84.
133. Luo, C., et al., *Interaction of calcineurin with a domain of the transcription factor NFAT1 that controls nuclear import.* Proc Natl Acad Sci U S A, 1996. **93**(17): p. 8907-12.
134. Song, Y., et al., *Species specific thyroid signal transduction: conserved physiology, divergent mechanisms.* Mol Cell Endocrinol, 2010. **319**(1-2): p. 56-62.
135. Sunahara, R.K., C.W. Dessauer, and A.G. Gilman, *Complexity and diversity of mammalian adenylyl cyclases.* Annu Rev Pharmacol Toxicol, 1996. **36**: p. 461-80.
136. Vanhaesebroeck, B., et al., *Phosphoinositide 3-kinases: a conserved family of signal transducers.* Trends Biochem Sci, 1997. **22**(7): p. 267-72.
137. Rhee, S.G. and Y.S. Bae, *Regulation of phosphoinositide-specific phospholipase C isozymes.* J Biol Chem, 1997. **272**(24): p. 15045-8.
138. Fatourechi, V., D.D. Ahmed, and K.M. Schwartz, *Thyroid acropachy: report of 40 patients treated at a single institution in a 26-year period.* J Clin Endocrinol Metab, 2002. **87**(12): p. 5435-41.
139. Winkler, A. and D. Wilson, *Thyroid acropachy. Case report and literature review.* Mo Med, 1985. **82**(12): p. 756-61.
140. Fatourechi, V., M. Pajouhi, and A.F. Fransway, *Dermopathy of Graves disease (pretibial myxedema). Review of 150 cases.* Medicine (Baltimore), 1994. **73**(1): p. 1-7.

141. Bartalena, L. and V. Fatourechi, *Extrathyroidal manifestations of Graves' disease: a 2014 update.* J Endocrinol Invest, 2014. **37**(8): p. 691-700.
142. Akasu, F., et al., *Localized myxedema on the nasal dorsum in a patient with Graves' disease: report of a case.* J Endocrinol Invest, 1989. **12**(10): p. 717-21.
143. Noppakun, N., K. Bancheun, and S. Chandraprasert, *Unusual locations of localized myxedema in Graves' disease. Report of three cases.* Arch Dermatol, 1986. **122**(1): p. 85-8.
144. Wright, A.L., P.K. Buxton, and D. Menzies, *Pretibial myxedema localized to scar tissue.* Int J Dermatol, 1990. **29**(1): p. 54-5.
145. Schwartz, K.M., et al., *Dermopathy of Graves' disease (pretibial myxedema): long-term outcome.* J Clin Endocrinol Metab, 2002. **87**(2): p. 438-46.
146. Lang, P.G., J.C. Sisson, and P.J. Lynch, *Intralesional triamcinolone therapy for pretibial myxedema.* Arch Dermatol, 1975. **111**(2): p. 197-202.
147. Susser, W.S., et al., *Elephantiasic pretibial myxedema: a novel treatment for an uncommon disorder.* J Am Acad Dermatol, 2002. **46**(5): p. 723-6.
148. Fatourechi, V., *Thyroid dermopathy and acropachy.* Best Pract Res Clin Endocrinol Metab, 2012. **26**(4): p. 553-65.
149. Lazarus, J.H., *Epidemiology of Graves' orbitopathy (GO) and relationship with thyroid disease.* Best Pract Res Clin Endocrinol Metab, 2012. **26**(3): p. 273-9.
150. Kendler, D.L., J. Lippa, and J. Rootman, *The initial clinical characteristics of Graves' orbitopathy vary with age and sex.* Arch Ophthalmol, 1993. **111**(2): p. 197-201.
151. Bartley, G.B., et al., *Chronology of Graves' ophthalmopathy in an incidence cohort.* Am J Ophthalmol, 1996. **121**(4): p. 426-34.
152. Weetman, A.P., *Graves' disease.* N Engl J Med, 2000. **343**(17): p. 1236-48.
153. Wiersinga, W.M., *Quality of life in Graves' ophthalmopathy.* Best Pract Res Clin Endocrinol Metab, 2012. **26**(3): p. 359-70.
154. Coulter, I., et al., *Psychological implications of Graves' orbitopathy.* Eur J Endocrinol, 2007. **157**(2): p. 127-31.
155. Bahn, R.S., *Graves' ophthalmopathy.* N Engl J Med, 2010. **362**(8): p. 726-38.
156. Bartley, G.B., *The epidemiologic characteristics and clinical course of ophthalmopathy associated with autoimmune thyroid disease in Olmsted County, Minnesota.* Trans Am Ophthalmol Soc, 1994. **92**: p. 477-588.
157. Eden, K.C. and W.R. Trotter, *LID-RETRACTION IN TOXIC DIFFUSE GOITRE.* The Lancet, 1942. **240**(6214): p. 385-387.
158. Feldon, S.E. and L. Levin, *Graves' ophthalmopathy: V. Aetiology of upper eyelid retraction in Graves' ophthalmopathy.* Br J Ophthalmol, 1990. **74**(8): p. 484-5.
159. Anderson, R.L., et al., *Dysthyroid optic neuropathy without extraocular muscle involvement.* Ophthalmic Surg, 1989. **20**(8): p. 568-74.
160. Rundle, F.F. and C.W. Wilson, *Development and course of exophthalmos and ophthalmoplegia in Graves' disease with special reference to the effect of thyroidectomy.* Clin Sci, 1945. **5**(3-4): p. 177-94.
161. Menconi, F., et al., *Spontaneous improvement of untreated mild Graves' ophthalmopathy: Rundle's curve revisited.* Thyroid, 2014. **24**(1): p. 60-6.
162. Hales, I.B. and F.F. Rundle, *Ocular changes in Graves' disease. A long-term follow-up study.* Q J Med, 1960. **29**: p. 113-26.
163. Perros, P., A.L. Crombie, and P. Kendall-Taylor, *Natural history of thyroid associated ophthalmopathy.* Clin Endocrinol (Oxf), 1995. **42**(1): p. 45-50.
164. Bartalena, L., et al., *The 2016 European Thyroid Association/European Group on Graves' Orbitopathy Guidelines for the Management of Graves' Orbitopathy.* Eur Thyroid J, 2016. **5**(1): p. 9-26.

165. Tellez, M., J. Cooper, and C. Edmonds, *Graves' ophthalmopathy in relation to cigarette smoking and ethnic origin.* Clin Endocrinol (Oxf), 1992. **36**(3): p. 291-4.
166. Shine, B., et al., *Association between Graves' ophthalmopathy and smoking.* Lancet, 1990. **335**(8700): p. 1261-3.
167. Pfeilschifter, J. and R. Ziegler, *Smoking and endocrine ophthalmopathy: impact of smoking severity and current vs lifetime cigarette consumption.* Clin Endocrinol (Oxf), 1996. **45**(4): p. 477-81.
168. Hagg, E. and K. Asplund, *Is endocrine ophthalmopathy related to smoking?* Br Med J (Clin Res Ed), 1987. **295**(6599): p. 634-5.
169. Winsa, B., A. Mandahl, and F.A. Karlsson, *Graves' disease, endocrine ophthalmopathy and smoking.* Acta Endocrinol (Copenh), 1993. **128**(2): p. 156-60.
170. Bartalena, L., et al., *More on smoking habits and Graves' ophthalmopathy.* J Endocrinol Invest, 1989. **12**(10): p. 733-7.
171. Eckstein, A., et al., *Impact of smoking on the response to treatment of thyroid associated ophthalmopathy.* Br J Ophthalmol, 2003. **87**(6): p. 773-6.
172. Bartalena, L., et al., *Cigarette smoking and treatment outcomes in Graves ophthalmopathy.* Ann Intern Med, 1998. **129**(8): p. 632-5.
173. Krassas, G.E., M. Segni, and W.M. Wiersinga, *Childhood Graves' ophthalmopathy: results of a European questionnaire study.* Eur J Endocrinol, 2005. **153**(4): p. 515-21.
174. Cawood, T.J., et al., *Smoking and thyroid-associated ophthalmopathy: A novel explanation of the biological link.* J Clin Endocrinol Metab, 2007. **92**(1): p. 59-64.
175. Baker, G.R., et al., *Altered tear composition in smokers and patients with graves ophthalmopathy.* Arch Ophthalmol, 2006. **124**(10): p. 1451-6.
176. Salvi, M., et al., *Increased serum concentrations of interleukin-6 (IL-6) and soluble IL-6 receptor in patients with Graves' disease.* J Clin Endocrinol Metab, 1996. **81**(8): p. 2976-9.
177. Mack, W.P., et al., *The effect of cigarette smoke constituents on the expression of HLA-DR in orbital fibroblasts derived from patients with Graves ophthalmopathy.* Ophthal Plast Reconstr Surg, 1999. **15**(4): p. 260-71.
178. Lim, S.L., et al., *Prevalence, risk factors, and clinical features of thyroid-associated ophthalmopathy in multiethnic Malaysian patients with Graves' disease.* Thyroid, 2008. **18**(12): p. 1297-301.
179. Kung, A.W., C.C. Yau, and A. Cheng, *The incidence of ophthalmopathy after radioiodine therapy for Graves' disease: prognostic factors and the role of methimazole.* J Clin Endocrinol Metab, 1994. **79**(2): p. 542-6.
180. Bartalena, L., et al., *Relation between therapy for hyperthyroidism and the course of Graves' ophthalmopathy.* N Engl J Med, 1998. **338**(2): p. 73-8.
181. Torring, O., et al., *Graves' hyperthyroidism: treatment with antithyroid drugs, surgery, or radioiodine--a prospective, randomized study. Thyroid Study Group.* J Clin Endocrinol Metab, 1996. **81**(8): p. 2986-93.
182. Jones, B.M., C.C. Kwok, and A.W. Kung, *Effect of radioactive iodine therapy on cytokine production in Graves' disease: transient increases in interleukin-4 (IL-4), IL-6, IL-10, and tumor necrosis factor-alpha, with longer term increases in interferon-gamma production.* J Clin Endocrinol Metab, 1999. **84**(11): p. 4106-10.
183. Almqvist, S. and P. Algvere, *Hypothyroidism in progressive ophthalmopathy of Graves' disease.* Acta Ophthalmol (Copenh), 1972. **50**(6): p. 761-70.
184. Prummel, M.F., et al., *Effect of abnormal thyroid function on the severity of Graves' ophthalmopathy.* Arch Intern Med, 1990. **150**(5): p. 1098-101.

185. Farid, N.R., E. Stone, and G. Johnson, *Graves' disease and HLA: clinical and epidemiologic associations.* Clin Endocrinol (Oxf), 1980. **13**(6): p. 535-44.
186. Weetman, A.P., et al., *Analysis of HLA-DQB and HLA-DPB alleles in Graves' disease by oligonucleotide probing of enzymatically amplified DNA.* Clin Endocrinol (Oxf), 1990. **33**(1): p. 65-71.
187. Yanagawa, T., et al., *CTLA-4 gene polymorphism associated with Graves' disease in a Caucasian population.* J Clin Endocrinol Metab, 1995. **80**(1): p. 41-5.
188. Huber, A.K., et al., *Interleukin (IL)-23 receptor is a major susceptibility gene for Graves' ophthalmopathy: the IL-23/T-helper 17 axis extends to thyroid autoimmunity.* J Clin Endocrinol Metab, 2008. **93**(3): p. 1077-81.
189. McKenzie, B.S., R.A. Kastelein, and D.J. Cua, *Understanding the IL-23-IL-17 immune pathway.* Trends Immunol, 2006. **27**(1): p. 17-23.
190. Farago, B., et al., *Functional variants of interleukin-23 receptor gene confer risk for rheumatoid arthritis but not for systemic sclerosis.* Ann Rheum Dis, 2008. **67**(2): p. 248-50.
191. Duerr, R.H., et al., *A genome-wide association study identifies IL23R as an inflammatory bowel disease gene.* Science, 2006. **314**(5804): p. 1461-3.
192. Marcocci, C., et al., *Selenium and the course of mild Graves' orbitopathy.* N Engl J Med, 2011. **364**(20): p. 1920-31.
193. Zang, S., K.A. Ponto, and G.J. Kahaly, *Clinical review: Intravenous glucocorticoids for Graves' orbitopathy: efficacy and morbidity.* J Clin Endocrinol Metab, 2011. **96**(2): p. 320-32.
194. Kahaly, G.J., et al., *Randomized, single blind trial of intravenous versus oral steroid monotherapy in Graves' orbitopathy.* J Clin Endocrinol Metab, 2005. **90**(9): p. 5234-40.
195. Marino, M., et al., *Acute and severe liver damage associated with intravenous glucocorticoid pulse therapy in patients with Graves' ophthalmopathy.* Thyroid, 2004. **14**(5): p. 403-6.
196. Le Moli, R., et al., *Determinants of liver damage associated with intravenous methylprednisolone pulse therapy in Graves' ophthalmopathy.* Thyroid, 2007. **17**(4): p. 357-62.
197. Stan, M.N., et al., *Randomized controlled trial of rituximab in patients with Graves' orbitopathy.* J Clin Endocrinol Metab, 2015. **100**(2): p. 432-41.
198. Salvi, M., et al., *Efficacy of B-cell targeted therapy with rituximab in patients with active moderate to severe Graves' orbitopathy: a randomized controlled study.* J Clin Endocrinol Metab, 2015. **100**(2): p. 422-31.
199. Prummel, M.F., et al., *A randomized controlled trial of orbital radiotherapy versus sham irradiation in patients with mild Graves' ophthalmopathy.* J Clin Endocrinol Metab, 2004. **89**(1): p. 15-20.
200. Kahaly, G.J., et al., *Low- versus high-dose radiotherapy for Graves' ophthalmopathy: a randomized, single blind trial.* J Clin Endocrinol Metab, 2000. **85**(1): p. 102-8.
201. Kahaly, G., et al., *Ciclosporin and prednisone v. prednisone in treatment of Graves' ophthalmopathy: a controlled, randomized and prospective study.* Eur J Clin Invest, 1986. **16**(5): p. 415-22.
202. Prummel, M.F., et al., *Prednisone and cyclosporine in the treatment of severe Graves' ophthalmopathy.* N Engl J Med, 1989. **321**(20): p. 1353-9.
203. Perros, P., et al., *Azathioprine in the treatment of thyroid-associated ophthalmopathy.* Acta Endocrinol (Copenh), 1990. **122**(1): p. 8-12.
204. Rajendram, R., et al., *Protocol for the combined immunosuppression & radiotherapy in thyroid eye disease (CIRTED) trial: a multi-centre, double-masked, factorial randomised controlled trial.* Trials, 2008. **9**: p. 6.

205. Kahaly, G., et al., *Randomized trial of intravenous immunoglobulins versus prednisolone in Graves' ophthalmopathy.* Clin Exp Immunol, 1996. **106**(2): p. 197-202.
206. Antonelli, A., et al., *High-dose intravenous immunoglobulin treatment in Graves' ophthalmopathy.* Acta Endocrinol (Copenh), 1992. **126**(1): p. 13-23.
207. Paridaens, D., et al., *The effect of etanercept on Graves' ophthalmopathy: a pilot study.* Eye (Lond), 2005. **19**(12): p. 1286-9.
208. Dickinson, A.J., et al., *Double-blind, placebo-controlled trial of octreotide long-acting repeatable (LAR) in thyroid-associated ophthalmopathy.* J Clin Endocrinol Metab, 2004. **89**(12): p. 5910-5.
209. Wemeau, J.L., et al., *Octreotide (long-acting release formulation) treatment in patients with graves' orbitopathy: clinical results of a four-month, randomized, placebo-controlled, double-blind study.* J Clin Endocrinol Metab, 2005. **90**(2): p. 841-8.
210. Galofre, J.C., A.M. Chacon, and R. Latif, *Targeting thyroid diseases with TSH receptor analogs.* Endocrinol Nutr, 2013. **60**(10): p. 590-8.
211. Khoo, D.H., et al., *The combination of absent thyroid peroxidase antibodies and high thyroid-stimulating immunoglobulin levels in Graves' disease identifies a group at markedly increased risk of ophthalmopathy.* Thyroid, 1999. **9**(12): p. 1175-80.
212. Goh, S.Y., et al., *Thyroid autoantibody profiles in ophthalmic dominant and thyroid dominant Graves' disease differ and suggest ophthalmopathy is a multiantigenic disease.* Clin Endocrinol (Oxf), 2004. **60**(5): p. 600-7.
213. Noh, J.Y., et al., *Thyroid-stimulating antibody is related to Graves' ophthalmopathy, but thyrotropin-binding inhibitor immunoglobulin is related to hyperthyroidism in patients with Graves' disease.* Thyroid, 2000. **10**(9): p. 809-13.
214. Morris, J.C., 3rd, et al., *Clinical utility of thyrotropin-receptor antibody assays: comparison of radioreceptor and bioassay methods.* Mayo Clin Proc, 1988. **63**(7): p. 707-17.
215. Lytton, S.D., et al., *A novel thyroid stimulating immunoglobulin bioassay is a functional indicator of activity and severity of Graves' orbitopathy.* J Clin Endocrinol Metab, 2010. **95**(5): p. 2123-31.
216. Kampmann, E., et al., *Thyroid Stimulating but Not Blocking Autoantibodies Are Highly Prevalent in Severe and Active Thyroid-Associated Orbitopathy: A Prospective Study.* Int J Endocrinol, 2015. **2015**: p. 678194.
217. Metcalfe, R., et al., *Demonstration of immunoglobulin G, A, and E autoantibodies to the human thyrotropin receptor using flow cytometry.* J Clin Endocrinol Metab, 2002. **87**(4): p. 1754-61.
218. Latif, R., et al., *The thyroid-stimulating hormone receptor: impact of thyroid-stimulating hormone and thyroid-stimulating hormone receptor antibodies on multimerization, cleavage, and signaling.* Endocrinol Metab Clin North Am, 2009. **38**(2): p. 319-41, viii.
219. Wess, J., *Molecular basis of receptor/G-protein-coupling selectivity.* Pharmacol Ther, 1998. **80**(3): p. 231-64.
220. Bouvier, M., *Oligomerization of G-protein-coupled transmitter receptors.* Nat Rev Neurosci, 2001. **2**(4): p. 274-86.
221. Weightman, D.R., et al., *Autoantibodies to IGF-1 binding sites in thyroid associated ophthalmopathy.* Autoimmunity, 1993. **16**(4): p. 251-7.
222. Tsui, S., et al., *Evidence for an association between thyroid-stimulating hormone and insulin-like growth factor 1 receptors: a tale of two antigens implicated in Graves' disease.* J Immunol, 2008. **181**(6): p. 4397-405.
223. Minich, W.B., et al., *Autoantibodies to the IGF1 receptor in Graves' orbitopathy.* J Clin Endocrinol Metab, 2013. **98**(2): p. 752-60.

224. Varewijck, A.J., et al., *Circulating IgGs may modulate IGF-I receptor stimulating activity in a subset of patients with Graves' ophthalmopathy.* J Clin Endocrinol Metab, 2013. **98**(2): p. 769-76.
225. Krieger, C.C., et al., *Bidirectional TSH and IGF-1 receptor cross talk mediates stimulation of hyaluronan secretion by Graves' disease immunoglobins.* J Clin Endocrinol Metab, 2015. **100**(3): p. 1071-7.
226. Vassart, G., et al., *Structure, expression and regulation of the thyroglobulin gene.* Mol Cell Endocrinol, 1985. **40**(2-3): p. 89-97.
227. Kriss, J.P., *Radioisotopic thyroidolymphography in patients with Graves' disease.* J Clin Endocrinol Metab, 1970. **31**(3): p. 315-23.
228. Konishi, J., M.M. Herman, and J.P. Kriss, *Binding of thyroglobulin and thyroglobulin-antithyroglobulin immune complex to extraocular muscle membrane.* Endocrinology, 1974. **95**(2): p. 434-46.
229. Ludgate, M., et al., *Definition, at the molecular level, of a thyroglobulin-acetylcholinesterase shared epitope: study of its pathophysiological significance in patients with Graves' ophthalmopathy.* Autoimmunity, 1989. **3**(3): p. 167-76.
230. Marino, M., et al., *Identification of thyroglobulin in orbital tissues of patients with thyroid-associated ophthalmopathy.* Thyroid, 2001. **11**(2): p. 177-85.
231. Lisi, S., et al., *Thyroglobulin in orbital tissues from patients with thyroid-associated ophthalmopathy: predominant localization in fibroadipose tissue.* Thyroid, 2002. **12**(5): p. 351-60.
232. Ludgate, M. and G. Vassart, *The molecular genetics of three thyroid autoantigens: thyroglobulin, thyroid peroxidase and the thyrotropin receptor.* Autoimmunity, 1990. **7**(2-3): p. 201-11.
233. Lai, O.F., et al., *Detection of thyroid peroxidase mRNA and protein in orbital tissue.* Eur J Endocrinol, 2006. **155**(2): p. 213-8.
234. Gunji, K., et al., *Cloning and characterization of the novel thyroid and eye muscle shared protein G2s: autoantibodies against G2s are closely associated with ophthalmopathy in patients with Graves' hyperthyroidism.* J Clin Endocrinol Metab, 2000. **85**(4): p. 1641-7.
235. Kubota, S., et al., *Reevaluation of the prevalences of serum autoantibodies reactive with "64-kd eye muscle proteins" in patients with thyroid-associated ophthalmopathy.* Thyroid, 1998. **8**(2): p. 175-9.
236. Dong, Q., M. Ludgate, and G. Vassart, *Cloning and sequencing of a novel 64-kDa autoantigen recognized by patients with autoimmune thyroid disease.* J Clin Endocrinol Metab, 1991. **72**(6): p. 1375-81.
237. Beard, N.A., D.R. Laver, and A.F. Dulhunty, *Calsequestrin and the calcium release channel of skeletal and cardiac muscle.* Prog Biophys Mol Biol, 2004. **85**(1): p. 33-69.
238. Gopinath, B., et al., *Can autoimmunity against calsequestrin explain the eye and eyelid muscle inflammation of thyroid eye disease?* Orbit, 2009. **28**(4): p. 256-61.
239. Qiu, Z., et al., *DNA synthesis and mitotic clonal expansion is not a required step for 3T3-L1 preadipocyte differentiation into adipocytes.* J Biol Chem, 2001. **276**(15): p. 11988-95.
240. Xu, J. and K. Liao, *Protein kinase B/AKT 1 plays a pivotal role in insulin-like growth factor-1 receptor signaling induced 3T3-L1 adipocyte differentiation.* J Biol Chem, 2004. **279**(34): p. 35914-22.
241. Ailhaud, G., P. Grimaldi, and R. Negrel, *Cellular and molecular aspects of adipose tissue development.* Annu Rev Nutr, 1992. **12**: p. 207-33.
242. Wu, Z., N.L. Bucher, and S.R. Farmer, *Induction of peroxisome proliferator-activated receptor gamma during the conversion of 3T3 fibroblasts into*

adipocytes is mediated by C/EBPbeta, C/EBPdelta, and glucocorticoids. Mol Cell Biol, 1996. **16**(8): p. 4128-36.
243. Kim, S.P., et al., *Transcriptional activation of peroxisome proliferator-activated receptor-gamma requires activation of both protein kinase A and Akt during adipocyte differentiation.* Biochem Biophys Res Commun, 2010. **399**(1): p. 55-9.
244. Fajas, L., et al., *The organization, promoter analysis, and expression of the human PPARgamma gene.* J Biol Chem, 1997. **272**(30): p. 18779-89.
245. Smith, T.J., et al., *Orbital fibroblast heterogeneity may determine the clinical presentation of thyroid-associated ophthalmopathy.* J Clin Endocrinol Metab, 2002. **87**(1): p. 385-92.
246. Sorisky, A., et al., *Evidence of adipocyte differentiation in human orbital fibroblasts in primary culture.* J Clin Endocrinol Metab, 1996. **81**(9): p. 3428-31.
247. Zhang, L., et al., *Biological effects of thyrotropin receptor activation on human orbital preadipocytes.* Invest Ophthalmol Vis Sci, 2006. **47**(12): p. 5197-203.
248. de Roux, N., et al., *A neomutation of the thyroid-stimulating hormone receptor in a severe neonatal hyperthyroidism.* J Clin Endocrinol Metab, 1996. **81**(6): p. 2023-6.
249. Fuhrer, D., et al., *Identification of a new thyrotropin receptor germline mutation (Leu629Phe) in a family with neonatal onset of autosomal dominant nonautoimmune hyperthyroidism.* J Clin Endocrinol Metab, 1997. **82**(12): p. 4234-8.
250. Lu, M. and R.Y. Lin, *TSH stimulates adipogenesis in mouse embryonic stem cells.* J Endocrinol, 2008. **196**(1): p. 159-69.
251. Kumar, S., et al., *A stimulatory TSH receptor antibody enhances adipogenesis via phosphoinositide 3-kinase activation in orbital preadipocytes from patients with Graves' ophthalmopathy.* J Mol Endocrinol, 2011. **46**(3): p. 155-63.
252. Sasisekharan, R., R. Raman, and V. Prabhakar, *Glycomics approach to structure-function relationships of glycosaminoglycans.* Annu Rev Biomed Eng, 2006. **8**: p. 181-231.
253. Itano, N., et al., *Three isoforms of mammalian hyaluronan synthases have distinct enzymatic properties.* J Biol Chem, 1999. **274**(35): p. 25085-92.
254. Meran, S., et al., *Involvement of hyaluronan in regulation of fibroblast phenotype.* J Biol Chem, 2007. **282**(35): p. 25687-97.
255. Selbi, W., et al., *Overexpression of hyaluronan synthase 2 alters hyaluronan distribution and function in proximal tubular epithelial cells.* J Am Soc Nephrol, 2006. **17**(6): p. 1553-67.
256. Selbi, W., et al., *Characterization of hyaluronan cable structure and function in renal proximal tubular epithelial cells.* Kidney Int, 2006. **70**(7): p. 1287-95.
257. Zhang, L., et al., *Possible targets for nonimmunosuppressive therapy of Graves' orbitopathy.* J Clin Endocrinol Metab, 2014. **99**(7): p. E1183-90.
258. Csoka, A.B., G.I. Frost, and R. Stern, *The six hyaluronidase-like genes in the human and mouse genomes.* Matrix Biol, 2001. **20**(8): p. 499-508.
259. Lokeshwar, V.B., et al., *Stromal and epithelial expression of tumor markers hyaluronic acid and HYAL1 hyaluronidase in prostate cancer.* J Biol Chem, 2001. **276**(15): p. 11922-32.
260. Franzmann, E.J., et al., *Expression of tumor markers hyaluronic acid and hyaluronidase (HYAL1) in head and neck tumors.* Int J Cancer, 2003. **106**(3): p. 438-45.
261. Stern, R. and M.J. Jedrzejas, *Hyaluronidases: their genomics, structures, and mechanisms of action.* Chem Rev, 2006. **106**(3): p. 818-39.
262. Zhang, L., et al., *Thyrotropin receptor activation increases hyaluronan production in preadipocyte fibroblasts: contributory role in hyaluronan*

accumulation in thyroid dysfunction. J Biol Chem, 2009. **284**(39): p. 26447-55.
263. van Zeijl, C.J., et al., *Effects of thyrotropin and thyrotropin-receptor-stimulating Graves' disease immunoglobulin G on cyclic adenosine monophosphate and hyaluronan production in nondifferentiated orbital fibroblasts of Graves' ophthalmopathy patients.* Thyroid, 2010. **20**(5): p. 535-44.
264. van Zeijl, C.J., et al., *Thyrotropin receptor-stimulating Graves' disease immunoglobulins induce hyaluronan synthesis by differentiated orbital fibroblasts from patients with Graves' ophthalmopathy not only via cyclic adenosine monophosphate signaling pathways.* Thyroid, 2011. **21**(2): p. 169-76.
265. Zhang, L., et al., *Adipose tissue depot-specific differences in the regulation of hyaluronan production of relevance to Graves' orbitopathy.* J Clin Endocrinol Metab, 2012. **97**(2): p. 653-62.
266. Smith, T.J. and N. Hoa, *Immunoglobulins from patients with Graves' disease induce hyaluronan synthesis in their orbital fibroblasts through the self-antigen, insulin-like growth factor-I receptor.* J Clin Endocrinol Metab, 2004. **89**(10): p. 5076-80.
267. Pritchard, J., et al., *Igs from patients with Graves' disease induce the expression of T cell chemoattractants in their fibroblasts.* J Immunol, 2002. **168**(2): p. 942-50.
268. Li, H., et al., *Independent adipogenic and contractile properties of fibroblasts in Graves' orbitopathy: an in vitro model for the evaluation of treatments.* PLoS One, 2014. **9**(4): p. e95586.
269. Douglas, R.S., et al., *Increased generation of fibrocytes in thyroid-associated ophthalmopathy.* J Clin Endocrinol Metab, 2010. **95**(1): p. 430-8.
270. Quan, T.E., et al., *Circulating fibrocytes: collagen-secreting cells of the peripheral blood.* Int J Biochem Cell Biol, 2004. **36**(4): p. 598-606.
271. Strieter, R.M., B.N. Gomperts, and M.P. Keane, *The role of CXC chemokines in pulmonary fibrosis.* J Clin Invest, 2007. **117**(3): p. 549-56.
272. Hong, K.M., et al., *Differentiation of human circulating fibrocytes as mediated by transforming growth factor-beta and peroxisome proliferator-activated receptor gamma.* J Biol Chem, 2007. **282**(31): p. 22910-20.
273. Smith, T.J., et al., *Evidence for cellular heterogeneity in primary cultures of human orbital fibroblasts.* J Clin Endocrinol Metab, 1995. **80**(9): p. 2620-5.
274. Koumas, L., T.J. Smith, and R.P. Phipps, *Fibroblast subsets in the human orbit: Thy-1+ and Thy-1- subpopulations exhibit distinct phenotypes.* Eur J Immunol, 2002. **32**(2): p. 477-85.
275. Borrello, M.A. and R.P. Phipps, *Differential Thy-1 expression by splenic fibroblasts defines functionally distinct subsets.* Cell Immunol, 1996. **173**(2): p. 198-206.
276. Koumas, L., et al., *Thy-1 expression in human fibroblast subsets defines myofibroblastic or lipofibroblastic phenotypes.* Am J Pathol, 2003. **163**(4): p. 1291-300.
277. Brandau, S., et al., *Orbital Fibroblasts From Graves' Orbitopathy Patients Share Functional and Immunophenotypic Properties With Mesenchymal Stem/Stromal Cells.* Invest Ophthalmol Vis Sci, 2015. **56**(11): p. 6549-57.
278. Eckstein, A.K., et al., *Current insights into the pathogenesis of Graves' orbitopathy.* Horm Metab Res, 2009. **41**(6): p. 456-64.
279. Forbes, G., et al., *Ophthalmopathy of Graves' disease: computerized volume measurements of the orbital fat and muscle.* AJNR. American journal of neuroradiology, 1986. **7**(4): p. 651-6.
280. Peplinski, L.S. and K. Albiani Smith, *Deepening of lid sulcus from topical bimatoprost therapy.* Optom Vis Sci, 2004. **81**(8): p. 574-7.

281. Filippopoulos, T., et al., *Periorbital changes associated with topical bimatoprost.* Ophthal Plast Reconstr Surg, 2008. **24**(4): p. 302-7.
282. Yam, J.C., N.S. Yuen, and C.W. Chan, *Bilateral deepening of upper lid sulcus from topical bimatoprost therapy.* Journal of ocular pharmacology and therapeutics : the official journal of the Association for Ocular Pharmacology and Therapeutics, 2009. **25**(5): p. 471-2.
283. Nakabayashi, K., et al., *Thyrostimulin, a heterodimer of two new human glycoprotein hormone subunits, activates the thyroid-stimulating hormone receptor.* J Clin Invest, 2002. **109**(11): p. 1445-52.
284. Okada, S.L., et al., *A glycoprotein hormone expressed in corticotrophs exhibits unique binding properties on thyroid-stimulating hormone receptor.* Mol Endocrinol, 2006. **20**(2): p. 414-25.
285. Tigas, S., et al., *Is excessive weight gain after ablative treatment of hyperthyroidism due to inadequate thyroid hormone therapy?* Thyroid : official journal of the American Thyroid Association, 2000. **10**(12): p. 1107-11.
286. Jansson, S., et al., *Overweight--a common problem among women treated for hyperthyroidism.* Postgraduate medical journal, 1993. **69**(808): p. 107-11.
287. Haluzik, M., et al., *Effects of hypo- and hyperthyroidism on noradrenergic activity and glycerol concentrations in human subcutaneous abdominal adipose tissue assessed with microdialysis.* J Clin Endocrinol Metab, 2003. **88**(12): p. 5605-8.
288. Dale, J., et al., *Weight gain following treatment of hyperthyroidism.* Clinical endocrinology, 2001. **55**(2): p. 233-9.
289. Ricciotti, E. and G.A. FitzGerald, *Prostaglandins and inflammation.* Arterioscler Thromb Vasc Biol, 2011. **31**(5): p. 986-1000.
290. Goldberg, B., H. Green, and G.J. Todaro, *Collagen Formation in Vitro by Established Mammalian Cell Lines.* Exp Cell Res, 1963. **31**: p. 444-7.
291. Eisenberg, D.L., C.B. Toris, and C.B. Camras, *Bimatoprost and travoprost: a review of recent studies of two new glaucoma drugs.* Survey of ophthalmology, 2002. **47 Suppl 1**: p. S105-15.
292. Woessner, J.F., Jr., *Matrix metalloproteinases and their inhibitors in connective tissue remodeling.* Faseb j, 1991. **5**(8): p. 2145-54.
293. Lindsey, J.D., et al., *Prostaglandin action on ciliary smooth muscle extracellular matrix metabolism: implications for uveoscleral outflow.* Surv Ophthalmol, 1997. **41 Suppl 2**: p. S53-9.
294. Weinreb, R.N., et al., *Prostaglandins increase matrix metalloproteinase release from human ciliary smooth muscle cells.* Invest Ophthalmol Vis Sci, 1997. **38**(13): p. 2772-80.
295. Jiang, W. and J.S. Bond, *Families of metalloendopeptidases and their relationships.* FEBS Lett, 1992. **312**(2-3): p. 110-4.
296. Curran, T. and B.R. Franza, Jr., *Fos and Jun: the AP-1 connection.* Cell, 1988. **55**(3): p. 395-7.
297. Lindsey, J.D., H.D. To, and R.N. Weinreb, *Induction of c-fos by prostaglandin F2 alpha in human ciliary smooth muscle cells.* Invest Ophthalmol Vis Sci, 1994. **35**(1): p. 242-50.
298. Tappeiner, C., et al., *[Orbital fat atrophy in glaucoma patients treated with topical bimatoprost--can bimatoprost cause enophthalmos?].* Klinische Monatsblatter fur Augenheilkunde, 2008. **225**(5): p. 443-5.
299. Aydin, S., et al., *Recovery of orbital fat pad prolapsus and deepening of the lid sulcus from topical bimatoprost therapy: 2 case reports and review of the literature.* Cutaneous and ocular toxicology, 2010. **29**(3): p. 212-6.
300. Park, J., H.K. Cho, and J.I. Moon, *Changes to upper eyelid orbital fat from use of topical bimatoprost, travoprost, and latanoprost.* Japanese journal of ophthalmology, 2011. **55**(1): p. 22-7.

301. Jayaprakasam, A. and S. Ghazi-Nouri, *Periorbital fat atrophy - an unfamiliar side effect of prostaglandin analogues.* Orbit, 2010. **29**(6): p. 357-9.
302. Serrero, G. and N.M. Lepak, *Prostaglandin F2alpha receptor (FP receptor) agonists are potent adipose differentiation inhibitors for primary culture of adipocyte precursors in defined medium.* Biochemical and biophysical research communications, 1997. **233**(1): p. 200-2.
303. Balapure, A.K., et al., *Structural requirements for prostaglandin analog interaction with the ovine corpus luteum prostaglandin F2 alpha receptor. Implications for development of a photoaffinity probe.* Biochemical pharmacology, 1989. **38**(14): p. 2375-81.
304. Abramovitz, M., et al., *Cloning and expression of a cDNA for the human prostanoid FP receptor.* The Journal of biological chemistry, 1994. **269**(4): p. 2632-6.
305. Sakamoto, K., et al., *Molecular cloning and expression of a cDNA of the bovine prostaglandin F2 alpha receptor.* J Biol Chem, 1994. **269**(5): p. 3881-6.
306. Vielhauer, G.A., H. Fujino, and J.W. Regan, *Cloning and localization of hFP(S): a six-transmembrane mRNA splice variant of the human FP prostanoid receptor.* Arch Biochem Biophys, 2004. **421**(2): p. 175-85.
307. Liang, Y., et al., *Identification and pharmacological characterization of the prostaglandin FP receptor and FP receptor variant complexes*, in *Br J Pharmacol*. 2008. p. 1079-93.
308. Black, F.M. and M.J. Wakelam, *Activation of inositol phospholipid breakdown by prostaglandin F2 alpha without any stimulation of proliferation in quiescent NIH-3T3 fibroblasts.* The Biochemical journal, 1990. **266**(3): p. 661-7.
309. Nakao, A., et al., *Characterization of prostaglandin F2 alpha receptor of mouse 3T3 fibroblasts and its functional expression in Xenopus laevis oocytes.* Journal of cellular physiology, 1993. **155**(2): p. 257-64.
310. Liu, L. and N.A. Clipstone, *Prostaglandin F2alpha inhibits adipocyte differentiation via a G alpha q-calcium-calcineurin-dependent signaling pathway.* Journal of cellular biochemistry, 2007. **100**(1): p. 161-73.
311. Neal, J.W. and N.A. Clipstone, *Calcineurin mediates the calcium-dependent inhibition of adipocyte differentiation in 3T3-L1 cells.* The Journal of biological chemistry, 2002. **277**(51): p. 49776-81.
312. Krassas, G.E. and A.E. Heufelder, *Immunosuppressive therapy in patients with thyroid eye disease: an overview of current concepts.* European journal of endocrinology / European Federation of Endocrine Societies, 2001. **144**(4): p. 311-8.
313. Bartalena, L., A. Pinchera, and C. Marcocci, *Management of Graves' ophthalmopathy: reality and perspectives.* Endocrine reviews, 2000. **21**(2): p. 168-99.
314. Yasumizu, T., *[Prostaglandins in human pregnancy and labor--studies on the levels of PGF2 alpha metabolites and in vitro production of PGE and PGF by uterus and placenta during human pregnancy and labor (author's transl)].* Nihon Sanka Fujinka Gakkai Zasshi, 1981. **33**(1): p. 1-10.
315. Toppozada, M., et al., *Induction of human luteolysis by high dose infusions of 150methyl PGF2 alpha.* Prostaglandins Med, 1981. **6**(2): p. 203-11.
316. Kang, K.H., et al., *PGF2 alpha causes bronchoconstriction and pulmonary vasoconstriction via thromboxane receptors in rat lung.* Korean J Intern Med, 1996. **11**(1): p. 74-81.
317. Todaro, G.J. and H. Green, *Quantitative studies of the growth of mouse embryo cells in culture and their development into established lines.* J Cell Biol, 1963. **17**: p. 299-313.

318. Green, H. and M. Meuth, *An established pre-adipose cell line and its differentiation in culture.* Cell, 1974. **3**(2): p. 127-33.
319. Gregoire, F.M., C.M. Smas, and H.S. Sul, *Understanding adipocyte differentiation.* Physiol Rev, 1998. **78**(3): p. 783-809.
320. Spiegelman, B.M. and J.S. Flier, *Adipogenesis and obesity: rounding out the big picture.* Cell, 1996. **87**(3): p. 377-89.
321. Kim, J. and M. Shim, *Prostaglandin F2alpha receptor (FP) signaling regulates Bmp signaling and promotes chondrocyte differentiation.* Biochim Biophys Acta, 2015. **1853**(2): p. 500-12.
322. Kim, J.W., *Topical prostaglandin analogue drugs inhibit adipocyte differentiation.* Korean J Ophthalmol, 2014. **28**(3): p. 257-64.
323. Casimir, D.A., C.W. Miller, and J.M. Ntambi, *Preadipocyte differentiation blocked by prostaglandin stimulation of prostanoid FP2 receptor in murine 3T3-L1 cells.* Differentiation; research in biological diversity, 1996. **60**(4): p. 203-10.
324. Miller, C.W., D.A. Casimir, and J.M. Ntambi, *The mechanism of inhibition of 3T3-L1 preadipocyte differentiation by prostaglandin F2alpha.* Endocrinology, 1996. **137**(12): p. 5641-50.
325. Reginato, M.J., et al., *Prostaglandins promote and block adipogenesis through opposing effects on peroxisome proliferator-activated receptor gamma.* J Biol Chem, 1998. **273**(4): p. 1855-8.
326. Hyman, B.T., L.L. Stoll, and A.A. Spector, *Accumulation of (n-9)-eicosatrienoic acid in confluent 3T3-L1 and 3T3 cells.* J Biol Chem, 1981. **256**(17): p. 8863-6.
327. Meyer zu Horste, M., et al., *A novel mechanism involved in the pathogenesis of Graves ophthalmopathy (GO): clathrin is a possible targeting molecule for inhibiting local immune response in the orbit.* The Journal of clinical endocrinology and metabolism, 2011. **96**(11): p. E1727-36.
328. Kumar, S., et al., *Evidence for enhanced adipogenesis in the orbits of patients with Graves' ophthalmopathy.* J Clin Endocrinol Metab, 2004. **89**(2): p. 930-5.
329. Seibold, L.K., D.A. Ammar, and M.Y. Kahook, *Acute effects of glaucoma medications and benzalkonium chloride on pre-adipocyte proliferation and adipocyte cytotoxicity in vitro.* Current eye research, 2013. **38**(1): p. 70-4.
330. Choi, H.Y., et al., *In vitro study of antiadipogenic profile of latanoprost, travoprost, bimatoprost, and tafluprost in human orbital preadiopocytes.* Journal of ocular pharmacology and therapeutics : the official journal of the Association for Ocular Pharmacology and Therapeutics, 2012. **28**(2): p. 146-52.
331. Silvestri, C., et al., *Anandamide-derived prostamide F2alpha negatively regulates adipogenesis.* J Biol Chem, 2013. **288**(32): p. 23307-21.
332. Starkey, K., et al., *Peroxisome proliferator-activated receptor-gamma in thyroid eye disease: contraindication for thiazolidinedione use?* J Clin Endocrinol Metab, 2003. **88**(1): p. 55-9.
333. Maxey, K.M., J.L. Johnson, and J. LaBrecque, *The hydrolysis of bimatoprost in corneal tissue generates a potent prostanoid FP receptor agonist.* Survey of ophthalmology, 2002. **47 Suppl 1**: p. S34-40.
334. Hellberg, M.R., et al., *The hydrolysis of the prostaglandin analog prodrug bimatoprost to 17-phenyl-trinor PGF2alpha by human and rabbit ocular tissue.* Journal of ocular pharmacology and therapeutics : the official journal of the Association for Ocular Pharmacology and Therapeutics, 2003. **19**(2): p. 97-103.
335. Woodward, D.F., et al., *The pharmacology of bimatoprost (Lumigan).* Survey of ophthalmology, 2001. **45 Suppl 4**: p. S337-45.

336. Ichhpujani, P., et al., *Comparison of human ocular distribution of bimatoprost and latanoprost.* Journal of ocular pharmacology and therapeutics : the official journal of the Association for Ocular Pharmacology and Therapeutics, 2012. **28**(2): p. 134-45.
337. Estcourt, S., et al., *The patient experience of services for thyroid eye disease in the United Kingdom: results of a nationwide survey.* European journal of endocrinology / European Federation of Endocrine Societies, 2009. **161**(3): p. 483-7.
338. Bartalena, L. and M.L. Tanda, *Clinical practice. Graves' ophthalmopathy.* The New England journal of medicine, 2009. **360**(10): p. 994-1001.
339. Marcocci, C. and M. Marino, *Treatment of mild, moderate-to-severe and very severe Graves' orbitopathy.* Best practice & research. Clinical endocrinology & metabolism, 2012. **26**(3): p. 325-37.
340. Serrero, G., N.M. Lepak, and S.P. Goodrich, *Prostaglandin F2 alpha inhibits the differentiation of adipocyte precursors in primary culture.* Biochemical and biophysical research communications, 1992. **183**(2): p. 438-42.
341. Mourits, M.P., et al., *Clinical activity score as a guide in the management of patients with Graves' ophthalmopathy.* Clinical endocrinology, 1997. **47**(1): p. 9-14.
342. Laurberg, P., et al., *Double vision is a major manifestation in moderate to severe graves' orbitopathy, but it correlates negatively with inflammatory signs and proptosis.* J Clin Endocrinol Metab, 2015. **100**(5): p. 2098-105.
343. Terwee, C.B., et al., *Development of a disease specific quality of life questionnaire for patients with Graves' ophthalmopathy: the GO-QOL.* Br J Ophthalmol, 1998. **82**(7): p. 773-9.
344. Draman, M.S., et al., *Prostaglandin F2alpha (PGF2alpha) Effects on Adipocyte Biology Relevant to Graves' Orbitopathy.* Thyroid, 2013.
345. Choi, H.G., et al., *Inhibition of prostaglandin D(2) production by trihydroxy fatty acids isolated from Ulmus davidiana var. japonica.* Phytother Res, 2013. **27**(9): p. 1376-80.
346. Draman, M.S. *Pathogenesis of Graves Orbitopathy*. 2011; Available from: http://www.eurekaselect.com/87911/article.
347. Terwee, C.B., et al., *Test-retest reliability of the GO-QOL: a disease-specific quality of life questionnaire for patients with Graves' ophthalmopathy.* J Clin Epidemiol, 1999. **52**(9): p. 875-84.
348. Ponto, K.A., et al., *Public health relevance of Graves' orbitopathy.* J Clin Endocrinol Metab, 2013. **98**(1): p. 145-52.
349. Higginbotham, E.J., et al., *One-year, randomized study comparing bimatoprost and timolol in glaucoma and ocular hypertension.* Arch Ophthalmol, 2002. **120**(10): p. 1286-93.
350. Reddy, S.V., et al., *Prevalence of Graves' ophthalmopathy in patients with Graves' disease presenting to a referral centre in north India.* Indian J Med Res, 2014. **139**(1): p. 99-104.
351. Wiersinga, W.M. and L. Bartalena, *Epidemiology and prevention of Graves' ophthalmopathy.* Thyroid, 2002. **12**(10): p. 855-60.
352. Tanda, M.L., et al., *Prevalence and natural history of Graves' orbitopathy in a large series of patients with newly diagnosed graves' hyperthyroidism seen at a single center.* J Clin Endocrinol Metab, 2013. **98**(4): p. 1443-9.
353. Bahn, R.S., et al., *Thyrotropin receptor expression in Graves' orbital adipose/connective tissues: potential autoantigen in Graves' ophthalmopathy.* J Clin Endocrinol Metab, 1998. **83**(3): p. 998-1002.
354. Hsu, S.Y., K. Nakabayashi, and A. Bhalla, *Evolution of glycoprotein hormone subunit genes in bilateral metazoa: identification of two novel human*

glycoprotein hormone subunit family genes, GPA2 and GPB5. Mol Endocrinol, 2002. **16**(7): p. 1538-51.
355. Okajima, Y., et al., *Biochemical roles of the oligosaccharide chains in thyrostimulin, a heterodimeric hormone of glycoprotein hormone subunits alpha 2 (GPA2) and beta 5 (GPB5).* Regul Pept, 2008. **148**(1-3): p. 62-7.
356. Vitt, U.A., S.Y. Hsu, and A.J. Hsueh, *Evolution and classification of cystine knot-containing hormones and related extracellular signaling molecules.* Mol Endocrinol, 2001. **15**(5): p. 681-94.
357. Lapthorn, A.J., et al., *Crystal structure of human chorionic gonadotropin.* Nature, 1994. **369**(6480): p. 455-61.
358. Alvarez, E., C. Cahoreau, and Y. Combarnous, *Comparative structure analyses of cystine knot-containing molecules with eight aminoacyl ring including glycoprotein hormones (GPH) alpha and beta subunits and GPH-related A2 (GPA2) and B5 (GPB5) molecules.* Reprod Biol Endocrinol, 2009. **7**: p. 90.
359. Ruddon, R.W., S.A. Sherman, and E. Bedows, *Protein folding in the endoplasmic reticulum: lessons from the human chorionic gonadotropin beta subunit.* Protein Sci, 1996. **5**(8): p. 1443-52.
360. Lantz, M., et al., *Thyrostimulin (a TSH-like Hormone) expression in orbital and thyroid tissue.* Thyroid, 2007. **17**(2): p. 113-8.
361. Denis-Henriot, D., et al., *Site-related differences in G-protein alpha subunit expression during adipogenesis in vitro: possible key role for Gq/11 alpha in the control of preadipocyte differentiation.* Biochem Biophys Res Commun, 1996. **220**(2): p. 443-8.
362. Paschke, R., et al., *Presence of nonfunctional thyrotropin receptor variant transcripts in retroocular and other tissues.* J Clin Endocrinol Metab, 1994. **79**(5): p. 1234-8.
363. Quellari, M., et al., *Role of cleavage and shedding in human thyrotropin receptor function and trafficking.* Eur J Biochem, 2003. **270**(17): p. 3486-97.
364. Rapoport, B. and S.M. McLachlan, *The thyrotropin receptor in Graves' disease.* Thyroid, 2007. **17**(10): p. 911-22.
365. Nagayama, Y., et al., *A novel murine model of Graves' hyperthyroidism with intramuscular injection of adenovirus expressing the thyrotropin receptor.* J Immunol, 2002. **168**(6): p. 2789-94.
366. Berchner-Pfannschmidt, U., et al., *Comparative assessment of female mouse model of Graves' orbitopathy under different environments, accompanied by pro-inflammatory cytokine and T cell responses to thyrotropin hormone receptor antigen.* Endocrinology, 2016: p. en20151829.
367. Evans, C., et al., *Development of a luminescent bioassay for thyroid stimulating antibodies.* J Clin Endocrinol Metab, 1999. **84**(1): p. 374-7.
368. Sun, S.C., et al., *Thyrostimulin, but not thyroid-stimulating hormone (TSH), acts as a paracrine regulator to activate the TSH receptor in mammalian ovary.* J Biol Chem, 2010. **285**(6): p. 3758-65.
369. Bassett, J.H., et al., *Thyrostimulin Regulates Osteoblastic Bone Formation During Early Skeletal Development.* Endocrinology, 2015. **156**(9): p. 3098-113.
370. Bodo, E., et al., *Human female hair follicles are a direct, nonclassical target for thyroid-stimulating hormone.* J Invest Dermatol, 2009. **129**(5): p. 1126-39.
371. Nagasaki, H., et al., *Differential expression of the thyrostimulin subunits, glycoprotein alpha2 and beta5 in the rat pituitary.* J Mol Endocrinol, 2006. **37**(1): p. 39-50.
372. Valyasevi, R.W., et al., *Differentiation of human orbital preadipocyte fibroblasts induces expression of functional thyrotropin receptor.* J Clin Endocrinol Metab, 1999. **84**(7): p. 2557-62.

373. Gillespie, E.F., et al., *Increased expression of TSH receptor by fibrocytes in thyroid-associated ophthalmopathy leads to chemokine production.* J Clin Endocrinol Metab, 2012. **97**(5): p. E740-6.
374. Bell, A., et al., *Functional TSH receptor in human abdominal preadipocytes and orbital fibroblasts.* Am J Physiol Cell Physiol, 2000. **279**(2): p. C335-40.
375. Nagayama, Y., et al., *Binding domains of stimulatory and inhibitory thyrotropin (TSH) receptor autoantibodies determined with chimeric TSH-lutropin/chorionic gonadotropin receptors.* J Clin Invest, 1991. **88**(1): p. 336-40.
376. Ploski, R., et al., *Thyroid stimulating hormone receptor (TSHR) intron 1 variants are major risk factors for Graves' disease in three European Caucasian cohorts.* PLoS One, 2010. **5**(11): p. e15512.
377. Paschke, R. and M. Ludgate, *The thyrotropin receptor in thyroid diseases.* The New England journal of medicine, 1997. **337**(23): p. 1675-81.
378. Seppel, T., A. Kosel, and R. Schlaghecke, *Bioelectrical impedance assessment of body composition in thyroid disease.* European journal of endocrinology / European Federation of Endocrine Societies, 1997. **136**(5): p. 493-8.
379. Lahesmaa, M., et al., *Hyperthyroidism increases brown fat metabolism in humans.* J Clin Endocrinol Metab, 2014. **99**(1): p. E28-35.
380. Obregon, M.J., *Adipose tissues and thyroid hormones.* Front Physiol, 2014. **5**: p. 479.
381. Pears, J., R.T. Jung, and A. Gunn, *Long-term weight changes in treated hyperthyroid and hypothyroid patients.* Scott Med J, 1990. **35**(6): p. 180-2.
382. Weinreb, J.T., Y. Yang, and G.D. Braunstein, *Do patients gain weight after thyroidectomy for thyroid cancer?* Thyroid, 2011. **21**(12): p. 1339-42.
383. Rotondi, M., et al., *Body weight changes in a large cohort of patients subjected to thyroidectomy for a wide spectrum of thyroid diseases.* Endocr Pract, 2014. **20**(11): p. 1151-8.
384. Wajchenberg, B.L., *Subcutaneous and visceral adipose tissue: their relation to the metabolic syndrome.* Endocr Rev, 2000. **21**(6): p. 697-738.
385. Diez, J.J. and P. Iglesias, *The role of the novel adipocyte-derived hormone adiponectin in human disease.* Eur J Endocrinol, 2003. **148**(3): p. 293-300.
386. Steppan, C.M., et al., *The hormone resistin links obesity to diabetes.* Nature, 2001. **409**(6818): p. 307-12.
387. Tseng, Y.H., A.M. Cypess, and C.R. Kahn, *Cellular bioenergetics as a target for obesity therapy.* Nat Rev Drug Discov, 2010. **9**(6): p. 465-82.
388. Sanchez-Gurmaches, J. and D.A. Guertin, *Adipocytes arise from multiple lineages that are heterogeneously and dynamically distributed.* Nat Commun, 2014. **5**: p. 4099.
389. Cannon, B. and J. Nedergaard, *Brown adipose tissue: function and physiological significance.* Physiol Rev, 2004. **84**(1): p. 277-359.
390. Cypess, A.M., et al., *Identification and importance of brown adipose tissue in adult humans.* N Engl J Med, 2009. **360**(15): p. 1509-17.
391. Virtanen, K.A., et al., *Functional brown adipose tissue in healthy adults.* N Engl J Med, 2009. **360**(15): p. 1518-25.
392. Cypess, A.M., et al., *Anatomical Localization, Gene Expression Profiling, and Functional Characterization of Adult Human Neck Brown Fat.* Nat Med, 2013. **19**(5): p. 635-9.
393. Seale, P., et al., *PRDM16 controls a brown fat/skeletal muscle switch.* Nature, 2008. **454**(7207): p. 961-7.
394. Kajimura, S., et al., *Initiation of myoblast to brown fat switch by a PRDM16-C/EBP-beta transcriptional complex.* Nature, 2009. **460**(7259): p. 1154-8.

395. Walden, T.B., et al., *Recruited vs. nonrecruited molecular signatures of brown, "brite," and white adipose tissues.* Am J Physiol Endocrinol Metab, 2012. **302**(1): p. E19-31.
396. Rosenwald, M., et al., *Bi-directional interconversion of brite and white adipocytes.* Nat Cell Biol, 2013. **15**(6): p. 659-67.
397. Lee, Y.H., et al., *In vivo identification of bipotential adipocyte progenitors recruited by beta3-adrenoceptor activation and high-fat feeding.* Cell Metab, 2012. **15**(4): p. 480-91.
398. Wu, J., et al., *Beige adipocytes are a distinct type of thermogenic fat cell in mouse and human.* Cell, 2012. **150**(2): p. 366-76.
399. Jespersen, N.Z., et al., *A classical brown adipose tissue mRNA signature partly overlaps with brite in the supraclavicular region of adult humans.* Cell Metab, 2013. **17**(5): p. 798-805.
400. Endo, T. and T. Kobayashi, *Thyroid-stimulating hormone receptor in brown adipose tissue is involved in the regulation of thermogenesis.* American journal of physiology. Endocrinology and metabolism, 2008. **295**(2): p. E514-8.
401. Lee, J.Y., et al., *Triiodothyronine induces UCP-1 expression and mitochondrial biogenesis in human adipocytes.* Am J Physiol Cell Physiol, 2012. **302**(2): p. C463-72.
402. Chance, B. and G.R. Williams, *Respiratory enzymes in oxidative phosphorylation. VI. The effects of adenosine diphosphate on azide-treated mitochondria.* J Biol Chem, 1956. **221**(1): p. 477-89.
403. Dalgaard, L.T. and O. Pedersen, *Uncoupling proteins: functional characteristics and role in the pathogenesis of obesity and Type II diabetes.* Diabetologia, 2001. **44**(8): p. 946-65.
404. Fisler, J.S. and C.H. Warden, *Uncoupling proteins, dietary fat and the metabolic syndrome.* Nutr Metab (Lond), 2006. **3**: p. 38.
405. Azzu, V. and M.D. Brand, *The on-off switches of the mitochondrial uncoupling proteins.* Trends Biochem Sci, 2010. **35**(5): p. 298-307.
406. Esterbauer, H., et al., *Human peroxisome proliferator activated receptor gamma coactivator 1 (PPARGC1) gene: cDNA sequence, genomic organization, chromosomal localization, and tissue expression.* Genomics, 1999. **62**(1): p. 98-102.
407. Liang, H. and W.F. Ward, *PGC-1alpha: a key regulator of energy metabolism.* Adv Physiol Educ, 2006. **30**(4): p. 145-51.
408. Tritos, N.A., et al., *Characterization of the peroxisome proliferator activated receptor coactivator 1 alpha (PGC 1alpha) expression in the murine brain.* Brain Res, 2003. **961**(2): p. 255-60.
409. Aruga, J., et al., *A novel zinc finger protein, zic, is involved in neurogenesis, especially in the cell lineage of cerebellar granule cells.* J Neurochem, 1994. **63**(5): p. 1880-90.
410. Shioda, T., M.H. Fenner, and K.J. Isselbacher, *msg1, a novel melanocyte-specific gene, encodes a nuclear protein and is associated with pigmentation.* Proc Natl Acad Sci U S A, 1996. **93**(22): p. 12298-303.
411. Yahata, T., et al., *Selective coactivation of estrogen-dependent transcription by CITED1 CBP/p300-binding protein.* Genes Dev, 2001. **15**(19): p. 2598-612.
412. Sharp, L.Z., et al., *Human BAT possesses molecular signatures that resemble beige/brite cells.* PLoS One, 2012. **7**(11): p. e49452.
413. Petrovic, N., et al., *Chronic peroxisome proliferator-activated receptor gamma (PPARgamma) activation of epididymally derived white adipocyte cultures reveals a population of thermogenically competent, UCP1-containing adipocytes molecularly distinct from classic brown adipocytes.* J Biol Chem, 2010. **285**(10): p. 7153-64.

414. Yamamoto, Y., et al., *Adipose depots possess unique developmental gene signatures.* Obesity (Silver Spring), 2010. **18**(5): p. 872-8.
415. Laurberg, P., et al., *TSH-receptor autoimmunity in Graves' disease after therapy with anti-thyroid drugs, surgery, or radioiodine: a 5-year prospective randomized study.* Eur J Endocrinol, 2008. **158**(1): p. 69-75.
416. Abe, E., et al., *TSH is a negative regulator of skeletal remodeling.* Cell, 2003. **115**(2): p. 151-62.
417. Marcus, C., et al., *Regulation of lipolysis during the neonatal period. Importance of thyrotropin.* J Clin Invest, 1988. **82**(5): p. 1793-7.
418. Lu, S., et al., *Role of extrathyroidal TSHR expression in adipocyte differentiation and its association with obesity.* Lipids Health Dis, 2012. **11**: p. 17.
419. Ma, S., et al., *Thyrotropin and obesity: increased adipose triglyceride content through glycerol-3-phosphate acyltransferase 3.* Sci Rep, 2015. **5**: p. 7633.
420. Muscogiuri, G., et al., *High-normal TSH values in obesity: is it insulin resistance or adipose tissue's guilt?* Obesity (Silver Spring), 2013. **21**(1): p. 101-6.
421. Endo, T. and T. Kobayashi, *Expression of functional TSH receptor in white adipose tissues of TSH receptor mutant mice induces lipolysis in vivo.* American journal of physiology. Endocrinology and metabolism, 2012.
422. Martinez-deMena, R., et al., *TSH effects on thermogenesis in rat brown adipocytes.* Mol Cell Endocrinol, 2015. **404**: p. 151-8.
423. de Lloyd, A., et al., *TSH receptor activation and body composition.* The Journal of endocrinology, 2010. **204**(1): p. 13-20.
424. Sera, N., et al., *Thyroid hormones influence serum leptin levels in patients with Graves' disease during suppression of beta-adrenergic receptors.* Thyroid, 2000. **10**(8): p. 641-6.
425. Paz-Filho, G., et al., *Congenital leptin deficiency: diagnosis and effects of leptin replacement therapy.* Arq Bras Endocrinol Metabol, 2010. **54**(8): p. 690-7.
426. Paz-Filho, G.J., et al., *Decrease in leptin production by the adipose tissue in obesity associated with severe metabolic syndrome.* Arq Bras Endocrinol Metabol, 2009. **53**(9): p. 1088-95.
427. Elledge, S.J., *Cell cycle checkpoints: preventing an identity crisis.* Science, 1996. **274**(5293): p. 1664-72.
428. Sakurai, M., et al., *Association between genetic polymorphisms of the prostaglandin F2alpha receptor gene, and response to latanoprost in patients with glaucoma and ocular hypertension.* Br J Ophthalmol, 2014. **98**(4): p. 469-73.

8 APPENDICES

8.1 Appendix 1: Supplier list

Fisher	https://www.fishersci.co.uk/
Promega	https://www.promega.com/b/uk/
Star lab	http://www.starlab.de/
Stratagene	http://www.genomics.agilent.com/
Melford	htpp://www.melford.co.uk
Sigma	http://www.sigmaaldrich.com/
Invitrogen	https://www.thermofisher.com/
Abcam	http://www.abcam.com/
Cell signalling	https://www.cellsignal.com/
Santa Cruz Biotechnology	https://www3.scbt.com/
Qiagen	https://www.qiagen.com/
New England Biolab	http://www.neb.uk.com/
GE Healthcare	http://www3.gehealthcare.com/
Cayman chemical	http://www.caymaneurope.com/
Cambridge Bioscience	http://www.bioscience.co.uk/
Allergan	http://www.allergan.co.uk/
Blumont healthcare	http://www.blumonthealthcare.com/

8.2 Appendix 2: Stock components

Pioglitazone stock (100nM-Takeda)

Dilute the stock 1 in 10 in DMSO (working solution 10 mM, e.g. 80 ul in 720 ul of DMSO). Aliquot 25 ul volume. Use 20 ul/200ml DM to give final concentration of 1 uM.

Insulin (100mg, I1882-Sigma)

Dissolve 100mg in 10 ml ultra-pure water and few drops glacial acetic acid, Filter sterilised. Mix 1ml of 0.01% BSA with 99 ml of HBSS. Add 90 ml of HBSS/0.01% BSA to 10 ml filtered insulin. Aliquot 600 ul each and freeze.

BSA (100mg, A7906-Sigma)

1% BSA was made by adding 100mg of BSA in 10 ml of ultra-pure water and filter sterilised. 0.01% concentration was achieved by adding 100 ul of 1% BSA to 9.9 ml of ultra-pure water.

Hydrocortisone (100mg, H2270-Sigma)

100mg was dissolved in 20 ml of ultra-pure water. Aliquot 200 ul and freeze -20 C. Use 20 ul of stock into 200 ml of DM.

Pantothenate (100g, P5155-Sigma)

100mg in 25ml of complete medium (4mg/ml). Aliquot 210 ul. Use 200 ul per 200 ml medium.

Biotin (500mg B4639-Sigma)

Dissolve 500mg in 20 mls of 1 M NaOH (25mg/ml). Aliquot 200 ul and freeze.

NaOH (100ml of 10M, 72068-Sigma)

Dilute 1:10 of water to get 1M NaOH.

T3 (1mg,T-5516-Sigma)

10x stock is prepared in 1M NaOH.1ml of 1M NaOH was added to 1mg T3 and gently swirled to dissolve. To this 49 ml of complete medium was added to give a stock solution of 20 ug/ul. Aliquots 200 ul and freeze.

OligodT (500ug/ml, C110A-Promega)

Dilute 1:5 (e.g. 40 ul in 160 ul of RNAse free water to give working solution 100 ug/ml)

dNTPs

dGTP (100nM, U121A- Promega), dATP (100nM, U120A- Promega), dCTP (100nM, U122A-Promega), dTTP (100nM, U123A- Promega).

Dilute 20 ul of each in 120 ul of water (1:10) to give working concentration of 10 nM.

PMSF (phenylmethylsulfonyl fluoride)

To prepare a 100 mM solution, add 17.4 mg of PMSF per millilitre of isopropanol. Store at −20°C.

Phosphate buffered saline (PBS)

NaCl	16g
Na_2HPO_4	2.9g
KH_2PO_4	0.5g
KCL	0.4g
Distilled water	2 l

Adjusted to pH 7.2 using 10N sodium hydroxide.

TAE 50x

242g TRIS

100ml 0.5M pH8 EDTA

57.1 ml glacial acetic acid

Make up to 1L with distilled water + autoclave this solution to give 50x solution.

100mls of TAE 50x in 4.9 Litre of distilled water = TAE x1

Stock pH 8.5

Ampicillin 100mg/ml

1g in 10 ml of distilled water and filtered sterilised. 1ml Aliquots was prepared.

X-Gal

100mg was dissolved in 2.5ml of Dimethylformamide and filtered sterilised, 40 ul per plate, spread over and left for 1 hour to diffuse.

Glycerol stock solution

67% Glycerol and 13 mM $MgCl_2$

Components	Amount
Glycerol	6.7 ml
$MgCl_2$ anhydrous	12.38 mg
H_2O	3.3 ml

Use 500 ul of the solution and mix with 200 ul of overnight *E. coli* culture.

8.3 Appendix 3: Websites

Genome restriction map
http://db.yeastgenome.org/cgi-bin/seqTools

Human genome database
http://genatlas.medecine.univ-paris5.fr/
http://www.ncbi.nlm.nih.gov/nucleotide
http://www.ncbi.nlm.nih.gov/tools/primer-blast/

Mouse genome database
http://www.informatics.jax.org/
http://vega.sanger.ac.uk/index.html

8.4 Appendix 4: BIMA Study

8.4.1 Protocol

Prostaglandin F2-alpha eye drops (Bimatoprost) in thyroid eye disease: a randomised controlled double blind crossover trial

Protocol V2

Bima Study

Confidential
Short title: Bimatoprost Eye Drops in Thyroid Eye Disease (BIMA Study)

Sponsor Number: SPON1266-14
EudraCT Number: 2014-000540-15

TABLE OF CONTENTS

LIST OF ABBREVIATONS

AE: Adverse Event
CI: Chief Investigator
CSRI: Client Service Receipt Inventory
CRF: Case Report Form
CU: Cardiff University
DSMB: Data Safety Monitoring Board
FT3: Free T3 (thyroid function test)
FT4: Free T4 (thyroid function test)
GCP: Good Clinical Practice
HCTU: Haematology Cancer Trials Unit
IMP: Investigational Medicinal Product
MHRA: Medicines & Healthcare Products Regulatory Agency
NIHR: National Institute for Health Research
NISCHR CRC: National Institute for Social Care & Health Research Clinical Research Centre
PGF2α: Bimatoprost
PI: Principal Investigator
REC: Research Ethics Committee
RIES: Research, Innovation and Enterprise Services
SAE: Severe Adverse Event
SAR: Severe Adverse Reaction
SPC: Summary of product characteristics
SUSAR: Suspected Unexpected Serious Adverse Reaction
TED: Thyroid Eye Disease
TEDtc: Thyroid Eye Disease Charitable Trust
TMG: Trial Management Group
TSC: Trial Steering Committee

1. TRIAL MANAGEMENT

3.5 SPONSOR

CARDIFF UNIVERSITY
Chris Shaw
Research Governance Coordinator
Research, Innovation and Enterprise Services (RIES)
Cardiff University
7th Floor, 30-36 Newport Road
Cardiff
CF24 0DE
Tel: (+44) 0 29 208 ex79130
Fax: (+44) 0 29 20874189
Email: ShawC3@cardiff.ac.uk

3.6 TRIAL CENTRE

Haematology Cancer Trials Unit
University Hospital of Wales
Heath Park, Cardiff CF14 4XW
Tel/Fax: (+44) 0 29 20744370

3.7 Trial Investigators

3.7.1 CHIEF INVESTIGATOR AND PRINCIPAL INVESTIGATOR

Colin M Dayan MA FRCP PhD
Professor of Clinical Diabetes and Metabolism
Director, Institute of Molecular and Experimental Medicine
Cardiff University School of Medicine
University Hospital of Wales, Heath Park, Cardiff CF14 4XN
Tel:(+44) 029 20 742182
Fax:(+44) 029 20 744671
Email: DayanCM@cf.ac.uk

3.7.2 LEAD OPHTHALMOLOGY INVESTIGATOR

Daniel Morris BSc(Hons) MBChB MRCOphth MFSEM(UK) FRCSEd(Ophth)
Consultant Ophthalmologist
Department of Ophthalmology
University Hospital of Wales, Heath Park, Cardiff CF14 4XW.
Tel: (+44) 029 20 742083
Fax: (+44) 029 20 748300
Email: dsm@doctors.org.uk

3.7.3 CO-INVESTIGATORS

Carol Lane BM, MRCP, FRCS FRCOphth DM FRCP
Consultant Ophthalmologist
Department of Ophthalmology
University Hospital of Wales, Heath Park, Cardiff CF14 4XW
Tel: (+44) 029 20 742083
Fax: (+44) 029 20 748300
Email: Carol.lane2@wales.nhs.uk

Onyebuchi Okosieme MD FRCP MBBS
NISCHR Research Fellow
Thyroid Research Group
Institute of Molecular and Experimental Medicine
Cardiff University School of Medicine
University Hospital of Wales, Heath Park, Cardiff CF14 4XN
Tel:(+44) 029 20 742182
Fax:(+44) 029 20 744671
Email: OkosiemeOE@cardiff.ac.uk

Mohd Shazli Draman MB BCh BAO (Hons) MRCPI
Clinical Lecturer
Thyroid Research Group
Institute of Molecular and Experimental Medicine
Cardiff University School of Medicine
University Hospital of Wales, Heath Park, Cardiff CF 14 4XN
Tel: (+44) 02920748481
Fax: (+44) 02920744671
Email: DramanYusofMS@cardiff.ac.uk

Marian Ludgate BSc PhD
Professor of Molecular Endocrinology
Thyroid Research Group
Institute of Molecular and Experimental Medicine
School of Medicine, Cardiff University

University Hospital of Wales, Heath Park
Cardiff CF14 4XN, UK
Tel: (+44) 02920 745457
Fax: (+44) 02920 744671
Email: ludgate@cf.ac.uk

3.7.4 TRIAL STATISTICIAN
Ms Rosemary Greenwood MSc(Leic)
Senior Statistician
University Hospitals Bristol NHS Foundation Trust
Level 3 Education Centre
Upper Maudlin Street
Bristol BS2 8AE
Tel: (+44) 0117 34 20234
Email: Rosemary.Greenwood@UHBristol.nhs.uk

3.7.5 SENIOR TRIALS MANAGER
Ian Thomas
Senior Trials Manager
Haematology Cancer Trials Unit
Cardiff University School of Medicine
University Hospital of Wales
Heath Park
Cardiff CF14 4XN
Tel: 02920 745397
Fax: 02920 742289
ThomasIF@cardiff.ac.uk

3.7.6 TRIAL COORDINATOR
Mrs Julie Pell PgC (Man)
Clinical Trials Coordinator
Institute of Molecular and Experimental Medicine
Cardiff University School of Medicine
C2 Link Corridor
University Hospital of Wales
Heath Park
Cardiff CF14 4XN, UK.
Tel & Fax (direct line): (+44) 029 20744370
Email: PellJC@cardiff.ac.uk

3.7.7 HEALTH ECONOMIST
Mr Chris Foy
Medical Statistician
Gloucestershire Research Support Service
Leadon House
Gloucestershire Royal Hospital
Great Western Road
Gloucester GL1 3NN
Tel: 0300 422 5461

Fax: 0300 422 5469
Email: Chris.Foy@glos.nhs.uk

3.8 Independent Members of Trial Advisory Committee

3.8.1 TRIAL STEERING COMMITTEE

(CHAIR) Mr Richard W J Lee BMedSci (Hons) BMBS MRCS (Eng) MRCOphth PhD
NIHR Clinical Lecturer in Ophthalmology
Dept. of Clinical Science at South Bristol, University of Bristol
School of Medical Sciences
University Walk
Bristol, BS8 1TD
Tel: (+44) 0117 331 2020
Fax: (+44) 0117 928 7896
Email: richard.lee@bristol.ac.uk

Dr. Daniel G. Ezra MA MBBS MMedEd MD FRCS FRCOphth FHEA
NIHR Biomedical Research Centre for Ophthalmology,
Moorfields Eye Hospital and UCL Institute of Ophthalmology,
London EC1V 2PD, UK.
Tel: (+44) 02084574571
Email: d.ezra@ucl.ac.uk

Dr Catey Bunce PhD
Research & Development Department
Moorfields Eye Hospital NHS Trust
City Road
London EC1V 2PD
Tel: (+44) 0207 566 2820
Email: c.bunce@ucl.ac.uk

7 BACKGROUND INFORMATION

Thyroid eye disease (TED) is the commonest extra thyroidal manifestation of Graves' hyperthyroidism. A key mechanism underlying TED is an increase in adipogenesis in the orbit resulting in orbital volume expansion and proptosis (eye protrusion). Proptosis may persist after inflammation has subsided in the late "burnt out" phase of TED and the persistent disfigured appearance of the eyes is a source of significant psychological distress and impaired quality of life for sufferers. Despite the negative impact of the condition, however, there are no specific medical treatments that target orbital volume reduction in late stage disease. Furthermore, a UK nationwide survey of patients with TED revealed low satisfaction levels with existing therapies [1]. In this study we propose to take advantage of the observation that enophthalmos (recession of the eye into the orbit) occurs in some patients treated with prostaglandin analogue eye drops like Bimatoprost (PGF2α) for glaucoma as well as the finding in in-vitro studies that prostaglandin analogues reduce fat expansion. We hypothesise that topical treatment with Bimatoprost may reduce orbital tissue volume in non-inflamed orbits and thereby improve quality of life in patients with TED.

3.9 BACKGROUND

Graves' disease affects about 1% of the general population and is the commonest cause of hyperthyroidism in iodine sufficient countries [2, 3]. Affected individuals suffer considerable morbidity and untreated disease may be complicated by multiple systemic manifestations including cardiac rhythm disorders, osteoporosis, and strokes [2, 3]. About 10-20% of patients with Graves' disease suffer with disfiguring eye disease or thyroid eye disease (TED) [4], equating to around 5,000 people in Wales. The majority of these patients have "burnt-out" or inactive disease in which the disfigurement persists, but there is no longer active inflammation. Women in the age range 30-50 are the group most commonly affected. The annual incidence of new TED is estimated at about 16 per 100,000 in women and 3 per 100,000 in men [5].

3.10 SYMPTOMS

In its mildest form TED causes marked irritation of the eye with excessive tearing, discomfort, and redness of the conjunctiva. Severe eye disease however leads to double vision and protrusion of the eyes, and in 3-5% of cases to sight loss [2, 3]. In addition most patients with TED have reduced quality of life [6] and suffer long-term psychological distress due to the disfiguring appearance resulting from the eye ball protrusion [7], an effect that is often underestimated by health care professionals. The course of the disease is highly unpredictable and treatment options are limited.

3.11 CURRENT TED MANAGEMENT

The natural history of TED comprises an early active inflammatory phase followed by a late or "burnt out" disease phase. For the majority of patients these treatments are supportive but in 5-10% of cases the disease is severe enough to merit major immunosuppressive therapy (e.g. high dose steroids or ciclosporin) and orbital radiotherapy during the inflamed "active" phase of the disease, or surgical decompression and rehabilitative surgery at a later stage [8]. Each of these treatment modalities has significant drawbacks in terms of side effects. Surgical decompression carries the risk of worsening double vision and local complications while high dose steroid therapy may be complicated by weight gain, diabetes mellitus, depression, or life threatening liver dysfunction and is not effective in "burnt-out" disease; orbital radiotherapy is not always effective and carries the potential risk of a tumour developing at the treatment site [9].

As mentioned above, most available non-surgical treatments are targeted towards control of inflammation during the active stage whereas rehabilitative surgery is the mainstay of treatment for the late disease phase. However, surgery is not always successful in reducing

proptosis and carries the attendant risks of anaesthesia and local complications, (decompression surgery is highly skilled and involves removal of bone around all three orbital walls). PGF2α agonists may thus be particularly useful in the late-phase of TED, a disease stage in which disfigurement and impairment of ocular function persists after resolution of the initial inflammatory process and which affects 5-10 times as many people as the early active phase. If PGF2α is confirmed to be effective in reducing proptosis in this study, it would indicate that PGF2α could represent a safe, locally acting agent in the management of TED, reducing the need for potentially high risk therapies such as surgical rehabilitation.

3.12 PATHOPHYSIOLOGY

The main pathological features of TED include expansion of orbital tissue fat, mononuclear cell infiltration of orbital connective tissue and extra ocular muscle, and tissue remodelling, a process that can culminate in fibrosis and diminished eye motility [10]. A key mechanism underlying TED is an increase in adipogenesis and associated secretion of glycosaminoglycans in the orbit, resulting in an increase in orbital volume and exophthalmos (protrusion of the eye) [11, 12]. The opposite effect, enophthalmos (recession of the eye into the orbit), has been described in patients with glaucoma treated with Bimatoprost (PGF2α), a prostaglandin analogue used topically in the management of intraocular hypertension (glaucoma). Cases of enophthalmos developing in patients treated with Bimatoprost have been reported worldwide, albeit in small numbers [13-15]. This side effect is more noticeable if only one eye is exposed to treatment as the treated eye is easily comparable with the unexposed eye. However, since most patients receive treatment to both eyes it is possible that the incidence of enophthalmos in Bimatoprost treated patients has been underestimated.

3.13 MECHANISM OF ACTION AND TRIAL RATIONALE

A possible mechanism by which PGF2α agonists might produce enophthalmos is through reduction of orbital fat volume [13]. A PGF2α receptor agonist has been shown to be a potent inhibitor of adipose differentiation in new-born rat precursor cells [16]. This raises the possibility that PGF2α exerts direct effects on adipose tissue precursors. We have confirmed this finding in in-vitro studies in our laboratory using 3T3L1 cell lines and human primary orbital fibroblast cultures [17, 18]. Thus, PGF2α agonists may be effective in reducing orbital fat expansion, ameliorating proptosis, and thus improving patient quality of life in patients with TED. There has been no clinical trial of PGF2α agonists in patients with TED.

3.14 TRIAL SUMMARY

This randomised controlled double blind crossover trial of Bimatoprost in TED will be the first to explore the role of a PGF2α agonist as a topical agent for TED. Only patients with stable late inactive disease will be enrolled and follow-up will continue for a minimum of 10 months with 2 months wash out period in between treatment. A cross over design is used to allow efficient use of patients.

2.7 CONDUCT OF TRIAL

The trial will be conducted according to the protocol and in compliance with the principles of the Declaration of Helsinki (1996), the principles of Good Clinical Practice (GCP) and in accordance with Medicines for Human Use (Clinical Trials) Regulations 2004, as amended in 2006, the Research Governance Framework for Health and Social Care, the Data Protection Act 1998 and other regulatory requirements as appropriate. The Protocol has been submitted for approval to an NHS Research Ethics Committee (REC) and to Medicines and Healthcare Products Regulatory Agency (MHRA)

8 OBJECTIVES

The overall objective is to determine if PGF2α eye drops can reduce proptosis in inactive thyroid eye disease.

3.15 PRIMARY ENDPOINT

The primary endpoint of this study will be comparison of the change in exophthalmometry readings over the two 3-month treatment periods. A treatment effect of reducing proptosis by 2mm for treatment compared to placebo will be considered clinically relevant.

3.16 SECONDARY ENDPOINTS

1. Change in quality of life scores on the TED quality of life questionnaire (GO-QOL) [19]
2. Change in intraocular pressures
3. Side effect profiles of Bimatoprost in TED patients during the study
4. Health economics consumption

9 TRIAL DESIGN

3.17 CROSS-OVER DESIGN

The study design is a randomised placebo controlled double blind cross over design. We have chosen this design for several reasons. First each participant serves as his or her own control thus reducing the influence of confounding variables (e.g. smoking status). Second, each patient is exposed to both control and treatment and thus the design is highly efficient in that it reduces the actual number of participants required for the study. This is particularly useful for conditions like thyroid eye disease (TED) in which the prevalence of the condition is relatively low. Lastly the quick onset and short duration of action of Bimatoprost eye drops (reversible in 3 days in vitro cell cultures [18]) makes this a feasible design to study its effects. The drawback of this study design is that the long term effect of the treatment on patient outcomes, side effects and costs cannot be estimated, however short term efficacy can be assessed with good value for money.

We have carefully considered the risk of carry over and discussed this with our advisory statisticians. As a result we have extended the wash-out period from 1 month in our initial plans to 2 months, since the evidence suggests that carryover effect is likely to be negligible with the 2 months wash out period, allowing us to take advantage of the crossover design. In human studies, the elimination half-life of topical Bimatoprost is 45 minutes and the intra ocular pharmacological effect is not known to exceed 24 hours [17]. By one month the drug is completely washed out and we have allowed an extra one month of recovery period for any tissue changes to stabilise. Clinical case reports [13-15] suggest that effects wear off in 4-6 weeks so that a 2 month washout period will allow subjects to experience both treatment and placebo equally. Therefore, the two month washout period should be adequate for complete elimination of the drug and for its biological effect to have worn off. Analysis of any treatment order effect will confirm this was the case at the end of the study.

3.17.1 TRIAL OVERVIEW

This is a randomised controlled double blind crossover trial of Bimatoprost in TED. Thirty one patients with stable late inactive disease will be enrolled. Patients will be allocated either Bimatoprost or placebo for 3 months, followed by 2 months wash out period before crossing over to the opposite treatment. Follow-up will continue for 10 months duration. The key eligibility criteria are patients with stable proptosis for at least 6 months duration. The primary outcome measured is the reduction in proptosis at the end of treatment period. The secondary outcome measured includes quality of life score, intraocular pressure reduction and side effect profile of Bimatoprost.

Patients will be recruited from the multidisciplinary thyroid eye disease clinic at University Hospital Wales. There is a database of 200 patients with inactive (previously treated) thyroid eye disease of which we expect 60% to be ineligible. This will leave 80 patients available for recruitment in the 6 months available for recruitment. If these patients can be consented with a recruitment rate of 60%, it will be possible to consent 31 by contacting just 50 of these patients. We intend to consent 31 patients with a diagnosis of TED in the late inactive disease stage meeting the inclusion and exclusion criteria. The diagnosis of TED will be made by a consultant ophthalmologist on the basis of clinical assessment. ***TED will be diagnosed clinically in the presence of one or more of the following features: soft tissue changes in the eye, proptosis, extra ocular muscle dysfunction, corneal abnormalities, and optic nerve involvement.*** To avoid inter-rater variability the same examiner, Mr Dan Morris, will

conduct the ophthalmological assessments. Each participant will be enrolled in the trial for approximately 10 months. Participants will receive either treatment or placebo for the first three months, followed by a two month washout phase before being crossed over to the opposite treatment. Patients will be followed for a further 2 months after treatment completion to allow us to determine reversibility of the treatment and to collect health economic data. We will randomly assign patients to start with either intervention or placebo such that the order of treatment is random.

3.17.2 Figure 1: Expected participant flow (Also see activity chart appendix 2)

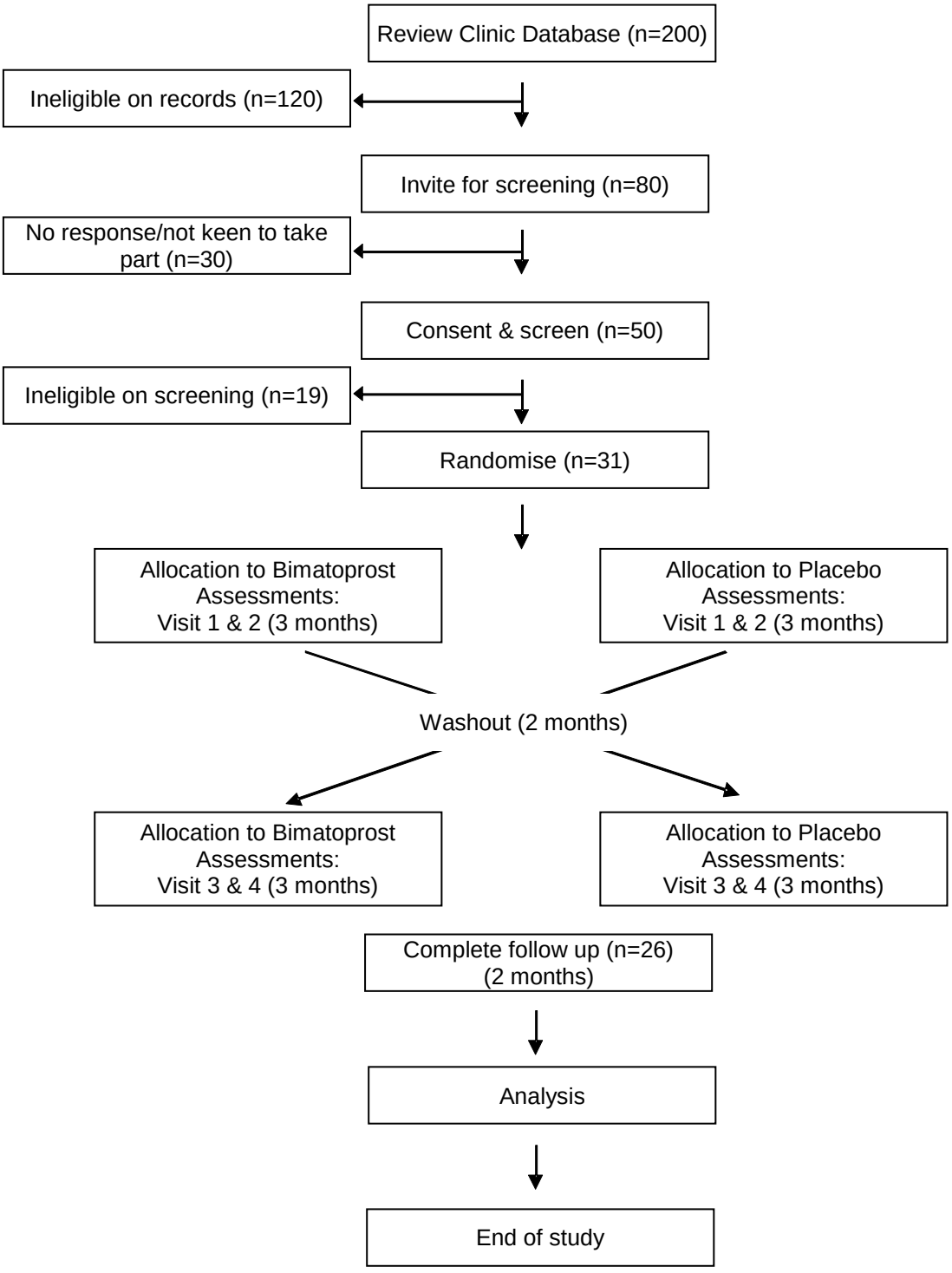

Trial participants will be randomised to receive Bimatoprost or placebo (illustrated above (n=expected number of participants)).

3.18 RANDOMISATION AND CODE BREAK SERVICE

Allocation of subjects will be by randomisation and minimisation to ensure balance between 2 trial arms. This service will be provided by remote computerised web-based allocation of treatment arm and will be supported by telephone service during working hours should network failure occur.

All investigators, trial staff, and participants will be blinded to the allocations. The trial pharmacist will use a web based format and receive treatment allocation from a Cardiff University validated randomisation system. A code of the allocations will be held by the pharmacist who will remain independent of the study and also by the clinical trials unit conducting the randomisation process. Code break during office hours will be via senior trial manager according to SOP. Out of hours code break service will be provided by UHW on-call pharmacist contactable via the hospital switchboard according to SOP agreed with pharmacy. The randomization information will be kept in the Bimatoprost trial pharmacy folder in the clinical trials room in the pharmacy. If a patient needs unmasking, this information will only be given to a doctor who is treating the patient. The pharmacist would say that the patient is receiving either Bimatoprost or placebo. If the doctor then needs to know whether the patient is receiving active or placebo, only then will the pharmacist reveal the treatment allocation. The PI will need to inform the senior trial manager within 24 hours of the code breaking.

3.19 MEASURE TO AVOID BIAS

3.19.1 Treatment Allocation

Allocation of patients to the 2 arms of the study will be done using minimisation. This is a process that allocates patients based on (a) their own characteristics, and (b) the allocations of patients with the same characteristics already in the trial. The process gains its name by minimising the imbalance in numbers in each of the trial arms with respect to a range of important prognostic variables simultaneously. It is a dynamic process and a randomisation schedule is therefore not drawn up in advance. The variables used to minimise patients are:

1. Degree of proptosis (Mild to moderate ≤ 22mm/Severe >23mm)
2. Eye involvement (Unilateral/bilateral)

The 2 trial arms to which minimisation will be applied in this study are:
(A) Starting Bimatoprost first
(B) Starting placebo first.

3.19.2 Masking

The placebo will be an artificial tear. To enhance masking the placebo will contain artificial tears with similar preservative (Benzalkonium chloride – marketed preparation) which will replicate any mild stinging sensation experienced with Bimatoprost. Both products (see section 6.1 for more details) will be relabelled by the trial pharmacist in accordance with EU Guidelines to Good Manufacturing Practice Medicinal Products for Human and Veterinary Use Annex 13. The relabelled product will be kept in an opaque medicine vial. However, it should be noted that the treatment and placebo bottles will be different sizes (3mls vs. 10mls), to avoid the need to repackage the agents. In an early proof of concept trial such as this, this lack of perfect placebo matching is justified to reduce costs – later confirmatory study will require this element to be addressed. However, in order not to unmask trial staff, the patients will be instructed not to bring their eye drop bottles to the eye clinic, but only to the hospital

pharmacy at the end of each treatment phase for disposal. Patients will be given a treatment log/diary to ensure compliance (Section 4.6.2). The PI and Consultant Ophthalmologists will not know the treatment allocation and will not have access to the eye drop bottles prescribed to patients – this will ensure maintenance of masking. Participants will be informed that the two treatments are in different sized vials, but with no indication of which is which.

3.19.3 OTHER MEASURES FOR MASKING AND PROTECTING AGAINST BIAS

Concealment of allocation as described above is very important. However, Bimatoprost eye drops do in some cases cause redness and irritation of the eyes, as well as iris colour and eyelash changes. We recognise that this may result in inadvertent unmasking during the trial of either the patient or the ophthalmologist. In addition only affected eyes will be treated (see section 6.1). This may mean that differences become apparent between the eye colours or eye lashes between the eyes. This will unavoidably have the potential to reduce masking amongst participants as well as trial staff and assessors. To minimise and evaluate this risk to concealment the following measures will be taken:

1. Participants will be asked to record any changes or adverse events in a standardised questionnaire, which will be designed to (a) not draw excessive attention to known unmasking effects of the treatment, (b) to allow this information to be collected prior to contact with trial staff, so that any influence of trial staff is minimised;
2. Only objective findings will be recorded by the assessor (e.g. proptosis measurements);
3. Assessor will have no access to prior assessment records/photos to compare with current measurement;
4. The success of blinding will be assessed at the 3-month and 8-month visits by asking patients and investigators to state whether they believe they know which treatment individual patients are receiving and assessing whether they can correctly identify this treatment. This will provide a degree of assessment of unmasking. Importantly, the quality of masking will be reported in the final trial report.
5. At the end of study, the masked photograph will be assessed by an independent ophthalmologist for treatment allocation. This will give information whether assessor/patients perception on treatment allocation is real.

3.19.3.1 Masked individuals

1. Patients
2. Clinical Investigators
3. Ophthalmologists
4. Endocrinologists
5. Clinical research fellow
6. Trial Coordinator
7. Data Analysts

3.19.3.2 Un-masked individuals:

1. Senior Trial Manager
2. Clinical Trial Pharmacists

Patients and the ophthalmic/endocrine clinical teams responsible for their care may request their treatment allocation which will be provided after the trial is completed (after last patient

completes follow up), unless unmasking is required for clinical reasons.

3.20 DETERMINATION OF SAMPLE SIZE

3.20.1 Primary outcome measure

The primary outcome of interest is the change in proptosis with Bimatoprost treatment and a reduction of 2mm or more is regarded as clinically relevant. Previous studies have shown a standard deviation of 2.5mm in proptosis measurements in patients with TED [19, 20]. We calculated that 26 participants (complete datasets) would be needed to be able identify a treatment effect of 1.6mm as statistically significant (p=0.05, two-sided, power 0.88). Allowing for a 15% dropout rate/incomplete datasets, we intend to recruit 31 participants. If the number of participants with incomplete datasets reaches 30% however there will still be 80% power to detect an effect of this size.

3.20.2 Secondary outcome measures

- Change in quality of life scores on the TED quality of life questionnaire (GO-QOL) [18]
- Change in intraocular pressures
- Side effect profiles of Bimatoprost in TED patients during the study
- Health economic consumption

3.21 TIMESCALES

3.21.1 Proposed Trial Start: January 2014

3.21.2 Projected Trial Completion: Feb 2016

3.21.3 Trial Duration: 26 months

3.21.4 Duration of Each Patient's Participation: 10 months

3.21.5 Follow up visits:

Following a baseline assessment (visit 1) follow up visits will be undertaken at 3 months (visit 2), 5 months (visit 3), 8 months (visit 4) and 10 months (visit 5). See appendix 2.

3.22 QUALITY CONTROL

3.22.1 Accountability for Investigational Products

Active Bimatoprost 0.03% and placebo artificial tear drop are being sourced via the St Mary's Pharmaceutical Unit. Both products will be relabelled by the trial pharmacist. The relabelled product will be kept in an opaque medicine vial. See section 6.1. Accountability logs will be kept in the Pharmacy Department and collected by the trial team at the end of the study.

3.22.2 Procedures for monitoring subject compliance
Each participant will be provided with a pre-designed log-book and asked to record each time the drug is taken. Compliance will be assessed at each visit by interviewing the participant and reviewing the log book (Appendix 9 - Patient Diary).

3.22.3 Site Monitoring
The Sponsor will delegate this responsibility to HCTU, who will have direct access to source data.

3.23 SAFETY

The safety of Bimatoprost is already established in its use in other indications. However, preliminary risk assessments will be conducted and the TMG will routinely review blinded adverse events on a three monthly basis. Since significant new adverse event information is not anticipated, a formal data safety monitoring board (DSMB) will not be established. However, if an unexpected rate of adverse event is observed, this will be discussed with the TSC and an independent DSMB able to review unmasked data will be convened if considered appropriate.

3.23.1 Interim analyses
No formal interim analyses are planned unless requested by the TSC.

3.23.2 Adverse Events
A list of adverse events will be compiled by the clinical research fellow and the trial coordinator and discussed at each TMG meeting along with a review of any early withdrawals from the protocol. All serious adverse events will be reported immediately to the sponsor who will manage these and report to the MHRA according to agreed procedures. See section 8.0 for adverse events classification.

3.23.3 Procedures for breaking randomisation codes
Randomisation codes may be broken prior to trial completion at the request of the patient's responsible clinician. Randomisation codes for individual patients may be broken for safety reasons and if clinically indicated. See section 4.2.

3.23.4 Criteria for termination of the trial
It is unlikely that the trial will be terminated prematurely due to safety issues, given the known safety record of the IMPs (active product and placebo). Should there be any unusual side effects detected, this will be discussed at TMG and reported to TSG. The trial can be terminated at the request of the TSG.

10 SELECTION AND WITHDRAWAL OF SUBJECTS

3.24 STUDY POPULATION

3.24.1 Inclusion criteria

1. Stable TED with no reported change in proptosis for at least 6 months. See section 4.1.1 for TED definition;
2. Clinical activity score <3 (Appendix 1);
3. Proptosis (subjective unilateral proptosis confirmed by asymmetry in exophthalmometry of >2mm OR greater than 20 mm on exophthalmometry measurement in one eye);
4. Euthyroid (FT3 and FT4 in the reference range);
5. If female, must be using a reliable form of contraception during the trial, e.g. oral contraceptive and condom, intra-uterine device (IUD) and condom, diaphragm with spermicide and condom.

3.24.2 Exclusion criteria

1. Age <18 yrs;
2. Dysthyroid optic neuropathy unless previously treated;
3. Pregnancy or lactation;
4. Previous Corneal Herpes Simplex infection;
5. On therapy for glaucoma or intraocular hypertension;
6. Less than 6 months from prior systemic steroid use;
7. Aphakia, pseudophakia with torn posterior lens capsule or anterior chamber lenses;
8. Patient with risk factors for cystoid macular oedema, iritis or uveitis;
9. Severe Asthma (risk of severe allergic reaction to medication);
10. Previous allergy to Bimatoprost or preservative.

3.25 RECRUITMENT AND IDENTIFICATION OF ELIGIBLE SUBJECTS

3.25.1 Advertising

Referrals will be from patients under the TED clinic at UHW and no specific advertising is planned.

3.25.2 Screening

Trial participants will be identified from the database of the multidisciplinary TED clinic in University Hospital Wales (UHW), Cardiff. The clinic database currently holds about 200 patients with TED who could potentially fulfil the study inclusion criteria. Potential participants meeting the inclusion criteria will be sent a letter informing them of the study and inviting their participation in the study. Patients who have been discharged from the clinic will be invited to re-attend the clinic.

3.25.3 Recruitment

Individuals who are clinically considered to have stable late stage TED, meeting the inclusion/exclusion criteria will be provided with an information sheet explaining the nature of the study in simple non-technical language. Participants will be recruited from current or previous attendees at the UHW TED clinic. In the unlikely event that adequate participant recruitment cannot be achieved from the multidisciplinary TED clinic in Cardiff and Vale Health Board, additional participants would be sought from other specialist eye clinics in neighbouring trusts including Aneurin Bevan Health Board, Cwm Taf Health Board and Abertawe Morgannwg University Health Board. Such sites will be added as Participant Identification

Sites (PICs) to identify and refer patients to C&V UHB. To our knowledge there are no major competing studies in this area which might impact our recruitment process.

REC and MHRA will be notified of end of study within 30 days of the last visit of the last participant taking part in the trial.

3.25.3.1 Screening and enrolment visit-Baseline assessment

Potentially eligible patients will be assessed by one of the Clinical Investigators. Patients will have received already a patient information sheet at least 24 hours before this visit. Any questions related to the trial will be answered prior to signing inform consent. Subjects fitting the clinical eligibility criteria will be invited to enter the trial.

The purpose of the baseline visit is to confirm eligibility, further discuss the pros and cons of taking part in the study, obtain consent if the patient wishes to take part and conduct the trial baseline assessments. A case record form (CRF) will be used to record the information and a modified version of the Initial Assessment Proforma published in 2002 by the European Group on Graves Orbitopathy (EUGOGO) will be used. The key components of the baseline visit are to document:

a) Medical history

- Duration and severity of TED symptoms
- TED treatment to date
- Prior and current thyroid status and treatments
- Ocular Co-morbidity
- General Past Medical History
- Current medications
- Smoking History
- Weight and Height (BMI)

b) Ophthalmological assessment:

- Proptosis (using an Oculus© exophthalmometer)
- Intraocular pressure in primary position and upgaze
- logMAR Visual Acuity
- Clinical activity score (CAS)* see appendix 1
- Palpebral aperture*
- Gorman's diplopia score
- Corneal integrity (Defined as healthy/dry (staining)/ulcerated)*
- Fundoscopy

*(*As per EUGOGO ATLAS)*

c) Photograph

Colour photographs of the eye in the lateral and anterior views according to standard operating procedure.

d) Blood tests:

Thyroid Function Tests (TSH, FT3, FT4). These will be analysed in chemical pathology lab University Hospital of Wales, as per standard practice. See appendix 6 for management of abnormal thyroid function test.

3.26 RANDOMISATION

Allocation of subjects will be by randomisation by minimisation. This is done to minimise the imbalance between the numbers of patients in each treatment group over 2 identified factors

(Degree of proptosis and uni/bilateral eyes involvement: See section 4.3.1). The service will be provided by a Cardiff University validated randomisation system. This is a remote computerised web-based allocation of treatment arm and will be supported by telephone service during working hours should network failure occurs. After a subject is deemed eligible, the trial coordinator will assign the patient a study number (1001-10xx) and fill an eligibility check list form which will include minimisation criteria.

Trial prescription will be written by clinical research fellow. The details will be entered into a randomisation web form by the trial coordinator. Treatment arm allocation will then be provided and confirmed via email to the clinical trial pharmacist. On receipt of the trial prescription, the pharmacist will provide the appropriate treatment materials for that subject at each visit.

3.27 WITHDRAWAL

3.27.1 Exit Criteria

AT ANY TIME

- Patient withdrawal of consent

AFTER RANDOMISATION

- Reactivation of TED
  - Increasing Clinical Activity Score (CAS) by ≥2 points, confirmed on repeat examination (within 14 days).
- Potential Serious Adverse Event attributable to Bimatoprost.
  - Iris cysts
  - Cystoid macular oedema
  - Anterior uveitis
  - Reactivation of herpes simplex virus infection

3.27.2 Treatment of Withdrawn Subjects

The patient, Consultant Ophthalmologist and Consultant Endocrinologist responsible for their care, will be informed of their treatment allocation on withdrawal from the trial.

Withdrawn subjects will be followed up as per standard care.

3.27.3 Follow-up of Withdrawn Subjects

Care for withdrawn subjects will return to their referring ophthalmologist, however they will also be invited to attend assessment visits at 3, 5, 8 and 10 months, to obtain outcome data in accordance with the planned intention-to-treat analysis.

3.27.4 Management of Data from Withdrawn Subjects

All withdrawn patients will be invited to produce outcome data for the purposes of the planned intention-to-treat analysis.

11 TRIAL TREATMENTS

3.28 Trial Interventions

Bimatoprost will be administered to affected eyes only. If both eyes are affected, both will be treated hence no comparison can be made between the 2 eyes. If one eye is affected, only the affected eye will be treated. The changes in the effected eyes could only be due to treatment (either placebo or Bimatoprost) or part of disease process itself. Treating only the affected eye will be acceptable to patients as treatment may restore normality.

3.28.1 Bimatoprost 0.03%

Bimatoprost (Lumigan®) will be administered at a strength of 0.03%. This will be purchased from the manufacture (Allergan). This is the strength used in the treatment of intraocular hypertension and glaucoma. It will be administered at a dose of one drop in the eye once daily between 6:00 - 00:00 pm starting from the day of allocation. It will be self-applied to the affected eye in unilateral involvement or in case of bilateral involvement, to both eyes. Treating both eyes will help to restore towards normality. Treating only affected eye in unilateral disease will be acceptable to patients as treatment may restore symmetry.

3.28.2 Placebo

The placebo will be an artificial tear purchased from manufacturer. To enhance masking the placebo will contain artificial tears with similar preservative (Benzalkonium chloride) which will replicate any mild stinging sensation experienced with Bimatoprost. It will be administered at a dose of one drop in the eye once daily between 6:00 - 00:00 pm starting from the day of allocation. It will be self-applied as per Bimatoprost eye drops.

3.28.3 Concomitant medication

Patients will be allowed to use preservative free eye drops during the trial. This has to be applied at least 30 minutes before/after IMP application. No other eye drops will be allowed during the trial period. Patients will be asked during each visit regarding any change in their regular medication especially recent steroid exposure.

3.28.4 Order of treatments and washout period

The order of treatment is by randomisation. Patient will be treated over 3 month period followed by 2 months washout period. Subsequently patient will cross over to the opposite treatment and continue further treatment for 3 month period.

3.28.5 Responsibility for Endocrine Care

Patients will either transfer responsibility for their Endocrine care to the trial team (under the supervision of the Endocrine Chief Investigator) for the duration of their participation in the study, or if they prefer to remain under the care of their own Endocrinologist the trial team will liaise closely with them in order to ensure that the patient is rendered euthyroid and maintained euthyroid for the duration of the trial.

3.28.6 Smoking advice

All trial subjects will be advised to stop smoking. We will monitor changes in smoking habits.

12 FOLLOW UP ASSESSMENT

3.28.7 STANDARD CLINICAL ASSESSMENTS AT EACH FOLLOW-UP VISIT

The primary outcome measure for the trial is based on exophthalmometry readings of proptosis measured using a Hertel exophthalmometer, according to a standard operating procedure by the same observer (as far as possible). These will be assessed by the lead ophthalmology investigator at each follow-up visit and their measurement recorded on the trial's Clinical Report Form. Please refer to visit schedule in Appendix 2 for more details.

The key components of the follow-up visits are:

10. Ophthalmological assessments;
11. Adverse events (Refer to Section 9 and Appendix 3);
12. Any Changes in medications (including thyroid treatments);
13. Any Changes in smoking habit;
14. Weight;
15. Colour photographs of the eye in the lateral and anterior views according to standard operating procedure;
16. GO-QOL (Appendix 4) done at clinic visits;
17. EQ-5D-5L (Appendix 5) done at clinic visits;
18. Review of clinical blood tests:

Thyroid Function Tests (TSH, FT4 & FT3) at visit 1, 2 and 4. See Appendix 6 for management of abnormal thyroid blood test.

13 HEALTH ECONOMIC EVALUATION

The primary intention of the economic evaluation is to explore the cost associated with TED treatment. In theory, Bimatoprost intervention would lead to the net cost savings to NHS in comparison to surgical rehabilitation that the patient otherwise would go through. We are aware of limitation in the trial design as this trial primary intention is to evaluate efficacy of Bimatoprost in TED, not to follow up patients until they might need surgery. However it would be useful to collect the resource use and quality of life data during this trial period on a pilot basis which may lead to a larger health economic focus study in the future. It is not envisaged that the crossover design will yield data that could allow a meaningful incremental cost-effectiveness ratio (ICER) to be calculated for Bimatoprost against placebo, as the duration of effects on perceived quality of life cannot be predicted in advance.

The different methods of patient care will be evaluated from the viewpoint of the National Health Service (NHS) and patients/carers. The data will be collected using Client Service Receipt Inventory (CSRI). Please see Appendix 7 and http://www.kcl.ac.uk/iop/depts/hspr/research/cemph/tools/csri.aspx. This is a questionnaire for collecting retrospective information about study participants' use of health and social care services, accommodation and living situation, income, employment and benefits. We have modified the CSRI in line with services used by our patient population. The questionnaire will

be filled by the patient at 0, 3, 5, 8 and 10 months.

The key domains and variables of the Client Service Receipt Inventory are:

- Socio-demographics: Age, gender, marital status, ethnicity, mother tongue, years of schooling, educational level
- Usual living situation: Living situation (alone, with relatives, etc.), type of accommodation, household composition
- Employment and income: Employment status, occupational category, days of work lost, state benefits, source/level of income
- Service receipt: Hospital in-patient days, out-patient attendances (e.g. endocrine & eye attendances) and community-based service contacts (private medical, counsellor, primary care etc.)
- Medication profile: Name/type of drug, dosage level and frequency

Quality of life

Participants will be asked to complete both a generic (EQ-5D-5L) and an eye-specific (GO-QOL) questionnaire concerning their quality of life (See appendix 4 and 5). Both questionnaires will be completed at 0, 3, 5, 8 & 10 months from recruitment, i.e. at baseline, at the end of the first treatment period and two months later, and at the end of the second treatment period.

Valuation of resource use

Analysis will be performed under the guidance of health economist.

National data sets such as the Unit Costs of Health and Social Care (http://www.kent.ac.uk/PSSRU/) will be used to value primary care contacts.

Visits to Walk-in Centres and calls to NHS Direct will be valued using information in the National Evaluations (http://www.epi.bris.ac.uk/wic/pdf/WIC%20Evaluation%20Report%20-%20Final.pdf and http://www.shef.ac.uk/scharr/mcru/reports/nhsd3.pdf)

The British National Formulary (http://bnf.vhn.net/bnf) will be used to value prescribed medication.

Secondary care use will be valued using the Department of Health National Reference Costs (http://www.doh.gov.uk/nhsexec/refcosts.htm).

14 PHARMACOVIGILANCE

There is established clinical experience of both trial interventions (Bimatoprost and placebo), and it is unlikely that this trial will contribute significantly to published safety data. However, Bimatoprost has not been used in this particular group of patients before. Adverse events will be monitored, reported in the trial publications and to the Trial Sponsor, Research Ethics Committee (REC) and Medicines and Healthcare products Regulatory Agency (MHRA) if appropriate.

SAE collection will start when the first participant is recruited and end at each patient's last visit.

3.29 PROCEDURES FOR RECORDING AND REPORTING ADVERSE EVENTS

Definitions used will be those under the Medicines for Human Use (Clinical Trials) Regulations 2004 and Amended Regulations 2006 as follows.

3.29.1 Definitions

An Adverse Event (AE) is any untoward medical occurrence in a participant to whom an investigational medicinal product (IMP) has been administered, including occurrences which are not necessarily caused by or related to that product.

An Adverse Reaction (AR) is any untoward and unintended response, in a participant, to an IMP which is related to any dose administered to that participant. An Adverse Reaction is an Adverse Event with a causal relationship to the IMP.

Serious Adverse Event (SAE), Serious Adverse Reaction (SAR) or Serious Unexpected Suspected Adverse Reaction (SUSAR) is defined as an Adverse Event, Adverse Reaction or unexpected Adverse Reaction that:

- results in death;
- is life-threatening;
  The term "life-threatening" in the definition of serious refers to an event in which the participant was at risk of death at the time of the event; it does not refer to an event which hypothetically might have caused death if it were more severe;
- requires hospitalisation or prolongation of existing hospitalisation. Hospitalization is defined as an inpatient admission, regardless of the length of stay, even if the hospitalization is a precautionary measure, for continued observation. Pre-planned hospitalisation e.g. for pre-existing conditions which have not worsened or elective procedures does not constitute an adverse event;
- results in persistent or significant disability or incapacity;
- consists of a congenital anomaly or birth defect; or
- is medically significant;
  Other events that may not result in death are not life-threatening, or do not require hospitalisation may be considered as a serious adverse event when, based upon appropriate medical judgement, the event may jeopardise the participant and may require medical or surgical intervention to prevent one of the outcomes listed above.

Pregnancy in either a participant or the partner of a participant taking trial medication should

be reported as a SAE.

A Suspected Unexpected Serious Adverse Reaction (SUSAR) is an adverse reaction that is both serious and unexpected (i.e. the nature and severity of which is not consistent with the information about the IMP in question set out in the Summary of Products Characteristics (SPC)).

Expected Adverse Reactions to the trial treatment(s) are detailed below:
a) Commonly occurring cosmetic effects (approximate incidence)

- Conjunctival redness (0.5%);
- Lengthening of eyelashes – (average elongation 0.7mm);
- Darkening of eye lashes (45-57%);
- Peri-ocular skin pigmentation (3%);
- Darkening of the iris (10.1%).

b) Rare but potentially serious side effects (limited information available)

- Iris cysts;
- Cystoid macular oedema;
- Anterior uveitis;
- Reactivation of herpes simplex virus infection.

The above list should not be relied upon. Always refer to the current Summary of Product Characteristics (SPC) when assessing the expectedness of an Adverse Reaction.

3.29.2 Prevention of Adverse Events
The trial exclusion criteria prevent patients especially at risk of developing adverse events from participating in the trial. In particular, patient with risk factors for cystoid macular oedema, iritis or uveitis is excluded. Also patient with corneal Herpes Simplex infection history is excluded to prevent potential reactivation of herpes simplex virus infection.

3.29.3 Eliciting Adverse Events
All trial subjects will have an enquiry about co-morbidities, medications and new or unexpected symptoms at each follow-up visit, as well as an ophthalmic and general examination.

3.29.4 Principal Investigator/Trial Centre Responsibilities
The lead ophthalmologist will be required to report all AEs/SAEs which occur during the Trial on an Adverse Event Form and keep a record in the case report form (CRF). AEs will be collected from the time the participant signs the trial consent form until one month after the last trial visit. The AEs will be reported monthly to TMG. TMG will report at least every 6 monthly to TSC and if there is any concern a DSMB will be convened.

3.29.5 Assessing AEs
The lead ophthalmologist should assess the AE for seriousness and causality. The lead ophthalmologist should exercise medical judgement in deciding whether an Adverse Event/Reaction is serious in other situations. All SAEs should be reported to the HCTU by the lead ophthalmologist immediately (within 24hrs) of becoming aware of the event. The lead ophthalmologist will be asked to grade all AEs in relationship to the study treatment according to their clinical judgement as follows:

Causality:
• Not related – temporal relationship of the onset of the event, relative to administration of the product, is not reasonable or another cause can by itself explain the occurrence of the

event.

- Unlikely to be related – temporal relationship of the onset of the event, relative to administration of the product, is likely to have another cause which can by itself explain the occurrence of the event.
- Possibly related – temporal relationship of the onset of the event, relative to administration of the product, is reasonable but the event could have been due to another, equally likely cause.
- Probably related – temporal relationship of the onset of the event, relative to administration of the product, is reasonable and the event is more likely explained by the product than any other cause.
- Very likely – temporal relationship of the onset of the event, relative to administration of the product, is reasonable and there is no other cause to explain the event, or a re-challenge is positive

Expectedness

No events other than those listed in section 9.1.1 and appendix 3 (SPC) are expected.

3.29.6 Reporting procedures

All SAEs must be reported immediately (within 24 hrs of being made aware of the event) by the lead ophthalmologist to HCTU.

Initial reports should be submitted as soon as the following minimum criteria are met:

- A suspected SAE is identified;
- An identifiable participant (e.g. trial participant code number);
- An AE assessed as serious and unexpected, and for which there is a reasonable suspected causal relationship;
- An identifiable reporting source (e.g. Clinical research fellow).

Following the Initial Report, all SAEs should be followed to resolution. Following the initial report the lead ophthalmologist may be requested to provide further information. The participant should only be identified by trial number, date of birth and initials. The participant's name should not be used on any correspondence. The lead ophthalmologist is also responsible for reporting AEs to their NHS Trust as per their local NHS Trust procedures.

3.29.7 Sponsor and Chief Investigator Responsibilities

The Sponsor (or delegate – HCTU) is responsible for ensuring all SAEs, SARs and SUSARs (except those specified in this protocol as not requiring reporting) will be reported in the appropriate timescale to the MHRA and REC.

HCTU is responsible for ensuring all SUSARs (except those specified in this protocol as not requiring reporting) will be reported in the appropriate timescale to the MHRA and REC.

Once an SAE is received by HCTU, the SAE will be sent to the CI (or appropriate delegate) for clinical review (assessment of causality and expectedness). Fatal and life threatening SAEs should be assessed by the CI within 24 hours of receipt. Non fatal or non life-threatening SAEs should be assessed by the CI within 4 days of receipt.

Only SUSARs should be reported immediately to MHRA and REC. HCTU will report according to the following timelines:

Fatal and life threatening SUSARs not later than 7 days after receipt at HCTU; Non fatal or non life-threatening SUSARs not later than 15 days after receipt at HCTU. Follow up information should be reported within 8 days of receipt of the follow up information. A copy of the SUSAR report should be provided to RIES.

In addition to reporting to the relevant REC and the MHRA, SUSARs will also be reported within 3 working days to all members of the TSC. The CI shall ensure that all co-investigators receive regular safety updates of SUSARs that occur in relation to the IMP in the trial.

15 PLANNED ANALYSES

3.30 INTERIM

No interim analysis is planned. See sections 4.7.1.

3.31 FINAL

Data cleaning and preparation process will be carried out prior to analysis. The process will involve monitoring the following:

1. Presence of duplicates in the file;
2. Presence non-existent patients;
3. Compulsory completion of a variable;
4. Out-of-range values;
5. Logical inconsistencies between variables;
6. Missing data investigated and data imputation considered where missing is not considered to be at random;
7. Data set preparation for multilevel modelling to include both eyes and both phases where appropriate;
8. Normality of outcome variables investigated.

Data analysis will proceed according to CONSORT guidelines for randomised controlled trials. This will be conducted under guidance of senior statistician. The first stage of the analysis will be to use descriptive statistics to describe the group of individuals recruited to the trial in relation to those eligible, and to investigate comparability of the trial arms at baseline.

A tabulation of demographic and clinical variables will be carried out to identify any chance imbalances at baseline between the two treatment groups

The mean change in proptosis measurement in the treated phase and control phase will be compared with a paired t-test in the first instance. In order to protect the independence of the data points, this will be carried out using the mean improvement of the two eyes where both have been treated. In addition to this proptosis both eyes for patients with both eyes treated and the one eye for patients with only one treated eye will be analysed using a multilevel model in STATA which will also give us the ability to use one data point for those patients who were unwilling or unable to proceed to the second phase of the protocol. Demographic and clinical variables (including baseline, the order of treatment and carryover effects) may be used in this multilevel model regression model to reduce the unexplained variance and obtain better estimates of effect size with tighter confidence intervals. The results will be expressed as millimetres effect from the treatment arm controlling for the placebo effect with 95% confidence intervals and p-values. Phase effects and carry over effects can be reported in this way also, but the study has not been designed to be powered to detect these effects as statistically significant unless they are as large as the treatment effect. The frequency of adverse effects will be compared in the treatment and control phases by observation of data tables and where appropriate use of the McNemar X2 for paired samples.

16 DATA HANDLING AND RECORD KEEPING

Source documents produced for this trial will be kept in the patient's hospital records and source data will be transcribed into trial-specific Clinical Record Forms (CRFs) at the end of each patient visit. These CRFs will be coded with the study number and will not include patients' names and addresses.

The paper CRFs will be maintained in the trial office at the Diabetes & Thyroid Research Group, C2 Link Corridor, University Hospital of Wales. Selected anonymised data will also be stored in electronic format. Paper records will be kept in a locked cabinet in secure premises within the Department at all times when the record is not in use for a study visit. Access to the records will be restricted to researchers working on the study, Sponsor representatives and representatives of regulatory authorities required to audit the conduct of the research study.

Photographs will be held electronically on University Health Board system.

Relevant data will be transferred (with double data entry/data checking) from the paper record in the trial office to an electronic database which will be stored and regularly backed up on a Cardiff University server. Identifiable data including the link between the patients' names and the study number will be stored separately from other data. All files will be password protected. Electronic data containing personalised information will be saved on Cardiff University computers only in password protected files and backed up regularly to hard copy on secure remote Cardiff University servers. Participant data will be anonymised by the use of study numbers. A copy of the study number code identifying subjects will be kept in a secure cabinet at local study sites accessible to the investigators at all times. Analysis will be conducted by the study team. Analysis will only be conducted on anonymised data.

The Chief Investigator, Professor Colin Dayan will act as custodian of the data, however for practical purposes this role will be delegated to HCTU. Personal data will be stored for a minimum of 15 years. Access will be controlled by Professor Dayan who will continue to act as custodian for all data held by the co-sponsors and will permit trial related monitoring, audits, REC review, and regulatory inspections (where appropriate) by providing direct access to source data and all other documents (i.e. patients' case sheets, blood test reports, etc).

17 FINANCIAL AND INSURANCE DETAILS

Support for this trial has been granted by the following charitable bodies:

- **NISCHR Research for Patient and Public Benefit Wales**
  For administrative and clinical research support; Investigational Medicinal Product (IMP) (Bimatoprost and placebo) and research related costs.

- **Cardiff and Vale LHB (University Hospital of Wales)**
  For NHS treatment excess cost and grant award administration; pharmacy and media supports.

Cardiff University has arranged clinical research insurance to cover the legal liability of the University for negligent harm. In addition the study doctors hold substantive or honorary NHS contracts, giving them the protection of the NHS clinical negligence arrangements.

18 PATIENT INVOLVEMENT

Our research group has a long tradition of involvement with the thyroid eye disease charitable trust (TEDct). This is a registered charity which provides information and support to individuals affected by thyroid eye disease. TEDct is associated with the British Thyroid Foundation and the British Thyroid Association and produces health information leaflets to promote awareness and understanding of the disease. The Chief Investigator has been working with TEDct for over 10 years, is Chairman of Trustees and Honorary Consultant Advisor to TEDct.

The current therapeutic options for patients with thyroid eye disease are unsatisfactory and the need for novel therapies which improve disfigurement and reduce the risk of sight loss has been a fundamental concern for most patients and clinicians. The current research question has thus evolved from discussions and feedback at past TEDct forum meetings as well as extensive patient surveys.

A UK nationwide survey of patients with thyroid eye disease revealed low satisfaction levels with existing therapies [1]. A "Thyroid Eye Disease Day", a workshop of patients and clinicians with the goal of advancing thyroid eye disease research, was held in December 2012, under the auspices of the NIHR Moorfields Biomedical Research Centre. The Chief investigator was present at the meeting and a consultation on the current research was held and received favourable feedback as to its relevance from the patient perspective.

We have been fortunate to have two patients who have very keen to be involved in the development of the study protocol and trial set up. Involving patients with TED from the outset strengthens the application by showing that the research is patient-centred and that patient participation has been welcomed, encouraged and facilitated. Our patient representatives have and will be involved in:

- Information leaflets design (participant information leaflets, patient invitation letter, consent form and GP letter);
- Protocol development;
- Trial management meetings;
- Trouble shooting to support recruitment and retention of participants;
- Reporting the final results to the trial participants;
- Preparing information for web site inclusion.

The study will be registered on the NIHR INVOLVE and NISCHR CRC Involving People (Cynnwys Pobl) databases once ethical approval is granted. These are national advisory groups that support greater public involvement in NHS, public health and social care research. INVOLVE provides a public information pack, newsletters and public networking to facilitate pubic involvement. Locally, Involving People provides excellent training and support for public involvement via local conferences, newsletters and public network.

Patient involvement, involvement of TEDct, and INVOLVE/Involving people will also facilitate dissemination of the study findings to as wide an audience as possible and will help set the agenda for future research in this field. Training and support for our patient representatives will be flexible and tailored to their individual needs. It will include training on the study background, methods and outcomes and where indicated IT training will be provided. Patients will be reimbursed in line with NISCHR's AcoRD guidance (Attributing the costs of Health and Social Care Research & Development).

19 PUBLICATION AND DESSIMINATION POLICY

It is intended that the results of the study will be reported and disseminated at local and international conferences and in peer-reviewed scientific journals. The result will be published further in eyes charity newsletter (e.g. TEDct). Written feedback will also be made available to the study participants.

20 TRIAL MANAGEMENT

1. Trial Steering Committee [TSC]

An independent Trial steering committee (TSC) will be convened (See membership section 1.4.1). The TSC will meet in person or by teleconference at a minimum of 6 monthly intervals during the trial. The TSC principal responsibilities will be to:

1. Review the protocol and comment on any major concerns in the trial design that they feel would prevent it addressing the primary objectives.
2. Review progress reports on the trial and provide advice if problems arise.
3. Comment on protocol amendments.
4. Ensure that any new information on the trial interventions which becomes available after the start of the trial is properly considered.
5. Protect the interests of patients should safety issues arise.
6. Ensure the integrity of the data as far as they are able.

2. Trial Management Group[TMG]

The project will be run by a Trial Management Group comprising trial coordinator, clinical research fellow, statistician, lead ophthalmology investigator and chief investigator and patient representatives. The TMG will oversee the day to day trial management and will meet in person or by teleconference at a minimum 2 monthly for the duration of the study. The TMG will overview and provide guidance on all aspects of regulatory approval, set-up, recruitment, protocol deviations, adverse events, data management, data analysis and dissemination. The TMG will report 6 monthly to the TSC and to the study sponsor as required.

21 ACKNOWLEDGEMENTS

The investigators wish to thank Chris Foy (Heath Economist), Mark Kelly and Kirsten McEwan (SEWTU Medical Statisticians) for initial advice on the trial design.

22 REFERENCES

1. Estcourt S, Hickey J, Perros P, Dayan C, Vaidya B. The patient experience of services for thyroid eye disease in the United Kingdom: results of a nationwide survey. Eur J Endocrinol. 2009; 161 (3):483-7.
2. Brent GA. Clinical practice. Graves' disease. N Engl J Med. 2008; 358 (24):2594-605.
3. Weetman AP. Graves' disease. N Engl J Med. 2000; 343 (17):1236-48.
4. Lazarus JH. Epidemiology of Graves' orbitopathy (GO) and relationship with thyroid disease. Best Pract Res Clin Endocrinol Metab. 2012; 26 (3):273-9.
5. Bartley GB. The epidemiologic characteristics and clinical course of ophthalmopathy associated with autoimmune thyroid disease in Olmsted County, Minnesota. Trans Am Ophthalmol Soc. 1994; 92:477-588.
6. Wiersinga WM. Quality of life in Graves' ophthalmopathy. Best Pract Res Clin Endocrinol Metab. 2012; 26 (3):359-70.
7. Coulter I, Frewin S, Krassas GE, Perros P. Psychological implications of Graves' orbitopathy. Eur J Endocrinol. 2007; 157 (2):127-31.
8. Bartalena L, Tanda ML. Clinical practice. Graves' ophthalmopathy. N Engl J Med. 2009; 360 (10):994-1001.
9. Marcocci C, Marino M. Treatment of mild, moderate-to-severe and very severe Graves' orbitopathy. Best Pract Res Clin Endocrinol Metab. 2012; 26 (3):325-37.
10. Eckstein AK, Johnson KT, Thanos M, Esser J, Ludgate M. Current insights into the pathogenesis of Graves' orbitopathy. Horm Metab Res. 2009; 41 (6):456-64.
11. Zhang L, Bowen T, Grennan-Jones F, Paddon C, Giles P, Webber J, et al. Thyrotropin receptor activation increases hyaluronan production in preadipocyte fibroblasts: contributory role in hyaluronan accumulation in thyroid dysfunction. J Biol Chem. 2009; 284 (39):26447-55.
12. Zhang L, Baker G, Janus D, Paddon CA, Fuhrer D, Ludgate M. Biological effects of thyrotropin receptor activation on human orbital preadipocytes. Invest Ophthalmol Vis Sci. 2006; 47 (12):5197-203.
13. Peplinski LS, Albiani Smith K. Deepening of lid sulcus from topical bimatoprost therapy. Optom Vis Sci. 2004; 81 (8):574-7.
14. Filippopoulos T, Paula JS, Torun N, Hatton MP, Pasquale LR, Grosskreutz CL. Periorbital changes associated with topical Bimatoprost. Ophthal Plast Reconstr Surg. 2008; 24 (4):302-7.
15. Yam JC, Yuen NS, Chan CW. Bilateral deepening of upper lid sulcus from topical Bimatoprost therapy. J Ocul Pharmacol Ther. 2009; 25 (5):471-2.
16. Serrero G, Lepak NM, Goodrich SP. Prostaglandin F2 alpha inhibits the differentiation of adipocyte precursors in primary culture. Biochem Biophys Res Commun. 1992; 183 (2):438-42.
17. Draman MS, Grennan-Jones F, Zhang L, Kyaw Tun T, McDermott JH, Sreenan S, et al. .Bimatoprost (PGF2α) Effects on Adipocyte Biology? Relevant to Graves' Orbitopathy. European Thyroid Journal 2012. 2012; 1 (1):195.
18. Draman MS, Grennan-Jones F, Zhang L, Taylor P, Kyaw Tun T, McDermott J, et al. Prostaglandin F2alpha (PGF2alpha) Effects on Adipocyte Biology Relevant to Graves' Orbitopathy. Thyroid : official journal of the American Thyroid Association. 2013.
19. Mourits MP, Prummel MF, Wiersinga WM, Koornneef L. Clinical activity score as a guide in the management of patients with Graves' ophthalmopathy. Clin Endocrinol (Oxf). 1997; 47 (1):9-14.
20. Haggerty H, Helen|Richardson,S,Sarah|Mitchell,KW,Keith W|Dickinson,AJ,A Jane. A modified method for measuring uniocular fields of fixation: reliability in healthy subjects and in

patients with Graves orbitopathy. Archives of ophthalmology. 2005; 123 (3):356-62.

23 SIGNATURE PAGE

1st July 2014

Chief Investigator

Date:

Professor Colin Dayan

24 Appendices

Appendix 1

Clinical Activity Score in TED
The Clinical Activity Score (CAS) [19] is calculated by assessing the presence or absence of each of the following clinical features using the trial's Standard Operating Procedures.

1. **Pain**
   - Pain on eye movement in the last 4 weeks
   - Painful, oppressive feeling on or behind globe in the last 4 weeks

2. **Redness**
   - Conjunctival redness
   - Eyelid redness

3. **Swelling**
   - Chemosis
   - Swollen caruncle
   - Eyelid oedema
   - Increasing proptosis of > 2mm

4. **Impaired Function**
   - Decreasing visual acuity of > 1 snellen line
   - Decreasing eye movement of ≥ 8^{o} [20]

Each feature = one point. The maximum score is 10 at each visit.

Appendix 2

Bima study activity chart						
	Baseline	**Randomisation**	**Follow-up**			
Visit Number	**-1**	**1**	**2**	**3**	**4**	**5**
Study month	Week -2	Month 0	3	5	8	10
Activity						
Ophthalmologist assessment	X		X	X	X	X
Blood test	X		X		X	
Pregnancy test	X	X	X	X	X	X
Weight		X	X	X	X	X
Height		X				
Photograph		X	X	X	X	X
Adverse Event Assessment			X	X	X	X
Send standard GP letter		X				
Sign Informed consent	X					
Complete GO-QOL & EQ5D-5L Questionnaire		X	X	X	X	X
Complete CSRI questionnaire		X	X	X	X	X
Start Treatment		X		X		
Stop Treatment			X		X	
Fill minimisation form and online randomisation service	X					
Transcribe CRF	X	X	X	X	X	X
If eligible to proceed, issue trial IMP prescription (Bimatoprost or placebo)	X			X		
Patient to return used eye drop bottles to pharmacy			X		X	
If eligible to proceed, issue trial diary		X				
Ask coordinator to chase blood results for this visit	X		X		X	
Masking Questionnaire (Dr and Patient)			X		X	
Trial Completion Summary Letter to inform post-exit clinic consult (cc GP +/- referring endocrinologist and ophthalmologist)						X

Appendix 3

ANNEX I

SUMMARY OF PRODUCT CHARACTERISTICS

1. NAME OF THE MEDICINAL PRODUCT

LUMIGAN 0.3 mg/ml eye drops, solution

2. QUALITATIVE AND QUANTITATIVE COMPOSITION

One ml of solution contains 0.3 mg Bimatoprost.

Excipient:
One ml of solution contains 0.05 mg benzalkonium chloride.

For the full list of excipients, see section 6.1.

3. PHARMACEUTICAL FORM

Eye drops, solution.

Colourless solution.

4. CLINICAL PARTICULARS

4.1 Therapeutic indications

Reduction of elevated intraocular pressure in chronic open-angle glaucoma and ocular hypertension in adults (as monotherapy or as adjunctive therapy to beta-blockers).

4.2 Posology and method of administration

Posology

The recommended dose is one drop in the affected eye(s) once daily, administered in the evening. The dose should not exceed once daily as more frequent administration may lessen the intraocular pressure lowering effect.

Paediatric population
The safety and efficacy of LUMIGAN in children aged 0 to 18 years has not yet been established.

Use in hepatic and renal impairment
LUMIGAN has not been studied in patients with renal or moderate to severe hepatic impairment and should therefore be used with caution in such patients. In patients with a history of mild liver disease or abnormal alanine aminotransferase (ALT), aspartate aminotransferase (AST) and/or bilirubin at baseline, bimatoprost 0.3 mg/ml eye drops, solution had no adverse effect on liver function over 24 months.

Method of Administration
If more than one topical ophthalmic medicinal product is being used, each one should be administered at least 5 minutes apart.

4.3 Contraindications

Hypersensitivity to the active substance or to any of the excipients listed in section 6.1.

4.4 Special warnings and precautions for use

Ocular

Before treatment is initiated, patients should be informed of the possibility of eyelash growth, darkening of the eyelid skin and increased iris pigmentation since these have been observed during treatment with LUMIGAN. Some of these changes may be permanent, and may lead to differences in appearance between the eyes when only one eye is treated. Increased iris pigmentation is likely to be permanent. The pigmentation change is due to increased melanin content in the melanocytes rather than to an increase in the number of melanocytes. The long term effects of increased iris pigmentation are not known. Iris colour changes seen with ophthalmic administration of Bimatoprost may not be noticeable for several months to years. Typically, the brown pigmentation around the pupil spreads concentrically towards the periphery of the iris and the entire iris or parts become more brownish. Neither naevi nor freckles of the iris appears to be affected by the treatment. At 12 months, the incidence of iris pigmentation with Bimatoprost 0.3mg/ml was 1.5% (see section 4.8) and did not increase following 3 years treatment. Periorbital tissue pigmentation has been reported to be reversible in some patients.

Cystoid macular oedema has been uncommonly reported (≥1/1000 to <1/100) following treatment with Bimatoprost 0.3 mg/ml eye drops. Therefore, LUMIGAN should be used with caution in patients with known risk factors for macular oedema (e.g. aphakic patients, pseudophakic patients with a torn posterior lens capsule).

There have been rare spontaneous reports of reactivation of previous corneal infiltrates or ocular infections with Bimatoprost 0.3 mg/ml eye drops, solution. LUMIGAN should be used with caution in patients with a prior history of significant ocular viral infections (e.g. herpes simplex) or uveitis/iritis.

LUMIGAN has not been studied in patients with inflammatory ocular conditions, neovascular, inflammatory, angle-closure glaucoma, congenital glaucoma or narrow-angle glaucoma.

Skin

There is a potential for hair growth to occur in areas where LUMIGAN solution comes repeatedly in contact with the skin surface. Thus, it is important to apply LUMIGAN as instructed and avoid it running onto the cheek or other skin areas.

Respiratory

LUMIGAN has not been studied in patients with compromised respiratory function and should therefore be used with caution in such patients. In clinical studies, in those patients with a history of a compromised respiratory function, no significant untoward respiratory effects have been seen.

Cardiovascular

LUMIGAN has not been studied in patients with heart block more severe than first degree or uncontrolled congestive heart failure. There have been a limited number of spontaneous reports of bradycardia or hypotension with Bimatoprost 0.3 mg/ml eye drops, solution. LUMIGAN should be used with caution in patients predisposed to low heart rate or low blood pressure

Other Information

In studies of Bimatoprost 0.3 mg/ml in patients with glaucoma or ocular hypertension, it has been shown that the more frequent exposure of the eye to more than one dose of Bimatoprost daily may decrease the IOP-lowering effect (see section 4.5). Patients using

LUMIGAN with other prostanglandim analogues should be monitored for changes to their intraocular pressure.

Bimatoprost 0.3 mg/ml eye drops, solution contains the preservative benzalkonium chloride, which may be absorbed by soft contact lenses. Eye irritation and discolouration of the soft contact lenses may also occur because of the presence of benzalkonium chloride. Contact lenses should be removed prior to instillation and may be reinserted 15 minutes following administration. Benzalkonium chloride, which is commonly used as a preservative in ophthalmic products, has been reported to cause punctate keratopathy and/or toxic ulcerative keratopathy. Since LUMIGAN contains benzalkonium chloride, monitoring is required with frequent or prolonged use in dry eye patients or where the cornea is compromised.

There have been reports of bacterial keratitis associated with the use of multiple dose containers of topical ophthalmic products. These containers had been inadvertently contaminated by patients who, in most cases, had a concurrent ocular disease. Patients with a disruption of the ocular epithelial surface are at greater risk of developing bacterial keratitis.

The tip of the bottle should not be allowed to contact the eye, surrounding structures, fingers or any other surface in order to avoid contamination of the solution.

4.5 Interaction with other medicinal products and other forms of interaction

No interaction studies have been performed.

No interactions are anticipated in humans, since systemic concentrations of Bimatoprost are extremely low (less than 0.2 ng/ml) following ocular dosing with Bimatoprost 0.3 mg/ml eye drops, solution. Bimatoprost is biotransformed by any of multiple enzymes and pathways, and no effects on hepatic drug metabolising enzymes were observed in preclinical studies.

In clinical studies, LUMIGAN was used concomitantly with a number of different ophthalmic beta-blocking agents without evidence of interactions.

Concomitant use of LUMIGAN and antiglaucomatous agents other than topical beta-blockers has not been evaluated during adjunctive glaucoma therapy.

There is a potential for the IOP-lowering effect of prostaglandin analogues (e.g. LUMIGAN) to be reduced in patients with glaucoma or ocular hypertension when used with other prostaglandin analogues (see section 4.4).

4.6 Pregnancy and lactation

Pregnancy

There are no adequate data from the use of Bimatoprost in pregnant women. Animal studies have shown reproductive toxicity at high maternotoxic doses (see section 5.3).

LUMIGAN should not be used during pregnancy unless clearly necessary.

Breast-feeding

It is unknown whether Bimatoprost is excreted in human breast milk. Animal studies have shown excretion of Bimatoprost in breast milk. A decision must be made whether to discontinue breast-feeding or to discontinue from LUMIGAN therapy taking into account the benefit of breast feeding for the child and the benefit of therapy for the woman.

Fertility

There are no data on the effects of Bimatoprost on human fertility.

4.7 Effects on ability to drive and use machines

LUMIGAN has negligible influence on the ability to drive and use machines. As with any ocular treatment, if transient blurred vision occurs at instillation, the patient should wait until the vision clears before driving or using machines.

Undesirable effects

In clinical studies, over 1800 patients have been treated with LUMIGAN 0.3 mg/ml eye drops, solution. On combining the data from phase III monotherapy and adjunctive LUMIGAN 0.3 mg/ml eye drops, solution usage, the most frequently reported treatment-related adverse events were: growth of eyelashes in up to 45% in the first year with the incidence of new reports decreasing to 7% at 2 years and 2% at 3 years, conjunctival hyperaemia (mostly trace to mild and thought to be of a non-inflammatory nature) in up to 44% in the first year with the incidence of new reports decreasing to 13% at 2 years and 12% at 3 years and ocular pruritus in up to 14% of patients in the first year with the incidence of new reports decreasing to 3% at 2 years and 0% at 3 years. Less than 9% of patients discontinued due to any adverse event in the first year with the incidence of additional patient discontinuations being 3% at both 2 and 3 years.

The following adverse reactions were reported during clinical trials with LUMIGAN 0.3 mg/ml eye drops, solution or in the post-marketing period. Most were ocular, mild to moderate, and none was serious:

Very common (≥1/10); common (≥1/100 to <1/10); uncommon (≥1/1,000 to <1/100); rare (≥1/10,000
to <1/1,000); very rare (<1/10,000) and not known (cannot be estimated from available data) adverse reactions are presented according to System Organ Class in Table 1. Within each frequency grouping, undesirable effects are presented in order of decreasing seriousness.

System Organ class	Frequency	Adverse reaction
Nervous system disorders	common	headache
	uncommon	dizziness
Eye disorders	very common	conjunctival hyperaemia, ocular pruritus, growth of eyelashes
	common	superficial punctate keratitis, corneal erosion, ocular burning, ocular irritation, allergic conjunctivitis, blepharitis, worsening of visual acuity, asthenopia, conjunctival oedema, foreign body sensation, ocular dryness, eye pain, photophobia, tearing, eye discharge, visual disturbance/blurred vision, increased iris pigmentation, eyelash darkening.

	uncommon	retinal haemorrhage, uveitis, cystoid macular oedema, iritis, blepharospasm, eyelid retraction, periorbital erythema
	not known	enophthalmos
Vascular disorders	common	hypertension
Gastrointestinal disorders	uncommon	nausea
Skin and subcutaneous tissue disorders	common	eyelid erythema, eyelid pruritus, pigmentation of periocular skin
	uncommon	eyelid oedema, hirsutism
General disorders and administration site conditions	uncommon	asthenia
Investigations	common	liver function test abnormal

4.8 Overdose

No case of overdose has been reported, and is unlikely to occur after ocular administration.

If overdose occurs, treatment should be symptomatic and supportive. If LUMIGAN is accidentally ingested, the following information may be useful: in two-week oral rat and mouse studies, doses up to 100 mg/kg/day did not produce any toxicity. This dose expressed as mg/m^2 is at least 70-times higher than the accidental dose of one bottle of LUMIGAN 0.3 mg/ml eye drops, solution in a 10 kg child.

5. PHARMACOLOGICAL PROPERTIES

5.1 Pharmacodynamic properties

Pharmacotherapeutic group: Ophthalmologicals, prostaglandin analogues, ATC code: S01EE03.

Mechanism of action

The mechanism of action by which Bimatoprost reduces intraocular pressure in humans is by increasing aqueous humour outflow through the trabecular meshwork and enhancing uveoscleral outflow. Reduction of the intraocular pressure starts approximately 4 hours after the first administration and maximum effect is reached within approximately 8 to 12 hours. The duration of effect is maintained for at least 24 hours.

Bimatoprost is a potent ocular hypotensive agent. It is a synthetic prostamide, structurally related to

prostaglandin F2α (PGF2α), that does not act through any known prostaglandin receptors. Bimatoprost selectively mimics the effects of newly discovered biosynthesised substances called prostamides. The prostamide receptor, however, has not yet been structurally identified.

During 12 months' monotherapy treatment with LUMIGAN 0.3 mg/ml in adults, versus timolol, mean change from baseline in morning (08:00) intraocular pressure ranged from -7.9 to -8.8 mm Hg. At any visit, the mean diurnal IOP values measured over the 12-month study period differed by no more than 1.3 mmHg throughout the day and were never greater than 18.0 mmHg.

In a 6-month clinical study with LUMIGAN 0.3 mg/ml, versus latanoprost, a statistically superior reduction in morning mean IOP (ranging from -7.6 to -8.2 mmHg for bimatoprost versus –6.0 to

-7.2 mmHg for latanoprost) was observed at all visits throughout the study. Conjunctival hyperaemia, growth of eyelashes, and eye pruritus were statistically significantly higher with Bimatoprost than with latanoprost, however, the discontinuation rates due to adverse events were low with no statistically significant difference.

Compared to treatment with beta-blocker alone, adjunctive therapy with beta-blocker and LUMIGAN 0.3 mg/ml lowered mean morning (08:00) intraocular pressure by -6.5 to -8.1 mmHg.

Limited experience is available in patients with open-angle glaucoma with pseudoexfoliative and pigmentary glaucoma, and chronic angle-closure glaucoma with patent iridotomy.

No clinically relevant effects on heart rate and blood pressure have been observed in clinical trials.

Paediatric population
The safety and efficacy of LUMIGAN in children aged 0 to less than 18 years has not been established.

5.2 Pharmacokinetic properties

Absorption
Bimatoprost penetrates the human cornea and sclera well in vitro. After ocular administration in adults, the systemic exposure of Bimatoprost is very low with no accumulation over time. After once daily ocular administration of one drop of LUMIGAN 0.3 mg/ml to both eyes for two weeks, blood concentrations peaked within 10 minutes after dosing and declined to below the lower limit of detection (0.025 ng/ml) within 1.5 hours after dosing. Mean Cmax and AUC 0-24hrs values were similar on days 7 and 14 at approximately 0.08 ng/ml and 0.09 ng•hr/ml respectively, indicating that a steady Bimatoprost concentration was reached during the first week of ocular dosing.

Distribution
Bimatoprost is moderately distributed into body tissues and the systemic volume of distribution in humans at steady-state was 0.67 l/kg. In human blood, Bimatoprost resides mainly in the plasma. The plasma protein binding of Bimatoprost is approximately 88%.

Biotransformation
Bimatoprost is the major circulating species in the blood once it reaches the systemic circulation following ocular dosing. Bimatoprost then undergoes oxidation, N-deethylation and glucuronidation to form a diverse variety of metabolites.

Elimination
Bimatoprost is eliminated primarily by renal excretion, up to 67% of an intravenous dose administered to healthy adult volunteers was excreted in the urine, 25% of the dose was excreted via the faeces. The elimination half-life, determined after intravenous administration, was approximately 45 minutes; the total blood clearance was 1.5 l/hr/kg.

Characteristics in elderly patients
After twice daily dosing of LUMIGAN 0.3 mg/ml, the mean AUC0-24hr value of 0.0634 ng•hr/ml

Bimatoprost in the elderly (subjects 65 years or older) were significantly higher than 0.0218 ng•hr/ml in young healthy adults. However, this finding is not clinically relevant as systemic exposure for both elderly and young subjects remained very low from ocular dosing. There was no accumulation of Bimatoprost in the blood over time and the safety profile was similar in elderly and young patients.

5.3 Preclinical safety data
Effects in non-clinical studies were observed only at exposures considered sufficiently in excess of the maximum human exposure indicating little relevance to clinical use.

Monkeys administered ocular Bimatoprost concentrations of ≥0.3 mg/ml daily for 1 year had an increase in iris pigmentation and reversible dose-related periocular effects characterised by a prominent upper and/or lower sulcus and widening of the palpebral fissure. The increased iris pigmentation appears to be caused by increased stimulation of melanin production in melanocytes and not by an increase in melanocyte number. No functional or microscopic changes related to the periocular effects have been observed, and the mechanism of action for the periocular changes is unknown.

Bimatoprost was not mutagenic or carcinogenic in a series of in vitro and in vivo studies.

Bimatoprost did not impair fertility in rats up to doses of 0.6 mg/kg/day (at least 103 -times the intended human exposure). In embryo/foetal developmental studies abortion, but no developmental effects were seen in mice and rats at doses that were at least 860-times or 1700-times higher than the dose in humans, respectively. These doses resulted in systemic exposures of at least 33- or 97 -times higher, respectively, than the intended human exposure. In rat peri/postnatal studies, maternal toxicity caused reduced gestation time, foetal death, and decreased pup body weights at ≥0.3 mg/kg/day (at least 41-times the intended human exposure). Neurobehavioural functions of offspring were not affected.

6. PHARMACEUTICAL PARTICULARS
6.1 List of excipients
Benzalkonium chloride
Sodium chloride
Sodium phosphate dibasic heptahydrate
Citric acid monohydrate
Hydrochloric acid or sodium hydroxide (to adjust pH)
Purified water

6.2 Incompatibilities
Not applicable.

6.3 Shelf life
2 years. 4 weeks after first opening.

6.4 Special precautions for storage
This medicinal product does not require any special storage conditions.

6.5 Nature and contents of container
White opaque low density polyethylene bottles with polystyrene screw cap. Each bottle has a fill volume of 3 ml.

The following pack sizes are available: cartons containing 1 or 3 bottles of 3 ml solution. Not all pack sizes may be marketed.

6.6 Special precautions for disposal
No special requirements for disposal.

7. MARKETING AUTHORISATION HOLDER
Allergan Pharmaceuticals Ireland

Castlebar Road
Westport
Co. Mayo
Ireland

8. MARKETING AUTHORISATION NUMBER

EU/1/02/205/001-002

9. DATE OF FIRST AUTHORISATION/RENEWAL OF THE AUTHORISATION

8 March 2002 / 20 February 2007

10. DATE OF REVISION OF THE TEXT

Detailed information on this product is available on the website of the European Medicines Agency (EMEA): http://www.emea.europa.eu

Appendix 4

EUGOGO
EUropean Group of Graves' Orbitopathy

GO-QOL English version

The following 15 questions deal specifically with your thyroid eye disease.
Please focus on the past week while answering these questions.
The boxes correspond with the answers above them. Tick the box that matches your answer. Please tick only one box for each question.

Q 1-7 During the past week, to what extent were you limited in carrying out the following activities because of your thyroid eye disease?

	Yes, seriously limited	Yes, a little limited	No, not at all limited
1. Driving [no drivers' licence ☐]	☐	☐	☐
2. Moving around in the house	☐	☐	☐
3. Walking outdoors	☐	☐	☐
4. Reading	☐	☐	☐
5. Watching TV	☐	☐	☐
6. Hobby or pastime ie.....	☐	☐	☐
	Yes, severely hindered	**Yes, a little hindered**	**No, not at all hindered**
7. During the past week, did you feel hindered from something that you wanted to do because of your thyroid eye disease?	☐	☐	☐

Q 8-15 The following questions deal with your thyroid eye disease <u>in general</u>

	Yes, very much so	Yes, a little	No, not at all
8. Do you feel that your appearance has changed because of your thyroid eye disease?	☐	☐	☐
9. Do you feel that you are stared at in the streets because of your thyroid eye disease?	☐	☐	☐

	Yes, very much so	Yes, a little	No, not at all
10. Do you feel that people react unpleasantly because of your thyroid eye disease?	☐	☐	☐
11. Do you feel that your thyroid eye disease has an influence on your self-confidence?	☐	☐	☐
12. Do you feel socially isolated because of your thyroid eye disease?	☐	☐	☐
13. Do you feel that your thyroid eye disease has an influence on making friends?	☐	☐	☐
14. Do you feel that you appear less often on photos than before you had thyroid eye disease?	☐	☐	☐
15. Do you try to mask changes in your appearance caused by your thyroid eye disease?	☐	☐	☐

Appendix 5

Health Questionnaire

English version for the UK

Under each heading, please tick the ONE box that best describes your health TODAY

MOBILITY

I have no problems in walking about ❑
I have slight problems in walking about ❑
I have moderate problems in walking about ❑
I have severe problems in walking about ❑
I am unable to walk about ❑

SELF-CARE

I have no problems washing or dressing myself ❑
I have slight problems washing or dressing myself ❑
I have moderate problems washing or dressing myself ❑
I have severe problems washing or dressing myself ❑
I am unable to wash or dress myself ❑

USUAL ACTIVITIES *(e.g. work, study, housework, family or leisure activities)*

I have no problems doing my usual activities ❑
I have slight problems doing my usual activities ❑
I have moderate problems doing my usual activities ❑
I have severe problems doing my usual activities ❑
I am unable to do my usual activities ❑

PAIN / DISCOMFORT

I have no pain or discomfort ❑
I have slight pain or discomfort ❑
I have moderate pain or discomfort ❑
I have severe pain or discomfort ❑
I have extreme pain or discomfort ❑

ANXIETY / DEPRESSION

I am not anxious or depressed ❑
I am slightly anxious or depressed ❑
I am moderately anxious or depressed ❑
I am severely anxious or depressed ❑
I am extremely anxious or depressed ❑

- We would like to know how good or bad your health is TODAY.
- This scale is numbered from 0 to 100.
- 100 means the best health you can imagine.
- 0 means the worst health you can imagine.
- Mark an X on the scale to indicate how your health is TODAY.
- Now, please write the number you marked on the scale in the box below.

YOUR HEALTH TODAY =

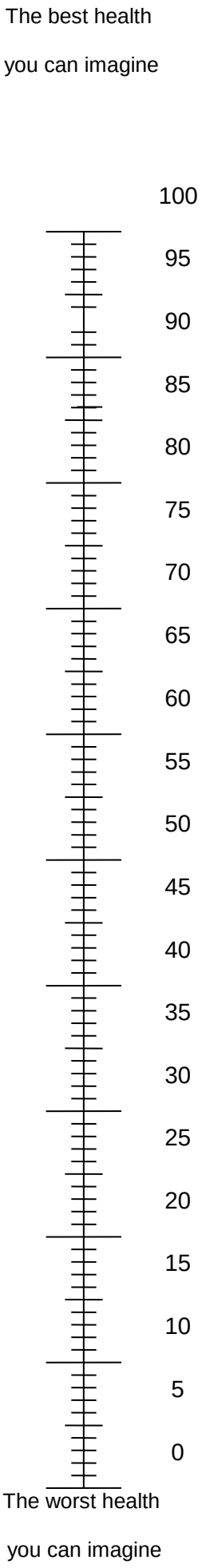

Appendix 6 Endocrine Management

Hyperthyroid patients will be treated with Carbimazole 40mg daily until euthyroid and then transferred to block-replace treatment (Carbimazole 40mg and Thyroxine 100µg daily) prior to study entry if recruitment time allowing.
Hypothyroid patients will be treated with Thyroxine, and the dose adjusted to normalise TSH levels. Previously controlled hyperthyroid patients (treated in the last 1 year) will remain on current treatment. If unstable, patient will be placed on block-replace treatment. Previously hypothyroid patients will have their dose adjusted (if required) according to their TSH levels. Euthyroid patients (5% of patients with TED have normal thyroid hormone levels) will not require any treatment for thyroid disease, but their Thyroid Function Tests (TSH, FT3, FT4) will be monitored at 3 month intervals and treated (as above) if changes develop.

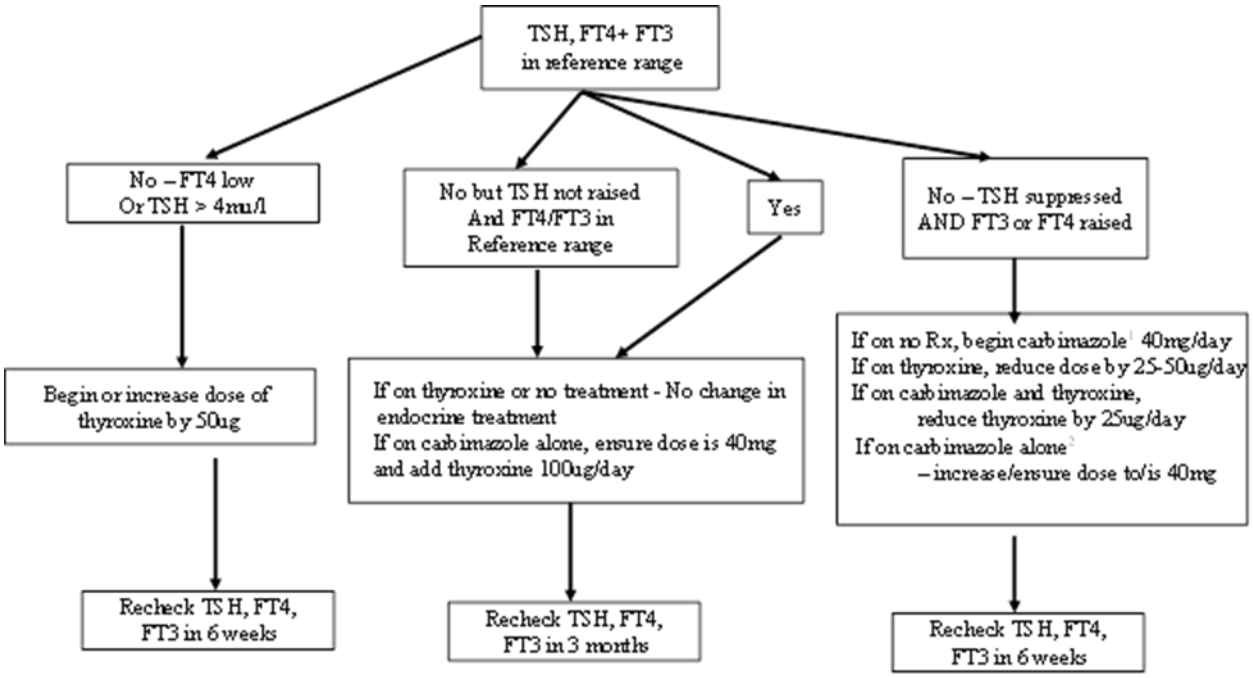

[1] If intolerant of carbimazole or on PTU, discuss with trial endocrinologist
[2] If this has already been done once, and patient remains thyrotoxic, discuss with trial endocrinologist
NB IF ON CARBIMAZOLE AND PT DEVELOPS SORES IN MOUTH WITHOLD MEDICATION + CHECK WCC within 24 hours – IF NEUTS< 1.0 discuss with trial endocrinologist within 24 hours

Appendix 7

University Hospital of Wales

Bima Study

Study Number ☐☐☐☐

Date ☐☐/☐☐/☐☐

Assessment 0 3 5 8 10

Firstly, please tell us about the health care you have received for your Thyroid Eye Disease

1) <u>In the last 2 months</u>, have you been to hospital <u>because of your thyroid or thyroid eye disease</u>?

Please tick 'yes' or 'no' for each line. If you answer 'yes' to any of them, please tell us how many times you used the service.

	No	Yes		
Had a hospital outpatient appointment	☐	☐	Total number of appointment	….…..….…....
Been to accident and emergency (casualty)	☐	☐	Total number of visits:	.....
Stayed in hospital overnight	☐	☐	Total number of nights:	.....

2) <u>In the last 2 months,</u> have you used any of the services below <u>because of your thyroid or thyroid eye disease</u>?

Please tick 'yes' or 'no' for each line. If you answer 'yes' to any of them, please tell us how many times you used the service, how long your contact with that person lasted (on average if more than once) and when applicable tick if the service was private.

	No	Yes	Number of times	On average, how many <u>minutes</u> did you see/talk to them for?	Cost (£)
GP and practice nurse					
Saw GP at the surgery	☐	☐	.....	.....	
Phoned GP for advice	☐	☐	.....	.....	
Saw practice nurse	☐	☐	.....	.....	
Phoned practice nurse for advice	☐	☐	.....	.....	
Got a repeat prescription (without seeing doctor)	☐	☐	.....	.....	
Blood test	☐	☐	.....	.....	
Other NHS Services					
NHS direct	☐	☐	.....	…….	
Other phone call (details) ……	☐	☐	.....	.....	
Other (details) ……..	☐	☐	.....	.....	
Non-NHS Services					
Private Medical	☐	☐	.....	.....	……...
Acupuncture	☐	☐	.....	.....	……...
Counsellor	☐	☐	.....	.....	……...
Support Group	☐	☐	.....	.....	……...
Other services					

Others *(e.g. alternative therapies)* ☐ ☐ .... ……..

……..…

We would now like to know about what thyroid eye disease has cost you and others

3) **<u>In the last 2 months</u>, what medicines have you used for your thyroid & thyroid eye disease and how did you pay for them altogether? (Include homeopathic/herbal medicines)**

Name of drug	Dosage (if known)	Dosage frequency (e.g. twice daily)
1.		
2.		
3.		
4.		
5.		

4) **<u>In the last 2 months</u>, how did you pay for the above medicines (Include homeopathic/herbal medicines) altogether?**

Please tick all that apply

☐ I did not have any medicines

☐ I got free prescriptions

☐ I have to pay for my private prescription

5) **<u>In the last 2 months</u>, have you, your relatives/friends, the NHS or social services paid for any of the following <u>because of your thyroid or thyroid eye disease</u>?**

Please tick 'yes' or 'no' for each line and tell us how much it cost

	No	Yes	How much has this cost altogether in the last 2 months?	Who paid for this?
Employing extra help *(e.g. childcare or cleaning)*	☐	☐	.....	.....
Transport to get healthcare *(e.g. to go to your GP surgery or hospital)*	☐	☐	.....	.....
Glasses	☐	☐	.....	.....
Cosmetics	☐	☐	.....	.....
Sunglasses	☐	☐	.....	.....

Any other costs due to thyroid eye disease..... ☐ ☐ ....
.

5) **<u>In the last 2 months</u>, have you taken any time off work <u>because of your thyroid or thyroid eye disease</u>?**

Note: Include any time taken off because you were suffering with thyroid eye disease or using any health services such as those listed in questions 1 & 2.

Yes ☐ ***If yes:*** Please give details below
No ☐
I have not been employed in the last 2 months ☐

	No	Yes	*Please tell us <u>either</u> the number of days <u>or</u> the number of hours you took off in the last 2 months* Number of whole working days	Number of hours
Took sick leave from work	☐	☐	.....	.....
Used your paid holiday time from work	☐	☐	.....	.....
Took unpaid leave from work	☐	☐	.....	.....
Just made up the time at work	☐	☐	.....	.....
Other arrangement *(please describe below)*	☐	☐	.....	.....

.....

Have you lost any pay because of this time off work?

Yes ☐ ***If yes:*** How much <u>gross</u> income you have lost in the last 2 months £.....
No ☐

6) **<u>In the last 2 months</u>, have friends and relatives helped you with tasks at home which you couldn't do <u>because of your thyroid or thyroid eye disease</u>?**

Yes ☐ ***If yes:*** Please tick below the tasks they helped you with and for how many hours per week.
No ☐

Did anyone help you with this task?	No	Yes	Typically, how many hours per week?
Personal care *(e.g. bathing, dressing)*	☐	☐	.....
Child care	☐	☐	.....
Housework / laundry	☐	☐	.....
Providing transport/taking you out	☐	☐	.....
Preparing meals	☐	☐	.....
Gardening	☐	☐	.....

Shopping	☐	☐	.....
Looking after pets	☐	☐	.....
Generally providing support	☐	☐	.....
Other *(Please describe below)*	☐	☐	.....

.....

7) **<u>In the last 2 months</u>, have friends and relatives stayed off work to help you because of your thyroid eye disease?**

Yes ☐ ***If yes:*** How many days did they take off work in the last 2 months? …….

No ☐

Now please tell us something about yourself

8) Which of the following best describes your <u>current</u> situation?

Please read the whole list first and then write '1' in the box that applies. If other categories apply, write '2' , '3' etc. to indicate the order that best describes your situation.

Working full time (30 hours or more per week) ☐
Working part time (less than 30 hours per week) ☐
Unemployed and looking for work ☐
Volunteer ☐
Job training/apprentice ☐
Student ☐
At home and not looking for work ☐
(e.g. looking after home and/or family)
Unable to work ☐ What is the reason for this?

Thyroid eye ☐ *Other illness* ☐ *Other reason* ☐

Made redundant/took early retirement ☐ What is the reason for this?

Thyroid eye ☐ *Other illness* ☐ *Other reason* ☐

Retired ☐
Other ☐ *Please describe* .....

9) Do you receive any state benefits?

Yes ☐ ***If yes:*** Please tick below which benefits you get and tell us how much you get altogether
No ☐

☐ Income support ☐ Invalidity allowance
☐ Jobseeker's allowance ☐ Disability living allowance

☐ Housing benefit ☐ Incapacity benefit
☐ Attendance allowance
☐ Others *(please describe)*
.....

How much do you receive altogether in benefits each week?
£.....

10) What is the total income of your <u>household per week from all sources before taxes and deductions</u>?

(Exclude housing benefit and council tax rebate)

Note: a household is either one person living alone, or a group of people (who may or may not be related) living, or staying temporarily, at the same address, with common housekeeping.

Please tick one

☐ £0 - £99	(£0 - £5199 per year)	☐ £350 - £449	(£18,200 - 23,399 per year)
☐ £100 - £149	(£5,200 - £7,799 per year)	☐ £450 - £599	(£23,400 - £31,199 per year)
☐ £150 - £249	(£7,800 - £12,999 per year)	☐ £600 - £749	(£31,200 - £38,999 per year)
☐ £250 - £349	(£13,000 - £18,199 per year)	☐ £750 or more	(£39,000 or more per year)

11) What kind of accommodation do you live in at the moment?

Please tick one

☐ Domestic housing (e.g. house, flat)
☐ Residential home
☐ Sheltered housing
☐ Nursing home

12) If you live in domestic housing, how many people are there in your household?

Number of adults (including yourself) ……..

Number of children under the age of 16 ……..

13) Which ethnic group do you consider yourself to belong to?

Please tick one

☐ White
☐ Indian
☐ Chinese
☐ Pakistani
☐ Black African
☐ Bangladeshi
☐ Black Caribbean
☐ None of these
☐ Black other

Thank you for completing this questionnaire

Appendix 8

Patient Diary

BIMA Study	Subject Diary
Screening No. / Study ID	Subject Initials

Investigator: Prof Dayan/Mr Morris/Mrs Lane Eye Unit Secretary: 029 20742083

Trial Doctor: Dr Shazli Draman: Tel: 029 20 748481 Mob: 07446624212

Julie Pell: Tel: 029 744370

Trial Coordinator: _____

Date of next scheduled visit: _____ Time of visit: _____

Study Reminders

1 Please bring this study diary with you to all clinic visits or have it to hand in case you need to call your study team

2 **Please notify your study doctor or nurse IMMEDIATELY if you are admitted to hospital for any reason**

BIMA Study	Subject Diary

Instructions on how to complete your diary

1 Please apply 1 drop of the eye drops into one or both eyes as instructed by your doctor daily anytime between 06:00 pm to 00:00 midnight.

2 Record the time you have administered the eye drops in provided box.

3 Please tick the appropriate box for the eye you have applied the eye drops.

4 If you notice any side effects please fill the Side Effect log

5 Record any illness or new medication used in the Illness and Medication log

Date	Time	Right Eye	Left Eye	Other	Date	Time	Right Eye	Left Eye	Other
01.01.2014 example	10:00 pm	√							

BIMA Study	Subject Diary-Side Effects

Side Effects - Instructions

1 In this section, please record any side effects you are experiencing from the trial medication

EXAMPLE

Side effect	Start Date	Stop Date	Side effect	Start Date	Stop Date	Comment
Example: Redness in right eye	01.01.14					

Side effect	Start Date	Stop Date	Side effect	Start Date	Stop Date	Comment

BIMA Study	Subject Diary-Illness and Medication Log

Illness and Medication Log - Instructions

1 In this section, new medication other than your prescribed eye drops should be recorded

2 Please record any new illnesses and medications (or medication changes) since your last study visit (include any vitamins and herbal remedies). Please bring medication packaging for doses if you are unsure.

3 Please record the date the new illness and medication STARTED and/or the date of medication (dose) change.

4 Please record the date the illness/ medication STOPPED and/or the stop date of medication (dose) change

5 If you are still taking the same medication(s) without any dose change at the time of your next study visit, record a dash (--) in the STOP DATE column (see example below)

EXAMPLE:

Illness	Start Date	Stop Date	Medication Name	Start Date	Stop Date	Total Daily Dose (Change)
headcold	15.7.11	20.7.11	paracetamol	15.7.11	18.7.11	4gms
headcold	15.7.11	21.7.11	paracetamol	19.7.11	21.7.11	2gms
ankle sprain	23.7.11	_ _ _	Ibuprofen	23.7.11	_ _ _	600mgs

Illness	Start Date	Stop Date	Medication Name	Start Date	Stop Date	Total Daily Dose (Change)

8.4.2 Patient information sheet (summary)

GIG CYMRU NHS WALES
Bwrdd Iechyd Prifysgol Caerdydd a'r Fro
Cardiff and Vale University Health Board

Ysbyty Athrofaol Cymru

University Hospital of Wales

Eich cyf/Your ref:
Ein cyf/Our ref:
Rhwydwaith Ffôn Iechyd Cymru/
Welsh Health Telephone Network:

Llinell uniongyrchol/Direct Line:

Parc y Mynydd Bychan
Caerdydd CF14 4XW
Ffôn 029 2074 7747
Ffacs 029 20743838
Minicom 029 2074 3632

Heath Park
Cardiff CF14 4XW
Phone 029 2074 7747
Fax 029 2074 3838
Minicom 029 2074 3632

Chief Investigator:	**Professor Colin Dayan**
Address:	Thyroid Research Group, Cardiff University School of Medicine, University Hospital of Wales, Heath Park, Cardiff CF14 4XW
Telephone:	029 20 742182 / Clinical Trials Office: 029 20 744370
Fax:	029 20744671
Email:	DayanCM@cardiff.ac.uk
Researchers:	**Mr Dan Morris / Mrs Carol Lane**
Telephone:	029 20 747747 (secretary extension: 2083)

SUMMARY PATIENT INFORMATION SHEET

1. **What is the purpose of the study?**
   To establish whether Bimatoprost eye drops, which are routinely used to treat glaucoma, are effective in making the eyes less prominent in Thyroid Eye Disease (TED).

2. **Why have I been sent this information sheet?**
   Because you are currently attending, have previously attended or have been referred to the eye clinic involved in this trial for the treatment of prominent ('starey') eyes due to Thyroid Eye Disease.

3. **Do I have to take part in this study?**
   No. It is up to you to decide whether or not to take part.

4. **What will happen to me if I take part?**
   You will be given two courses of treatment each of 3 months with a two month gap in between. One course will be with once daily eye drops containing Bimatoprost and the other will be with dummy (called a placebo) eye drops.

5. **Will I be asked to give any blood samples?**
   Yes. You will be asked to give blood samples on 3 occasions, 3 months apart.

6. **Will I (or my doctor) know what treatments I am taking?**

To ensure the study is well designed, neither you nor the doctors will know which treatment you receive first or second (Bimatoprost or placebo) until all patients have completed the study.

7. How will the decision about which treatments I receive be made?
This will be selected by a computer on the basis of chance, like flipping a coin.

8. How long will I be in the study?
10 months – 2 treatment periods of 3 months and 2 rest periods of 2 months each.

9. What are the possible benefits of taking part?
If the treatment you receive is found to be better than the current standard treatment used at your Eye Hospital, you will benefit from participating in this study. Otherwise, taking part may not be of direct benefit to you. It should, however, help us to develop better care for TED patients in the future.

10. What safety assurances will I have if I take part?
If your TED gets worse at any stage you will be withdrawn from the study and given standard treatment.

11. Who is organising and funding the research?
This research has been organised by a group of doctors (Ophthalmologists and Endocrinologists) who are specialists in the treatment of Thyroid Eye Disease. It has been funded by National Institute for Social Care and Health Research (NISCHR) which is a Welsh government body.

12. What do I do if I want more information?
For more information please contact:

Mr Dan Morris and Mrs Carol Lane, Consultant Ophthalmologists, University Hospital of Wales, Heath Park, Cardiff CF14 4XW
Tel: 029 20 747747 (secretary extension: 2083)

Or

Professor Colin Dayan, Professor Clinical Diabetes and Metabolism, School of Medicine Centre for Endocrine and Diabetes Science, Cardiff University, Heath Park, Cardiff CF14 4XW
Tel: 029 20 742182 (secretary)

Or

Trials Office:
Julie Pell, Trials Coordinator: 029 21847942, pelljc@cardiff.ac.uk
Dr Draman, Study Doctor: 02920 748481, Dramanyusofms@cardiff.ac.uk

8.4.3 Patient information sheet (detailed)

GIG CYMRU NHS WALES
Bwrdd Iechyd Prifysgol Caerdydd a'r Fro
Cardiff and Vale University Health Board

Ysbyty Athrofaol Cymru
University Hospital of Wales

Parc y Mynydd Bychan
Caerdydd CF14 4XW
Ffôn 029 2074 7747
Ffacs 029 20743838
Minicom 029 2074 3632

Heath Park
Cardiff CF14 4XW
Phone 029 2074 7747
Fax 029 2074 3838
Minicom 029 2074 3632

Eich cyf/Your ref:
Ein cyf/Our ref:
Rhwydwaith Ffôn Iechyd Cymru/
Welsh Health Telephone Network:
Llinell uniongyrchol/Direct Line:

Prostaglandin F2-alpha eye drops (Bimatoprost) in thyroid eye disease: A randomised controlled double blind crossover trial
(BIMA Study)

Principal Investigator:	**Professor Colin Dayan**
Address:	Thyroid Research Group, Cardiff University School of Medicine, University Hospital of Wales, Heath Park, Cardiff CF14 4XW
Telephone:	029 20 742182 / Clinical Trials Office: 029 20 744370
Fax:	029 20744671
Email:	DayanCM@cardiff.ac.uk
Researchers:	**Mr Dan Morris/ Mrs Carol Lane**
Telephone:	029 20 747747 (secretary extension: 2083)

DETAILED PATIENT INFORMATION SHEET

Part 1

1. Invitation to take part in this research project

You have been sent this information because you are currently attending or have been referred to the eye clinic involved in this trial for the treatment of prominent ('starey') eyes due to Thyroid Eye Disease (TED). If we confirm at your outpatient visit that you still have prominent and inactive TED for at least 6 month duration prior to the visit, you will be invited to take part.

2. What is the purpose of the study?

To establish whether Bimatoprost eye drops are effective in making the eyes less ('starey') in thyroid eye disease and improving quality of life in patients with TED.

3. Do I have to take part in this study?

It is up to you to decide whether or not to take part. If you do decide to take part you will be asked to sign a consent form.

If you decide to take part you are still free to withdraw at any time and without giving a reason. If you change your mind and withdraw, this will not affect the standard of care that

you receive.

4. What are Bimatoprost eye drops and are they safe?

Bimatoprost eye drops are normally being used to treat people with glaucoma (this is a condition that increases the pressure in the eye. Bimatoprost eye drops work by increasing the amount of fluid that drains out of your eye, which reduces the pressure. We will be using the dose that is regularly prescribed for glaucoma. The expected benefit may not last after you stop the treatment. This medication has been used since 2002 with an excellent safety profile. Its role in TED has not been studied yet.

5. What other medicines could I have instead?

There is currently no other eye drop licenced for this purpose. The majority of the patients will be on some form of artificial tears.

6. What are its side-effects?

The most common side effects after using Bimatoprost eye drops are an itching sensation in the eyes and/or eye redness. This was reported in approximately 4% of patients. Bimatoprost may cause other less common side effects which typically occur on the skin close to where it is applied, or in the eyes. These include skin darkening, longer or thicker eyelashes, dryness of the eyes and redness of the eyelids. Any eyelid skin darkening or eye lashes thickening/elongation are expected to reverse after several weeks to months after stopping the eye drops. Bimatoprost use may also cause increased brown pigmentation (reported in approximately 1% of patients) of the coloured part of the eye known as iris which may be permanent. If you develop any other eye problems with your eyes you can contact your eye specialist for advice.

7. What will happen to me if I take part?

You will have 6 visits in total as part of clinical assessments in the outpatient clinic. At the start of the trial you will be given either Bimatoprost eye drops or dummy eye drops (called a placebo). You will be on 3 month course of either eye drops. You then will have 2 month break before commencing the eye drops that you have not used at the start of the trial. At all visits, apart from the first, we will take photographs of your eyes. We will ask you to consent separately for publication of any photographs. Although you have the right to withdraw consent, it would not be possible to withdraw published material.

You also will be asked to fill in a short questionnaire regarding your thyroid eye condition throughout the study period.

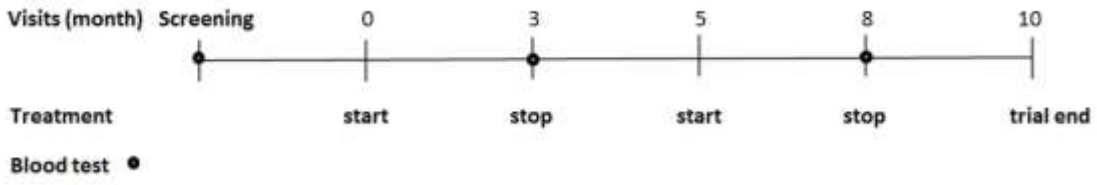

8. Will I know what treatments I am taking?

No, not until the end of the study. It is an important part in the design to ensure that neither you nor your doctor will know what treatments you receive (a procedure called ‘masking’).

This is because it is well known that if patients receive what they and / or their doctor believes is the 'best' or 'worst' treatment; it influences the way they measure the benefit of the treatment.

9. How will I be prevented from knowing what treatments I am taking?

All patients enrolled in the study will be given the eye drops to take once a day. Half will receive Bimatoprost eye drops and half will receive a dummy eye drops (placebo), which looks like the real thing but is not. Both products will be relabelled by the trial pharmacist. The relabelled product will be kept in an opaque medicine vial. You will be asked to not bring your eye drop bottles to the hospital when you come for your trial visits, but ONLY to return your eye drop bottles to the pharmacy department at the end of each 3 month course of treatment.

10. In an emergency, can I find out what treatments I am taking?

Yes. Your doctor can contact our trial pharmacist or on-call pharmacist (outside working hours) via the hospital switchboard (029 2074 7747). However, if you find out which treatments you have been given you will no longer be able to continue on treatment, but you would be invited to attend for the remaining follow up visits.

11. How will the decision about which order I receive the treatment be made?

Everyone in the study will receive both treatments (Bimatoprost and placebo). Neither you nor the study staff will have any influence over which treatments you receive first. This will be selected by a computer on the basis of chance, like flipping a coin. You have an equal chance of being allocated to either treatment first.

12. How long will I be in the study?

10 months.

13. If I take part in the study will I be asked to give any <u>extra</u> blood samples (apart from routine check), or have any other tests?

No. You will only have routine blood tests for your thyroid gland that would be carried out even if you were not taking part in the study and may normally be done by your GP. If you take part in the study, the blood tests would be carried out here in the hospital as part of your study visits or with your GP whichever is more convenient for you.

14. What will happen at each of the follow-up visits?

You will be seen by an Eye Specialist and a Clinical Research Fellow at each visit. The clinic visit will last as your routine clinic visit.

They will conduct a detailed examination of your eyes (like a routine eye clinic visit) and ask questions about your Thyroid Eye Disease, general health, and medications. In addition photographs of your eyes will be undertaken. You also will be asked to complete a short quality of life questionnaire and a health related cost questionnaire at each visit.

15. What if my Thyroid Eye Disease gets worse during this research, or if I receive Bimatoprost eye drops and do not tolerate it?

If your Thyroid Eye Disease gets worse at one of your follow-up visits you will be recalled 2 weeks later to double check the measurements. If these have not improved at the second visit you will be withdrawn from the trial (we will stop your study eye drops and treat you accordingly).

If you are concerned that your Thyroid Eye Disease is getting worse you can contact your research doctor at any time and they can arrange to review you before your planned appointment. If they confirm that your condition is deteriorating (as above) you will be withdrawn from the trial.

16. Expenses and payments

You will be paid any travel expenses incurred in coming to trial visits. Your contact details will be given to Cardiff University finance department in order that they can process payment to you.

17. What happens to my treatment when I finish the trial?

Your ophthalmologist will continue to follow you up in the NHS eye clinic, if it is considered necessary and decide whether you need to be treated with Bimatoprost after you have finished the trial.

18. If I did not take part in this research what treatment would I receive?

The standard treatments for patients with inactive Thyroid Eye Disease currently used at University Hospital of Wales involve artificial tears or surgery if required. For further information please ask your doctor to explain the usual care patients receive for inactive Thyroid Eye Disease.

19. Is there anything else to be worried about if I take part?

Please share this information with your partner if it is appropriate. You should not take part in this study if you are pregnant, breast-feeding or you may become pregnant during the study period. If you could become pregnant, we will ask you to have a pregnancy test (urine or blood) before taking part. You must agree to use a reliable form of contraception during the trial, e.g. oral contraceptive and condom, intra-uterine device (IUD) and condom, diaphragm with spermicide and condom. This should be continued for at least 2 months after the treatment has finished. If you do become pregnant during the course of the study, we would ask you to tell your study doctor immediately so we can help decide appropriate action.

20. Will my taking part in the study be kept confidential?

Yes. All information which is collected about you during the course of the research will be kept strictly confidential. Parts of your medical records and the data collected for the study will be looked at by authorised persons from Cardiff University, Cardiff & Vale University Health Board and the regulatory authorities – who are required to check that the study is being carried out correctly.

You will be assigned a study identification number so that the information collected about you (data) held on Cardiff University IT systems will be anonymised.

With your permission, your GP will be told that you are taking part in the study, as will any other doctors who are involved in your care, such as your endocrinologist.

21. What if new information becomes available?

Sometimes during the course of a research project, new information becomes available about the treatments that are being studied. If this happens, your research doctor will tell you about it and discuss with you whether you want to continue in the study. If you decide to withdraw, your research doctor will make arrangements for your normal care to continue. If you decide to continue in the study you will be asked to sign an updated consent form.

Also, on receiving new information your research doctor might consider it to be in your best interests to withdraw you from the study. They will explain the reasons and arrange for your care to continue.

22. What if something goes wrong?

If you are harmed by taking part in this research project or if you are harmed due to someone's negligence, then you may have grounds for a legal action.

Regardless of this, if you have concerns about any aspect of the way you have been approached or treated during the course of this study you may wish to contact the

following:

University Hospital of Wales, Cardiff
Complaints Manager at Cardiff and Vale UHB is Angela Hughes, Cardiff and Vale University Health Board Headquarters, Whitchurch Hospital, Park Road, Whitchurch, Cardiff CF14 7XB, Tel: 029 20 742202.

23. What will happen to the results of the research study?

The results of the study may be presented at relevant medical and scientific meetings and published in an appropriate medical or scientific journal. When all patients have completed the study, we can provide you with a summary of the results if you request it.

24. Who is organising and funding the research?

The study is being organised by Professor Colin Dayan in endocrine department and Mr Dan Morris and Mrs Carol Lane from Ophthalmology department. Funding for the study is provided from National Institute for Social Care and Health Research (NISCHR) which is a Welsh government body.

25. Who has reviewed the study?

This study has been reviewed by the South East Wales Research Ethics Committee, Medicines and Healthcare products Regulatory Agency (MHRA), National Institute for Social Care and Health Research (NISCHR), Cardiff University and Cardiff and Vale NHS Trust Research and Development Office.

26. Contact for Further Information

Mr Dan Morris and Mrs Carol Lane, Consultant Ophthalmologists, University Hospital of Wales, Heath Park, Cardiff CF14 4XW
Tel: 029 20 747747 (secretary extension: 2083)

Or

Professor Colin Dayan, Professor Clinical Diabetes and Metabolism, School of Medicine Centre for Endocrine and Diabetes Science, Cardiff University, Heath Park, Cardiff CF14 4XW
Tel: 029 20 742182 (secretary)

Or

Trials Office:
Julie Pell, Trials Coordinator: 02921 847942, pelljc@cardiff.ac.uk
Dr Draman, Study Doctor: 02920 748481, Dramanyusofms@cardiff.ac.uk
Mob: 07446624212

This information sheet is yours to keep. Thank you for taking time to read it.

8.4.4 Consent form

Bima Study

Patient Identification Number for this trial: _____

Bwrdd Iechyd Prifysgol Caerdydd a'r Fro
Cardiff and Vale University Health Board

Ysbyty Athrofaol Cymru

University Hospital of Wales

Eich cyf/Your ref:

Ein cyf/Our ref:

CONSENT FORM

Title of Project: Prostaglandin F2-alpha eye drops (Bimatoprost) in thyroid eye disease: a randomised controlled double blind crossover trial (BIMA study)

Chief Investigator: Professor Colin Dayan, Consultant Endocrinologist

Consultant Ophthalmologists: Mr Dan Morris / Mrs Carol Lane, Consultant Ophthalmologists, University Hospital of Wales, Heath Park, Cardiff CF14 4XW

Please initial boxes

1. I confirm that I have read and understand the information sheet,

V2, 20 March 2014 for the above study and have had the opportunity to ask questions.

2. I understand that my participation is voluntary and that I am free to withdraw at any time, without giving any reason, without my medical care or legal rights being affected. ☐

3. I understand that sections of my medical notes may be looked at by responsible individuals from Cardiff University, Cardiff & Vale University Health Board and the regulatory authorities, where it is relevant to my taking part in research, and that my personal details may be shared between research staff working at the institutions involved in the trial. I give permission for these individuals to have access to my records, and for my personal data to be used in this way. ☐

5. I agree to having photographs of my eyes taken for the purposes of research. ☐

6. I agree to my GP being informed of my participation in the study. ☐

7. I agree to take part in the above study ☐

<u>OPTIONAL (you can still take part in the study, even if you do not want to initial the box below)</u>

1. I consent to photographs of my eyes being published in an open access journal,

textbook or other form of medical publication (which may include the internet), and therefore may be seen by the general public as well as medical professionals. I understand that no other information about me would be published – only the photographs.

☐

_____	_____	_____
Name of Patient	Date	Signature
_____	_____	_____
Name of Person taking consent (if different from researcher)	Date	Signature
_____	_____	_____
Researcher	Date	Signature

1 for patient; 1 for researcher; 1 to be kept with hospital notes

8.4.5 Standard operating procedure list

BIMA Study: Study specific SOPs:

SOP	Author	Latest version	Date
Eye photograph	Dr S Draman	V1.0	06 May 2014
Height measurement	Dr S Draman	V1.0	26 Nov 2013
Weight measurement	Dr S Draman	V1.0	27 Nov 2013
Emergency code break procedure	J Pell/UHW Pharmacy	V1.0	23 July 2014
Pharmacy notification of allocation and dispensing of study treatments	Dr S Draman/UHW Pharmacy	V1.0	1 May 2014
Ophthalmology assessments	Dan Morris/S Draman	V1.0	06 May 2014
Endocrine Care	Dr S Draman	V1.0	26 Nov 2013
Smoking advice	Dr S Draman	V1.0	26 Nov 2013
Pregnancy Testing (*to be used in conjunction with PCTO -*	Dr S Draman Point of Care Testing	V1.0 E1.3	06 May 2014 21 Dec 2012

All Wales Pregnancy Training			
Randomisation Testing Plan	Dr S Draman		22 May 2014
Contacting patient after invite letter has been sent	Dr S Draman	V1.0	20 Mar 2014
Patient Pathway – Trial Visit	Dr S Draman/Julie Pell	V1.0	21 May 2014
Patient Pathway – To appt and subsequent trial visit appts	Dr S Draman/Julie Pell	V1.0	May 2014